Mixed-Mode Electrokinetic Chromatography of Low Molecular Weight Anions and Cations

by

Philip Zakaria

Chemistry

A thesis submitted in fulfilment of the requirements for the degree

of

Doctor of Philosophy

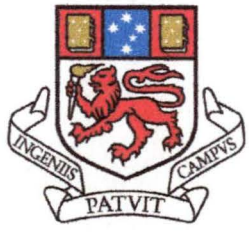

UNIVERSITY
OF TASMANIA

Submitted 14th March 2003

DECLARATION

To the best of my knowledge, this thesis contains no copy or paraphrase of material previously published or written by another person, except where due reference is made in the text of the thesis.

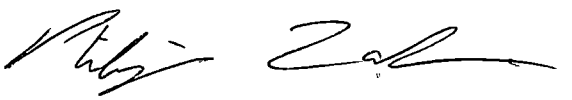

Philip Zakaria
14th March 2003

This thesis may be available for loan and limited copying in accordance with the Copyright Act 1968.

Philip Zakaria
14th March 2003

ACKNOWLEDGMENTS

None of the work presented here would have been possible without the help and support of numerous people over the past few years and I would like to offer my sincere thanks to the following people:

Firstly to my supervisor Professor Paul Haddad for all his help and support without which the following work would have not been possible.

My co-supervisor, Dr. Mirek Macka, whose help and suggestions over the course of the last few years has been a major reason things have gone as smoothly as they have.

Professor Jim Fritz for his helpful suggestions and enthusiasm over the warm summer months.

All past and present members of ACROSS (aka SSG) including John Madden, Cameron Johns, Helmy Cook, John O'Reilly, Greg Dicinoski, Narumol Vachirapatama, Baoguo Sun, Takashi Yokoyama, Matt Shaw, Andrew Grosse, Chisato Obara, Amanda Glover, Wenchu Yang, Joe Hutchinson, Fang Wang, Samra Tulumovic, Andy Bowie and the courageous fish of Rm 413 whose fighting spirit is an inspiration to us all. I would also like to especially thank those members who participate in a few quiet ales come a Friday afternoon, without which I most certainly would not have got this far.

The staff and students of the School of Chemistry for providing such a friendly working environment, especially the morning tea which is certainly a highlight of each day.

Rod Minett, David Wilkinson and Mike Whitby of Agilent Technologies Australia for technical and financial support. Financial support from the Australian Research Council and Dionex Corporation is also gratefully acknowledged.

All my friends in Hobart and interstate for providing many fun times over the past few years and also to the members of Not Div ½ (aka Einherger TS) for many fun (and some not so fun) games of indoor soccer.

I would also like to thank my parents, even though they have not been around much in the last few years their support via email and visits has been greatly appreciated.

Finally I would like to offer my most heartfelt thanks to my wife, Jane, for all her love and support over the past 6 years. Without her I'm not sure what I would have been doing right now and so a large part of this work has to be dedicated to her.

LIST OF ABBREVIATIONS

ANN	Artificial neural network
BGE	Background electrolyte
CD	Cyclodextrin
CE	Capillary electrophoresis
EKC	Electrokinetic chromatography
EOF	Electroosmotic flow
ID	Internal diameter
IE	Ion-exchange
IP	Ion-pair
MR	Minimum resolution
NRP	Normalised resolution product
PDDAC	Poly(diallydimethylammonium chloride)
p-SP	Pseudo-stationary phase
PVS	Polyvinylsulfonate
s-β-CD	Sulfated-β-cyclodextrin
Tris	Tris(hydroxymethyl)aminomethane

LIST OF PUBLICATIONS

Type of Publication	Number	Reference
Papers in refereed journals	7	1-7
Posters at international meetings	4	8-11
Oral presentations at international meetings	3	12-14
Presentations at student conferences	2	15-16

1. P. Zakaria, M. Macka and P. R. Haddad, Electrokinetic chromatography utilizing two pseudo-stationary phases providing ion-exchange and hydrophobic interactions, *Anal. Chem.*, 74 (2002) 1241. *(Chapter 3)*

2. P. Zakaria, M. Macka and P. R. Haddad, Modelling, optimisation and control of selectivity in the separation of aromatic bases by electrokinetic chromatography using a neutral cyclodextrin as a pseudo-stationary phase, *Electrophoresis*, 23 (2002) 1844. *(Chapter 5)*

3. P. Zakaria, M. Macka, J. S. Fritz and P. R. Haddad, Modelling and optimisation of the electrokinetic chromatographic separation of mixtures of organic anions and cations using poly(diallydimethylammonium chloride) and hexanesulfonate as mixed pseudo-stationary phases, *Electrophoresis*, 23 (2002) 2821. *(Chapter 7)*

4. P. Zakaria, M. Macka and P. R. Haddad, Separation of opiate alkaloids using electrokinetic chromatography with sulfated-cyclodextrin as a pseudo-stationary phase, *J. Chromatogr. A.*, 985 (2003) 493. *(Chapter 4)*

5. P. Zakaria, M. Macka and P. R. Haddad, Mixed-mode electrokinetic chromatography of aromatic bases with two pseudo-stationary phases and pH control, *J. Chromatogr. A.*, 997 (2003) 207. *(Chapter 5)*

6. P. Zakaria, M. Macka and P. R. Haddad, Selectivity Control in the Separation of Aromatic Amino Acid Enantiomers using Sulfated β-cyclodextrin, *J. Chromatogr. A*, submitted for publication. *(Chapter 6)*

7. P. Zakaria, M. Macka and P. R. Haddad, Optimisation of Selectivity in the Separation of Aromatic Amino Acid Enantiomers using Sulfated β-cyclodextrin and Dextran Sulfate as Pseudostationary Phases, *Electrophoresis*, submitted for publication. *(Chapter 6)*

8. P. Zakaria, M. Macka and P. R. Haddad, Modelling the CEC separation of aromatic bases using a neutral cyclodextrin, IICS 2001, Chicago, USA.

9 P. Zakaria, M. Macka, J. S. Fritz and P. R. Haddad, Use of ion-exchange and hydrophobic pseudo-stationary phases for mixed-mode separations in capillary electrochromatography, ISCC 2002, Riva del Garda, Itali.

10. P. Zakaria, M. Macka, J. S. Fritz and P. R. Haddad, Modelling and optimisation of the electrokinetic chromatographic separation of mixtures of organic anions and cations using poly(diallydimethylammonium chloride) and hexanesulfonate as mixed pseudo-stationary phases, ISCC 2002, Riva del Garda, Itali.

11. P. Zakaria, M. Macka and P. R. Haddad, Modelling the separation of six opiate compounds in electrokinetic chromatography using a sulfated-cyclodextrin as a pseudo-stationary phase, IICS 2002, Baltimore, USA.

12. P. Zakaria, M. Macka and P. R. Haddad, Mixed-mode separations in pseudo-phase capillary electrochromatography involving ion-exchange, hydrophobic interactions and electrophoresis, IICS 2001, Chicago, USA, as presenting author.

13. P. Zakaria, M. Macka and P. R. Haddad, Modelling the separation of six opiate compounds in electrokinetic chromatography using a sulfated cyclodextrin as a pseudo-stationary phase, Interact 2002, Sydney, Australia.

14. P. Zakaria, M. Macka and P. R. Haddad, Optimisation of selectivity in the separation of aromatic amino acid Enantiomers using a sulfated-β-cyclodextrin and temperature as selectivity modifiers, IICS 2003, San Diego, USA, as presenting author.

15. P. Zakaria, M. Macka and P. R. Haddad, Multi-mode capillary electrochromatography, *poster presentation*, R&D 2000, Wagga Wagga, Australia.

16. P. Zakaria, M. Macka and P. R. Haddad, Mixed-mode electrokinetic chromatography of aromatic bases utilizing two pseudo-stationary phases and pH control, *oral presentation*, R&D 2002, Warrnambool, Australia.

ABSTRACT

This work presents a comprehensive study into selectivity control over electrokinetic chromatography (EKC) systems for the determination of small organic anions and cations using various additives.

For the separation of anions an electrolyte system comprising a cationic soluble polymer (poly(diallydimethylammonium chloride), PDDAC) and a neutral β-cyclodextrin (β-CD) as pseudo-stationary phases was used. The separation mechanism was a combination of electrophoresis, ion-exchange (IE) interactions with PDDAC, and hydrophobic interactions with β-CD. The extent of each chromatographic interaction was independently variable, allowing for control of the separation selectivity of the system.

Various cationic analytes were also examined, including opiate alkaloids, aromatic bases and amino acids. In the case of the opiate alkaloids (morphine, thebaine, 10-hydroxy thebaine, codeine, oripavine and laudanine) a system utilising sulfated-β-cyclodextrin (s-β-CD) as a pseudo-stationary phase was used. Cation-exchange interactions between the cationic analytes and the anionic s-β-CD (7-11 moles of sulfate groups per mole CD) were found to be the predominant separation mechanism.

The separation of a series of aromatic bases was achieved utilising an electrolyte system comprising an anionic soluble polymer (polyvinylsulfonic acid, PVS) and β-CD as pseudo-stationary phases. The separation mechanism was based on a combination of electrophoresis, IE interactions with PVS, and hydrophobic interactions with β-CD. The extent of each chromatographic interaction was independently variable, allowing for control of the separation selectivity of the

system. The IE and the hydrophobic interactions could be varied by changing the concentrations of PVS and β-CD, respectively. Additionally, mobilities of the bases could be controlled by varying pH, due to their large range of pK_a values.

Selectivity control of the enantiomeric separation of the three aromatic amino acids (phenylalanine, tyrosine and tryptophan) was demonstrated utilising temperature and s-β-CD and dextran sulfate as pseudo-stationary phases. Two systems were explored using s-β-CD as the chiral selector. In these systems either temperature or the addition of dextran sulfate was used to increase the selectivity control.

The possibility of the simultaneous separation of anions and cations was demonstrated using a series of aromatic carboxylic acids, sulfonates and opiates as analytes. Separation was achieved using electrokinetic chromatography employing a mixture of PDDAC and the amphiphilic anion hexanesulfonate as pseudo-stationary phases. In this system, the PDDAC pseudo-stationary phase interacted with the anionic analytes, whereas the hexanesulfonate interacted with the cationic analytes. A further interaction between the combined PDDAC-hexanesulfonate complex and the more hydrophobic analytes was also evident.

Mathematical modelling based on physical equilibrium and artificial neural networks was also undertaken, with the models successfully describing each system (r^2>0.98 for predicted versus observed migration times). The models were then used to not only optimise each system, but also to allow predictable selectivity control leading to attainment of desired migration orders.

TABLE OF CONTENTS

Chapter 1

Introduction and Literature Review

1.1 Introduction

Capillary electrophoresis (CE) is an analytical separation technique that utilises the electrophoretic motion of ions in solution upon application of an external electric field, with species being separated due to their differing migration velocities. While application of an external electric field is necessary for separation, it generates a current which in turn increases the temperature of the electrolyte. Efficient heat dissipation is therefore of practical importance when performing the technique. A simple means to achieve heat dissipation is the use of smaller diameter capillaries to perform the electrophoretic separation, due to increased surface to volume ratios allowing for more effective heat removal.

The first demonstration of free solution electrophoresis in small diameter tubing was in 1967 by Hjerten [1] who used 3mm internal diameter (ID) capillaries. Virtanen in 1974 [2] and Mikkers *et al.* [3] in 1979 extended this work by using 0.2-0.5mm ID glass capillaries and 200μm ID polymer capillaries, respectively.

The major advantage of CE over conventional liquid chromatographic techniques is the high efficiency that can be obtained due to the plug-like flow profile of the electroosmotic flow (EOF) compared to the parabolic profile of pump-driven systems. The EOF is generated by the movement of the diffuse layer of ions in the vicinity of the capillary wall. These ions can either be cations or anions depending on the charge on the capillary wall and so the EOF can either move towards the cathode or anode

depending on the particular application. The high efficiencies obtainable with CE was first demonstrated by Jorgenson and Lukacs in 1981 who used high electric field strengths with small ID capillaries (less than 100μm). In 1989 the first commercially available CE system was introduced and since this time CE has been widely applied to a large range of different samples and analytes [4,5].

1.2 Selectivity Manipulation in CE

In CE, separation is achieved due to the difference in migration velocities (electrophoretic mobilities) of the analytes of interest. Therefore, analytes with sufficiently different mobilities are reasonably easy to separate in a CE system. However, analytes with similar mobilities often do not separate fully and migrate as a single peak. Neutral analytes cannot be separated by CE due to their lack of mobility and these migrate as a single peak with the EOF. The mobility of an analyte in a given electrolyte system is a physical property of that analyte and is related to its charge to size ratio. That is, smaller analytes with higher charge migrate faster than larger analytes with lower charge. Generally then, the mobility of an analyte can be modified via two means, either varying its effective charge, or varying its size. For the purpose of discussion, CE here is assumed to be any separation where additives to the electrolyte, such as micelles, ion pair reagents, polymers etc., are not used. These separations are termed electrokinetic chromatography separations and will be discussed below.

Modifying the selectivity in straight CE systems is generally achieved by varying electrolyte conditions such as pH, ionic strength, temperature, voltage or using organic modifiers. Instrumental parameters such as temperature, voltage, use of external pressure or capillary dimensions generally have a limited effect on selectivity

since they tend to affect all analytes in a similar manner. Varying the pH is one of the most effective means of changing the selectivity of a system. It is especially useful for the separation of weak acids and bases as the pH directly affects the degree of charge on the analytes, and hence their observed mobility. Use of organic modifiers is also a popular approach when trying to control the selectivity of a system. Modifiers can act in a variety of ways including affecting the relative hydration enthalpies of ions or varying the effective pK_a values of weak acids and bases. Several reviews into selectivity control in CE have been published dealing with a range of analytes [6-8].

Although methods to control selectivity in CE do exist, they tend to either only bring about relatively small changes in selectivity or only be applicable to certain analytes, ultimately limiting the number of applications to which CE can be successfully applied.

1.3 Micellar Electrokinetic Chromatography

Electrokinetic chromatography (EKC) is a variation of CE whereby an additive is included in the electrolyte. This additive is chosen so as to interact with an analyte of interest thereby varying the charge and/or size of the analyte and hence its effective mobility. Differences in the strength of interaction between the additive and the different analytes present in the sample lead to selectivity changes in the system. These additives are termed pseudo-stationary phases (p-SP) since they interact with the analytes in a similar manner to a solid stationary phase, however, they themselves do not strictly remain stationary within the system.

To date, micelles have been the most common additive used in EKC, with the technique here being termed micellar electrokinetic chromatography (MEKC).

MEKC was first introduced by Terabe *et al.* in 1984 [9] and has since been extended to the analysis of a large variety of analytes using cationic, anionic, neutral and zwitterionic surfactants. Separation in MEKC relies on the different partitioning of analytes between the electrolyte and surfactant phases. In this way both charged and neutral analytes can be separated due to the apparent mobility of neutral analytes when incorporated into the micellar phase.

1.3.1 Sodium Dodecyl Sulfate

The most common surfactant used since the introduction of MEKC has been sodium dodecyl sulfate (SDS). The use of SDS greatly increases the selectivity control offered over straight CE and examples are summarised in Table 1.1. SDS was used as long ago as 1985 during the pioneering work of Terabe and co-workers [10]. In this work SDS was used to separate neutral and partially ionised chlorinated phenols with separation attributed to partitioning of the phenols into the hydrophobic region of the SDS micelles, with the extent of partitioning found to differ for each analyte, shown by calculated retention factors. It was also found that for partially ionised solutes the retention factor decreased as the pH increased whereas for neutral solutes it stayed virtually constant. This was attributed to an increase in the electrophoretic mobility of the solute (counter to the EOF) and/or to an increased repulsion of the solute from the anionic micelle. Whatever the mechanism, it shows the potential for increased selectivity control compared to that of a straight CE system. This allows the selectivity to be controlled in a 2-dimensional manner by varying both the concentration of SDS and the pH of the system.

This 2-dimensional approach to selectivity control was extended by Quang et al. [11] who used the parameters [SDS] and pH to optimise the MEKC separation of acidic

Table 1.1: Selectivity in MEKC using SDS

Analytes	Optimisation Parameters	Electrolyte	Separation Conditions	Detection	Ref.
Chlorinated phenols	[SDS], pH	Phosphate-borate	50μm x 65cm (50cm to detector), 35°c	Direct UV at 220nm	[10]
Catecholamines	[SDS], voltage	Phosphate, pH 7.0	53μm x 58cm (44.5cm to detector), 40°c	Direct UV at 254nm	[12]
Illicit heroin and amphetamine samples	[SDS], %ACN	Phosphate-borate + ACN, pH 9.0	50μm with effective separation length of 50cm	Direct UV at 214nm	[13]
Substituted phenols and aromatic amines	[SDS], pH	Phosphate-carbonate	50μm x 57cm, 40°c	Direct UV at 214nm	[11]
Free and glucuronidated opioids	[SDS], pH, voltage, %ethylene glycol	Phosphate	50μm x 41cm (22cm to detector), 35°c	Direct UV at 210nm	[14]
Histamine, tyramine, cadaverine and spermidine (derivatized)	[SDS]	Phosphate-borate, pH 10	50μm with effective separation length of 75cm	Absorbance at 340nm or in-capillary derivatization with fluorescence detection at 450nm (excitation at 340nm)	[15]
Metal complexes with HEDTC	[SDS], %MeOH	NS	NS	NS	[16]

ACN – Acetonitrile; HEDTC - Bis(2-hydroxyethyl)dithiocarbamate; MeOH – Methanol; NS – Not stated

and basic compounds, substituted phenols and aromatic amines, respectively. The basic mechanism of separation was the same as that shown previously but the authors derived equilibrium-based expressions to describe the observed separations. These expressions took into account both interactions of the analytes with the micelle as well as interactions with free surfactant monomers present in the electrolyte. The model could then be used to predict migration times for any inputted SDS concentration and pH.

A further parameter that can be used to vary the selectivity of a MEKC system is the addition of organic modifiers and this was demonstrated by Zhang and Thormann [14] who showed that the addition of ethylene glycol to the SDS separation of free and glucuronidated opioids led to an improvement in the separation due to weakening of the solute-surfactant interactions.

1.3.2 Other Ionic Surfactants

Although SDS has been the most widely used surfactant in MEKC, several other ionic surfactants have also been used to modify the selectivity of MEKC systems, as summarised in Table 1.2.

The use of different surfactants allows for altered selectivities compared to that obtained using SDS. Tanaka *et al.* [17] used the double-chain anionic surfactant disodium 5,12-bis(dodecyloxymethyl)-4,7,10,13-tetraoxa-1,16-hexadecane-disulphonate (DBTD) for the separation of benzene and naphthalene derivatives. DBTD showed several advantages over SDS while giving comparable separations. It has a lower Krafft point and critical micellar concentration (CMC), meaning less DBTD was required, 7.5mM compared to 50mM SDS. It was also shown that the migration order of the solutes differed in the DBTD system compared to the

Table 1.2: Selectivity in MEKC using various surfactants

Surfactant	Analytes	Optimisation Parameters	Electrolyte	Separation Conditions	Detection	Ref.
DBTD (anionic)	Benzene and naphthalene derivatives	[DBTD]	Phosphate-borate, pH 7.0	50μm x 72cm (50cm to detector), 35°c	Direct UV at 210nm	[17]
CTAB (cationic)	Morphine and related alkaloids	pH, type and concentration of organic modifiers	Phosphate-borate + organic modifiers	50μm x 70cm (45cm to detector), 28°c	Direct UV at 254nm	[18]
SDBS (anionic)	PAHs	[SDBS], %ACN	Tris + ACN, pH 7.2	50μm x 67cm (53cm to detector),	Direct UV at 254nm	[19]
ALE (anionic) and LMT (anionic)	Phenol and alanine derivatives	pH, surfactant functional group	Phosphate-borate	50μm x 62cm (50cm to detector), 30°c	Direct UV at 270nm	[20]
Sulfonated Brij-30 (anionic)	Polar organic compounds, testosterones and PAHs	[sulfonated Brij-30], voltage, %ACN	Borate, pH 9 and 10	50 or 75μm x 60cm (52.5cm to detector), 25°c	Direct UV at 214 or 254nm	[21]
MAPS (zwitterionic) + alkylsulfonates (anionic)	Opiates and adulterants found in heroin seizures	[surfactant], [alkylsulfonates]	6-ACA + 10% ACN	50μm x65cm (60cm to detector),	Direct UV at 214nm	[22]
CAS U (zwitterionic) + TTAB (cationic)	Inorganic anions	[surfactant]	Chromate, pH 8.0	75μm x 47cm (40cm to detector)	Indirect UV at 254nm	[23]
ALE (anionic), LMT (anionic) and LSA (anionic)	Aniline derivatives	Surfactant functional group	Phosphate-borate, pH 7.0	50μm x 62cm (50cm to detector), 30°c	Direct UV at 240nm	[24]

Table 1.2: Selectivity in MEKC using various surfactants (ctd)

Surfactant	Analytes	Optimisation Parameters	Electrolyte	Separation Conditions	Detection	Ref.
SC (anionic), TTAB (cationic) and SDS+Brij-35 (anionic + neutral)	Tetracyclines	pH, [surfactant]	Ammonium acetate	75μm x 43cm (36cm to detector), 25°c	Direct UV at 265nm	[25]
DDAPS (zwitterionic)	Inorganic anions	[DDAPS]	Phosphate, pH 7.2 and chromate, pH 8.0	50μm x 47cm (40cm to detector), 25°c	Direct and indirect UV at 254nm	[26]
CTAB (cationic)	Small organic acids, aminoglycosides and benzene derivatives	[CTAB], voltage	Imidazole-acetate, pH 5.0 for indirect detection, Tris-acetate, pH 7.5, or Tris-benzoate, pH 8.0, for direct detection	75μm x 56.8cm (50cm to detector), 30°c	Direct and indirect UV detection at 214nm	[27]
LDS + LPFOS (anionic + anionic)	Neutral aromatic organics	[surfactant]	Phosphate, pH 7.0	50μm x 47cm (40cm to detector), 25°c	Direct UV at 214nm	[28]

DBTD - 5,12-bis(dodecyloxymethyl)-4,7,10,13-tetraoxa-1,16-hexadecanedisulphonate; CTAB – Cetyltrimethylammonium bromide; SDBS – Sodium dodecylbenzenesulfonate; PAHs – Polycyclic aromatic hydrocarbons; Tris – Tris(hydroxymethyl)aminomethane; ALE - Sodium N-lauroyl-N-methyl-β-alaninate; LMT – Sodium N-lauroyl-N-methyltaurate; Brij-30 - Polyoxyethylene 4 lauryl ether; MAPS – 3-N,N-dimethylmyristylammoniopropanesulfonate; 6-ACA – 6-aminocaproic acid; ACN – Acetonitrile; CAS U – coco amidopropylhydroxyldimethylsulfobetaine; TTAB – Tetradecyltrimethylammonium bromide; LSA – Sodium laurylsulfoacetate; SC – Sodium cholate, Brij-35 - Polyoxyethylene 23 lauryl ether; DDAPS – 3-(N,N-dimethyldodecylammonio)propane sulfonate; LDS – Lithium dodecyl sulfate; LPFOS – Lithium perfluorooctanesulfonate

corresponding SDS system. Baseline resolution of 1- and 2-naphthol was also not possible with the SDS system but was readily achieved using the DBTD system. Varying the functional group of surfactants is also a useful means for changing the selectivity of a system. Takeda and co-workers [20,24] have demonstrated the differing selectivities for phenol and aniline derivatives using surfactants based on carboxylate, sulfonate and sulfate (using SDS) functionalities. The analyte-micelle interaction was found to be not only associated with hydrophobic partitioning into the micellar phase, but to also be affected by electrostatic interactions with analytes possessing higher pK_a values interacting more strongly with SDS than the other surfactants.

The use of cationic surfactants also allows for differing selectivities since the micelles now migrate in the opposite direction to that of anionic micelles. Quaternary ammonium surfactants such as tetradecyltrimethylammonium bromide (TTAB) and cetyltrimethylammonium bromide (CTAB) have long been used to modify surface properties of fused silica capillaries (due to interaction between the cationic surfactant and anionic silanol groups on the capillary surface), but they can also be used as micellar p-SPs. Several classes of analyte have been successfully separated using both TTAB and CTAB [18,25,27].

A further group of ionic surfactants that has been used successfully for selectivity control in MEKC are zwitterionic surfactants. These have the advantage over other ionic surfactants that they can be added to electrolytes without affecting the conductivity, allowing larger concentrations to be added without causing current and Joule heating problems [26]. These surfactants have also been shown to give a unique selectivity, especially for inorganic anions. Work by Woodland and Lucy [26] has shown that the use of 3-(N,N-dimethyldodecylammonio)propane sulfonate (DDAPS)

for the separation of inorganic anions dramatically altered the selectivity, in particular for the more polarizable anions such as thiocyanate, iodide, nitrate and bromide, consistent with the retention observed in electrostatic ion chromatography. The separation mechanism was attributed to simultaneous electrostatic attraction and repulsion of the anions with the zwitterionic surfactant.

1.3.3 Neutral Surfactants

Neutral micelles have also been used for MEKC as shown in Table 1.3. Since these micelles possess no mobility they migrate with the EOF. Neutral surfactants, like zwitterions, have the advantage that they can be added to a system without increasing the ionic strength or current and can therefore be added at greater concentrations than most ionic surfactants. Brij-35 (polyoxyethylene 23 lauryl ether) is the most commonly used neutral surfactant and is a strong hydrogen bond base and weak hydrogen bond acid and has been shown to have a great capacity for attraction interactions between ion pairs [29]. Brij-35 has been used for the separation of pharmaceutical compounds [30], naphthalenedisulfonate isomers [29] and derivatized amino acids [31].

1.4 Microemulsion Electrokinetic Chromatography

Microemulsion electrokinetic chromatography (MEEKC) is a modification of a MEKC system where a lipophilic organic solvent has been dissolved in the micelles. These microemulsions are defined as macroscopically homogeneous, fully optically transparent fluids having more than one liquid phase [32]. A typical composition of a microemulsion consists of 0.8% *n*-octane + 3.3% SDS + 6.6% n-butanol + 89.3% 10mM borate buffer at pH 9.2 [32]. The main separation mechanism in MEEKC is

Table 1.3: Selectivity in MEKC using neutral surfactants

Surfactant	Analytes	Optimisation Parameters	Electrolyte	Separation Conditions	Detection	Ref.
Brij-30 and Brij-35	Pharmaceutical bases and weakly acidic positional isomers	[surfactant], pH	Phosphate, ACES, pH 6.5-7.0	DOI-CE, 50μm x 60cm (25cm to detector),	Direct UV at 214 and 234nm	[30]
Brij-35	Substituted and unsubstituted naphthalene-disulfonate isomers	[Brij-35], temperature, concentration and type of organic modifier	Borate, pH 9.1	75μm x 64.5cm (66.5cm to detector)	Direct UV at 230nm	[29]
Brij-35	Amino acids derivatized with DTAF	[Brij-35]	Borate, pH 9.5	50μm x 57cm (50cm to detector, 35°c	LIF detection with excitation at 488nm and emission at 520nm	[31]

Brij-30 – Polyoxyethylene 4 lauryl ether; Brij-35 – Polyoxyethylene 23 lauryl ether; ACES – N-(2-acetamido)-2-aminoethanesulfonic acid; DOI-CE - Dual opposite injection capillary electrophoresis; LIF – Laser induced fluorescence; DTAF – 5-(4,6-dichloro-s-triazin-2-ylamino)fluorescein

similar to that of MEKC with the solutes partitioning between the aqueous phase and the organic phase (present as oil droplets that are solubilised by the addition of a surfactant such as SDS). An advantage of MEEKC is the high solubilising ability of the microemulsions, allowing for the separation of relatively large organic analytes. Although the number of additives used potentially allows for many different parameters to be changed to modify observed selectivities, in reality this is limited since the range of conditions for which the microemulsions are stable is relatively small. This means full control of the selectivity can be difficult to achieve due to loss of the microemulsion as certain parameters are varied over a large range. Despite this applications of MEEKC to a wide variety of analytes have been reported and the technique has been the subject of reviews [32,33].

1.5 Ion-Pair Additives

In many EKC systems, such as MEKC and MEEKC, the separation mechanism involves partitioning of the solutes between the electrolyte phase and the p-SP. Separation then occurs due to the difference in interaction strengths between the analytes and the micelles, as well as the modified mobility of the analytes when incorporated into the p-SP. Additives for EKC systems, however, do not necessarily have to form secondary phases in the electrolyte. Any additive that can interact with the analytes of interest can be potentially used as a p-SP. A common interaction that is utilised is an electrostatic interaction between analytes and oppositely charged additives. This association is termed an ion-pair (IP) interaction and several small additives have been successfully used as IP reagents in EKC systems and these are summarised in Table 1.4.

Table 1.4: Selectivity in EKC using ion-pair additives

Additive	Analytes	Optimisation Parameters	Electrolyte	Separation Conditions	Detection	Ref.
Phytic acid	Peptides	[phytic acid],	Phosphate, pH 7.0	75μm x 95cm (87cm to detector)	Direct UV at 214nm	[34]
Alkylsulfonic acids and tetra-alkylammonium salts	Neuro-transmitters, peptides and protiens	[additive], pH	Phosphate, pH 2.5, 7.0 and 9.0	50 and 75μm x 75 and 42cm (8cm from capillary end to detector, 25°c	Direct UV at 210nm	[35]
Ethanesulfonic acid and triethylamine	Protonated anilines	[additive], pH, type and concentration of organic solvent	Phosphate + 7.5% 2-propanol	50μm x45cm (37cm to detector)	Direct UV at 229nm	[36]
Ammonium, TMA, TEA and TBA	Metal cations chelated to PAR	Concentration and type of additive	Phosphate + PAR, pH 8	50μm x 70cm (62.5cm to detector), 25°c	Direcct UV at 510nm	[37]
Short chain TAA salts	Pyrroloquinoline quinone and three isomeric analogues	Concentration and type of additive	Phosphate, pH 7.4	50μm x 30cm (20cm to detector), 25°c	Direct UV at 254nm	[38]
tBuCQN	Peptides	[tBuCQN], composition of non-aqueous electrolyte, pH, ionic strength	MeOH-EtOH buffered with acetic acid and triethylamne	50μm x 64.5cm (56cm to detector), 15°c	Direct UV at 254nm	[39]

PAR – 4-(2-pyridylazo)resorcinol; TAA – Tetraalkylammonium; tBuCQN – *tert.*-Butylcarbamoylquinine

Generally small organic molecules such as alkylsulfonates and alkylammonium salts are used most commonly. These additives however possess both a hydrophobic and an ionic group and may therefore alter both the hydrophobicity as well as the charge on the analyte. An alternative IP reagent that has been successfully used is phytic acid. Phytic acid consists of cyclohexane with 6 phosphoric acid groups connected to the 6 carbons. Phytic acid exhibits very little hydrophobicity and due to its large number of acidic groups should interact strongly with cationic analytes in basic conditions. Kornfelt *et al.* [34] used phytic acid as an IP reagent for the separation of peptides and it was found that peptides with p*I* values above that of the electrolyte interacted the strongest with phytic acid. This corresponds to those peptides that are cationic at the electrolyte pH, leading to a strong interaction with the anionic phytic acid.

IP reagents can be thought of as selective additives, that is, they can be added to a system to interact only with those analytes of opposite charge while showing very little interaction with neutral or similarly charged analytes. A review into the use of IP reagents in EKC has been published by Shelton *et al.* [40].

1.6 Dendrimers

Dendrimers are large molecules obtained by repetitive "cascade" synthesis starting from an initiator core of a branched building block [41]. Commercially available dendrimers based on a initiator core of ethylene diamine are now available and are collectively termed starburst™ (poly-[amido-amine]; PAMAM) dendrimers. The use of dendrimers as p-SPs in EKC separations is summarised in Table 1.5.

Commercially available starburst™ dendrimers have proven a popular choice for EKC separations. Due to the cascade synthesis of these dendrimers, both anionic

Table 1.5: Selectivity in EKC using dendrimers as additives

Dendrimer	Analytes	Optimisation Parameters	Electrolyte	Separation Conditions	Detection	Ref.
Poly(propyleneimine) dendrimer	Aromatic alcohols	Comparison with SDS	Tris, pH 8.2	50μm x 30cm (25.4cm to detector), 25°c	Direct UV at 200nm	[42]
Starburst dendrimer	Dansylamino acids	[dendrimer], temperature, voltage	Phosphate-triethylamine + 20% MeOH, pH 8.3	75μm x 56.5cm (50cm to detector), 25°c	Direct UV at 254nm	[43]
Polyacid dendrimer	Parabens	[dendrimer], temperature	Tris-borate, pH 8.5	50μm x 30cm (25.4cm to detector)	Direct UV at 254nm	[44]
Sulfonic acid modified starburst dendrimer	Positional isomers of neutral phenols	[dendrimer], pH,	Phosphate-borate	60μm x 90cm (53.4cm to detector), 25°c	Direct UV at 254nm	[45]
Starburst dendrimer	Protein profiling	[dendrimer]	Phosphate, pH 7.2	75μm x 60cm (52cm to detector)	Direct UV at 214nm	[46]

Tris - Tris(hydroxymethyl)aminomethane; Starburst – poly(amido-amine) dendrimer; MeOH – Methanol

(carboxylate) and cationic (amino) dendrimers are possible depending on where the synthesis is halted. Dendrimers can therefore be used as ion-exchange (IE) p-SPs for both anionic and cationic analytes. The hydrophobic core of the dendrimers also introduces the possibility of hydrophobic interactions with organic analytes, similar to that seen when using micelles. Dendrimers are therefore potentially applicable to both charged and neutral analytes.

Gray and Hsu [45] have shown the separation of neutral phenols with and without the addition of an anionic starburst dendrimer. Without the addition of the dendrimer coelution of phenol isomers was observed, but these isomers could be successfully separated in the presence of the dendrimer. The dendrimer separation was also compared to that obtained using SDS and was found to give an almost two-fold increase in efficiency over the MEKC system.

Dendrimers have also been shown to exhibit IE interactions with charged analytes. Castagnola *et al.* [43] used different generations of anionic starburst™ dendrimer for the separation of dansylamino acids and found that the predominant interaction with the dendrimers was IE in nature. It was also concluded that the observed selectivity of the system could be varied depending on the generation of dendrimer used due to the difference in size and amount of charge present on the dendrimer.

Classification and use of dendrimers as p-SPs has been reviewed by Castagnola *et al.* [41].

1.7 Crown Ethers

Crown ethers are macrocyclic polyethers that are known to form stable complexes with alkali, alkaline-earth and primary ammonium cations. Crown ethers have been used as additives to EKC systems while chiral crown ethers have been successfully

used for enantiomeric separations. The use of crown ethers for selectivity control in EKC systems is summarised in Table 1.6.

Francois *et al.* [49] have shown the selectivity changes that can be introduced when using 18-crown-6 as an electrolyte additive for the separation of ammonium, alkali and alkaline-earth cations. Mobility changes are brought about due to differing complexation strengths between the various cations and the crown ether. Of the analytes, barium was found to interact most strongly with the crown ether while ammonium had the weakest interaction. This is due to the close match of the ionic radius of barium (1.36Å) and the cavity radius of 18-crown-6 (1.38Å) while the radius of ammonium (1.51Å) is too large to be incorporated into the crown ether cavity. The same set of analytes was also examined by Oehrle [50] who included 15-crown-5 and 12-crown-4 as electrolyte additives. However, it was found that 18-crown-6 provided the best separation of the cations investigated.

Introduction of chiral groups to crown ethers allows these additives to be used for enantiomeric separations. The most commonly used chiral crown ether is 18-crown-6 tetracarboxylic acid, which has been employed for the separation of several optically active compounds [47,48,51]. The separation mechanism involves complexation of the analyte into the cavity of the crown ether by three hydrogen bonds with the crown ether oxygen atoms and additional lateral interactions with the four carboxylate groups are necessary for the discrimination of the enantiomers [51].

1.8 Soluble Polymers

Soluble polymers have proven to be one of the most popular additives for EKC systems. They have the advantages that numerous backbones and functional groups can be used to form these polymers, potentially allowing them to be custom-made for

Table 1.6: Selectivity in EKC using crown ethers as additives

Crown Ether	Analytes	Optimisation Parameters	Electrolyte	Separation Conditions	Detection	Ref.
18-crown-6 tetracarboxylic acid (chiral separations)	Optically active aromatic amines	Temperature	Tris-citrate, pH 2.2 and BTAC-Tris, pH 2.2.	75μm x 50cm, 25°c	Direct UV at 254nm and Indirect UV at 214nm	[47]
18-crown-6 tetracarboxylic acid (chiral separations)	5,6-dihydroxy-2-aminotetralin	[crown ether], temperature	Tris-citrate, pH 2.2	75μm x 57cm (50cm to detector), 25°c	Direct UV at 280nm	[48]
18-crown-6	Ammonium, alkali and alkaline-earth cations	[18-crown-6], pH, temperature, voltage	Imidazole	75μm x 57cm (50cm to detector), 25°c	Indirect UV at 214nm	[49]
18-crown-6, 15-crown-5 and 12-crown-4	Ammonium, alkali and alkaline-earth cations	[crown ether]	UV Cat-2 (waters) + tropolone	75μm x 60cm	Indirect UV at 185nm	[50]

BTAC – Benzyltrimethylammonium chloride; Tris – Tris(hydroxymethyl)aminomethane

particular analytical problems. A recent article by Liu and Armes [52] highlights the recent advances in the synthesis of soluble polymers with a range of molecular architectures and functional groups.

The addition of soluble polymers to EKC systems provides a convenient means to predictably control the selectivity of the separation system. Several analyte-polymer interactions are possible depending on the particular polymer being used. These include IE interactions, chelation, hydrophobic interactions, H-bonding etc.

1.8.1 Cationic Polymers

Cationic polymers have proven to be the most popular when used as additives in EKC systems and their use is summarised in Table 1.7.

Cationic polymers were first used by Terabe and Isemura in 1990 for the separation of naphthalenesulfonic acid isomers [53] and aromatic carboxylic acids [54]. For the separation of naphthalenesulfonic acid isomers the cationic polymer poly(diallyldimethylammnonium chloride) (PDDAC) was used. It was found that in the absence of the polymer the disulfonates migrated faster than the monosulfonates (due to a greater charge), but all monosulfonate and disulfonate isomers co-migrated. The addition of PDDAC to the electrolyte successfully separated all isomers and also reversed the migration order between the mono- and disulfonates. The separation mechanism was attributed to IE interactions, meaning that divalent ions should have a stronger interaction than monovalent ions. This agreed with the observation that the disulfonates showed larger changes in migration time in the presence of PDDAC than the monosulfonates. Similar effects were observed for aromatic carboxylic acids [54], with the divalent acids showing a greater interaction with PDDAC than the

Table 1.7: Selectivity in EKC using cationic polymers as additives

Polymer	Analytes	Optimisation Parameters	Electrolyte	Separation Conditions	Detection	Ref.
PDDAC	Isomers of naphthalene-sulfonates and naphthalene-disulfonates	[PDDAC]	Phosphate, pH 7.0	50μm x 71cm (46cm to detector), 25°c	Direct UV at 210nm	[53]
Polybrene and PDDAC	Aromatic carboxylic acids	[polymer]	Phosphate, pH 7.0	50μm x 75cm (50cm to detector), 25°c	NS	[54]
PDDPiCr, HDMCr, PDDPyCr and DEAEDCr	Inorganic anions	[polymer], pH	Chromate	75μm x 60cm (52cm to detector)	Indirect UV at 254nm	[55]
PDDPy and PDDPi	Inorganic and small organic anions	pH, %MeOH and %CAN	Chromate, benzoate	77μm x 60cm (53cm to detector)	Direct UV at 214 and Indirect UV at 254nm	[56]
Polybrene, PDDAC and PVPyBr	Inorganic anions and metal PAR chelates	[polymer]	Chromate, pH 8.8	50μm x 60cm (46cm to detector)	Direct UV at 490nm and Indirect UV at 254nm	[57]
PEI	Substituted phenols	[PEI], pH	MES and Tris	75μm x 75cm (60cm to detector)	Direct UV at 210nm	[58]
PEI	Mono- and oligophenols	[PEI]	MES, pH 7.0	100μm x 46.9cm (40.3cm to detector), 20-25°c	Direct UV at 214nm	[59]

Table 1.7: Selectivity in EKC using cationic polymers as additives (ctd)

Polymer	Analytes	Optimisation Parameters	Electrolyte	Separation Conditions	Detection	Ref.
PDDAC	Metal EDTA complexes	[PDDAC], [competing ion]	Acetate-sulfate, pH 7.0	50μm x 50cm (45cm to detector)	Direct UV at 200-220nm	[60]
PEI	Benzyl alcohols and phenols	%MeOH, %ACN	MES, pH 7.0	100μm x 47cm (40.3cm to detector), 26°c	Direct UV at 214nm	[61]
PDDAC	Inorganic and small organic anions	[PDDAC], pH, PDDAC molecular mass, [competing ion], %CAN	Borate	50μm x 40cm (32.5cm to detector)	Direct UV at 214nm	[62]
PDDAC	Inorganic and small organic anions	[PDDAC], type and concentration of competing ion	Tris, pH 8.05	50μm x 50cm (41.5cm to detector)	Direct UV at 214nm	[63]
PDDAC and PDDAOH	Metal complexes with HBED	[polymer], [competing ion], pH	Acetate-borate and sulfate-borate	50μm x 50cm (45.5cm to detector)	Direct UV at 242nm	[64]
PDDAC	Small neutral aromatics	[PDDAC]	Acetate, pH 5.2	50μm x 27 and 32.1cm (20 and 23.6cm to detector), 25°c	Direct UV at 205, 210 and 214nm	[65]
PDDAC, TMA, TEA and DMP	Small neutral aromatics	Comparison of PDDAC with monomeric units	Acetate, pH 5.2	50μm x 27 and 32.1cm (20 and 23.6cm to detector), 25°c	Direct UV at 214nm	[66]

Table 1.7: Selectivity in EKC using cationic polymers as additives (ctd)

Polymer	Analytes	Optimisation Parameters	Electrolyte	Separation Conditions	Detection	Ref.
PDDAC	Phenols	[PDDAC]	Acetate, pH 5.2	75μm x 45.6cm (37.1cm to detector), 25°c	Direct UV at 214nm	[67]
PDDAC	Olanzapine, carbamazepine and their main metabolites	[PDDAC]	Formate, pH 4.0	50μm x 42cm (22cm to detector)	Direct UV at 190nm	[68]
$PDDA^+$	Inorganic and small organic anions	[$PDDA^+$], type and concentration of competing ion	Tris, pH 7.7	50μm x 50cm (41.5cm to detector)	Indirect UV at 214 and 254nm	[69]
Polysiloxane polymers utilizing TACN complexed with Co^{3+}	Substituted benzenes	[polymer]	Tris	75μm x 29.7cm (20.4cm to detector)	Direct UV at 214nm	[70]

PDDAC – Poly(diallyldimethylammonium chloride); NS – Not stated; PDDPi – Poly(1,1-dimethylenepiperidinium); HDM – Hexadimethrine; PDDPy – Poly(1,1-dimethylenepyrrolidinium); DEAED – Diethylaminoethyl dextran; MeOH – Methanol; ACN – Acetonitrile; PVPyBr – Poly(N-ethyl-4-vinylpyridinium bromide); PAR – 4-(2-pyridylazo)resorcinolato; PEI – Polyethyleneimine; MES – 2-(N-morpholino)ethanesulfonic acid; Tris – Tris(hydroxymethyl)aminomethane; EDTA – Ethylenediaminetetraacetic acid; PDDAOH – Poly(diallydimethylammonium hydroxide); HBED – N,N'-bis(hydroxybenzyl)ethylenediamine-N,N'-diacetic acid; TMA – Tetramethylammonium; TEA – Tetraethylammonium; DMP – Dimthylpyrrolidinium; $PDDA^+$ - Poly(diallydimethylammonium); TACN – 1,4,7-triazacyclononane

monovalent acids. In this work PDDAC was also compared to another cationic polymer, polybrene, and it was found that although PDDAC showed a greater interaction with the acids, the selectivity offered by each additive was similar, most likely due to similar quaternary ammonium functionalities.

PDDAC and similar polymers have also been used in combination with indirect detection. Stathakis and Cassidy [55] have used PDDAC, polybrene and associated polymers for the separation of inorganic anions using chromate as the probe. Since most of the polymers are obtained as chloride salts, conversion to the associated chromate salt is required to minimise system peak problems. Selectivity changes for the analyte anions were observed for all the polymers tested, with the divalent anion sulfate showing the strongest interaction with all the polymers except diethylaminoethyl dextran chromate (DEAEDCr). This was attributed to steric effects associated with the bulkier polymeric cation and/or reduced charge density within the polymer.

The use of PDDAC as an IE additive for the separation of inorganic and small organic anions was comprehensibly investigated by Breadmore *et al.* [63] who examined the effects of polymer ion concentration as well as the effect of different competing ions for selectivity control. The strength of the competing ion was found to increase in the order of fluoride, acetate, chloride and sulfate, while the selectivity was found to be similar to that observed when using a strong-base anion-exchange resin. An equilibrium model based on IE theory was also developed that accurately described the observed separations. This model was then successfully used to optimise the separation of 16 anions in systems comprising of the four different competing ions used. The same authors extended this work to indirect detection [69] with the determination of 24 inorganic and small organic anions using probes of differing

elution strength (benzoate, chromate and phthalate). As in previous work the chloride salt of PDDAC had to be replaced with the corresponding probe anion so as to minimise system peaks that interfered with the analysis.

Although PDDAC has proven a popular additive to induce IE interaction with anions, it has also been used for the separation of a variety of neutral analytes. Gas and co-workers used PDDAC for the separation of small neutral analytes [66,67]. The exact separation mechanism in these examples is unclear, but it is likely to be due to some interaction between the polymer and heteroatoms contained on the analytes and not simply due to hydrophobic partitioning. This is supported by work using the cationic polymer polyethyleneimine (PEI) as an additive for the separation of a similar group of small neutral organics. It was found that selectivity was not dependent on the position of alkyl groups contained on the analytes and it was concluded for such separations that ion-dipole interactions seem to be the predominant mechanism of separation, thus separation depended on the number and position of the OH-groups contained on the analyte, not differing hydrophobicities.

1.8.2 Anionic Polymers

Anionic polymers have also proven to be popular as additives to EKC systems and have the advantage over cationic polymers due to the larger number of anionic functionalities such as carboxylate, sulfonate and sulfate groups whereas in the case of cations, generally only amine based functional groups are used. Work using anionic polymers to modify selectivity is summarised in Table 1.8.

To date most anionic polymers have been used for the separation of neutral organic analytes, thus many of these polymers incorporate alkyl chains of varying length.

Table 1.8: Selectivity in EKC using anionic polymers as additives

Polymer	Analytes	Optimisation Parameters	Electrolyte	Separation Conditions	Detection	Ref.
Alkylated PAA with carboxylate groups	Alkyl phenyl ketones and PAHs	Length of alkyl chains, %MeOH	Borate, pH 9.3	50μm x 48cm (33cm to detector)	Direct UV at 254nm	[71]
Partially hydrolyzed polyacrylamide	Neutral organics	NS	Phosphate, pH 7.0	100μm x 27cm (20cm to detector)	Direct UV at 214nm	[59]
Amphiphilic block copolymer of PAIE and PPIE	Phenols	[SDS], pH	Phosphate, pH 7.0, phthalate, pH 5.0 and borate, pH 9.0	50μm x 70cm (50cm to detector), 25°c	Direct UV at 230nm	[73]
Alkylated PAA with carboxylate groups	Alkyl phenyl ketones and PAHs	[polymer], length of alkyl chains, %MeOH	Borate, pH 9.3 and borate + ACN, pH 9.3	50μm x 48cm (33cm to detector)	Direct UV at 254nm	[72]
Poly(Na 11-AAU)	Alkyl phenyl ketones, benzene and naphthalene derivatives and PAHs	[polymer]	Phosphate-borate + ACN, pH 9.3	50μm x 65cm (50cm to detector)	Direct UV at 215 and 254nm	[74]
AGESS, AGENT, APDSS and PAGENT	Alkyl phenyl ketones and substituted benzene and naphthalene compounds	[polymer]	Borate, pH 9.2	50μm x 50cm (42cm to detector), 25°c	Direct UV at 214 and 254nm	[75]

Table 1.8: Selectivity in EKC using anionic polymers as additives (ctd)

Polymer	Analytes	Optimisation Parameters	Electrolyte	Separation Conditions	Detection	Ref.
PVS	Cationic amines	[PVS]	Citrate, pH 3.0	50μm x 55cm (46.8cm to detector)	Direct UV at 214nm	[76]
Amphiphilic copolymers of AMPS with pDHCHAt or ptOAm	Ketones, benzene derivatives and PAHs	Concentration and type of polymer	Borate, pH 9.2	50μm x 53.5cm (45cm to detector), 25°c	Direct UV at 214 and 254nm	[77]
Alkyl-modified anionic siloxane polymers	Alkyl phenyl ketones and PAHs	%ACN and %MeOH	Borate	50μm x 50cm (42cm to detector), 25°c	Direct UV at 215 and 244nm	[78]

PAA – Polyallylamine; PAH – Polycyclic aromatic hydrocarbon; MeOH – Methanol; NS – Not stated; PAIE – Poly[(N-acetylimino)ethylene]; PPIE – Poly[(N-pentanoylimino)ethylene]; SDS – Sodium dodecyl sulfate; Poly(Na 11-AAU) – 11-Acrylamidoundecanoate; Allyl glycidyl ether sulfite-modified siloxane; AGENT – Allylglycidyl ether N-methyl taurine-modified siloxane; APDSS – Alloxy propane diol sulfate modified siloxane; PAGENT – Pentane allyl glycidyl ether N-methyl taurine-modified siloxane; PVS – Polyvinylsulfonate; AMPS – 2-Acrylamido-2-methyl-1-propane sulfonic acid; pDHCHAt – Dihydrocholesteryl acrylate; ptOAm – tert-octyl acrylamide; ACN – Acetonitrile

Tanaka and co-workers have incorporated C_8- to C_{16}- alkyl chains into polyallylamine (PAA) based polymers [71,72]. These polymers have then been used for the separation of alkyl phenyl ketones and polycyclic aromatic hydrocarbons with the longer alkyl chain polymer interacting more strongly with the analytes. Methanol (MeOH) and acetonitrile (ACN) were found to suppress the interaction between the polymer and the analytes. The same approach, but based on alkyl- modified siloxane polymers, has been reported by Peterson and Palmer who separated a similar group of analytes [75,78]. It was found that both the PAA and siloxane polymers gave comparable results indicating that the interaction was between the analyte and the alkyl chain and not the polymer backbone.

Since anionic polymers have been mainly applied to the separation of neutral analytes the presence of the charge is mainly used to increase the solubility of the polymer as well as impart some mobility to the p-SP. Unlike cationic polymers, the potential for introducing IE interactions between anionic polymers and cationic analytes has not been comprehensibly investigated. One report into the use of an anionic polymer, polyvinylsulfonate (PVS), for the separation of cations was by Bendahl *et al.* [76]. Here a relatively small amount of PVS was added to the electrolyte and this induced small mobility changes for the cationic analytes, which was attributed to IE interactions. Although the changes were relatively small, only 0-0.1% PVS was tested and it is likely that larger changes would be observed at higher concentration of PVS.

1.8.3 Neutral Polymers

Neutral polymers have also been successfully used for the separation of a variety of different analytes and this is summarised in Table 1.9.

Table 1.9: Selectivity in EKC using neutral polymers as additives

Polymer	Analytes	Optimisation Parameters	Electrolyte	Separation Conditions	Detection	Ref.
PVP	Synthetic cationic dyes	[PVP]	Tris-citrate, pH 3.0	75μm x 26.9cm (20.2cm to detector), 25°c	Direct UV at 214nm	[80]
PVP, PEG and PAA	Diastereomeric derivatives of amino acids	[polymer]	Phosphate, pH 5.8	100μm x 56cm (39cm to detector), 24-25°c	Direct UV at 233nm	[79]
PVP	Central nervous systems drugs	[PVP]	Phosphate, pH 2.5	50μm x 43.2cm (23.0cm to detector)	Direct UV at 206 and 245nm	[81]
PEG	Alkylpyridines	%PEG and nature of co-ion	Phosphate, pH 2.5	75μm x 75cm (45cm to detector)	Direct UV at 260nm	[82]
PVP	Antipsychotic drugs (clozapine and loxapine)	%PVP	Phosphate, pH 2.5	50μm x 45cm (25.2cm to detector)	Direct UV at 206 and 254nm	[83]
HPC	Dendro[60]fullerene	%HPC, pH, and buffer concentration	Phosphate	50μm x 47cm (40cm to detector), 30°c	Direct UV at 254nm	[84]
Pluronic F127	Proteins and peptides	%Pluronic F127	Phosphate, pH 2.5	75μm x 27cm (20cm to detector), 20°c	Direct UV at 214nm	[85]

PVP – Polyvinylpyrrolidone; PEG – Poly(ethylene glycol); PAA – Poly(acrylamide); HPC – Hydroxypropylcellulose; Pluronic F127 – (polyethylene oxide)$_{106}$(polypropylene oxide)$_{70}$(polyethylene oxide)$_{106}$

The most commonly used neutral polymers have been poly(vinylpyrrolidone) (PVP) and poly(ethylene glycol). Schutzner *et al.* [79] have used these two polymers as well as poly(acrylamide) for the separation of diastereomeric derivatives of amino acids. It was found that although addition of the polymers has a significant effect on the viscosity of the electrolyte, the variation of analyte mobilities did not reflect these changes. Hence, specific selectivity effects were the result of analyte-polymer interactions. It was also found that selectivities differed for the various polymers used, implying that specific analyte-polymer interactions based on the analyte or polymer composition and structure are important for the separation.

1.9 Cyclodextrins

Cyclodextrins (CDs) are oligosaccharides made up of several D(+)-glucopyranose units. Generally those with 6, 7 and 8 glucopyranose units, termed α-, β- and γ-cyclodextrins, are the most commonly used. CDs can be thought of as a truncated cone comprising a hydrophobic central cavity with hydroxyl groups situated on the rim which aid in increasing its solubility in aqueous solutions. Analytes are separated due to partitioning into the hydrophobic core of the cyclodextrin with secondary interactions also being possible between the analyte and the hydroxyl groups. The advantages of cyclodextrins are their relatively high solubility, precisely defined structure and the ability to modify functional groups to introduce a charge, modify the selectivity or to increase solubility.

The major use of cyclodextrins has been for enantiomeric separations although they have been successfully applied to non-chiral separations as well.

1.9.1 Neutral Cyclodextrins

Neutral cyclodextrins have been used for a variety of separations and their use as selectivity modifiers is summarised in Table 1.10.

Neutral cyclodextrins possess no electrophoretic mobility of their own and thus induce selectivity changes by reducing analyte mobility due to complexation. Complexation of analytes into neutral cyclodextrins is driven by hydrophobic partitioning into the relatively hydrophobic core of the cyclodextrin. Analytes that "fit best" into the cavity will show the greatest change in mobility on addition of the cyclodextrin. As well as hydrophobic partitioning, secondary interactions such as hydrogen bonding also play a major role, often allowing for the separation of structurally similar molecules. Quang and Khaledi have proposed a more formal "three point" interaction model for the interaction between pseudoephedrine and ephedrine with β-CD [103]. This model involves inclusion of the hydrophobic aromatic group into the cavity of the cyclodextrin as well as hydrogen bond interactions between the hydroxyl and amino groups with the secondary C-2 and C-3 hydroxyl groups at the wider opening of the β-CD.

Selectivity control in cyclodextrin systems can be achieved by either varying the cyclodextrin size (α-, β- or γ-) or substituents on the rim of the cyclodextrin. Lindner *et al.* [88] showed the advantages of various CDs for the separation of amino acids derivatized with several derivatizing agents. It was found that voluminous fluorescent derivatives showed best resolution with the larger γ-CDs whereas the smaller derivatives could be efficiently separated with β-CDs. Hydrogen bonding was also found to play an important role agreeing with the three-point interaction model proposed by Quang and Khaledi [103].

Table 1.10: Selectivity in EKC using neutral cyclodextrins as additives

Cyclodextrin	Chiral Separation	Analytes	Optimisation Parameters	Electrolyte	Separation Conditions	Detection	Ref.
HP-β-CD	Yes	Propranolol	pH, [HP-β-CD], voltage, temperature	Aminocaproic acid, MES, AMPSO and TAPSO adjusted to pH with with methanesulfonic acid and TBAH + 0.4% hydrophilic polymeric additive	25μm x 27cm (20cm to detector)	Direct UV at 230nm	[86]
β-CD	No	Food additive dyestuffs	[β-CD]	Borate, pH 7.5	50μm x 77cm (60cm to the detector)	Direct UV at 245nm	[87]
α-CD, β-CD, γ-CD, HP-β-CD, Me-β-CD, HP-γ-CD and Me-γ-CD	Yes	Amino acids derivatized with various labeling agents	[CD], pH, temperature	Phosphate, borate and citrate	50μm x 70cm (50cm to detector)	Direct UV at 214nm with a bubble cell (3x extended path length	[88]
β-CD, γ-CD, DM-β-CD TM-β-CD, HP-β-CD and SB-β-CD	No	Opium alkaloids	[CD]	6-ACA, pH 4.0	50μm x 55cm, 30°c	Direct UV at 214nm	[89]
β-CD	Yes	Tioconazole	[β-CD], %ACN, %MeOH	Phosphate-TEA, pH 3.0	50μm x 57cm (50cm to detector), 25°c	Direct UV at 230nm	[90]
β-CD	Yes	Dansyl-amino acids	[β-CD]	Phosphate-borate, pH 9.0 and NMF electrolyte for NACE	50μm x 58.5cm (50cm to detector), 25°c	Direct UV at 254nm	[91]

Table 1.10: Selectivity in EKC using neutral cyclodextrins as additives (ctd)

Cyclodextrin	Chiral Separation	Analytes	Optimisation Parameters	Electrolyte	Separation Conditions	Detection	Ref.
HP-β-CD	No	Benzoic acid isomers	[HP-β-CD]	Phosphate, pH 4.0	75μm x 35cm (30cm to detector)	Direct UV at 225nm	[92]
DM-β-CD	No	Morphine in pharmaceuticals	NS	6-ACA, pH 4.0	50μm x 64cm (55.5cm to detector), 30°c	Direct UV at 214nm	[93]
α-CD, β-CD and γ-CD	Yes	Amphetamine related substances	pH	Phosphate	50μm x 45cm (36.5cm to detector)	Direct UV at 200nm	[94]
α-CD, β-CD and γ-CD	No	Small inorganic and organic anions	[CD]	Chromate, pH 8.0 and phthalate, pH 6.0	75μm x 60cm (52cm to detector)	Indirect UV at 254nm	[95]
α-CD	Yes	Aromatic amino acids	[α-CD], voltage, pH	Phosphate	75μm x 57cm (50cm to detector), 25°c	Direct UV at 214nm	[96]
α-CD	No	Inorganic anions	[α-CD]	NS	300μm x 23cm (13cm to detector)	On-column contactless conductivity detector	[97]
α-CD	Yes	Aromatic amino acids	[α-CD], pH, electrolyte concentration	Phosphate	75μm x 42.5cm (35.5cm to detector), 25°c	Direct UV at 214nm	[98]

Table 1.10: Selectivity in EKC using neutral cyclodextrins as additives (ctd)

Cyclodextrin	Chiral Separation	Analytes	Optimisation Parameters	Electrolyte	Separation Conditions	Detection	Ref.
β-CD, γ-CD, HP-β-CD HP-γ-CD and DM-β-CD	No	Morphine and its oxidation products	[CD], pH, voltage, temperature	Tris-phosphate	50μm x 48.5 and 64.5cm (40 and 50cm to detector), 25°c	Direct UV at 210nm with a bubble cell (3x extended path length	[99]
α-CD and β-CD	No	Cationic surfactants	[CD], %MeOH, %Can, pH	Phosphate	75μm x 57.5cm (44cm to detector)	Direct UV at 210nm	[100]
HP-β-CD	No	Deoxyribonucleotides	[HP-β-CD]	Borate, pH 9.0	50μm x 37cm (30cm to detector), 25°c	Direct UV at 254nm	[101]
β-CD, M-β-CD, DM-β-CD, TM-β-CD, HP-β-CD and HP-γ-CD	No	Naphthalene sulfonic acids	[CD], external pressure	Borate, pH 9.0	50μm x 75cm (60cm to detector), 35°c	Direct UV at 230nm	[102]

HP – Hydroxypropyl; MES – 2-(N-morpholino)ethanesulfonic acid, AMPSO – 3-[(1,1-dimethyl-2-hydroxyethyl)amino]-2-hydroxypropanesulfonic acid; TAPSO – 3-[N-tris(hydroxymethyl)methylamino]-2-hydroxypropanesulfonic acid; TBAH – Tetrabutylammonium hydroxide; Me – 2,3,6-methyl; DM – Heptakis(2,6-di-O-methyl; TM – Heptakis(2,3,6-tri-O-methyl); SB – Sulphobutyl ether-IV; 6-ACA – 6-Amino caproic acid; TEA – Triethanolamine, NACE – Non-aqueous capillary electrophoresis; NMF – N-methylformamide; NS – Not stated; MeOH – Methanol; ACN - Acetonitrile

Inorganic anions have also been successfully separated using neutral cyclodextrins as selectivity modifiers. Work by Stathakis and Cassidy [95] showed that the selectivity for inorganic anions was dependent on the cyclodextrin type, concentration and on the electrolyte co-ions used. For the inorganic anions investigated, α-CD was found to give the largest selectivity changes while the larger β- and γ-CDs showed little interaction with the anions. The more polarizable anions, iodide, perchlorate and thiocyanate were also found to interact more strongly than the other anions investigated.

1.9.2 Anionic Cyclodextrins

Charged cyclodextrins have been used successfully for a variety of different analytes and have the advantage that they can be more soluble and, due to their inherent mobility, can lead to larger selectivity changes compared to neutral cyclodextrins. To date, anionic cyclodextrins have been used more frequently than cationic cyclodextrins and their use as selectivity modifiers is summarised in Table 1.11.

As with neutral cyclodextrins, partitioning of analytes into the hydrophobic core of the cyclodextrin is the major interaction leading to separation. However, with anionic cyclodextrins a further electrostatic interaction is possible between cationic analytes and the anionic functionalities contained on the cyclodextrins. Hellriegel *et al.* [104] used ultraviolet (UV) spectrophotometry, mass spectrometry (MS) and nuclear magnetic resonance (NMR) experiments to elucidate the exact chiral separation mechanism of ephedrines in the presence of neutral and anionic cyclodextrins. They found that in the case of neutral cyclodextrins 1:1 inclusion complexes were formed by inclusion of the phenyl ring (agreeing with the three point interaction mechanism proposed by Quang and Khaledi [103]). However, in the case of anionic

Table 1.11: Selectivity in EKC using anionic cyclodextrins as additives

Cyclodextrin	Chiral Separation	Analytes	Optimisation Parameters	Electrolyte	Separation Conditions	Detection	Ref.
S-β-CD	Yes	Anesthetics, antiarrhythmics, antidepressants, anticonvulsants, antihistamines, antihypertensives, antimalarials, relaxants and bronchodilators	NS	Phosphate, pH 3.8	75μm x 60cm (52.4cm to detector)	Direct UV at 214nm	[105]
CM-β-CD of differing degrees of substitution	Yes	Oxprenolol, AMEBD and ephedrine	[CD], pH, degree of substitution	Phosphate, pH 2.45, citrate, pH 3.50, acetate, pH 5.45 and Tris-borate, pH 8.20	50μm x 35 and 72cm (13 and 47cm to detector), 26°c	Direct UV at 220nm	[106]
S-β-CD	Yes	Trimipramine	[S-β-CD]	Tris-citrate, pH* 5.1	50μm x 42cm (31cm to detector), 25°c	Direct UV at 254nm	[107]
H6S-β-CD	Yes	Noncharged, acidic, basic and zwitterionic analytes	[H6S-β-CD]	Phosphate, pH 2.5, ethanolamine, pH 9.5	25μm x 45 cm (39cm to detector), 20°c	Direct UV at 214nm	[108]
S-β-CD and SBE-γ-CD	Yes	Labetol and Propranolol	[CD], pH	Phosphate and borate	50μm x 47cm (40cm to detector), 30°c	Direct UV at 200nm	[109]

Table 1.11: Selectivity in EKC using anionic cyclodextrins as additives (ctd)

Cyclodextrin	Chiral Separation	Analytes	Optimisation Parameters	Electrolyte	Separation Conditions	Detection	Ref.
S-β-CD	Yes	Terbutaline	[S-β-CD], %ACN, %MeOH	Phosphate, pH 3.0	25μm x 24cm (19.6cm to detector), 20°c	Direct UV at 211nm	[110]
HS-α-CD, HS-β-CD, HS-γ-CD and S-β-CD	Yes	Aspartyl di- and tripeptides	CD size	Phosphate-TEA, pH 2.5	50μm x 57cm (50cm to detector), 25°c	Direct UV at 200nm	[111]
SBE(IV)-β-CD, SBE(VII)-β-CD, SBE(XII)-β-CD, SBE(IV)-γ-CD, SBE(VII)-γ-CD, SU(XI)-α-CD, SU(VII)-β-CD, SU(XII)-β-CD, and SU(XIII)-γ-CD	Yes	Phenethylamines and achiral neutral impurities in illicit methamphetamine	Degree of substitution	Phosphate, pH 8.5 + 10% MeOH	50μm x 57cm (50cm to detector), 30°c	Direct UV at 200nm	[112]
HDAS-β-CD, HDMS-β-CD, HS-β-CD and S-β-CD	Yes	Pharmaceutical compounds	[CD], pH, concentration and type of organic modifier, temperature, buffer type and concentration, voltage	Phosphate, pH 2.5 and Phosphate-TEA, pH 2.5	75μm x 63cm (56 cm to detector)	Direct UV at 200nm	[113]

Table 1.11: Selectivity in EKC using anionic cyclodextrins as additives (ctd)

Cyclodextrin	Chiral Separation	Analytes	Optimisation Parameters	Electrolyte	Separation Conditions	Detection	Ref.
HAD-β-CD and HDAS-β-CD	Yes	Ephedrine derivatives	NS	Phosphate, pH 3.0	50μm x 60cm (50cm to detector), 25°c	Direct UV at 194nm	[104]
CM-β-CD	Yes	β-Adrenolytics	[CM-β-CD]	Tris-phosphate, pH 2.18 and 2.60, Tris-acetate, pH 4.70, Triethanolamine-acetate, pH 5.50	50μm x 48.5cm (40cm to detector), 25°c	Direct UV at 215nm	[114]
S-β-CD	Yes	Epoxides	[S-β-CD], %MeOH	Phosphate-triethanolamine, pH 4.0	75μm x 37cm (30cm to detector), 15°c	Direct UV at 214nm	[115]
CM-β-CD and CM-γ-CD	Yes	Pharmaceutical compounds containing amine groups	pH, electrolyte type and concentration, temperature	Phosphate and borate	75μm x 60cm (50cm to detector)	Direct UV at 200nm	[116]
S-β-CD	No	Metal ions	[S-βCD]	Pyridine + formic acid, pH 4.1	75μm x 67cm (59.5cm to detector), 25°c	Indirect UV at 254nm	[117]
SBE-β-CD	Yes	Reboxetine	[SBE-β-CD], pH, electrolyte concentration, temperature, %MeOH, %ACN	Phosphate	50μm x 48.5cm (40cm to detector), 25°c	Direct UV at 206nm	[118]

Table 1.11: Selectivity in EKC using anionic cyclodextrins as additives (ctd)

Cyclodextrin	Chiral Separation	Analytes	Optimisation Parameters	Electrolyte	Separation Conditions	Detection	Ref.
SU(XIII)-γ-CD	Yes	Amphetamine type stimulants	[SU(XIII)-γ-CD]	Phosphate, pH 2.6 and 7.0	50μm x 32.5cm (24cm to detector), 30°c	Direct UV at 195nm	[119]

S – Sulfated; NS – Not stated; AMEBD – Aminomethyl-benzodioxane derivative; pH* - Apparent pH in organic solvent; H6S – Hepta-6-sulfato; SBE - Sulfobutylether; ACN – Acetonitrile; MeOH – Methanol; HS – Highly sulfated; TEA – Triethylamine; SBE(IV) – Sulfobutyl(IV)-ether; SBE(VII) – Sulfobutyl(VII)-ether; SBE(XII) – Sulfobutyl(XII)-ether; SU(XI) – Sulfated(XI); SU(VII) – Sulfated(VII); SU(XII) – Sulfated(XII); SU(XIII) – Sulfated(XIII); HDAS – Heptakis(2,3-diacetyl-6-sulfato); HDMS – Heptakis(2,3-dimethyl-6-sulfato); HS – Heptakis-6-sulfato; HAD – Heptakis(2,3-*O*-diacetyl)

cyclodextrins a different orientation was adopted which was likely to stabilise electrostatic interactions between cationic groups on the analyte and the anionic functionalities on the cyclodextrin. This could lead to different selectivities when using anionic cyclodextrins and also introduced the possibility of achieving an IE type interaction between analytes and charged cyclodextrins.

An IE interaction between anionic cyclodextrins and metal cations has been demonstrated by Muzikar *et al.* [117]. They found that divalent cations interacted far more strongly with the sulfated-β-CD than monovalent cations and likened this to the effect observed on a sulfonated cation exchanger. It was also noted that no interaction between the cations and neutral cyclodextrins was observed and they concluded that it was unlikely that the cations were complexed into the cyclodextrin cavity but rather were associated with the anionic groups on the surface of the cyclodextrin.

1.9.3 Cationic Cyclodextrins

Although the use of cationic cyclodextrins has not been as common as anionic cyclodextrins, several have been synthesized and used successfully for the separation of various analytes and are summarised in Table 1.12.

Bunke and Jira [120] have shown that cationic cyclodextrins can be used for the separation of acidic and basic aromatic organic compounds. The separation mechanism was generally attributed to partitioning of the phenyl group into the cyclodextrin cavity as well as hydrogen bonding. Electrostatic interactions appear to play a much smaller role with cationic cyclodextrins than with anionic cyclodextrins, however, the reasons for this are unclear and may be more due to the choice of analytes rather than a lack of IE interaction.

Table 1.12: Selectivity in EKC using cationic cyclodextrins as additives

Cyclodextrin	Chiral Separation	Analytes	Optimisation Parameters	Electrolyte	Separation Conditions	Detection	Ref.
HTAP-β-CD	Yes	Acidic and basic organics	[CD], pH	Acetate and acetate-phosphate	50μm x 37cm (30cm to detector), 25°c	Direct UV at 214nm	[120]
QA-β-CD	Yes	Anti-inflammatory drugs	[CD], pH*, type of organic solvent used as the electrolyte	Tris-acetate in formamide, *N*-methylformamide, MeOH and dimethylsulfoxide, pH* 7.5	50μm x 42cm (31cm to detector), 30°c	Direct UV at 254nm	[121]
PMMA-β-CD	Yes	Pyrethroic acids	[CD], pH	Borate-acetate-phosphate	50μm x 58.5cm (50cm to detector), 25°c	Direct UV at 202 and 220nm	[122]
TMA-β-CD chloride	Yes	Acetylphenylalanine	[CD]	Phosphate, pH 6.8	50μm x 50cm (37.8cm to detector), 25°c	Direct UV at 216nm	[123]
HHEAD-β-CD	Yes	Anionic and neutral organics	[CD], pH	Phosphate	50and 75μm x 64.5cm (56cm to detector),14°c	Direct UV at 214nm	[124]

TMA – 6-Trimethylammonio-6-deoxy; HHEAD – Heptakis(6-hydroxyethylamino-6-deoxy); PMMA – Permethylmonoamino; QA – Quaternary ammonium; pH* - Apparent pH in organic solvents; MeOH – Methanol; HTAP – 2-Hydroxy-3-trimethylammoniopropyl

1.10 Mixed Systems

Selectivity in EKC separations can be modified by the addition of more than one additive, thereby utilising several different separation mechanisms. The advantage of EKC systems is that since the additives are simply dissolved in the electrolyte, several additives can be easily combined to yield a system with a unique selectivity. Various combinations of additives have been successfully used to modify the selectivity of EKC systems.

1.10.1 Mixed Cyclodextrin Systems

The presence of different substituents on cyclodextrins can vary the observed selectivity offered for different analytes. Systems comprising more than one cyclodextrin have been successfully utilised to improve the separation of various analytes over that obtained using single cyclodextrin systems and these are summarised in Table 1.13.

Dual cyclodextrin systems generally combine a neutral and charged cyclodextrin and are often used for the separation of neutral analytes. The charged cyclodextrin can either be used simply as a carrier or it can aid in the separation by having different formation constants with the analytes. In such systems the observed separation is generally a result of the combined effects from both cyclodextrins. Work by Culha *et al.* [125] has shown that by using a simple model and derived distribution coefficients it is possible to explain observed selectivities and to predict selectivities for various binary mixtures of neutral cyclodextrins with carboxymethyl-β-CD (CM-β-CD) for the separation of naphthalene derivatives.

Table 1.13: Selectivity in EKC using mixed cyclodextrin systems

Cyclodextrins	Chiral Separation	Analytes	Optimisation Parameters	Electrolyte	Separation Conditions	Detection	Ref.
CM-β-CD, β-CD, HP-β-CD and γ-CD	No	PAHs	Different combination and concentration of the CDs	Phosphate-borate, pH 6.0 and 9.0 + 20-30% ACN	50μm x 50cm (40cm to detector),	LIF detection using a He-Cd laser	[127]
α-CD + S-β-CD	Yes	Monoterpenes	Different combination and concentrations of the CDs	Phosphate, pH 3.3	75μm x 57.6cm (50cm to detector), 21°c	Direct UV at 214nm	[128]
HP-β-CD, SB-β-CD, M-β-CD, α-CD and γ-CD	No	PAHs	Different combination and concentrations of the CDs	Borate, pH 9.2	50μm x 57cm (50cm to detector)	Direct UV at 254nm	[129]
α-CD, HP-α-CD, β-CD, DM-β-CD, TM-β-CD, HP-β-CD, Glu-β-CD, Mal-β-CD, HP-γ-CD and γ-CD	Yes	Various drug compounds	Different combination and concentrations of the CDs	Phosphate-TEA, pH 3.0	75μm and 40cm to detector, 20°c	Direct UV at 210nm	[130]
β-CD, HP-β-CD, HDM-β-CD and HTM-β-CD	Yes	Methamphetamine and related compounds	Different combination and concentrations of the CDs	Tris-phosphate, pH 2.5	75μm x 80.5cm (72cm to detector), 25°c	Direct UV at 195nm	[131]

Table 1.13: Selectivity in EKC using mixed cyclodextrin systems (ctd)

Cyclodextrins	Chiral Separation	Analytes	Optimisation Parameters	Electrolyte	Separation Conditions	Detection	Ref.
β-CD, CM-β-CD, γ-CD and HDMS-β-CD	No	Naphthalene compounds	Different combination and concentrations of the CDs	Phosphate, pH 5.0 and 7.5	50μm x 48cm (39.5cm to detector), 24°c	Direct UV 205-254nm	[125]
HS-β-CD and HDM-β-CD	Yes	Profens	Different concentrations of the CDs	Phosphate-triethanolamine, pH 2.5	50μm x 45cm (40.3cm to detector), 25°c	Direct UV at 214nm	[126]
HTM-β-CD, HS-β-CD and HDMS-β-CD	Yes	Propranolol and ibuprofen	Different concentrations of the CDs	Phosphate, pH 2.5	50μm x 48.5cm (40cm to detector), 25°c	Direct UV at 214nm	[132]

CM – Carboxymethyl; HP – Hydroxypropyl; PAH – Polycyclic aromatic hydrocarbon; ACN – Acetonitrile; LIF – Laser induced fluorescence, S – Sulfated; SB – Sulfobutyloxy; M – Methyl; DM – Dimethyl; TM – Trimethyl; Glu – 6-*O*-α-D-glucosyl; Mal – 6-*O*-α-D-maltosyl; TEA – Triethylamine; HDM – Heptakis(2,6-di-*O*-methyl); HTM – Heptakis(2,3,6-tri-*O*-methyl; HDMS – Heptakis(2,3-dimethyl-6-sulfato); HS – Heptakis-6-sulfato

The use of mixtures of neutral and charged cyclodextrins is also the subject of a recent review by Fillet and Crommen [126].

1.10.2 Cyclodextrins and Surfactants

Increasing the number of p-SPs present in the electrolyte potentially increases the selectivity control offered since analytes can now partition into multiple phases. A common approach to this is the combination of cyclodextrins with surfactants, termed CD-modified MEKC (CD-MEKC). Analytes in these systems can now partition into the hydrophobic phase of the micelles or complex with the cyclodextrin. IP interactions with surfactant monomers as well as IE interactions with charged cyclodextrins are also possible, adding to the potential selectivity control of such systems. Examples of CD-MEKC are shown in Table 1.14.

Luong and Guo have shown the possibilities for selectivity control of the separation of polycyclic aromatic hydrocarbons (PAHs) using a combination of sodium dioctyl sulfosuccinate (DOSS) and the anionic sulfobutylether-β-CD (SB-β-CD). It was found that although the DOSS did not form micelles at the electrolyte conditions used (20-40% acetonitrile (ACN)), it did lead to separation of 14 out of the 16 PAHs investigated. The separation mechanism was attributed to hydrophobic interactions between the PAHs and the hydrophobic chains of the surfactant, rather than to partitioning into a micellar phase. Compared to DOSS, SB-β-CD was found to give a different selectivity for the PAHs due to a different interaction mechanism. Using a combined system it was demonstrated that the observed selectivity could be varied between that of the pure DOSS system and that of the pure SB-β-CD system,

Table 1.14: Selectivity in EKC using mixed cyclodextrin and surfactant systems

Cyclodextrins	Surfactants	Analytes	Optimisation Parameters	Electrolyte	Separation Conditions	Detection	Ref.
γ-CD	SDS	Aniline derivatives	[Additives], pH	Phosphate-borate	50μm x 72cm (50cm to detector), 30°c	Direct UV at 210nm	[133]
γ-CD	Sodium cholate	Phenols, anilines and PAHs	[Additives]	Borate, pH 8.35 + 10% acetone, THF or MeOH	50μm x 27cm (20cm to the detector)	Direct UV at 214nm	[134]
β-CD and γ-CD	SDS	Chiral polychlorinated biphenyls	[Additives]	Ches-urea, pH 10	50μm x 65cm (50.5cm to detector), 45°c	Direct UV at 235nm	[135]
α-CD, β-CD, γ-CD, HP-β-CD, DM-β-CD and TM-β-CD	SDS	Neutral pesticides	[CDs], %ACN, %MeOH	Borate + 100mM SDS, pH 9.0	75μm x 57cm (50cm to detector), 30°c	Direct UV at 200nm	[136]
β-CD and γ-CD	SDS	PAHs	[CDs]	Borate-urea + 100mM SDS, pH 9.0	50μm x 65cm (50.5cm to detector), 35°c	Direct UV at 230nm	[137]
SB-β-CD and HP-β-CD	DOSS	PAHs	[Additives], %ACN	Borate, pH 9.0	50μm x 47cm (40cm to detector)	Direct UV at 254nm	[138]
HP-β-CD and S-β-CD	SDS	Nitroaromatic explosive isomers	[Additives], %ACN	Borate, pH 9.0	50μm x 47cm (40cm to detector)	Direct UV at 214nm	[139]

Table 1.14: Selectivity in EKC using mixed cyclodextrin and surfactant systems (ctd)

Cyclodextrins	Surfactants	Analytes	Optimisation Parameters	Electrolyte	Separation Conditions	Detection	Ref.
α-CD, β-CD and γ-CD	SDS	Amino acids derivatized with FITC	[Additives], %ACN, %2-propanol	Borate, pH 9.5	50μm x 74.4 and 99cm (55.7 and 85cm to detector), RT	LIF detection with excitation at 488nm and emission at 520nm	[140]
DM-β-CD, TM-β-CD, HP-β-CD, HP-γ-CD, β-CD and γ-CD	SDS	Monohydroxy-benzo[a]pyrene positional isomers	[Additives], pH, temperature	Phosphate-borate, pH 8.5	75μm x 56cm, 20°c	Direct UV at 280nm with a bubble cell (3x extended path length)	[141]
γ-CD	SDS	Amino acids derivatized with CBQCA	[NaCl] in the electrolyte	Borate, pH 9.5	50μm x 67cm (60cm to detector), 25°c	LIF detection with excitation at 488nm and emission at 520nm	[142]
β-CD	SDS	Amino acids derivatized with DTDP	[Additives], pH, %ACN, %2-propanol	Borate	50μm x 65cm (45cm to detector), 25°c	Direct UV at 282nm	[143]
α-CD and β-CD	Sodium cholate and sodium taurocholate	Anthraquinone derivatives and a distyrene derivative in rhubarb	[Additives], pH	Borax, pH 11	50μm (45cm to detector), 25°c	Direct UV at 254nm	[144]

SDS – Sodium dodecyl sulfate; PAH – Polycyclic aromatic hydrocarbon; THF – Tetrahydrofuran; MeOH – Methanol; HP – Hydroxypropyl; DM – Dimethyl; TM – Trimethyl; ACN – Acetonitrile; SB – Sulfobutylether; DOSS – Sodium dioctyl sulfosuccinate; S – Sulfated; SUC – Succinyl; FITC – Fluoresceine isothiocyanate isomer I; RT – Room temperature; LIF – Laser induced fluorescence; CBQCA – 3-(4-carboxybenzoyl)-quinoline-2-carboxaldehyde; DTDP – 3-(4,6-dichloro-1,3,5-triazinylamino)-7-dimethylamino-2-methylphenazine

although it was found that comparable amounts of both DOSS and SB-β-CD were needed to give a selectivity substantially different from the individual systems.

A complicating factor when using combined cyclodextrin-micellar systems is the potential interaction between the cyclodextrin and surfactant monomers. This interaction has been examined by Lin *et al.* [145] using SDS and β-CD. They found that analyte-cyclodextrin interactions could be greatly diminished or even lost when SDS was included in the electrolyte. Addition of a cyclodextrin can also increase the critical micellar concentration (CMC) of surfactants due to incorporation into the cyclodextrin cavity. For SDS-(β-CD) interactions a 1:1 stoichiometry was found to predominate with the 2:1 complex probably present at less than 10%. The interaction between multiple p-SP is thus an important consideration when trying to increase selectivity control by combining additives.

1.10.3 Other Mixed Systems

As well as CD-MEKC, several other mixed p-SP EKC systems have been used for the separation of a variety of different analytes and these are summarised in Table 1.15.

Tananka *et al.* [146] used a mixture of C_{10}- and C_{16}- modified polyallylamine (PAA) to vary the migration times of several organic analytes. It was found that the mixed system gave a selectivity that differed from that obtained when either the C_{10}-modified PAA or the C_{16}-modified PAA were used alone. Although this work introduced two p-SPs, both interacted with the analytes via the same mechanism, namely hydrophobic partitioning, so independent control of the selectivity offered by each SP was difficult to achieve.

The use of multiple SPs that exhibit different interactions with the analytes of interest has the potential to increase the selectivity control over a system since individual

Table 1.15: Selectivity in EKC using other mixed systems

Additive 1	Additive 2	Analytes	Optimisation Parameters	Electrolyte	Separation Conditions	Detection	Ref.
α-CD, β-CD, γ-CD and HDM-β-CD	MHEC, HPMC and HEC	Isomeric organic compounds	[Additives]	Tris-tricine, pH 8.5 and Tris-acetate, pH 3.5	49μm x 50-65cm	Direct UV at 254nm	[147]
BM-β-CD, TM-β-CD, HP-β-CD, HE-β-CD, γ-CD and α-CD	18-Crown-6	Non-polar primary amines	[Additives]	Phosphate, pH 2.0	50μm x 67cm (60cm to detector), 23°c	Direct UV at 214nm	[148]
HP-β-CD, M-β-CD, β-CD and γ-CD	Alkylsuflonates, alkanoic acids and quinine (IP reagents)	Acidic and basic organics	[Additives], alkyl chain length on the alkylsulfonic acids, pH	Phosphate, pH 2.0 and acetate, pH 5.0	50 and 75μm x 37, 44 and 57cm (30, 37 and 50cm to detector), 25°c	Direct UV at 214nm	[149]
Sulfonated-Brij-30	Ethanesulfonic acid	Acidic, basic and neutral organics including PAHs	[Additives], %ACN, %2-propanol	Phosphate, pH 2.40	50μm x 45cm (37.5cm to detector), 25°c	Direct UV at 214 and 254nm	[150]
SDS	TMAB and TBAB	Aniline and substituted anilines	[Additives]	Borate, pH 10	50μm x 67cm (60cm to detector), 25°c	Direct UV at 214nm	[151]
Alkylated PAA with carboxylate groups	Alkylated PAA with carboxylate groups	Alkyl phenyl ketones and PAHs	[Additives], alkyl chain length on PAA, %MeOH, %ACN	Borate, pH 9.3	50μm x 48cm (33cm to detector), RT	Direct UV at 254nm	[146]

Table 1.15: Selectivity in EKC using other mixed systems (ctd)

Additive 1	Additive 2	Analytes	Optimisation Parameters	Electrolyte	Separation Conditions	Detection	Ref.
β-CD and S-β-CD	TBAB	Sulfonium ions	[Additives], %MeOH	Phosphate, pH 2.5	50μm x 50cm (45.4cm to detector), 20°c	Direct UV at 220nm	[152]
α-CD, β-CD, γ-CD, HDM-β-CD and HTM-β-CD	18-Crown-6	Chiral organic compounds containing primary amine functionalities	[Additives], pH, [K^+]	Phosphate and tris-citrate	75μm x 57cm (50cm to detector), 25°c	Direct UV at 254nm	[153]
DM-β-CD and γ-CD	18-Crown-6	THNA and MPPA	[Additives]	Phosphate, pH 2.0 and tris-citrate, pH 2.0	50μm x 67cm (60cm to detector), 23°c	Direct UV at 214nm	[154]
SDS	TMAB, TEAB, TPAB, TBAB and TPAC	Mesalazine or 5-aminosalicylic acid and its major impurities	[Additives], temperature, voltage, pH	CAPSO	50μm x 48.5cm (40cm to detector), 30°c	Direct UV at 230, 254 and 300nm	[155]
HP-γ-CD	Poly-D-SUV	Polychlorinated biphenyls	[Additives], %MeOH, voltage, [CHES], temperature	CHES, pH 10	50μm x 78cm (71.4cm to detector), 45°c	Direct UV at 200, 214, 254 and 280nm	[156]

HDM – Heptakis(2,6-di-O-methyl); MHEC – Methylhydroxyethylcellulose; HPMC – Methylhydroxypropylcellulose; HEC – Hydroxyethylcellulose; DM – 2,6-di-O-methyl; TM – 2,4,6-tri-O-methyl; HP – Hydroxypropyl; HE – Hydroxyethyl; M – Methyl; IP – Ion-pair; Brij-30 – Polyoxyethylene 4 lauryl ether; ACN – Acetonitrile; PAH – Polycyclic aromatic hydrocarbons; SDS – Sodium dodecyl sulfate; TMAB – Tetramethylammonium bromide; TBAB – Tetrabutylammonium bromide; PAA – Polyallylamine; RT – Room temperature; MeOH – Methanol; S – Sulfated; HTM – Heptakis(2,3,6-tri-O-methyl); THNA – 1,2,3,4-Tetrahydro-1-naphthylamine; MPPA – 1-Methyl-3-phenylpropylamine; TEAB – Tetraethylammonium bromide; TPAB – Tetrapentylammonium bromide; TPAC – Tetrapentylammonium chloride; CAPSO – [3-(cyclohexylamino)2-hydroxy-1-propane sulfonic acid]; Poly-D-SUV – Polysodium N-undecanoyl-D-valinate; CHES – 2-(N-cyclohexylamino)ethanesulfonic acid

characteristic of analytes can be targeted. The use of IP reagents combined with hydrophobic additives, such as cyclodextrins or micelles, has been a common approach. Jira *et al.* used anionic and cationic IP reagents combined with neutral cyclodextrins for the chiral separation of acidic and basic compounds. The alkyl chain length on the IP reagents was found to play an important role in the observed separation. It was concluded that the more hydrophobic IP reagents with the longer alky chains were included more strongly into the cyclodextrin cavity and hence more effectively displaced the analytes from the cyclodextrin phase. The role of the IP reagent can thus be seen to have a multiple effect on the observed selectivity of the system, namely it can either form IPs with the analytes or it can act as a displacing ion, modifying the analyte-cyclodextrin interaction. Interestingly, it was noted that the use of cationic IP reagents influenced the chiral separation of cationic analytes in the presence of neutral cyclodextrins. Presumably in such systems IP interactions do not play a role and the influence of the cationic IP reagent is most likely solely due to competition between analyte cations and the cationic IP reagents for the cyclodextrin cavity.

The use of more than one additive also allows multiple complexes to be formed. An example of this is the separation of primary amines using mixtures of cyclodextrins and crown ethers. Armstrong *et al.* [153] have shown the advantages of including the achiral crown ether, 18-crown-6, in the cyclodextrin-mediated separation of a large range of primary amine compounds. The mechanism of separation is attributed to a "three-body" complex with the aromatic group on the analyte situated within the cyclodextrin cavity and the protonated amino group outside the cavity. This amino group is then free to complex the crown ether giving rise to a "sandwich" cyclodextrin -analyte-crown ether complex. The stability of the complex is dependent on the

presence of competing species (for both the cyclodextrin cavity and the crown ether) and the protonation of the amine group. This fact allows the observed selectivity of such systems to be varied by varying system parameters such as pH and $[K^+]$ (known to complex strongly with crown ethers).

1.11 Project Aims

From the preceding survey of the literature it can be seen that many additives have been used to increase the selectivity of a variety of EKC systems. However, most of the work to date has focused mainly on the use of single additive systems. These systems generally only allow selectivity intermediate between that of the pure CE system and that of the corresponding SP system. Furthermore, detailed investigation into the separation mechanisms with a focus on predicably varying the selectivity has been limited.

The systems that have been developed utilising more than one additive often only deal with selectivity in a qualitative fashion, describing observed changes rather than actively predicting separations.

Therefore the general aim of this work has been to extend the selectivity control offered over EKC systems using multiple analyte interactions. This can either be done using a single additive that exhibits multiple interactions with the analytes of interest or by including more than one additive in the electrolyte. The specific aims of the project were to:

- Investigate which additives can be utilised to exhibit predictable interactions with various analytes and to determine which parameters in these systems can be varied to alter the selectivity.

- Examine the possibility of using combined systems to exploit specific characteristics of the analytes investigated and determine which experimental parameters can be varied to exhibit predictable selectivity changes.
- Develop theoretical models that can be used to not only give useful information about the described system, but also to optimise and predict separations over defined experimental spaces.
- Examine the possibility of combining predictable selectivity changes with chiral separations to increase the selectivity control over these systems.

1.12 References

1. S. Hjerten, *Chromatogr. Rev.*, 9 (1967) 122.
2. R. Virtanen, *Acta Polytech. Scand.*, 123 (1974) 1.
3. F.E.P. Mikkers, F.M. Everaerts and T.P.E.M. Verheggen, *J. Chromatogr.*, 11 (1979) 169.
4. S.F.Y. Li, *Capillary Electrophoresis: Principles, Practice and Applications*, Elsevier, Amsterdam. 1992.
5. F. Foret, L. Krivankova and P. Bocek, *Capillary Zone Electrophoresis*, VCH Verlagsgesellschaft, Weinheim, 1993.
6. K. Sarmini and E. Kenndler, *J. Chromatogr. A*, 792 (1997) 3.
7. J.S. Fritz, *J. Chromatogr. A*, 884 (2000) 261.
8. A.H. Harakuwe and P.R. Haddad, *TrAC*, 20 (2001) 375.
9. S. Terabe, K. Otsuka, K. Ichikawa, A. Tsuchiya and T. Ando, *Anal. Chem.*, 56 (1984) 111.
10. K. Otsuka, S. Terabe and T. Ando, *J. Chromatogr.*, 348 (1985) 39.
11. C. Quang, J.K. Strasters and M.G. Khaledi, *Anal. Chem.*, 66 (1994) 1646.
12. J.K. Strasters and M.G. Khaledi, *Anal. Chem.*, 63 (1991) 2503.
13. M. krogh, S. Brekke, F. Tonnesen and K.E. Rasmussen, *J. Chromatogr. A*, 674 (1994) 235.
14. C. Zhang and W. Thormann, *J. Chromatogr. A*, 764 (1997) 157.
15. S. Oguri, S. Watanabe and S. Abe, *J. Chromatogr. A*, 790 (1997) 177.
16. J. Havel, M.C. Breadmore, M. Macka and P.R. Haddad, *J. Chromatogr. A*, 850 (1999) 345.
17. M. Tanaka, T. Ishida, T. Araki, A. Masuyama, Y. Nakatsu, M. Okahara and S. Terabe, *J. Chromatogr.*, 648 (1993) 469.
18. V.C. Trenerry, R.J. Wells and J. Robertson, *J. Chromatogr. A*, 718 (1995) 217.
19. G. Kavran and F.B. Erim, *J. Chromatogr. A*, 949 (2002) 301.
20. S. Takeda, S. Wakida, M. Yamane, K. Higashi and S. Terabe, *J. Chromatogr. A*, 781 (1997) 11.

21. W. Ding and J.S. Fritz, *Anal. Chem.*, 69 (1997) 1593.

22. O. Naess and K.E. Rasmussen, *J. Chromatogr. A*, 760 (1997) 245.

23. K.K. Yeung and C.A. Lucy, *J. Chromatogr. A*, 804 (1997) 319.

24. S. Takeda, S. Wakida, M. Yamane, Z. Siroma, K. Higashi and S. Terabe, *J. Chromatogr. A*, 817 (1998) 59.

25. Y. Chen and C. Lin, *J. Chromatogr. A*, 802 (1998) 95.

26. M.A. Woodland and C.A. Lucy, *Analyst*, 126 (2001) 28.

27. J.L. Beckers and P. Bocek, *Electrophoresis*, 23 (2002) 1947.

28. E. Fuguet, C. Rafols, J.R. Torres-Lapasio, M.C. Garcia-Alvarez-Coque, E. Bosch and M. Roses, *Anal. Chem.*, 74 (2002) 4447.

29. M.J. Cugat, F. Borrull and M. Calull, *Analyst*, 125 (2000) 2236.

30. D. Durkin and J.P. Foley, *Electrophoresis*, 21 (2000) 1997.

31. M. Molina and M. Silva, *Electrophoresis*, 23 (2002) 2333.

32. S. Hansen, C. Gabel-Jensen and D. El-Sherbiny, *TrAC*, 20 (2001) 614.

33. K.D. Altria, *J. Chromatogr. A*, 892 (2000) 171.

34. T. Kornfelt, A. Vinther, G.N. Okafo and P. Camilleri, *J. Chromatogr. A*, 726 (1996) 223.

35. M.K. Weldon, C.M. Arrington, P.L. Runnels and J.F. Wheeler, *J. Chromatogr. A*, 758 (1997) 293.

36. J. Li and J.S. Fritz, *J. Chromatogr. A*, 840 (1999) 269.

37. B. Liu, L. Liu and J. Cheng, *J. Chromatogr. A*, 848 (1999) 473.

38. A.R. Smith, J.R. Kirchhoff, Z. Zhang, L.M.V. Tillekeratne and R.A. Hudson, *J. Chromatogr. A*, 876 (2000) 193.

39. C. Czerwenka, M. Lammerhofer and W. Lindner, *Electrophoresis*, 23 (2002) 1887.

40. C.M. Shelton, J.T. Koch, N. Desai and J.F. Wheeler, *J. Chromatogr. A*, 792 (1997) 455.

41. M. Castagnola, C. Zuppi, D.V. Rossetti, F. Vincenzoni, A. Lupi, A. Vitali, E. Meucci and I. Messana, *Electrophoresis*, 23 (2002) 1769.

42. P.H.M. Muijselaar, H.A. Claessens, C.A. Cramers, J.F.G.A. Jansen, E.W. Meijer, E.M.M. de Brabander-van den Berg and S. van-der Wal, *J. High Res. Chromatogr.*, 18 (1995) 121.

43. M. Castagnola, L. Cassiano, A. Lupi, I. Messana, M. Patamia, R. Rabino, D.V. Rossetti and B. Giardina, *J. Chromatogr. A*, 694 (1995) 463.

44. S.A. Kuzdzal, C.A. Monnig, G.R. Newkome and C.N. Moorefield, *J. Am. Chem. Soc.*, 119 (1997) 2255.

45. A.L. Gray and J.T. Hsu, *J. Chromatogr. A*, 824 (1998) 119.

46. C. Stathakis, E.A. Arriaga and N.J. Dovichi, *J. Chromatogr. A*, 817 (1998) 233.

47. R. Kuhn, F. Erni, T. Bereuter and J. Hausler, *Anal. Chem.*, 64 (1992) 2815.

48. P. Castelnovo and C. Albanesi, *J. Chromatogr. A*, 715 (1995) 143.

49. C. Francois, P. Morin and M. Dreux, *J. Chromatogr. A*, 706 (1995) 535.

50. S. Oehrle, *J. Chromatogr. A*, 745 (1996) 87.

51. R. Kuhn, *Electrophoresis*, 20 (1999) 2605.

52. S. Liu and S.P. Armes, *Current Opinion in Colloid & Interface Science*, 6 (2001) 249.

53. S. Terabe and T. Isemura, *Anal. Chem.*, 62 (1990) 650.

54. S. Terabe and T. Isemura, *J. Chromatogr.*, 515 (1990) 667.

55. C. Stathakis and R.M. Cassidy, *Anal. Chem.*, 66 (1994) 2110.

56. C. Stathakis and R.M. Cassidy, *J. Chromatogr. A*, 699 (1995) 353.

57. O.V. Krokhin, H. Hoshino, O.A. Shpigun and T. Yotsuyanagi, *J. Chromatogr. A*, 776 (1997) 329.

58. F.B. Erim, *J. Chromatogr. A*, 768 (1997) 161.

59. B. Maichel, B. Potocek, B. Gas, M. Chiari and E. Kenndler, *Electrophoresis*, 19 (1998) 2124.

60. O.V. Krokhin, Adamov.A.V., H. Hoshino, O.A. Shpigun and T. Yotsuyanagi, *J. Chromatogr. A*, 850 (1999) 269.

61. B. Maichel, B. Potocek, B. Gas and E. Kenndler, *J. Chromatogr. A*, 853 (1999) 121.

62. J. Li, W. Ding and J.S. Fritz, *J. Chromatogr. A*, 879 (2000) 245.

63. M.C. Breadmore, P.R. Haddad and J.S. Fritz, *Electrophoresis*, 21 (2000) 3181.

64. O.V. Krokhin, H. Hoshino, O.A. Shpigun and T. Yotsuyanagi, *J. Chromatogr. A*, 895 (2000) 255.

65. B. Maichel, B. Gas and E. Kenndler, *Electrophoresis*, 21 (2000) 1505.

66. B. Maichel, K. Gogova, B. Gas and E. Kenndler, *J. Chromatogr. A*, 894 (2000) 25.

67. B. Potocek, E. Chmela, B. Maichel, E. Tesarova, E. Kenndler and B. Gas, *Anal. Chem.*, 72 (2000) 74.

68. G. Izzo, M. Raggi, B. Maichel and E. Kenndler, *J. Chromatogr. B*, 752 (2001) 47.

69. M.C. Breadmore, P.R. Haddad and J.S. Fritz, *J. Chromatogr. A*, 920 (2001) 31.

70. Q. Wu, M.L. Lee and R.G. Harrison, *J. Chromatogr. A*, 954 (2002) 247.

71. N. Tanaka, K. Nakagawa, H. Iwasaki, K. Hosoya, K. Kimata, T. Araki, Patterson and DG, *J. Chromatogr. A*, 781 (1997) 139.

72. N. Tanaka, K. Nakagawa, H. Nagayama, K. Hosoya, T. Ikegami, A. Itaya and M. Shibayama, *J. Chromatogr. A*, 836 (1999) 295.

73. T. Nakamura, A. Ohki, M. Mishiro, O. Tsuyashima and S. Maeda, *Anal. Sci.*, 15 (1999) 879.

74. C. Fujimoto, Y. Fujise and S. Kawaguchi, *J. Chromatogr. A*, 871 (2000) 415.

75. D.S. Peterson and C.P. Palmer, *Electrophoresis*, 22 (2001) 1314.

76. L. Bendahl, S. Hansen and B. Gammelgaard, *Electrophoresis*, 22 (2001) 2565.

77. W. Shi and C.P. Palmer, *Electrophoresis*, 23 (2002) 1285.

78. D.S. Peterson and C.P. Palmer, *J. Chromatogr. A*, 959 (2002) 255.

79. W. Schutzner, S. Fanali, A. Rizzi and E. Kenndler, *Anal. Chem.*, 67 (1995) 38666.

80. P. Blatny, C.H. Fischer and E. Kenndler, *Fres. J. Anal. Chem.*, 352 (1995) 712.

81. V. Pucci, M. Raggi and E. Kenndler, *J. Chromatogr. B*, 728 (1999) 263.

82. P. Bednar, Z. Stransky, P. Bartak and P. Adamovsky, *J. Chromatogr. A*, 838 (1999) 89.

83. V. Pucci, M. Raggi and E. Kenndler, *J. Chromatogr. A*, 853 (1999) 461.

84. S.L. Tamisier-Karolak, S. Pagliarusco, C. Herrenknecht, A. Brettreich, A. Hirsch, R. Ceolin, R.V. Bensasson, H. Szwarc and F. Moussa, *Electrophoresis*, 22 (2001) 4341.

85. I. Miksik, A. Eckhardt, E. Forgacs, T. Cserhati and Z. Deyl, *Electrophoresis*, 23 (2002) 1882.

86. A. Guttman and N. Cooke, *J. Chromatogr. A*, 680 (1994) 157.

87. S. Razee, A. Tamura and T. Masujima, *J. Chromatogr. A*, 715 (1995) 179.

88. W. Lindner, B. Bohs and V. Seidel, *J. Chromatogr. A*, 697 (1995) 549.

89. I. Bjornsdottir and S.H. Hansen, *J. Pharm. Bio. Anal.*, 13 (1995) 687.

90. P.D. Ferguson, D.M. Goodall and J.S. Loran, *J. Chromatogr. A*, 745 (1996) 25.

91. I.E. Valko, H. Siren and M.L. Riekkola, *J. Chromatogr. A*, 737 (1996) 263.

92. M. Hsieh, Y. Kuo, M. Lyu and H. Chang, *J. Chromatogr. A*, 898 (2000) 133.

93. I. Bjornsdottir and S.H. Hansen, *J. Pharm. Bio. Anal.*, 15 (1997) 1083.

94. F. Tagliaro, G. Manetto, S. Bellini, D. Scarcella, F.P. Smith and M. Marigo, *Electrophoresis*, 19 (1998) 42.

95. C. Stathakis and R.M. Cassidy, *Can. J. Chem.*, 76 (1998) 194.

96. P. Dzygiel, P. Wieczorek and J.A. Jonsson, *J. Chromatogr. A*, 793 (1998) 414.

97. M. Masar, R. Bodor and D. Kanianski, *J. Chromatogr. A*, 834 (1999) 179.

98. V. Dohnal, M. Farkova and J. Havel, *Chirality*, 11 (1999) 616.

99. B. Proksa, *J. Pharm. Bio. Anal.*, 20 (1999) 179.

100. T.S.K. So and C.W. Huie, *J. Chromatogr. A*, 872 (2000) 269.

101. P. Britz-McKibbin and D.D.Y. Chen, *Electrophoresis*, 23 (2002) 880.

102. V. Stanek, P. Jandera and H.A. Claessens, *J. Chromatogr. A*, 948 (2002) 235.

103. C. Quang and M.G. Khaledi, *Anal. Chem.*, 65 (1993) 3354.

104. C. Hellriegel, H. Handel, M. Wedig, S. Steinhauer, F. Sorgel, K. Albert and U. Holzgrabe, *J. Chromatogr. A*, 914 (2001) 315.

105. A.M. Stalcup and K. Gahm, *Anal. Chem.*, 68 (1996) 1360.

106. J. Szeman, K. Ganzler, A. Salgo and J. Szejtli, *J. Chromatogr. A*, 728 (1996) 423.

107. F. Wang and M.G. Khaledi, *Anal. Chem.*, 68 (1996) 3460.

108. J.B. Vincent, D.M. Kirby, T.V. Nguyen and G. Vigh, *Anal. Chem.*, 69 (1997) 4419.

109. I. Le Potier, S.L. Tamisier-Karolak, P. Morin, F. Megel and M. Taverna, *J. Chromatogr. A*, 829 (1998) 341.

110. S.R. Gratz and A.M. Stalcup, *Anal. Chem.*, 70 (1998) 5166.

111. K. Verleysen, S. Sabah, G. Scriba, A. Chen and P. Sandra, *J. Chromatogr. A*, 824 (1998) 91.

112. I.S. Lurie, N.G. Odeneal II, T.D. McKibben and J.F. Casale, *Electrophoresis*, 19 (1998) 2918.

113. L. Zhou, B.D. Johnson, C. Miller and J.M. Wyvratt, *J. Chromatogr. A*, 875 (2000) 389.

114. B. Proksa and R. Cizmarikova, *Anal. Chim. Acta*, 434 (2001) 75.

115. W. Jianjun, Z. Guojun, Y. Liu and S. Wanru, *Analyst*, 126 (2001) 438.

116. J. Zukowski, V. De Biasi and A. Berthod, *J. Chromatogr. A*, 948 (2002) 331.

117. M. Muzikar, J. Havel and M. Macka, *Electrophoresis*, 23 (2002) 1796.

118. M. Raggi, R. Mandrioli, C. Sabbioni, C. Parenti, G. Cannazza and S. Fanali, *Electrophoresis*, 23 (2002) 1870.

119. Y.T. Iwata, A. Garcia, T. Kanamori, H. Inoue, T. Kishi and I.S. Lurie, *Electrophoresis*, 23 (2002) 1328.

120. A. Bunke and T. Jira, *J. Chromatogr. A*, 798 (1998) 275.

121. F. Wang and M.G. Khaledi, *J. Chromatogr. A*, 817 (1998) 121.

122. R. Ivanyi, L. Jicsinszky and Z. Juvancz, *Electrophoresis*, 22 (2001) 3232.

123. H. Yamamura, A. Akasaki, Y. Yamada, K. Kano, T. Katsuhara, S. Araki, M. Kawai and T. Tsuda, *Electrophoresis*, 22 (2001) 478.

124. D. Lee and S.A. Shamsi, *Electrophoresis*, 23 (2002) 1314.

125. M. Culha, S. Fox and M.J. Sepaniak, *Anal. Chem.*, 72 (2000) 88.

126. A.M. Abushoffa, M. Fillet, P. Hubert and J. Crommen, *J. Chromatogr. A*, 948 (2002) 321.

127. M.J. Sepaniak, C.L. Copper, K.W. Whitaker and V.C. Anigbogu, *Anal. Chem.*, 67 (1995) 2037.

128. K. Gahm, L.W. Chang and D.W. Armstrong, *J. Chromatogr. A*, 759 (1997) 149.

129. A. Nguyen and J.H.T. Luong, *Anal. Chem.*, 69 (1997) 1726.

130. S. Izumoto and H. Nishi, *Electrophoresis*, 20 (1999) 189.

131. S. Chinaka, S. Tanaka, N. Takayama, K. Komai, T. Ohshima and K. Ueda, *J. Chromatogr. B*, 749 (2000) 111.

132. J. Magnusson, H. Wan and L.G. Blomberg, *Electrophoresis*, 23 (2002) 3013.

133. S. Takeda, S. Wakida, M. Yamane, A. Kawahara and K. Higashi, *J. Chromatogr. A*, 653 (1993) 109.

134. W.C. Brumley and W.J. Jones, *J. Chromatogr. A*, 680 (1994) 163.

135. M.L. Marina, I. Benito, J.C. Diez-Masa and M.J. Gonzalez, *J. Chromatogr. A*, 752 (1996) 265.

136. Ph. Schmitt, A.W. Garrison, D. Freitag and A. Kettrup, *J. Chromatogr. A*, 792 (1997) 419.

137. B. Jimenez, D.G. Patterson, J. Grainger, Z. Liu, M.J. Gonzalez and M.L. Marina, *J. Chromatogr. A*, 792 (1997) 411.

138. J.H.T. Luong and Y. Guo, *Electrophoresis*, 19 (1998) 723.

139. J.H.T. Luong and Y. Guo, *J. Chromatogr. A*, 811 (1998) 225.

140. L.J. Jin, I. Rodriguez and S.F.Y. Li, *Electrophoresis*, 20 (1999) 1538.

141. S. Kodama, A. Yamamoto, A. Matsunaga, A. Toriba and K. Hayakawa, *Analyst*, 125 (2000) 1555.

142. D.G. McLaren, O. Boulat and D.D.Y. Chen, *Electrophoresis*, 23 (2002) 1912.

143. H. Ma, Z. Wang and M. Su, *J. Chromatogr. A*, 955 (2002) 125.

144. X. Shang and Z. Yuan, *Anal. Chim. Acta*, 456 (2002) 183.

145. C. Lin, H. Huang and H. Chen, *J. Chromatogr. A*, 917 (2001) 297.

146. N. Tanaka, K. Nakagawa, K. Hosoya, C.P. Palmer and S. Kunugi, *J. Chromatogr. A*, 802 (1998) 23.

147. J. Snopek, H. Soini, M. Novotny, E. Smolkova-Keulemansova and I. Jelinek, *J. Chromatogr.*, 559 (1991) 215.

148. W.X. Huang, S.D. Fazio and V.V. Vivilecchia, *J. Chromatogr. A*, 781 (1997) 129.

149. T. Jira, A. Bunke and A. Karbaum, *J. Chromatogr. A*, 798 (1998) 281.

150. W. Ding and J.S. Fritz, *Anal. Chem.*, 70 (1998) 1859.

151. C.M. Knapp and J.J. Breen, *J. Chromatogr. A*, 799 (1998) 289.

152. F.A. Valenzuela, T.K. Green and D.B. Dahl, *Anal. Chem.*, 70 (1998) 3612.

153. D.W. Armstrong, L.W. Chang and S.S.C. Chang, *J. Chromatogr. A*, 793 (1998) 115.

154. W.X. Huang, H. Xu, S.D. Fazio and V.V. Vivilecchia, *J. Chromatogr. A*, 875 (2000) 361.

155. R. Gotti, R. Pomponio, C. Bertucci and V. Cavrini, *J. Chromatogr. A A*, 916 (2001) 175.

156. S.H. Edwards and S. Shamsi, *Electrophoresis*, 23 (2002) 1320.

Chapter 2

General Experimental

This section describes the instrumentation, chemicals and procedures used throughout this work, unless specified otherwise in a particular chapter.

2.1 Instrumentation

All separations were performed using a Hewlett-Packard HP ^{3D}CE system (Agilent Technologies, Waldbronn, Germany), equipped with a diode array detector. Data acquisition was performed using HP ^{3D}CE Chemstation (Agilent).

All CE separations were performed using fused silica capillaries (25, 50 and 75μm ID x 360μm OD) obtained from Polymicro Technologies Inc. (Phoenix, AZ, USA). Separations were performed at ±30kV unless otherwise stated.

Detection windows approximately 5mm in length were burnt 8.5cm from the end of the capillary using a butane torch and cleaned with acetone. Standard metallic interfaces of either 50 or 75μm were used for all separations.

2.2 Reagents

Unless specified otherwise all chemicals were of analytical reagent grade and are listed in Table 2.1-Table 2.6.

Table 2.1: Chemicals used as electrolytes

Electrolyte	pK_a	Formula	Supplier
Bis[2-hydroxyethyl]imino-tris [hydroxymethyl]-methane (Bis-Tris)	6.5	$C_8H_{19}NO_5$	Aldrich, Milwaukee, Wi, USA

Citric acid	3.128, 4.761, 6.396	$HOC(CO_2H)(CH_2CO_2H)_2$	Aldrich
Citric acid, trisodium salt	3.128, 4.761, 6.396	$HOC(CO_2Na)(CH_2CO_2Na)_2$	Aldrich
Phosphoric acid	2.16, 7.21, 12.32	H_3PO_4	BDH Chemicals, Kilsyth, Vic, Australia
Tris(hydroxymethyl)aminomethane (Tris)	8.05	$C_4H_{11}NO_3$	Aldrich

Table 2.2: Chemicals used as additives

Additive	Formula	Supplier
β-cyclodextrin	-	Sigma, St Louis, MO, USA
β-cyclodextrin, sulfated, sodium salt	-	Aldrich
Dextran sulfate	-	Sigma
Hexanesulfonic acid, sodium salt	$CH_3(CH_2)_5SO_3Na$	Aldrich
Octanesulfonic acid, sodium salt	$CH_3(CH_2)_7SO_3Na$	Aldrich
Poly(diallydimethylammonium chloride) (PDDAC)	$(C_8H_{16}NCl)_n$	Aldrich
Poly(vinylsulfonic acid, sodium salt) (PVS)	$[-CH_2CH(SO_3Na)-]_n$	Aldrich

Table 2.3: Chemicals used to condition or coat capillaries

Name	Formula	Supplier
Dextran sulfate	-	Sigma
PDDAC	$(C_8H_{16}NCl)_n$	Aldrich
Sodium hydroxide	NaOH	Ajax Chemicals, Sydney, NSW, Australia

Table 2.4: Chemicals used as competing ions

Competing ion	Formula	Supplier
Magnesium chloride	$MgCl_2$	BDH
Sodium chloride	NaCl	Ajax

Table 2.5: Chemicals used as analytes

Analyte	pK_a	Formula	Supplier
m-Aminopyridine	6.03(+)	$NH_2C_5H_4N$	Aldrich
o-Aminopyridine	6.71(+)	$NH_2C_5H_4N$	Aldrich
p-Aminopyridine	9.11(+)	$NH_2C_5H_4N$	Aldrich
Aniline	4.60(+)	$C_6H_5NH_2$	Aldrich
Benzenesulfonic acid, sodium salt	2.554	$C_6H_5SO_3Na$	Aldrich
Benzoic acid	4.204	C_6H_5COOH	Aldrich
Benzylamine	9.35(+)	$C_6H_5CH_2NH_2$	Aldrich
4-*tert*-Butylbenzoic acid	4.389	$(CH_3)_3CC_6H_4CO_2H$	Aldrich
4-*tert*-Butylpyridine	5.99(+)	$(CH_3)_3CC_5H_4N$	Aldrich
Codeine	7.95(+)	$C_{18}H_{21}NO_3$	Tasmanian Alkaloids
4-Ethylbenzenesulfonic acid	-	$C_2H_5C_6H_4SO_3H$	Aldrich
4-Ethylaniline	5.00(+)	$C_2H_5C_6H_4NH_2$	Aldrich
4-Ethylpyridine	5.87(+)	$CH_3CH_2C_5H_4N$	Aldrich
4-Heptylaniline	5.27(+)*	$CH_3(CH_2)_6C_6H_4NH_2$	Aldrich
4-Heptylbenzoic acid	-	$CH_3(CH_2)_6C_6H_4CO_2H$	Aldrich
Laudanine	-	$C_{20}H_{25}NO_4$	Tasmanian Alkaloids
4-Methylbenzylamine	9.52(+)*	$CH_3C_6H_4CH_2NH_2$	Aldrich
Morphine	7.87(+)	$C_{17}H_{19}NO_3$	Tasmanian Alkaloids
2-Naphthalenesulfonic acid, sodium salt	-	$C_{10}H_7SO_3Na$	Aldrich

Oripavine	-	$C_{18}H_{19}NO_3$	Tasmanian Alkaloids
4-Pentylaniline	5.10(+)*	$CH_3(CH_2)_4C_6H_4NH_2$	Aldrich
DL-Phenylalanine	2.58(+), 9.24	$C_6H_5CH_2CH(NH_2)COOH$	Sigma
Phthalic acid	2.950, 5.408	$C_6H_4(COOH)_2$	BDH Chemicals
Picoline	6.00(+)	$CH_3C_5H_4N$	Aldrich
4-Propylbenzoic acid	-	$CH_3(CH_2)_2C_6H_4CO_2H$	Aldrich
Pyridine	5.17(+)	C_5H_5N	Aldrich
Quinoline	4.80(+)	C_9H_7N	Aldrich
Sodium bromide	-	NaBr	Sigma
Sodium iodide	-	NaI	Aldrich
Sodium nitrate	-	$NaNO_3$	Ajax Chemicals
Thebaine	7.95(+)	$C_{19}H_{21}NO_3$	Tasmanian Alkaloids
10-OH Thebaine	-	$C_{19}H_{21}NO_4$	Tasmanian Alkaloids
4-Toluenesulfonic acid	-	$CH_3C_6H_4SO_3H$	Sigma
Toluic acid	4.362	$CH_3C_6H_4CO_2H$	Aldrich
DL-Tryptophan	2.38(+), 9.39	$C_{11}H_{12}N_2O_2$	Sigma
DL-Tyrosine	2.18(+), 9.21	$C_9H_{11}NO_3$	Sigma

(+) – Protonated species; * - Calculated using ACD/pK_a v4.56, Advanced Chemistry Development Inc, Toronto, Canada

Table 2.6: Other chemicals used in this work

Chemical	Formula	Supplier
Acetone	$(CH_3)_2CO$	BDH Chemicals
Acetonitrile	CH_3CN	BDH Chemicals
Hydrochloric acid	HCl	BDH Chemicals
Methanol	CH_3OH	BDH Chemicals

2.3 Procedures

2.3.1 Electrolyte and standard preparation

All electrolytes and analyte standards were prepared with water purified using a Milli-Q (Millipore, Bedford, MA, USA) water system. Electrolytes were filtered through a 0.45μm membrane filter of Type HA (Millipore) and degassed using vacuum sonification on an ultrasonic bath.

The opiates were obtained as codeine phosphate, morphine, thebaine barbiturate, 10-β-hydroxythebaine/thebaine (~1:1 mixture), oripavine and laudanine. These were prepared as 500mg/L stock solutions and further diluted to prepare the 50mg/L mixed standards.

2.3.2 Sample injection

Injection was performed using 50mbar pressure in all cases. Injection times depended on the diameter of capillary being used but were typically 2, 5 and 10s for 75, 50 and 25μm ID capillaries respectively.

2.3.3 Calculations

Acetone was used as the EOF marker in all cases.

Electrophoretic mobilities were calculated using the equation:

$$\mu_{eff} = \frac{L_T L_D}{V t_m} \qquad (2\text{-}1)$$

where L_T is the total length of the capillary and L_D is the length from the injection end of the capillary to the detector both in metres. V is the separation voltage in volts and t_m is the observed migration time in seconds.

All modelling work and non-linear regression was performed using the solver function in Microsoft Excel 97.

2.3.4 Optimisation

In all cases optimisation was undertaken using either the normalised resolution product (NRP) or minimum resolution (MR) criteria. The NRP criterion is defined by the following equation [1]:

$$r_{\text{min}} = \prod_{i=1}^{n=1} \left(\frac{R_{s(i,i+1)}}{\frac{1}{n-1} \sum_{i=1}^{n-1} R_{s(i,i+1)}} \right) \qquad (2\text{-}2)$$

where $R_{s(i,i+1)}$ is the resolution between adjacent peaks and n is the number of peaks in the separation. r ranges from 0-1, with 0 implying complete overlap of at least one pair of peaks while a value of 1 being reached all the analytes are evenly spaced over the electropherogram.

The MR criterion is defined by the following equation [1]:

$$r_{\text{min}} = \min \left(\sum_{i=1}^{n-1} R_{s(i,i+1)} \right) \qquad (2\text{-}3)$$

where $R_{s(i,i+1)}$ is the resolution between adjacent peaks and n is the number of peaks in the separation. The MR criterion takes into account only the peak pair having the worst resolution.

The process followed in the optimisation involved calculation of r using a defined set of experimental data covering the parameter space and then performing a separation under the predicted optimal conditions. Observed mobilities were then compared with predicted values and if the discrepancies exceeded 5%, the retention data were

added to the optimisation data set and the process repeated until agreement between predicted and observed mobilities was <5%.

2.4 References

1. M.C. Breadmore, P.R. Haddad and J.S. Fritz, *Electrophoresis*, 21 (2000) 3181.

Chapter 3

Selectivity Control of Inorganic and Small Organic Anions using PDDAC and β-CD as Mixed Pseudo-Stationary Phases

3.1 Introduction

In the analysis of anions, cationic polymers have proven popular and have been applied to a wide variety of analytes. Poly(diallyldimethylammonium chloride) (PDDAC) has been one cationic polymer that has been successfully used by several authors. Breadmore *et al.* [1] fully investigated the selectivity control that can be achieved using PDDAC for the separation of inorganic and small organic anions. The separation mechanism is based on an IE interaction, that is anions with larger interaction constants (such as divalent anions) will be more retained in a PDDAC system.

Pseudo-SPs have the advantage that they can be potentially added together to increase the selectivity control offered over a particular system. For such systems maximum selectivity control will be obtained if the nature and strength of the analyte-SP interactions differ for each analyte and SP used. This chapter examines the possibility for increased selectivity control in a system in which electrophoretic migration is combined with two independent chromatographic interactions, namely IE and hydrophobicity. The aim of this chapter is to thus demonstrate the possibility for independent control of the IE and the hydrophobic interactions using PDDAC and

β-CD as the p-SPs and to develop a suitable mathematical migration model which will allow the system to be optimised readily.

3.2 Experimental

The general details are given in Chapter 2. Detailed conditions are given in each figure caption.

3.2.1 Capillary coating procedures

To obtain a reversed EOF, capillaries were coated with PDDAC since this has been shown to produce a stable, reversed EOF [2]. When using electrolytes containing PDDAC the capillary was simply flushed with the electrolyte for 15min prior to separations being performed. In the case where PDDAC was not included in the electrolyte, the coating was applied and renewed as required by flushing the capillary with a 0.5% PDDAC solution for 2min followed by 15min with the new electrolyte. This procedure was repeated each time the electrolyte was changed and resulted in stable EOF values.

3.2.2 Electrolyte preparation

Stock 100mM Tris/Cl^- solutions were prepared by titration of 100mM TRIS to pH 8.05 with HCl, providing a background concentration of 50 mM Cl^- in the stock solution. Individual electrolytes were prepared by dilution of this stock solution to 20 mM Tris/10mM Cl^-, PDDAC was added to the electrolytes as a 2% solution to give concentrations up to 1.0% and β-CD was dissolved in each electrolyte to give the desired concentration. NaCl was added to the electrolyte as required, bearing in mind

each electrolyte already contained a background level of 10mM Cl^- from the titration of TRIS with HCl.

3.3 Choice of analytes

Since IE and hydrophobic partitioning were expected to be the two main interactions leading to separation, a series of test analytes exhibiting different IE interactions with PDDAC as well as having differing hydrophobicities was chosen and these are listed in Table 3.1. Ion-exchange selectivity coefficients on a strong base quaternary ammonium anion-exchange material have been determined for some of these analytes by Breadmore *et al.* [1] and these values are a useful guide to the IE affinities of the analytes for PDDAC. Octanol-water partition coefficients for most of the analytes are not available, but values for their neutral precursors (i.e. without the sulfonate or carboxylate functionalities) are listed in Table 3.1 and show that the selected analytes cover a reasonable range of hydrophobicities.

3.4 Selectivity

There are two main requirements for maximum control over the separation selectivity of an EKC system exhibiting multiple interactions. Firstly, it is desirable for several complementary separation mechanisms to be operating since this increases the number of possible sequences in which the analytes can migrate. Secondly, the magnitude of each interaction should be subject to independent control so that the selectivity of the system can be manipulated in a predictable manner. The suitability of using PDDAC and β-CD as dual additives in a EKC system is illustrated in Figure 3.1 which shows the effects on analyte mobilities caused by independent control of the hydrophobic and IE interactions. A fixed amount of PDDAC (0.5%) was used in

Table 3.1: Characteristics of the test analytes.

Analyte	K_{IE}[1]	P_{ow}[2]	P_{ow} *of the unfunctionalised molecule*[3]
Iodide	2.242	-	-
Nitrate	0.451	-	-
Benzenesulfonate	0.613	-	2.13
p-Toluenesulfonate	1.527	-	2.73
4-Ethylbenzenesulfonate	-	-	3.15
2-Naphthalenesulfonate	2.847	-	3.34
Benzoate	0.168	1.88	2.13
p-Toluate	-	2.34	2.73
4-Propylbenzoate	-	-	3.69
4-*t*-Butylbenzoate	-	-	4.11
4-Heptylbenzoate	-	-	5.52-6.30[4]

1 - Ion-exchange selectivity coefficients from Breadmore et al. [1]; 2 - Octanol-water partition coefficients from the CRC Handbook [3]; 3 - P_{ow} of the equivalent unfunctionalised molecule, e.g. for ethylbenzenesulfonate the equivalent molecule is ethylbenzene; 4 - The two extreme values shown are for hexyl and octylbenzene since these represent upper and lower limits for the expected P_{ow} for heptylbenzene.

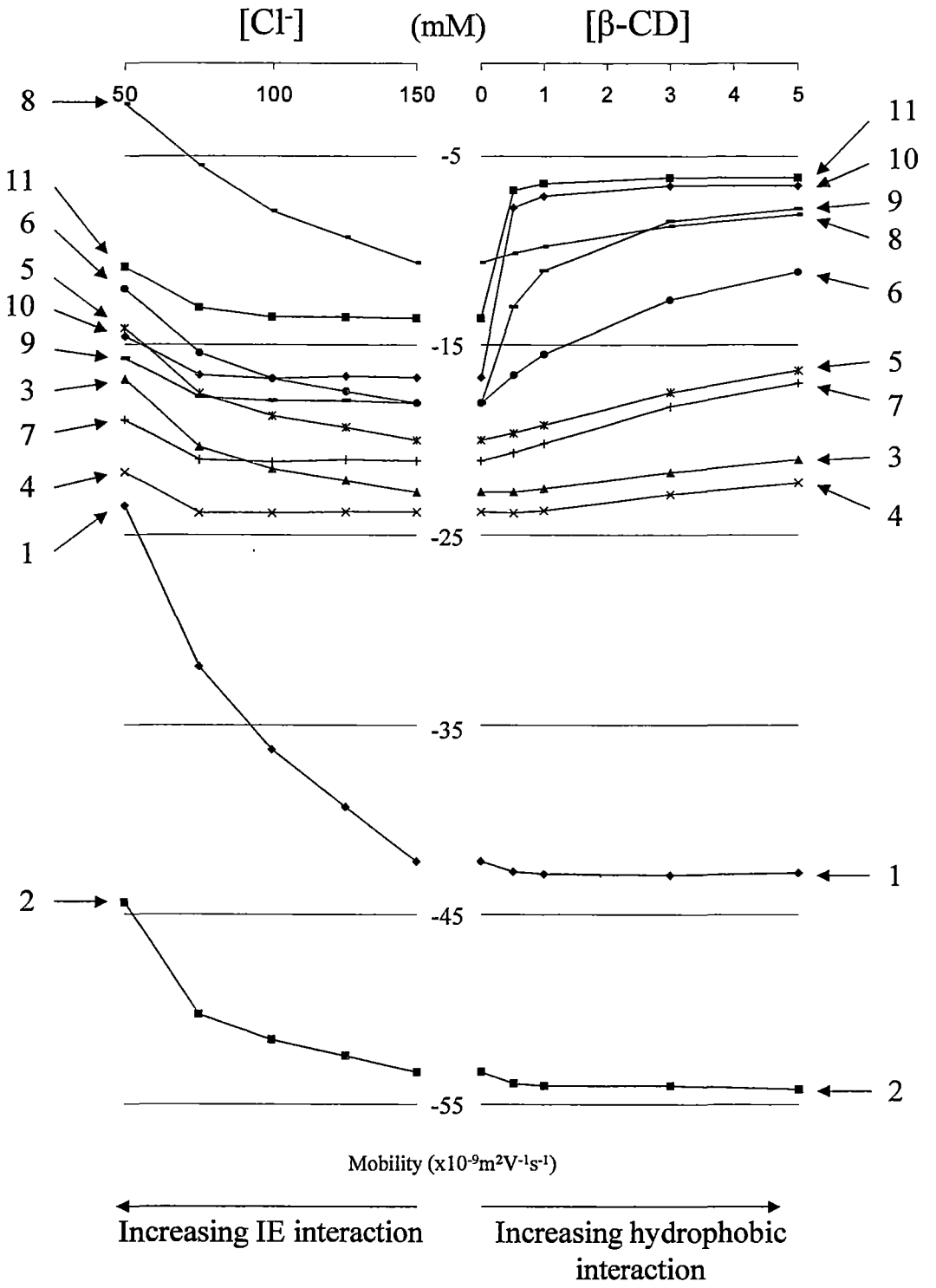

Figure 3.1: Separation selectivity on varying [Cl⁻] (left) and [β-CD] (right). Experimental Conditions: 20mM Tris electrolyte + 0.5%PDDAC. Peaks are 1=iodide, 2=nitrate, 3=benzenesulfonate, 4=benzoate, 5=toluenesulfonate, 6=ethylbenzenesulfonate, 7=toluate, 8=naphthalenesulfonate, 9=propylbenzoate, 10=*t*-butylbenzoate and 11=heptylbenzoate.

the electrolyte and the concentrations of chloride (as an IE competing ion) and β-CD were varied.

IE interactions were controlled by the amount of chloride added to the electrolyte. High levels of chloride competed effectively for the IE sites on PDDAC and hence reduced the IE interactions occurring with the analyte anions, leading to higher negative mobilities. Conversely, negative mobilities were lower under conditions where there was stronger interaction between the analytes and the PDDAC pseudo-SP. Selectivity effects offered by PDDAC were therefore predominantly IE in nature, such that the changes in mobility caused by addition of chloride to the electrolyte were greater for iodide and the sulfonates than the other analytes. This is in agreement with the behaviour expected from the elution order of these analytes on a strong-base anion exchange resin [4]. The extent of these IE interactions could be manipulated by varying either the concentration of PDDAC or chloride (the eluting ion) in the electrolyte [1].

Varying the concentration of the second additive, β-CD, also has a large effect on many of the analytes, especially the more hydrophobic analytes (propyl, butyl and heptylbenzoate), but a less pronounced effect on the mobilities of the smaller organic species and the inorganic anions, see Figure 3.1. In all cases except for the inorganic anions, mobilities of the analytes were decreased as the concentration of β-CD was increased due to inclusion of the analytes into the β-CD. It can also be noted that similar behaviour was observed for pairs of analytes in which only the functional groups differed (benzoate/benzenesulfonate, and toluate/toluenesulfonate). This suggested that the functional group on the analyte played little part in the analyte-CD interaction, implying that the mechanism of interaction involved partitioning of the alkyl-aromatic backbone of the analytes into the hydrophobic core of the cyclodextrin.

The magnitude of this interaction should, therefore, be directly controllable either by varying the concentration of β-CD or by the addition of organic solvents to the electrolyte in order to suppress hydrophobic interactions with the β-CD. In the present study, the first approach was used since the addition of organic solvents to the electrolyte would also affect the electrophoretic component of the separation through solvation and viscosity effects, complicating the mathematical modelling of the system. Moreover, whilst the use of organic solvents was found to have strong effects on analyte mobilities in electrolytes containing β-CD (as shown in Figure 3.2 for methanol), changes in separation selectivity were relatively minor up to 30% MeOH. Only iodide and nitrate showed any selectivity change with the peaks co-eluting at 30% MeOH. The reason for this is unclear, but since the changes were minor for a relatively large change in organic modifier concentration, they were not considered significant for the work presented here.

An important feature of the current EKC system is that both pseudo-SPs acted more or less independently and both PDDAC and the CD could be added to the system without affecting the other. A further advantage was the stability of the EOF which varied by less than 2.4% RSD. Reproducibility of migration times was also excellent with RSD values less than 0.7% for 10 consecutive runs.

3.5 Modelling the system

The independent nature of the two pseudo-SPs enables the current EKC system to be modelled from first principles. The following two equilibria apply:

$$A^-_{bge} \overset{K_{cd}}{\rightleftharpoons} A^-_{cd} \qquad (3\text{-}1)$$

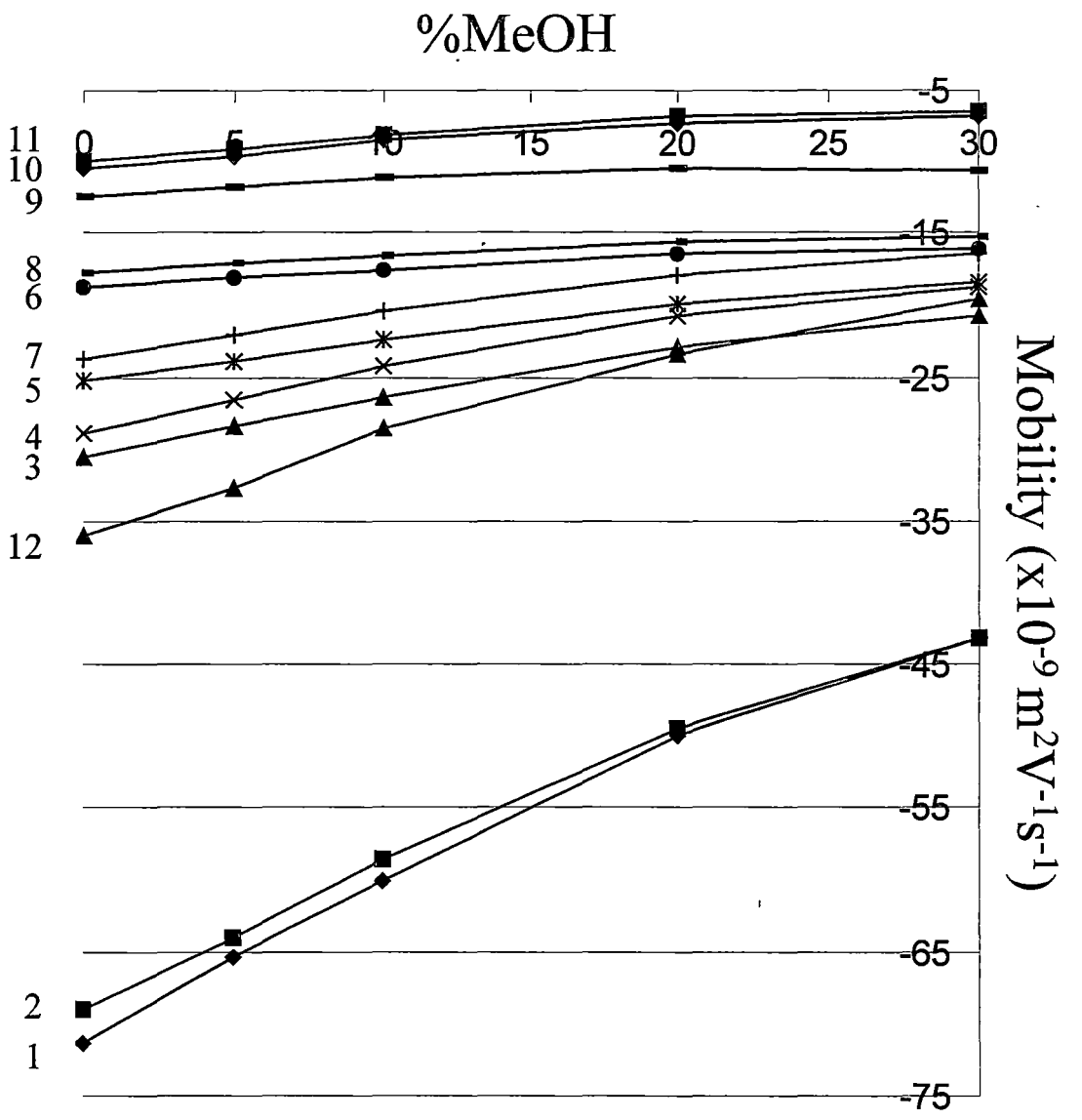

Figure 3.2: Effect on mobilities of the test analytes from addition of MeOH to the electrolyte. Conditions: 20mM Tris electrolyte + 3.0mM β-CD. Peaks: 1=iodide, 2=nitrate, 3=benzenesulfonate, 4=benzoate, 5=toluenesulfonate, 6=ethylbenzenesulfonate, 7=toluate, 8=2-naphthalenesulfonate, 9=propylbenzoate, 10=*t*-butylbenzoate 11=heptylbenzoate and 12=EOF.

$$A^-_{bge} + E^-_{poly} \overset{K_{poly}}{\rightleftharpoons} A^-_{poly} + E^-_{bge} \qquad (3\text{-}2)$$

where A and E are the analyte and competing ion, respectively. The subscripts "bge", "cd" and "poly" refer to the free species in the electrolyte, and bound to the cyclodextrin or polymer phases, respectively. These equilibria are characterised by the equilibrium constants K_{cd} and K_{poly}, with the former being a hydrophobic interaction constant and the latter being an ion-exchange selectivity coefficient. These equilibrium constants are defined as:

$$K_{cd} = \frac{[A^-]_{cd}}{[A^-]_{bge}} \qquad (3\text{-}3)$$

$$K_{poly} = \frac{[A^-]_{poly}[E^-]_{bge}}{[A^-]_{bge}[E^-]_{poly}} \qquad (3\text{-}4)$$

where $[A^-]_{bge}$, $[A^-]_{poly}$ and $[A^-]_{cd}$ are analyte concentrations in the electrolyte, PDDAC or cyclodextrin phases respectively. For two non-interacting SPs the total retention factor, k'_t of an analyte can be expressed in terms of the individual retention factors, k'_{cd} and k'_{poly} for the cyclodextrin and the polymer, respectively, where:

$$k'_t = k'_{cd} + k'_{poly} \qquad (3\text{-}5)$$

An expression for k'_{poly} can be derived from ion-chromatography theory [1],

$$k'_{poly} = \frac{w_{poly}}{V_{bge}} (K_{poly})^{1/y} (Q/y)^{x/y} [E]^{-x/y} \qquad (3\text{-}6)$$

where w_{poly} is the weight of the PDDAC pseudo-SP, V_{bge} is the volume of the electrolyte, Q is the ion-exchange capacity of the ion-exchange pseudo-SP, $[E]$ is the concentration of the competing ion (Cl^- for all the work presented here) while x and y are the charges on the analyte and eluent ion respectively (both 1 in the current work).

An equivalent expression for k'_{cd} can be derived from first principles:

$$k'_{cd} = \frac{n(A^-)_{cd}}{n(A^-)_{bge}} = \frac{[A^-]_{cd} V_{cd}}{[A^-]_{bge} V_{bge}} \tag{3-7}$$

Substituting in for $[A^-]_{cd}$ from eqn (3-3) leads to:

$$k'_{cd} = \frac{V_{cd}}{V_{bge}} K_{cd} \tag{3-8}$$

where V_{cd} is the volume of the cyclodextrin phase. Substituting for k'_{poly} and k'_{cd} in eqn (3-5) leads to a final expression for the total retention factor of the system.

$$k'_t = \frac{V_{cd}}{V_{bge}} K_{cd} + \frac{w_{poly}}{V_{bge}} \left(K_{poly}\right)^{1/y} (Q/y)^{x/y} [E]^{-x/y} \tag{3-9}$$

The observed mobility of an analyte can be expressed in terms of this retention factor [1]

$$\mu_{ob} = \frac{1}{1+k'} \mu_{bge} + \frac{k'}{1+k'} \mu_{sp} \tag{3-10}$$

where μ_{ob} is the observed mobility of the analyte while μ_{bge} and μ_{sp} are the mobilities of the analytes in the electrolyte and pseudo-SP respectively. In the case of two independent pseudo-SPs, eqn (3-10) can be rewritten as

$$\mu_{ob} = \frac{1}{1+k'_t} \mu_{bge} + \frac{k'_{cd}}{1+k'_{cd}} \mu_{cd} + \frac{k'_{poly}}{1+k'_{poly}} \mu_{poly} \tag{3-11}$$

where μ_{cd} and μ_{poly} are the mobilities of the analytes in the cyclodextrin and polymer phases, respectively. Expanding eqn (3-11) by including previous equations gives:

$$\mu_{ob} = \frac{1}{1+\frac{V_{cd}}{V_{bge}}K_{cd}+\frac{w_{poly}}{V_{bge}}K_{poly}Q[E]^{-1}}\mu_{bge} + \frac{\frac{V_{cd}}{V_{bge}}K_{cd}}{1+\frac{V_{cd}}{V_{bge}}K_{cd}}\mu_{cd} + \frac{\frac{w_{poly}}{V_{bge}}K_{poly}Q[E]^{-1}}{1+\frac{w_{poly}}{V_{bge}}K_{poly}Q[E]^{-1}}\mu_{poly} \quad (3\text{-}12)$$

In previous work [1] the influence of increasing ionic strength, I, of the electrolyte on mobilities was taken into account by replacing the μ terms with a ($b/\sqrt{I}$) term, where b is a constant related to the mobility at zero ionic strength. For the work presented here the change in mobility of all the analytes over the range of ionic strengths used was less than 5% and did not appear to follow a $1/\sqrt{I}$ relationship. For these reasons no correction term for ionic strength was included in the model equation.

In eqn (3-12) w_{poly}/V_{bge} is defined by the %(w/v) of PDDAC in the electrolyte. Q is also related to the %PDDAC and can be estimated by the number of repeat units in the polymer. V_{cd} can be estimated from the individual cavity volume of each β-CD molecule ($0.346nm^3$) [5]. $[E]$ is defined by the concentration of NaCl added to the electrolyte while the remaining parameters, K_{cd}, K_{poly}, μ_{bge}, μ_{cd} and μ_{poly} must be determined by non-linear regression.

3.6 Application of the migration model

Since eqn (3-12) contained 5 unknown constants with three variables, namely %PDDAC, [β-CD] and [Cl^-], a minimum of 6 experiments was needed to determine the unknowns. A three dimensional set of data for retention factors covering the parameter space determined by 0-1% PDDAC, 0-5mM β-CD (the β-CD had limited solubility above 10mM) and 50-150mM Cl^- was chosen. Although theoretically only six experiments were needed, termed the primary data set, for the non-linear

regression, a primary data set of 13 experiments was found to provide the best results. The experimental data used for the non-linear regression were measured at the 8 corner points of the 3-dimensional parameter space, as well as a 5 point "star" layout of points on the 0.5% PDDAC plane. Data were also acquired using a further 28 points throughout the parameter space, termed the "validation set", and these were used to evaluate the predictive power of the model.

Of the 5 parameters obtained from the non-linear regression, three are related to the analytes (K_{poly}, K_{cd} and μ_{bge}) while two (μ_{cd} andμ_{poly}) relate to the electrolyte system used and would only vary if the electrolyte was altered, for example by using a different competing ion such as sulfate. Table 3.2 shows the values of the parameters obtained from the non-linear regression and these values show the expected trends. The K_{poly} values follow the IE selectivity coefficients of the analytes observed on strong base anion-exchangers, while the K_{cd} values reflect the increasing hydrophobicities of the analytes given from the data in Table 3.1. Naphthalenesulfonate and iodide show the greatest affinity for PDDAC (in agreement with that shown by Breadmore *et al.* [1]), the remaining sulfonates have similar IE interactions and as a group interact with PDDAC more strongly than the carboxylates, while the carboxylates as a group also have similar IE interactions. The K_{cd} values reflect hydrophobicity and follow the trends expected from the P_{ow} values given in Table 3.1. It can be seen that ethylbenzene and naphthalenesulfonate, which have different structures but similar P_{ow} values, show similar K_{cd} values implying that octanol-water partition coefficients are a reasonable guide to the strength of interaction between the analytes and the neutral cyclodextrin.

Figure 3.3 shows the correlation between mobilities predicted for the validation set (using eqn (3-12) solved with the primary data set) and the observed mobilities. A

Table 3.2: Parameters derived from non-linear regression of eqn (3-12)

Analyte	K_{poly}[1]	K_{cd}[1]	μ_{cd}[2]
Iodide	0.73	0.02	-73.4
Nitrate	0.16	0.01	-65.4
Benzenesulfonate	0.29	0.16	-31.1
Benzoate	0.10	0.12	-28.3
p-Toluenesulfonate	0.35	0.38	-28.6
p-Toluate	0.12	0.37	-25.8
4-Ethylbenzenesulfonate	0.42	1.09	-26.8
2-Naphthalenesulfonate	1.99	0.98	-26.5
4-Propylbenzoate	0.15	2.54	-22.6
4-*t*-Butylbenzoate	0.14	3.50	-21.1
4-Heptylbenzoate	0.20	3.08	-18.3
μ_{poly}[2]		1.50	
μ_{cd}[2]		-2.86	

[1] - $x10^{3}$; [2] - $x10^{-9} m^2 V^{-1} s^{-1}$.

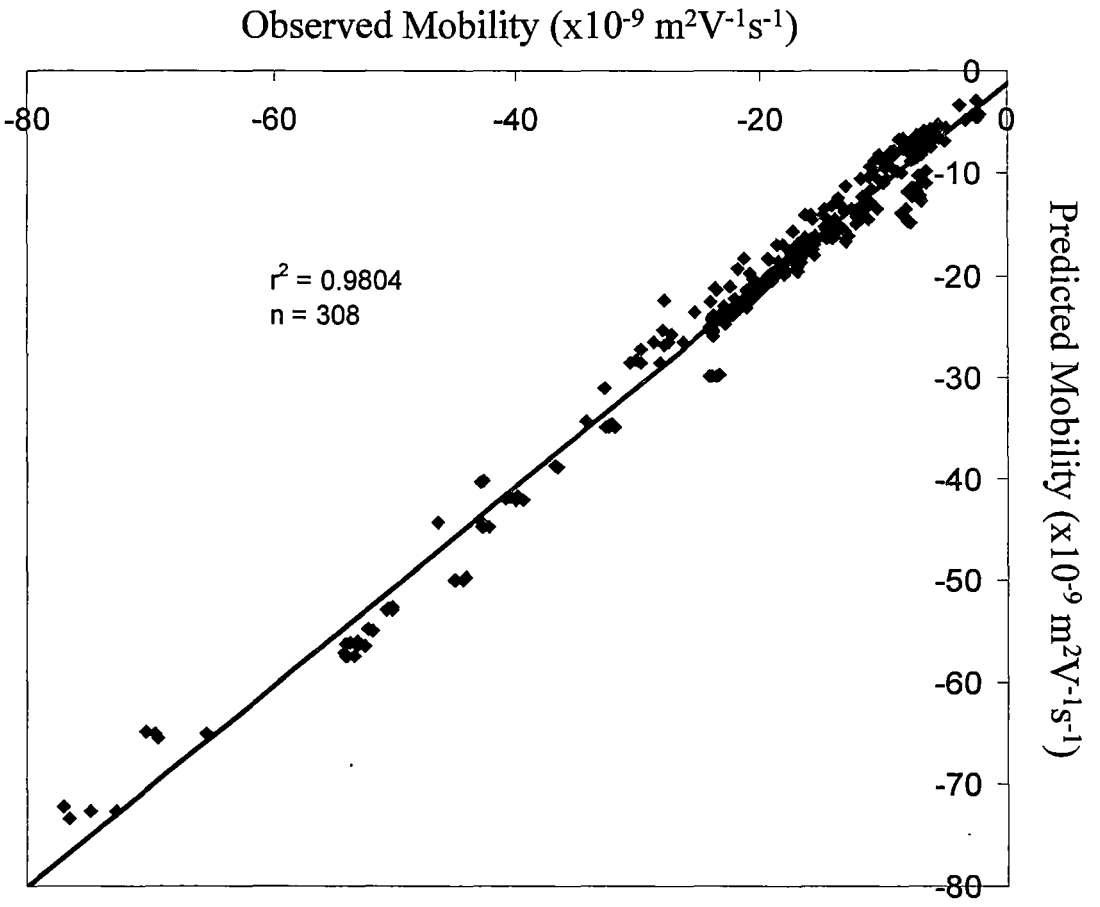

Figure 3.3: Correlation between predicted and observed mobilities using 28 different electrolyte compositions, calculated using parameters derived from non-linear regression performed using 13 experimental conditions.

total of 308 data points is contained in the validation set and a high degree of correlation was obtained. It should also be noted that the validation set was obtained using more than one capillary, showing that the system was very reproducible even after replacement of the capillary and re-coating with a fresh layer of PDDAC.

Determining the precision of the K values obtained is difficult due to the fact that the errors (% RSD) of the input (experimental) values do not translate to errors in the modelled constants. However, an estimation of precision can be obtained by comparison of the numbers acquired when the entire dataset is used to derive the constants. We found that K_{poly} values differed by less than 10%, while the K_{cd} values differed by less than 25%. These are reasonable values considering the model has to calculate these constants over three independent variables. It should also be noted that this analysis only gives an approximate guide to the precision of the results, relying on that fact that the values become more accurate as the size of the dataset is increased.

3.7 Optimisation

The availability of a model to describe the migration behaviour of the analytes introduces the possibility of optimizing the system using a suitable algorithm. Optimisation was performed using the normalised resolution product (NRP) criterion, as shown in Chapter 2, designed to reach a maximum value when all analytes are evenly separated.

Figure 3.4 shows the resolution surface obtained using the constants shown in Table 3.2, and indicates that the optimal conditions were 0.6%PDDAC, 3.5mM β-CD and 100mM Cl^-. A separation obtained using these conditions is shown in Figure 3.5 for a

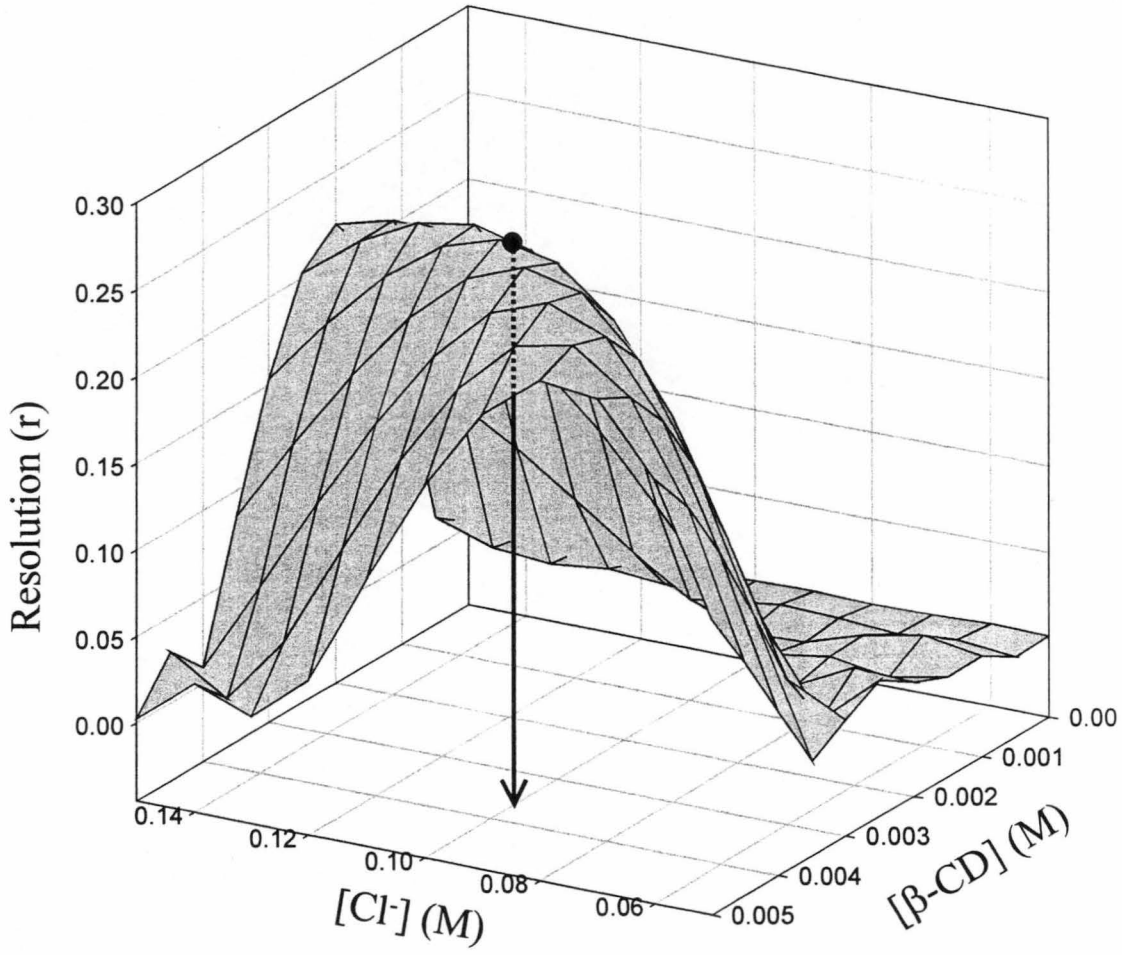

Figure 3.4: Resolution surface showing the normalised resolution product (*r*) plotted over the selected experimental space for 11 analytes using a electrolyte containing 0.6% PDDAC. The global optimum conditions are at 0.6% PDDAC, 3.5mM β-CD and 100mM Cl⁻.

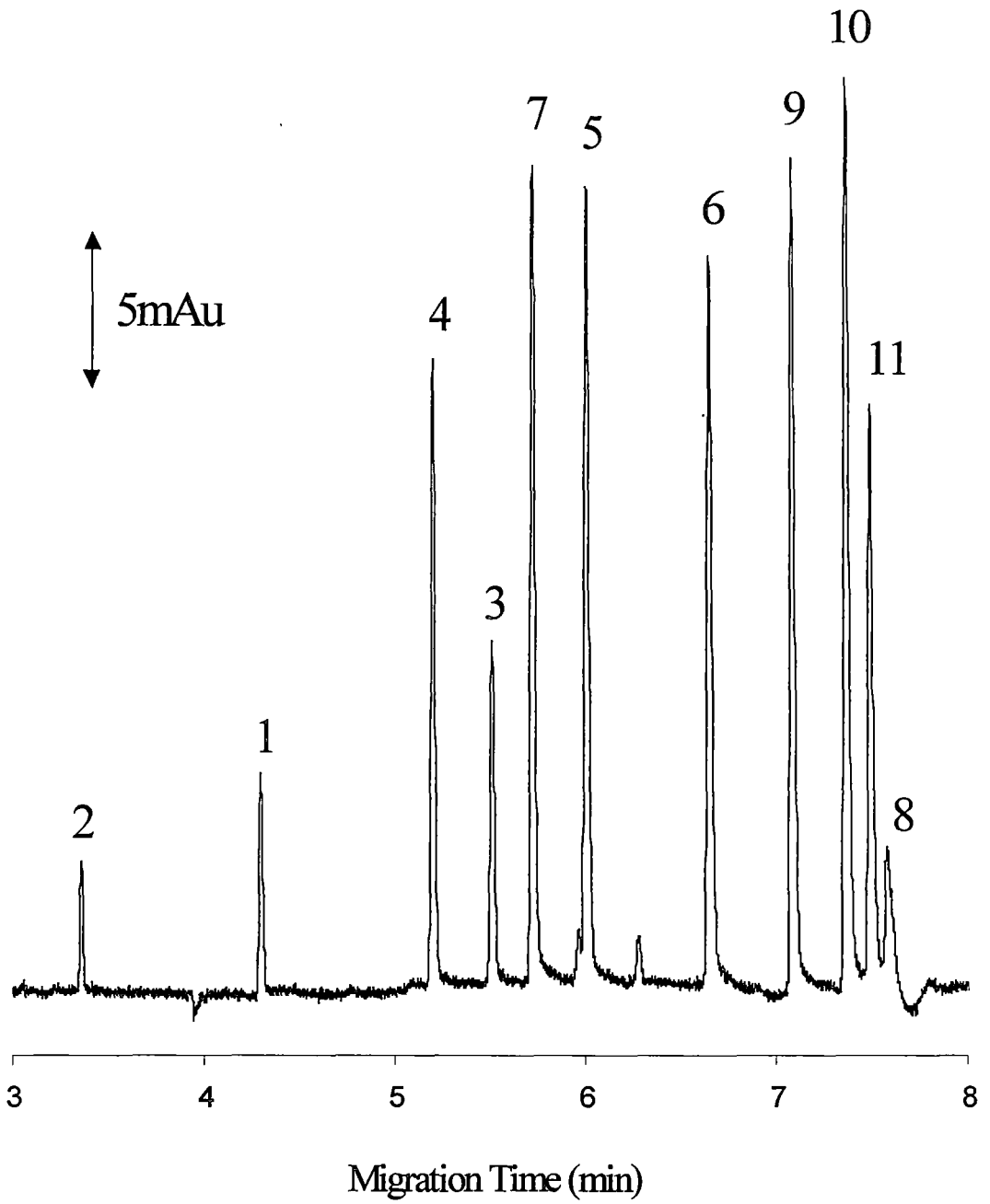

Figure 3.5: Optimal separation determined under the conditons predicted in Error! Reference source not found.. **Peaks are 1=iodide, 2=nitrate, 3=benzenesulfonate, 4=benzoate, 5=toluenesulfonate, 6=ethylbenzenesulfonate, 7=toluate, 8=naphthalenesulfonate, 9=propylbenzoate, 10=*t*-butylbenzoate and 11=heptylbenzoate. Capillary: 50μm x 50cm (41.5cm to detector), detection at 195nm.**

mixture of 11 analytes. Agreement between predicted and observed mobilities for this mixture was good, with differences being less than 0.8 x $10^{-9}m^2V^{-1}s^{-1}$.

3.8 Tuning the separation selectivity

Increasing the number of interactions in an EKC system improves the selectivity control. This can be used to predictably attain a desired separation selectivity. To this end studies were undertaken on the separation of particular pairs of analytes. The aim was to find conditions giving optimal separation and a desired migration order. Thus, the migration model was used to maximise the mobility difference between a pair of analytes, A_1 and A_2, subject to the condition that, for example $\mu_1>\mu_2$ so that A_1 migrates faster than A_2. It should be noted that although the work undertaken here was limited to two analytes, it is straightforward to extend the number of analytes. The ability to control the separation selectivity in this way offers advantages where co-migration is a problem or where peaks are masked by other components present in the sample at much larger concentrations.

Figure 3.6 and Table 3.3 show three examples of tuning the separation selectivity. Figure 3.6 shows separations which have been optimised for pairs of analytes, with these analytes migrating in a particular order in one electropherogram, and then in the reverse order in the next. Figure 3.6 (a) shows manipulation of the iodide and nitrate peaks. Since iodide interacts more strongly with PDDAC than nitrate it can be expected that for nitrate to migrate faster than iodide, significant IE effects would be needed (i.e. a high %PDDAC and a low [Cl^-] as the competing ion). The reverse situation should apply when iodide is to migrate faster than nitrate (e.g. when the electrolyte contains no PDDAC). The predicted optimal electrolyte compositions reflect these expectations (Table 3.3). It can also be seen that in both cases no β-CD

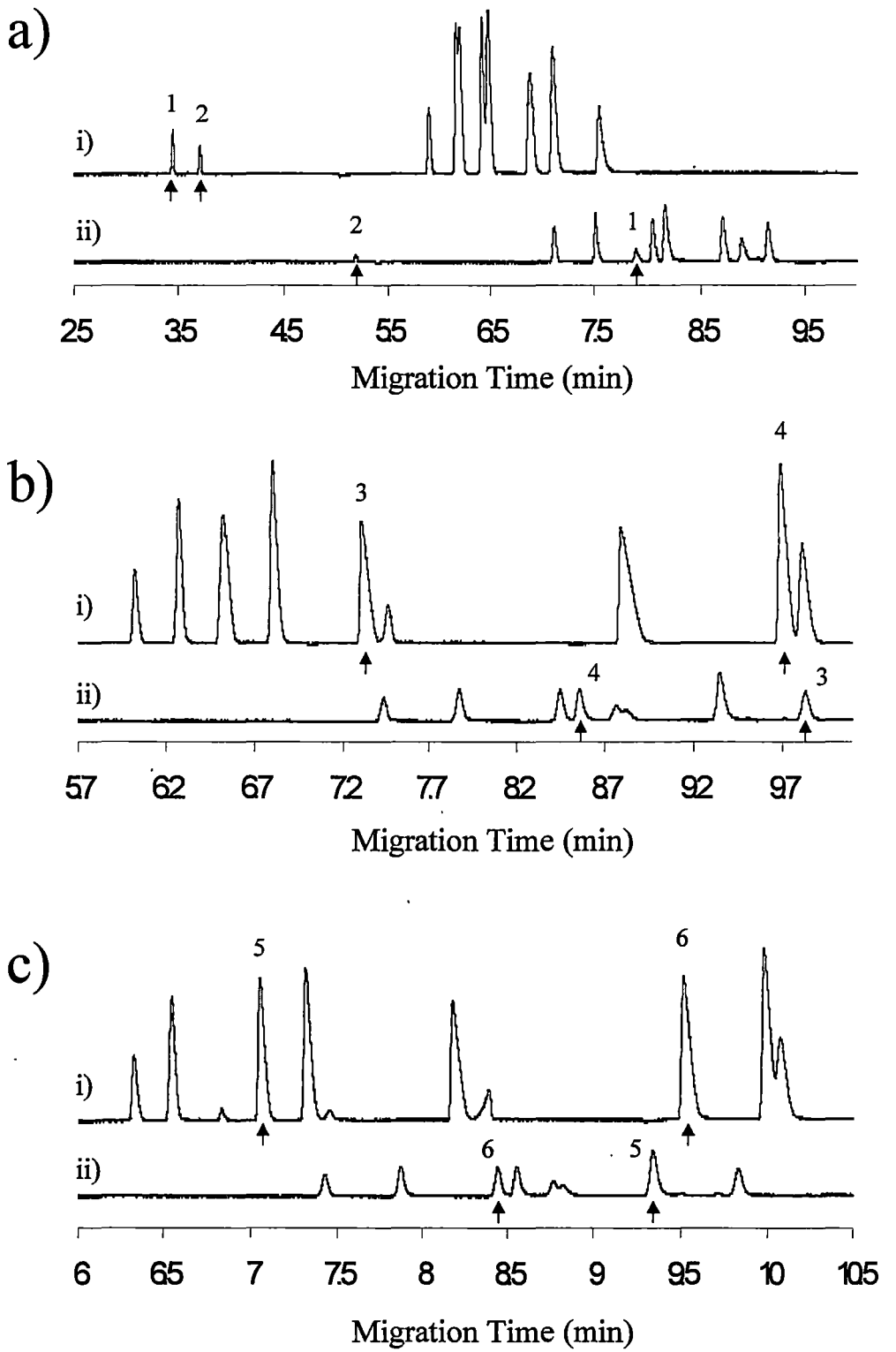

Figure 3.6: Control of migration order for selected pairs of analytes. (a) iodide and nitrate, b) *t*-butylbenzoate and ethylbenzenesulfonate and (c) propylbenzoate and toluenesulfonate. Conditions are given in Table 3.3. Capillary: 50μm x 50cm (41.5cm to detector), detection at 195nm.

Table 3.3: Experimental conditions used for the separations shown in Figure 3.6.

Figure	*Desired migration order*	*Optimal conditions*		
		%PDDAC	*[β-CD] (mM)*	*[Cl⁻] (mM)*
3.6 (a)i.	μ(iodide)>μ(nitrate)	0	0	150
3.6 (a)ii.	μ(nitrate)>μ(iodide)	0.7	0	50
3.6 (b)i.	μ(4-ethylbenzenesulfonate)> μ(4-*t*-butylbenzoate)	0	1.5	150
3.6 (b)ii.	μ(4-*t*-butylbenzoate)> μ(4-ethylbenzenesulfonate)	1.0	0	50
3.6 (c)i.	μ(4-toluenesulfonate)> μ(4-propylbenzoate)	0	3.6	150
3.6 (c)ii.	μ(4-propylbenzoate)> μ(4-toluenesulfonate)	1.0	0	50

is needed, resulting from the minimal interaction between the inorganic analytes and β-CD. It should be noted that for electrolytes lacking PDDAC, [Cl^-] has no effect on the calculated mobilities and as such the selected value for the [Cl^-] arises from the arbitrary starting value chosen. Thus, for the separation shown in Figure 3.6 (a), the model would predict the same mobilities for any [Cl^-].

Figure 3.6 (b) shows the manipulation of the *t*-butylbenzoate and ethylbenzenesulfonate peaks. Again the predicted electrolyte compositions for each migration order agree with those that would be expected. In the case where *t*-butylbenzoate is to migrate faster then ethylbenzenesulfonate, maximum IE interactions are needed (i.e. high %PDDAC and low [Cl-]) since the sulfonates have higher IE selectivity coefficients than the carboxylates. The reverse migration order should be achievable when the electrolyte contains no PDDAC, but with some β-CD since *t*-butylbenzoate interacts more strongly with the β-CD than ethylbenzenesulfonate. From Table 3.3 it can be seen that the predicted electrolyte compositions agree with these points. Similar trends can be seen in Figure 3.6 (c) for the separation of propylbenzoate and toluenesulfonate.

In the case were a particular migration order cannot be achieved, the optimisation yields conditions that provide the separation which is closest to the desired order, usually by bringing the two analytes as close together as possible. An example of this is the separation of benzoate and toluate, which can be achieved only with benzoate migrating faster than toluate. It should also be noted that the process used to attain a desired migration order considered only the analytes in question and the identified optimal conditions could therefore result in co-migration of an analyte with another component of the sample. Again, a straightforward modification of the optimisation algorithm could be used to overcome this deficiency. In a similar manner, the process

used here could also be adapted to find the conditions needed to elute a particular analyte in the shortest possible time.

3.9 Conclusions

The EKC system consisting of PDDAC and β-CD combines two complementary chromatographic separation mechanisms with an electrophoretic separation. The IE and hydrophobic interactions between anionic analytes and both p-SPs can be varied independently and used to control the separation selectivity of the system using the parameters %PDDAC, [Cl^-] and [β-CD]. The system can also be described using a mathematical model which adequately describes the analyte mobilities under changing electrolyte conditions and this model can be used to optimise the conditions for separation of an analyte mixture or to obtain conditions where desired peak pairs migrate in a particular order.

The described separation system is potentially applicable to any analytes exhibiting different interactions with the PDDAC and the cyclodextrin. One particular area of application could be the analysis of pharmaceutically important compounds, and especially in the area of enantiomeric separations. The ability to control selectivity via different analyte-SP interactions could potentially allow for both an enantioselective separation and the separation of closely migrating compounds.

It should be noted that although the system described here provides control of separation selectivity, it is applicable only to those analytes which show appreciable interactions with one or both of the pseudo-SPs. A further limitation is the lack of electrophoretic mobility of the neutral β-CD, which restricts the degree to which interactions with β-CD can be used to alter analyte mobilities. This could be overcome by using a cationic CD that migrated in the opposite direction to the analyte

anions, but this could also possibly introduce further IE interactions, adding to the complexity of the system.

3.10 References

1. M.C. Breadmore, P.R. Haddad and J.S. Fritz, *Electrophoresis*, 21 (2000) 3181.
2. Y. Wang and P.L. Dubin, *Anal. Chem.*, 71 (1999) 3463.
3. *CRC Handbook of Chemistry and Physics*, CRC Press, Boca Raton, 1999.
4. P.R. Haddad and P.E. Jackson, *Ion Chromatography. Principles and Applications*, Amsterdam, 1990.
5. J. Snopek, I. Jelinek and E. Smolkova-Keulemansova, *J. Chromatogr.*, 452 (1988) 571.

Chapter 4

Selectivity Control for the Separation of Opiate Alkaloids using Sulfated-β-Cyclodextrin as a Pseudo-Stationary Phase

4.1 Introduction

Opiate compounds have long been used either therapeutically or illicitly and as such their determination is important in the pharmaceutical industry or forensic analysis. Traditionally, capillary gas chromatography (cGC) and high-performance liquid chromatography (HPLC) have been the most popular techniques for the determination of opiate compounds. However, these techniques have some limitations and problems can arise for compounds that are thermally degradable, polar or non-volatile [1]. Recently, the use of capillary electrophoresis (CE) has proven to be a viable alternative which overcomes many of the problems encountered when using cGC or HPLC. Generally CE separations of opiates are performed either in acidic or basic electrolytes where the opiates are either fully or partially protonated, respectively. Unger *et al.* [2] separated various alkaloid classes, including the opiates thebaine, codeine and morphine, using a 1:1 ammonium acetate acetonitrile electrolyte at pH 3.1 while Tagliaro *et al.* [3] used CE to analyse hair samples for cocaine and morphine using borate electrolytes at pH 9.2.

Although straight CE has been applied successfully to the determination of opiates, this approach is limited due to lack of a convenient method to vary the separation

selectivity and thereby to enable the method to be used with samples of widely differing compositions.

The use of additives to improve separation has become a popular approach to the analysis of many pharmaceutical compounds, including opiates. Several papers dealing with the micellar electrokinetic chromatography (MEKC) separation of opiate related compounds using sodium dodecylsulfate (SDS) have been reported for both acidic and basic electrolytes [4-6]. As well as SDS, cationic surfactants such as cetyltrimethylammonium bromide (CTAB) [7] and zwitterionic surfactants such as 3-N,N-dimethylmyristylammoniopropanesulfonate [8] have also been used.

Cyclodextrins have been widely used in the analysis of many pharmaceutical compounds, especially for enantiomeric separations. Bjornsdottir *et al.* [5] successfully separated 6 opiates including morphine, thebaine and codeine using heptakis(2,6-di-O-methyl)-β-cyclodextrin and then applied this to real samples of opium and drug preparations.

Although previous reports on the separation of opiate compounds using EKC have been published, generally these have not included a detailed study of the mechanism of separation and have employed a qualitative approach to optimisation. Furthermore, these separations have generally relied on partitioning of the opiate between the aqueous electrolyte phase and a hydrophobic p-SP. The use of an anionic cyclodextrin to vary the selectivity of opiate-related compounds has been investigated briefly by Jelinek *et al.* [9] who used 2-O-carboxymethy-β-cyclodextrin (CM-CD) to separate morphine, codeine, thebaine and papaverine. It was found that the addition of CM-CD to an acidic electrolyte at pH 3.7 reduced the mobility of all analytes and this was attributed to formation of complexes between the opiates and the oppositely migrating CM-CD.

To date no EKC system based on ion-exchange (IE) interactions has been demonstrated, especially for the analysis of opiate related compounds. The aim of this chapter is to investigate an EKC system based on an anionic sulfated-β-cyclodextrin for the separation of opiate-related compounds. A further aim is to investigate the possibility of modelling and optimising the system based on IE interactions.

4.2 Experimental

The general details are given in Chapter 2. Detailed conditions are given in each figure caption.

4.2.1 Capillary coating procedures

A dual-coated capillary which gave a pH-independent EOF was used for all separations. For this purpose a coated capillary similar to that described by Katayama *et al.* [10] was used, where the capillary surface was first coated with the cationic polymer polybrene resulting in a reversed EOF, and then with the anionic polymer dextran sulfate resulting in a pH-independent cathodic EOF. For the work presented here polybrene was replaced by poly(diallydimethylammonium chloride) (PDDAC) which resulted in a very similar pH-independent EOF in the final capillary. The capillary was coated by flushing for 30 min with NaOH, 15 min with water, allowing to stand for 30 min, flushing for 15 min with 1% PDDAC, standing for 15 min, flushing for 2 min with water, 15 min with dextran sulfate, standing for 30 min and finally flushing for 5 min with water. Capillaries prepared in this manner were very robust and produced stable EOF values for the entire range of electrolytes used. Figure 4.1 shows the resultant systems used for the analysis of the opiates. Capillaries

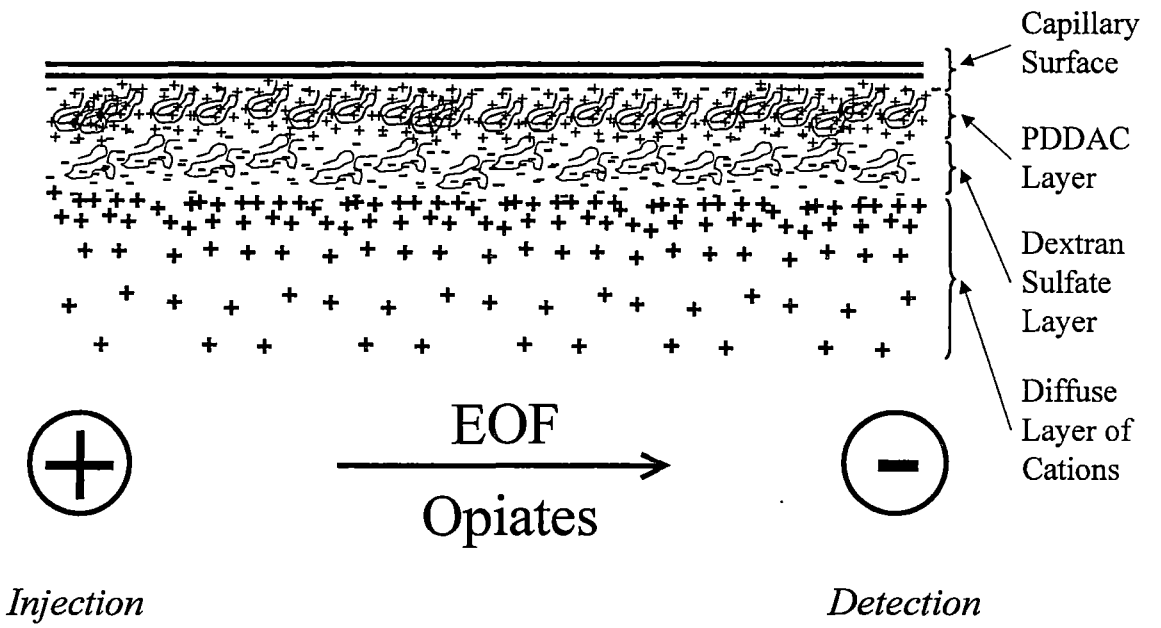

Figure 4.1: System used for separation of the organic bases.

were equilibrated by flushing with each new electrolyte for 15 min prior to use. This produced stable, reproducible migration times for all electrolytes tested.

4.2.2 Electrolyte preparation

Stock solutions of 100mM citric acid and sodium citrate were prepared from the appropriate solid. Citrate electrolytes were prepared by mixing 1.5ml of 100mM citric acid with 0.5ml of 100mM sodium citrate, producing a 20mM electrolyte. The appropriate mass of s-β-CD was then dissolved in the electrolyte and the pH adjusted to 3.50 with 1M HCl.

4.3 Selectivity

It can be expected that two possible interactions will occur between s-β-CD and the opiates, namely partitioning into the hydrophobic cavity of the CD and, since the opiates are protonated at the pH of the electrolyte, electrostatic interaction with the sulfate groups on s-β-CD. Figure 4.2 shows the effect on mobility of varying both the concentration of s-β-CD and NaCl in the electrolyte. It can be seen that increasing the concentration of s-β-CD decreased the mobility of the three opiates shown (this effect was also observed for the other opiates but these have been omitted from the figure for clarity). This resulted from the opposing migration directions of the opiates and the s-β-CD, towards the detector and injection end of the capillaries, respectively. This trend did not clarify the exact nature of the interaction between the opiates and the s-β-CD since both hydrophobic partitioning and electrostatic interactions would result in decreased analyte mobilities. However, if the interaction with the s-β-CD was predominantly IE in nature, then varying the nature and concentration of a competing cation in the electrolyte should increase the observed mobility by

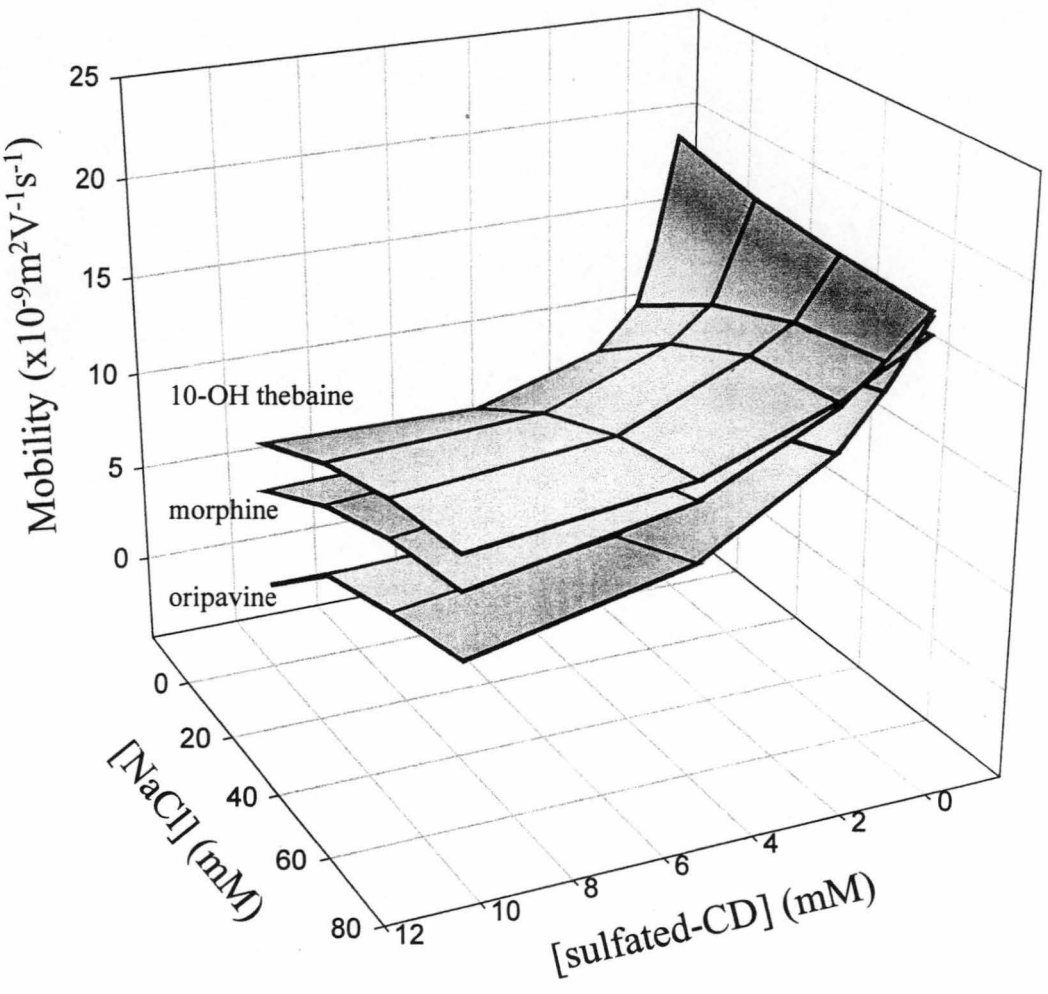

Figure 4.2: Plot of mobility versus [s-β-CD] and [NaCl] for morphine, 10-OH thebaine and oripavine. Conditions: 20mM Citrate electrolyte at pH 3.50, 50μm x 50cm (41.5cm to detector) capillary.

decreasing the interaction between the opiates and the s-β-CD. This is indeed observed in Figure 4.2 as [Na^+] was increased and also in Figure 4.3 where increasing concentrations of the competing cation (Na^+ or Mg^{2+}) increased the observed mobility of all the opiates. Figure 4.3 also shows the effect of changing the competing cation from Na^+ to Mg^{2+}. It can be seen that Mg^{2+} exerted a much stronger effect than Na^+, as would be expected due to higher charge and stronger IE interaction with the sulfate groups on the cyclodextrin. However, when using Mg^{2+} as the competing ion, there was also a large increase in the observed EOF [t_m for EOF of 6.7min (μ_{EOF} = $34 \times 10^{-9} m^2V^{-1}s^{-1}$) at 0mM $MgCl_2$, compared to t_m for EOF of 14min (μ_{EOF} = $16 \times 10^{-9} m^2V^{-1}s^{-1}$) at 50mM $MgCl_2$) so that the migration times of the opiates remained approximately the same. The change in EOF was far less pronounced when Na^+ was used as the competing ion with the migration time of the EOF going from 6.5min ($\mu_{EOF} = 35 \times 10^{-9} m^2V^{-1}s^{-1}$) at 0mM NaCl to 7.5min ($\mu_{EOF} = 31 \times 10^{-9} m^2V^{-1}s^{-1}$) at 100mM NaCl. Baselines at >2 mM $MgCl_2$ were also less stable than when NaCl was used. The most probable reason for these observations was the stronger interaction of Mg^{2+} with the negative wall of the capillary (due to the final layer of dextran sulfate), leading to decreased EOF. Due to these phenomena NaCl was used as the competing ion in all subsequent work.

From these results it can be reasonably concluded that the predominant interaction between the opiates and the s-β-CD is IE in nature rather than hydrophobic partitioning. It can also be seen that at high competing ion concentrations the observed migration order approached that of the standard CE separation, which also indicated that IE was the main interaction. Finally, it was also found that the use of neutral β-CD as a p-SP exerted very little effect on the separation of the opiates, again

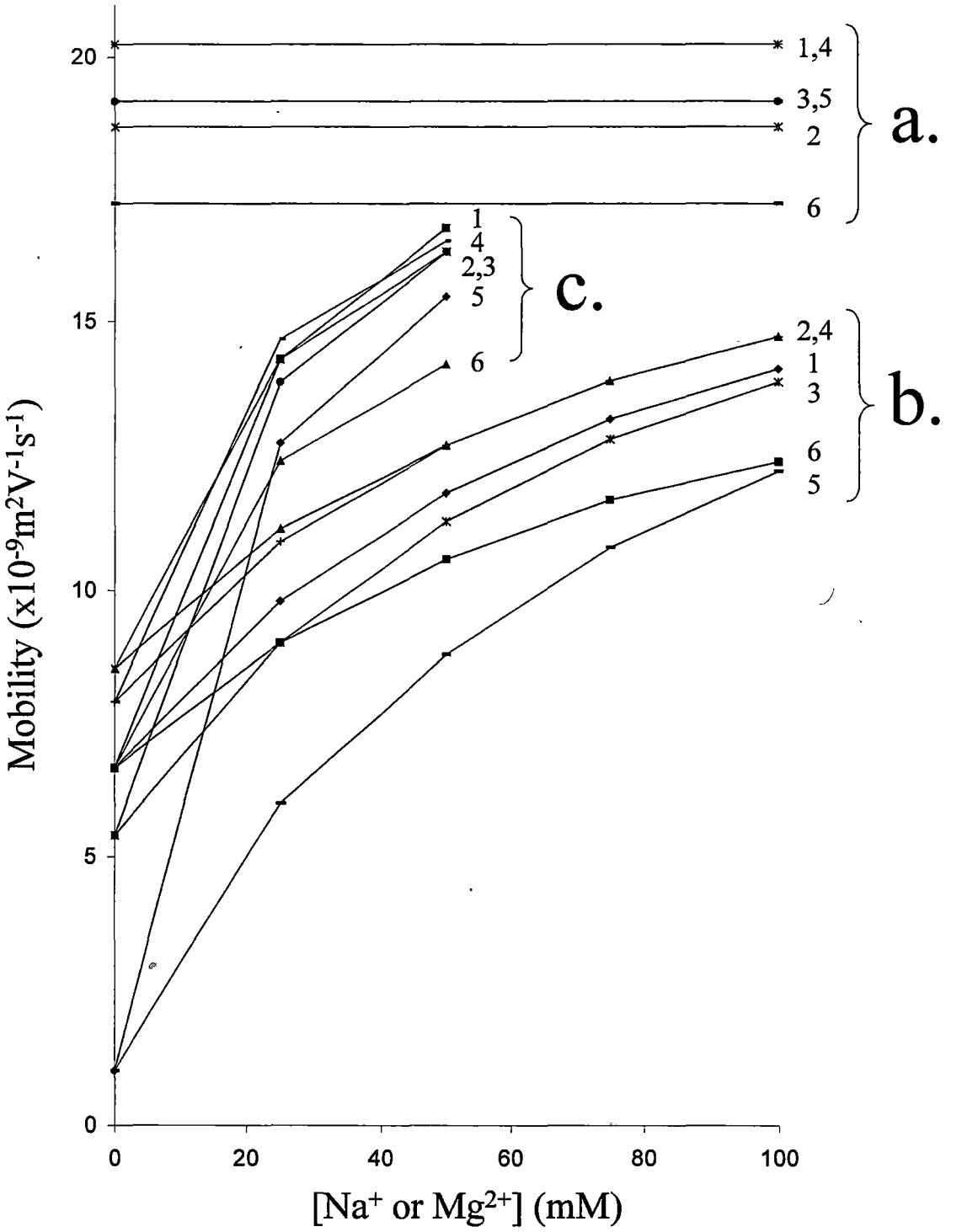

Figure 4.3: Effect of competing ion on the separation of opiates in a electrolyte containing 3.0mM s-β-CD. a) Observed electrophoretic mobility with no IE interaction (i.e. no additives in the electrolyte), b) Effect on mobility of increasing Na^+ concentration and c) Effect on mobility of increasing Mg^{2+} concentration. Analytes: 1=morphine, 2=10-OH thebaine, 3=thebaine, 4=codeine, 5=oripavine and 6=laudanine. Conditions: 20mM Citrate electrolyte at pH 3.50, 50μm x 50cm (41.5cm to detector) capillary.

suggesting that the interaction between the opiates and the β-CD ring is rather small, especially at acidic pH values.

4.4 Modelling the system

Since the interaction between the opiates and the s-β-CD involved IE interactions, it was possible to model the system using a similar IE model to that used by Breadmore *et al.* [11] for the separation of inorganic anions using PDDAC.

If IE interactions are the predominant mechanism of separation then the interaction of the analytes with the s-β-CD can be represented by the following equilibrium:

$$Op^+_{bge} + Na^+_{cd} \overset{K_{ie}}{\rightleftharpoons} Op^+_{cd} + Na^+_{bge} \qquad (4\text{-}1)$$

where Op^+ represents the opiate, Na^+ the competing ion and the subscripts "bge" and "cd" refer to the species in the electrolyte and bound to the cyclodextrin, respectively. The equilibrium constant for eqn. (4-1) is:

$$K_{ie} = \frac{[Op^+]_{cd}[Na^+]_{bge}}{[Op^+]_{bge}[Na^+]_{cd}} \qquad (4\text{-}2)$$

An expression for the analyte retention factor can be derived from first principles [11]

$$k' = w_{\%} K_{ie} Q [E^+]^{-1} \qquad (4\text{-}3)$$

where $w_{\%}$ is the weight percent of the p-SP, Q is the ion-exchange capacity of the p-SP and $[E^+]$ is the concentration of the competing ion in the electrolyte (Na^+ for the work presented here).

As shown in Chapter 3, the observed mobility of an analyte can be expressed in terms of this retention factor:

$$\mu_{ob} = \frac{1}{1+k'}\mu_{bge} + \frac{k'}{1+k'}\mu_{cd} \qquad (4\text{-}4)$$

where μ_{ob} is the observed mobility and μ_{bge} and μ_{cd} are the mobilities of the free opiate in the electrolyte and bound to the cyclodextrin, respectively.

Combining eqns (4-3) and (4-4) leads to a final equation describing the separation of the opiates in the presence of the s-β-CD

$$\mu_{ob} = \frac{1}{1 + w_{\%} K_{ie} Q [Na^+]^{-1}} \mu_{bge} + \frac{w_{\%} K_{ie} Q [Na^+]^{-1}}{1 + w_{\%} K_{ie} Q [Na^+]^{-1}} \mu_{cd} \qquad (4\text{-}5)$$

In equation (4-5), $w_{\%}$ and $[Na^+]$ are known parameters. Q can be estimated from the average degree of substitution of the s-β-CD or can be included as one of the unknown parameters, along with K_{ie}, μ_{bge} and μ_{cd}, and determined by non-linear regression.

Initial application of eqn (4-5) to the separation of the opiates showed that the $[Na^+]^{-1}$ relation ship did not accurately represent the observed trends in μ_{ob}. Replacing this with an $[Na^+]^{-x}$ term (eqn (4-6)) dramatically improved the results allowing the model to accurately predict the observed separations of the opiates. This outcome is most probably due to the fact that the displacement of Na^+ ions by the opiates is not a 1:1 process, as assumed in eqn (4-1). Since the exact displacement ratio will depend on a range of parameters and will be difficult to predict, its value was determined by non-linear regression, together with other unknown parameters in eqn (4-6).

$$\mu_{ob} = \frac{1}{1 + w_{\%} K_{ie} Q [Na^+]^{-x}} \mu_{bge} + \frac{w_{\%} K_{ie} Q [Na^+]^{-x}}{1 + w_{\%} K_{ie} Q [Na^+]^{-x}} \mu_{cd} \qquad (4\text{-}6)$$

4.5 Application of the migration model

Eqn (4-6) has five unknown parameters, K_{ie}, μ_{bge}, μ_{cd}, Q and x, with two variables, $w_{\%}$ and $[Na^+]$. This implied that a minimum of 6 experimental data points was required to determine all of the unknowns. A two dimensional data set of observed mobilities

was obtained over the parameter space determined by 0, 1, 2, 5, 10mM s-β-CD and 0, 25, 50, 75mM NaCl, comprising 20 data points. From these data non-linear regression was performed using the primary dataset consisting of the four corner points and two points taken close to the centre of the parameter space. The total dataset comprising all 20 points was then used to evaluate the predictive power of the model. Table 4.1 shows the constants obtained by non-linear regression of the primary dataset. Two of the five constants are related to the analytes themselves, i.e. K_{ie} and μ_{bge}, while the other three, μ_{cd}, number of IE sites (Q) and x, are related to the electrolyte system and would vary only when a new electrolyte or p-SP was used. The constants obtained agreed well with expected and observed trends. The analytes are listed in Table 4.1 in order of decreasing affinity for the s-β-CD and this order supports the observed trends seen in Figure 4.2. Oripavine showed the strongest affinity for the s-β-CD, 10-OH thebaine the weakest and morphine gave an intermediate value. μ_{bge} values also agreed with observed trends, with migration times predicted for a pure CE separation (i.e. in the absence of s-β-CD and NaCl) varying by less than 0.66% compared to the observed migration times. Table 4.1 shows a μ_{cd} value (relating to the mobility of the opiate-cyclodextrin complex) of -78.9×10^{-9} $m^2V^{-1}s^{-1}$, showing that the negative charge on the s-β-CD was not fully neutralised on complexing with the opiates. Q is related to the number of IE sites contained on each of the s-β-CD molecules and Table 4.1 shows a value 4.7, which was reasonable since the average degree of substitution quoted by the manufacturer is 7-11 mol sulfate/mol of s-β-CD and it can be assumed that not every sulfate group will be available for interaction with the bulky opiate ions. The final constant shown in Table 4.1 is x and the calculated value of 2.1 implies that there was an inverse

Table 4.1: Parameters derived from non-linear regression applied to eqn (4-6)

Opiate	K_{ie}	μ_{bge}^{1}
Analyte Specific Constants		
Oripavine	29.7	19.2
Morphine	22.5	20.2
Thebaine	22.1	19.2
Codeine	19.8	20.2
Laudanine	18.1	17.2
10-OH Thebaine	15.7	18.7
Electrolyte Specific Constants		
μ_{cd}^{1}	-78.9	
No. of IE sites	4.7	
x	2.1	

[1] - $x10^{-9} m^2 V^{-1} s^{-1}$

square relationship between the analyte retention factor and the competing ion concentration. Figure 4.4 shows the correlation between observed mobilities and those calculated using eqn (4-6) and the constants shown in Table 4.1. It can be seen that excellent correlation is obtained with an r^2 value of 0.996 obtained.

4.6 Optimisation

The availability of a model to describe the migration behaviour of the opiates allows for optimisation using a suitable algorithm. Optimisation was performed using the NRP criterion as shown in Chapter 2. Optimisation was also carried out using the minimum resolution (MR) criterion. This criterion takes into account only the peak pair having the worst resolution and is also shown in Chapter 2.

Figure 4.5 shows the resolution surface obtained using the NRP criterion. It can be seen that the optimum separation, i.e. that producing the highest resolution, was calculated to be at 1mM s-β-CD and 45mM NaCl. This should result in a separation where the peaks are as evenly spread over the entire separation as possible. The optimum separation is shown in Figure 4.6 a) with the predicted separation shown in Figure 4.6 b). Although it can be seen that full separation is not obtained using these conditions, the agreement obtained between predicted and observed migration times was <0.83%. However since all of the opiates migrated in a very small time window (less than 30s), even this small deviation between observed and predicted mobilities led to co-migration. A further complicating factor was the slightly tailed nature of the peaks which also contributed to the co-migration of 10-OH thebaine with thebaine and oripavine with laudanine. This was especially evident for oripavine which interacted strongly with the s-β-CD, leading to broadened peaks. Laudanine also

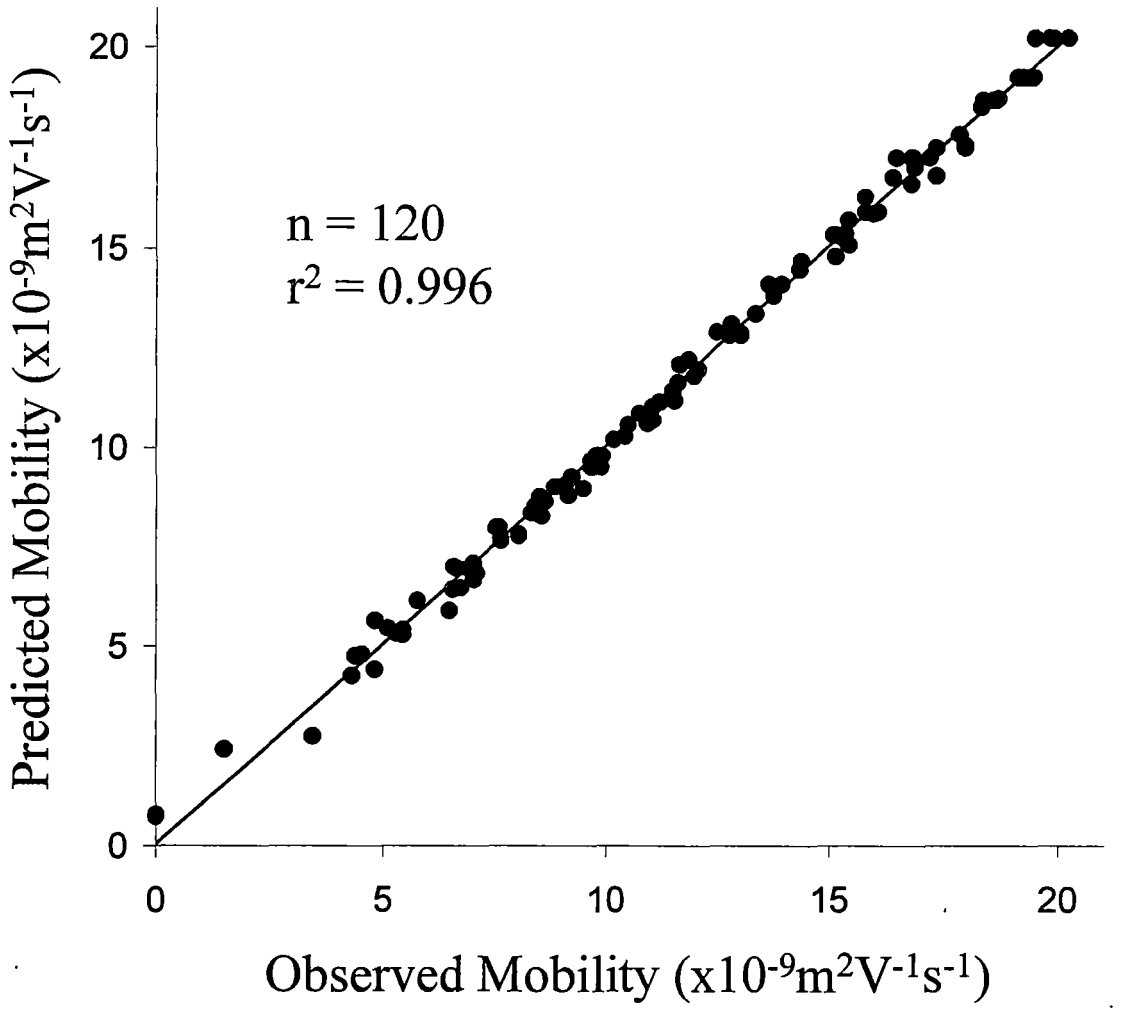

Figure 4.4: Correlation between observed and predicted mobilities using eqn (4-6) and the constants shown in Table 4.1. A total of 120 data points was used for the correlation including the 36 points used to derive the constants.

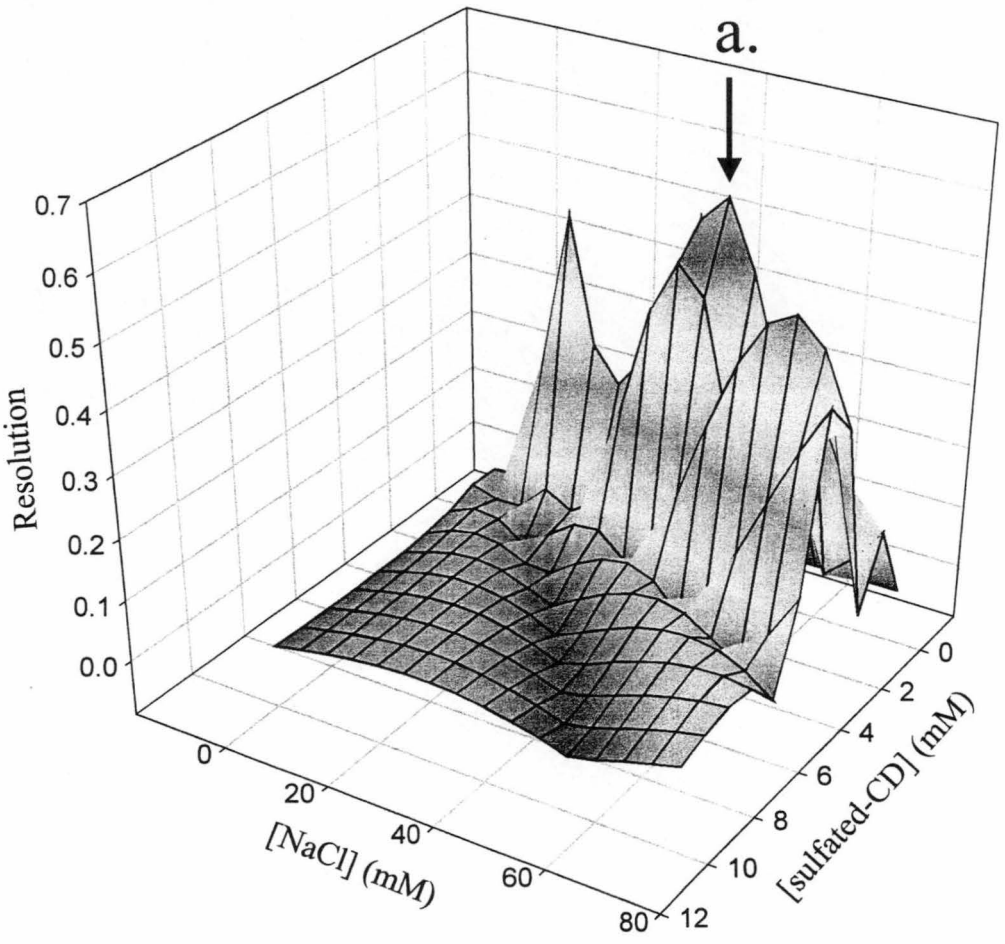

Figure 4.5: Resolution surface obtained using the NRP criterion. a) optimum at 1mM s-β-CD and 45mM NaCl.

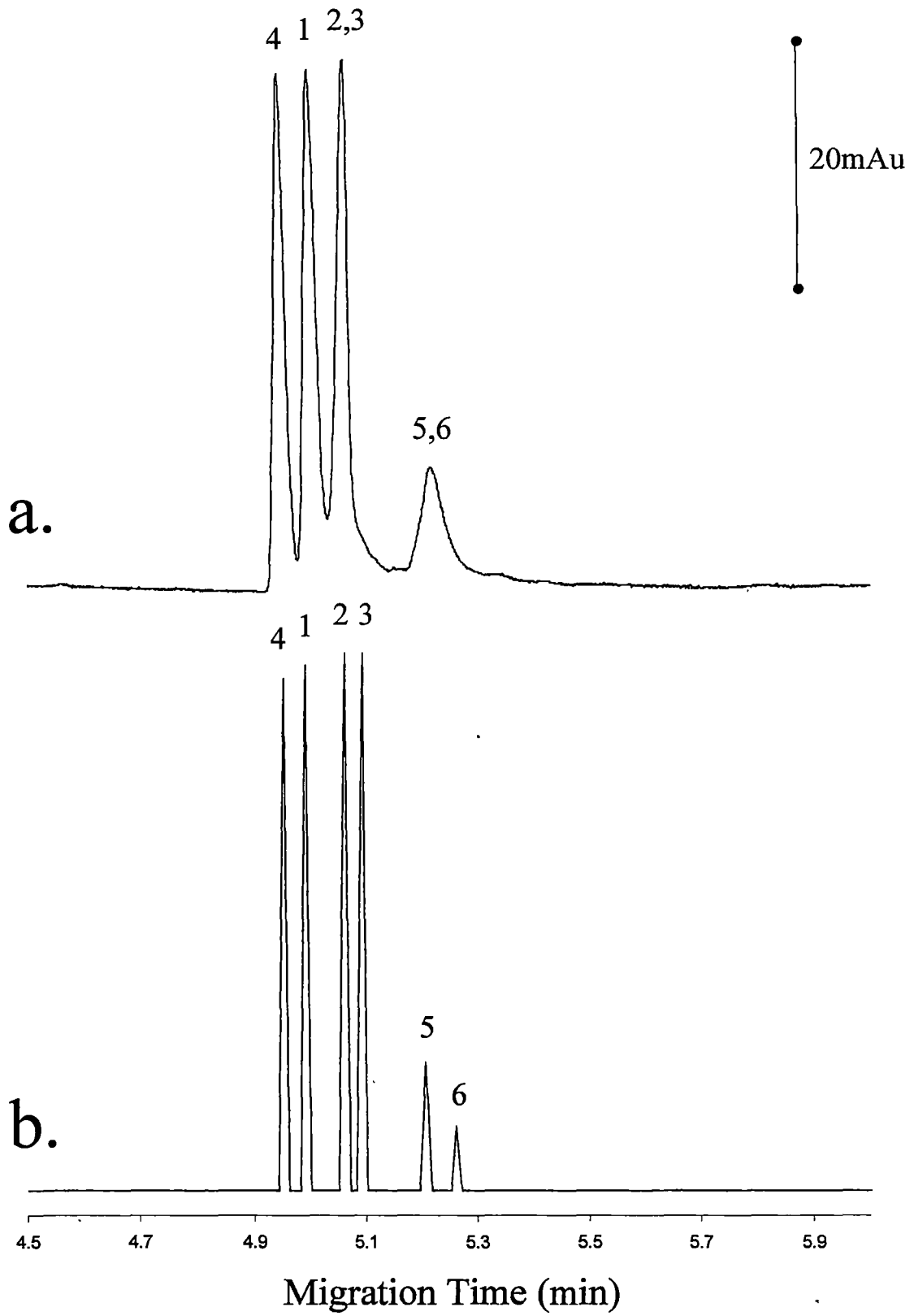

Figure 4.6: Optimal separation calculated using the normalised resolution product criterion. a) Observed separation, b) Predicted separation. Conditions: 1mM s-β-CD and 45mM NaCl. Peaks are 1=morphine, 2=10-OH thebaine, 3=thebaine, 4=codeine, 5=oripavine and 6=laudanine. Electrolyte: 20mM Citrate at pH 3.50, 50μm x 50cm (41.5cm to detector) capillary. Detection at 210nm.

produced a relatively small peak at 210nm, which further contributed to the lack of resolution between oripavine and laudanine.

The system was also modelled using the MR criterion. This criterion considers only the two adjacent peaks having the worst resolution and as such could possibly give a better optimum than that calculated using the normalised resolution product criterion. Figure 4.7 shows the resolution surface obtained using the minimum resolution criterion. It can be seen that the optimum separation was calculated to be at 5mM s-β-CD and 10mM NaCl and Figure 4.8 shows the separation obtained at these conditions. Full resolution was again not obtained but the separation was superior to that obtained using the NRP criterion. The difference between observed and predicted migration times was <1%, as can be seen when comparing Figure 4.8 a) and b). The cause for the co-migration of morphine and laudanine was again the small error in prediction and the fact that the peak for laudanine was very much smaller than morphine at 210nm and it migrated within the tail of the morphine peak. Lowering the wavelength of detection did not alleviate the problem. A further complication with the separation was the system peak seen after oripavine, see Figure 4.8 a). This occurred in a reproducible manner, particularly at higher s-β-CD concentrations, and caused problems with quantification of oripavine which has the strongest interaction with s-β-CD. This problem could be overcome by including the system peak in the optimisation process.

4.7 Conclusions

A sulfated cyclodextrin has been demonstrated to be a suitable cation-exchange p-SP additive for separation of opiate alkaloids. The extent of the IE interactions between the s-β-CD and the protonated opiates can be easily controlled by varying either the

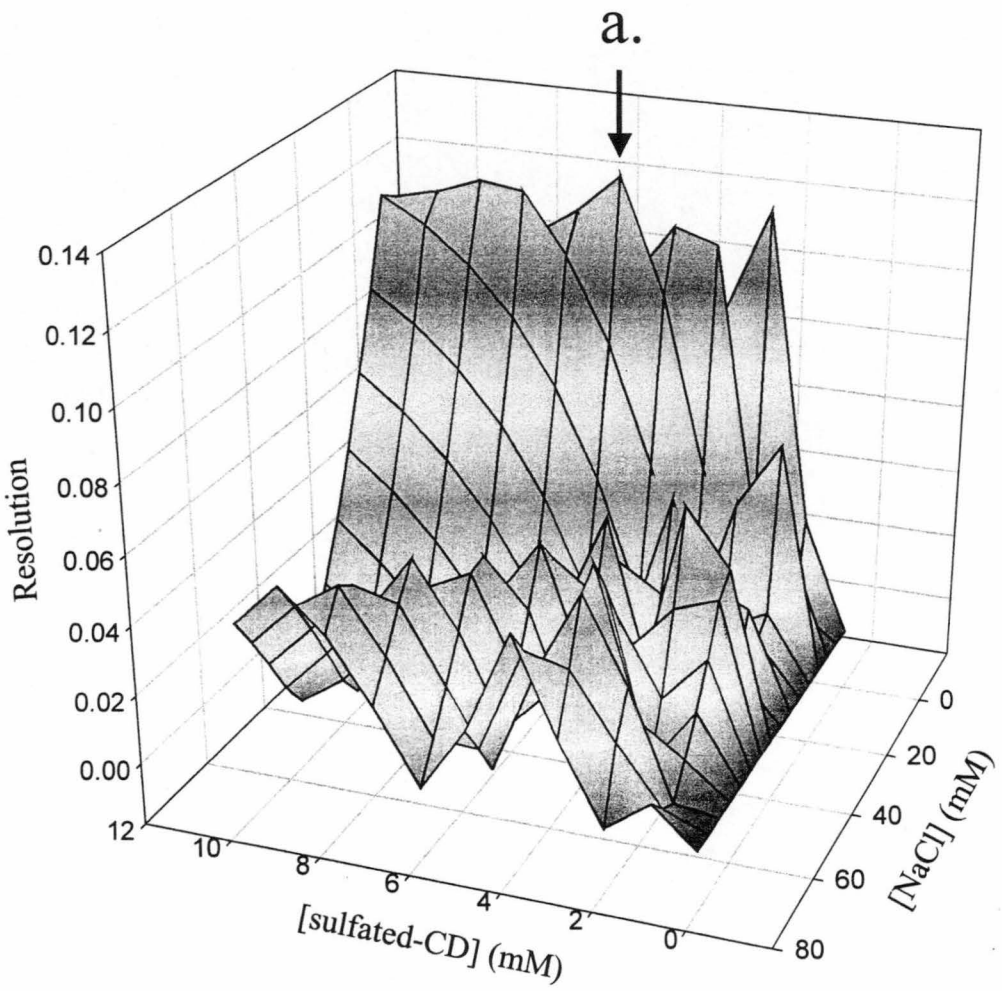

Figure 4.7: Resolution surface obtained using the MR criterion a) optimum at 5mM s-β-CD and 10mM NaCl.

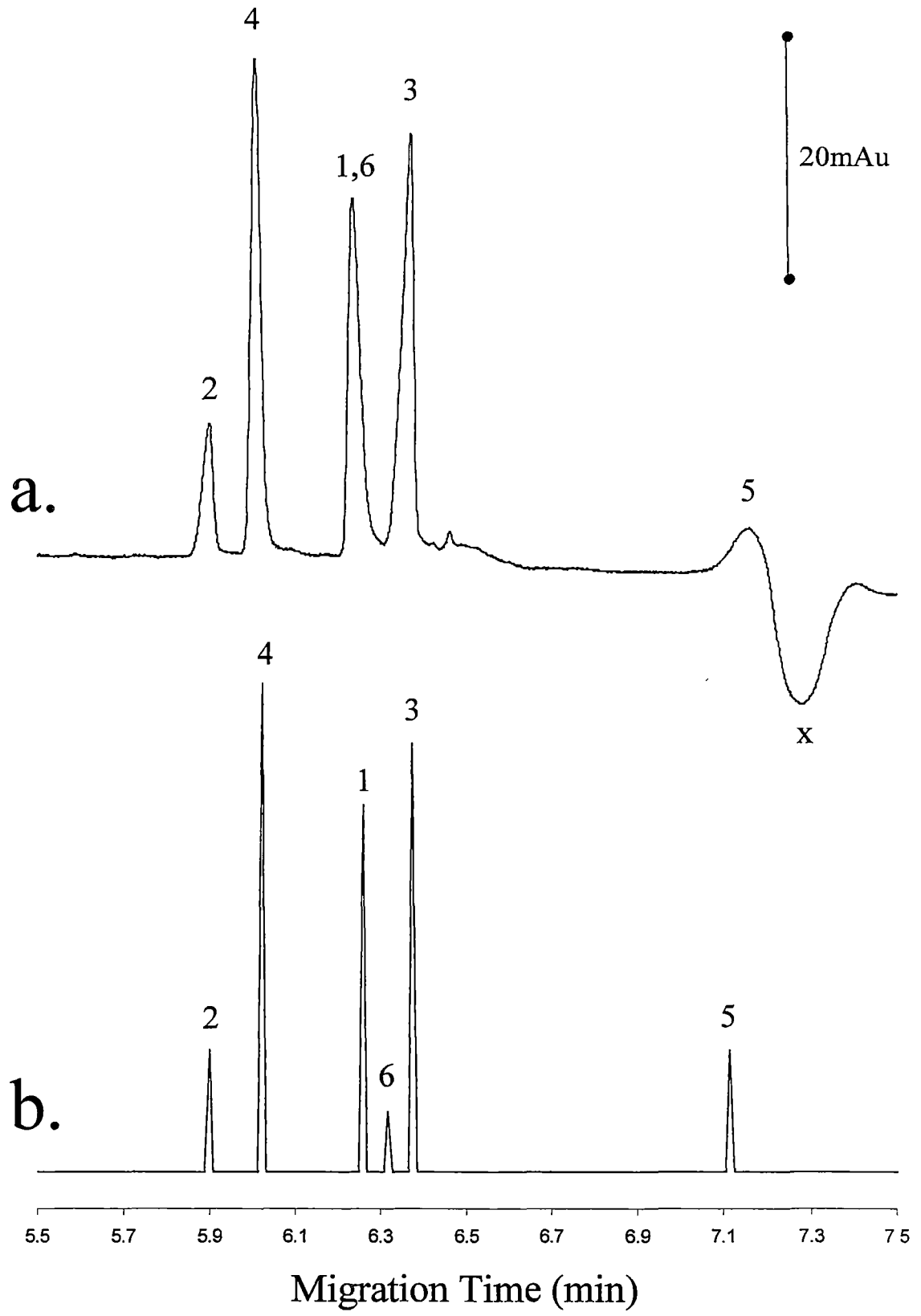

Figure 4.8: Optimal separation calculated using the minimum resolution criterion. a) Observed separation, b) Predicted separation. Conditions: 5mM s-β-CD and 10mM NaCl. Peaks are 1=morphine, 2=10-OH thebaine, 3=thebaine, 4=codeine, 5=oripavine 6=laudanine and x=system peak occurring prior to the EOF. Electrolyte: 20mM Citrate at pH 3.50, 50μm x 50cm (41.5cm to detector) capillary. Detection at 210nm.

concentration of s-β-CD in the electrolyte or the nature and concentration of the competing ion, such as Na^+ or Mg^{2+}. A mathematical model derived from first principles in terms of the IE equilibrium taking place can be used to accurately describe observed separations at any concentration within the experimental space using an initial subset comprising only 6 individual experiments. The system is not only useful for the opiates studied but potentially can be applied to any organic cation that exhibits an IE interaction with s-β-CD, possibly including many classes of pharmaceutically important compounds. The possibility also arises to include further cyclodextrins in the system to permit for simultaneous enantiomeric separations.

4.8 References

1. I.S. Lurie, *J. Chromatogr. A*, 780 (1997) 265.
2. M. Unger, D. Stockigt, D. Belder and J. Stockigt, *J. Chromatogr. A*, 767 (1997) 263.
3. F. Tagliaro, C. Poiesi, R. Aiello, R. Dorizzi, S. Ghielmi and M. Marigo, *J. Chromatogr.*, 638 (1993) 303.
4. C. Zhang and W. Thormann, *J. Chromatogr. A*, 764 (1997) 157.
5. I. Bjornsdottir and S.H. Hansen, *J. Pharm. Bio. Anal.*, 13 (1995) 687.
6. M. Krogh, S. Brekke, F. Tonnesen and K.E. Rasmussen, *J. Chromatogr. A*, 674 (1994) 235.
7. V.C. Trenerry, R.J. Wells and J. Robertson, *J. Chromatogr. A*, 718 (1995) 217.
8. O. Naess and K.E. Rasmussen, *J. Chromatogr. A*, 760 (1997) 245.
9. I. Jelinek, B. Gas, I. Zuskova, E. Niklickova and I. Buben, *Chem. Listy.*, 91 (1997) 487.
10. H. Katayama, Y. Ishihama and N. Asakawa, *Anal. Chem.*, 70 (1998) 2254.
11. M.C. Breadmore, P.R. Haddad and J.S. Fritz, *Electrophoresis*, 21 (2000) 3181.

Chapter 5

Selectivity Control of Aromatic Bases using PVS and β-CD as Mixed Pseudo-Stationary Phases

5.1 Introduction

Cyclodextrins (CDs) have become increasingly popular in recent years, due mainly to intense interest in enantiomeric separations where cyclodextrins have been used to establish chiral interactions with analytes.

Extensive work has been focussed on modelling the observed separations. Wren and Rowe introduced a simple equilibrium-based model for the separation of pairs of enantiomers using neutral cyclodextrins [1]. This model was extended in subsequent papers to take into account resolution and the use of organic modifiers [2,3]. However, the model was used mainly to support observed trends, rather than to predict conditions needed for optimum separations. A more detailed equilibrium model was derived from first principles by Rawjee *et al.* [4] and could be used for weak acids and bases. It took into account three different types of analytes, namely "type I" enantiomers where only the non-ionic forms of the enantiomers interacted differently with the cyclodextrin, "type II" enantiomers where only the dissociated forms of the analytes interacted differently with the cyclodextrin, and "type III" enantiomers where both the ionic and non-ionic forms of the enantiomers interacted differently with the cyclodextrin. To solve the model and to determine the conditions needed for the best enantiomeric separation, model constants (analyte mobilities, analyte-cyclodextrin mobilities and formation constants between the cyclodextrin and

the neutral and charged forms of the enantiomers) needed to be obtained. This required three specific experiments, firstly varying the pH at 0mM cyclodextrin, secondly varying [CD] at high pH, and finally varying [CD] at low pH. This model was applied successfully to weak acids [5] and bases [6]. Williams and Vigh [7] extended the work to take into account charged cyclodextrins. Their model, dubbed the CHARM model (characteristics of the charged resolving agent migration model), was used to predict operating conditions and verified in aqueous and non-aqueous solvents [8,9].

Although several models have been proposed for enantiomeric separations these tend to be quite complicated, especially if useful constants and quantitative conditions needed for optimal separations are to be gained. These models are also not generally applicable to non-enantiomeric separations using cyclodextrins as p-SPs. A simple model yielding useful constants related to analyte-cyclodextrin interactions for non-enantiomeric separations in an electrophoretic system has not been demonstrated. In this chapter a simple model to describe an EKC system containing a neutral β-CD and an anionic polymer (polyvinylsulfonate, PVS) for the separation of a series of aromatic bases is demonstrated. The aims of the chapter are to be able to derive constants related to analyte-cyclodextrin and analyte-PVS interactions and to optimise such a system simply and rapidly.

5.2 Experimental

The general details are given in Chapter 2. Detailed conditions are given in each figure caption.

5.2.1 Capillary coating procedures

Double-coated capillaries utilising PDDAC and dextran sulfate were used. These were prepared using the same procedure outlined in Chapter 4 and resulted in a pH-independent EOF, see Figure 5.1. The resultant coatings were also very robust over the range of pH, [β-CD] and [PVS] values used in this work.

5.2.2 Electrolyte preparation

Stock solutions of 100mM citric acid and sodium citrate were prepared from the appropriate solid. Citrate electrolytes were prepared by mixing various ratios of acid and base to produce 20mM electrolytes with the appropriate pH. Table 5.1 shows the ratio needed for each electrolyte used. The appropriate amounts of β-CD and PVS were then added to each electrolyte to give the desired concentration.

5.2.3 Artificial neural networks

Calculations involving artificial neural networks (ANN) were performed using the Trajan Neural Network Simulator, Release 3.0 (Trajan Software Ltd, Durham, UK).

5.3 Choice of analytes

A series of aromatic bases was chosen as analytes, similar in basic structure to the aromatic acids and sulfonates used in Chapter 3. These exhibited differing functional groups, pK_a values and hydrophobicities, thereby permitting selectivity changes to be achieved by either varying the pH or the concentrations of β-CD and PVS in the electrolyte. Table 5.2 lists the analytes chosen, together with their pK_a values. In some cases pK_a values were not found in the literature and were calculated using ACD/pK_a v4.56, software (Advanced Chemistry Development Inc., Toronto). To test

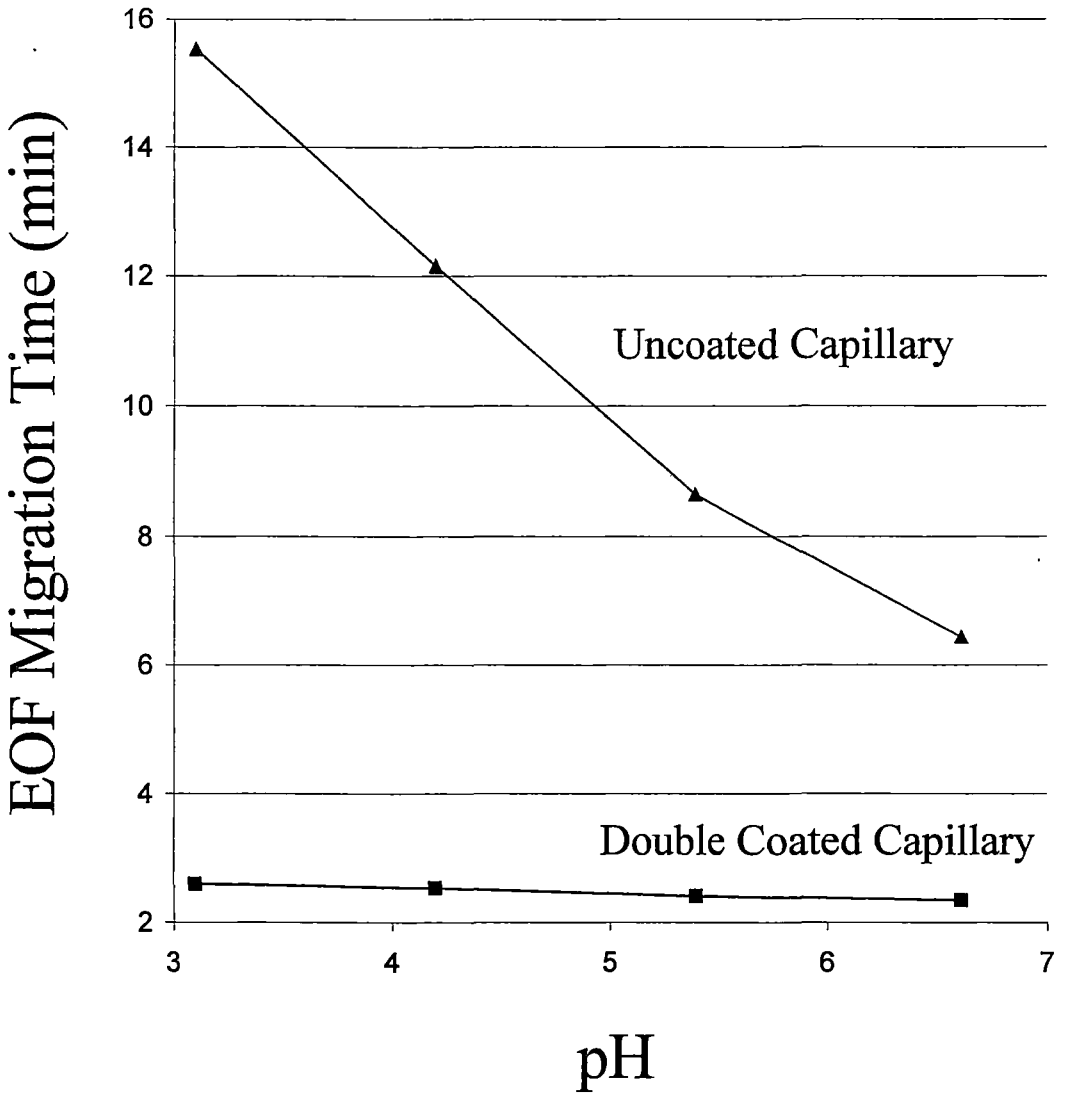

Figure 5.1: EOF vs pH for an uncoated and PDDAC/dextran sulfate coated capillary. Conditions: 20mM Citrate, 50 μm x 35 cm (26.5 cm to detector) capillary. All the conditions (i.e. applied voltage, electrolyte, temperature, capillary length and diameter) were kept constant when measuring EOF migration times for different pH values and capillary types.

Table 5.1: Ratios of citric acid to sodium citrate used to prepare electrolyte of various pH

V(100mM Citric Acid) (ml)	V(100mM Sodium Citrate) (ml)	Electrolyte pH
1.5	0.5	3.45
1.0	1.0	4.50
0.5	1.5	5.50
0.25	1.75	6.10
0.10	1.90	6.60
0.025	1.975	7.20

Table 5.2: pK_a values of the analytes used

Analyte	*pK_a*[1]
Pyridine	5.17
Picoline	6.00
4-Ethylpyridine	5.87
4-t-Butylpyridine	5.99
Quinoline	4.80
p-Aminopyridine	9.11
m-Aminopyridine	6.03
o-Aminopyridine	6.71
Aniline	4.60
4-Ethylaniline	5.00
4-Pentylaniline	5.10[2]
4-Heptylaniline	5.27[2]
Benzylamine	9.35
4-Methylbenzylamine	9.52[2]

1 - from Lange's Handbook of Chemistry, J. A. Dean, McGraw-Hill, New York, 1992, 14. Ed. 2 - Calculated using the ACD/pKa v4.56, Advanced Chemistry Development Inc, Toronto, Canada.

the accuracy of the software, pK_a values of several the analytes with known pK_a's were calculated. Predicted and literature values were 4.61 and 4.60, 5.09 and 5.0, and 9.40 and 9.35 for aniline, 4-ethylaniline and benzylamine, respectively. Based on these results, the calculated values of pK_a were used for pentylaniline, heptylaniline and 4-methylbenzylamine, see Table 5.2.

5.4 Simplified systems

From Figure 5.2 it can be seen that the complete separation system is relatively complex and involves four simultaneous equilibria. Modelling this system by deriving a mathematical model from first principles is relatively complex, and for this reason two simplifications of the system are considered first. System I involves removing pH as a variable, leading to the separation system shown by the following equilibria.

$$BH^{+}_{bge} + E^{+}_{pvs} \overset{K_{pvs}}{\rightleftharpoons} BH^{+}_{pvs} + E^{+}_{bge}$$

$$K_{cd+} \uparrow\downarrow$$

$$BH^{+}_{cd}$$

System I

In this system the pH was maintained at pH 3.50 to ensure that all the bases were protonated fully. System II involved removing [PVS] as a variable, leading to the separation system shown by the following equilibria.

$$B_{bge} + H^{+}_{bge} \overset{K_a^{-1}}{\rightleftharpoons} BH^{+}_{bge}$$

$$K_{cd} \uparrow\downarrow \qquad\qquad \uparrow\downarrow K_{cd+}$$

$$B_{cd} \qquad\qquad BH^{+}_{cd}$$

System II

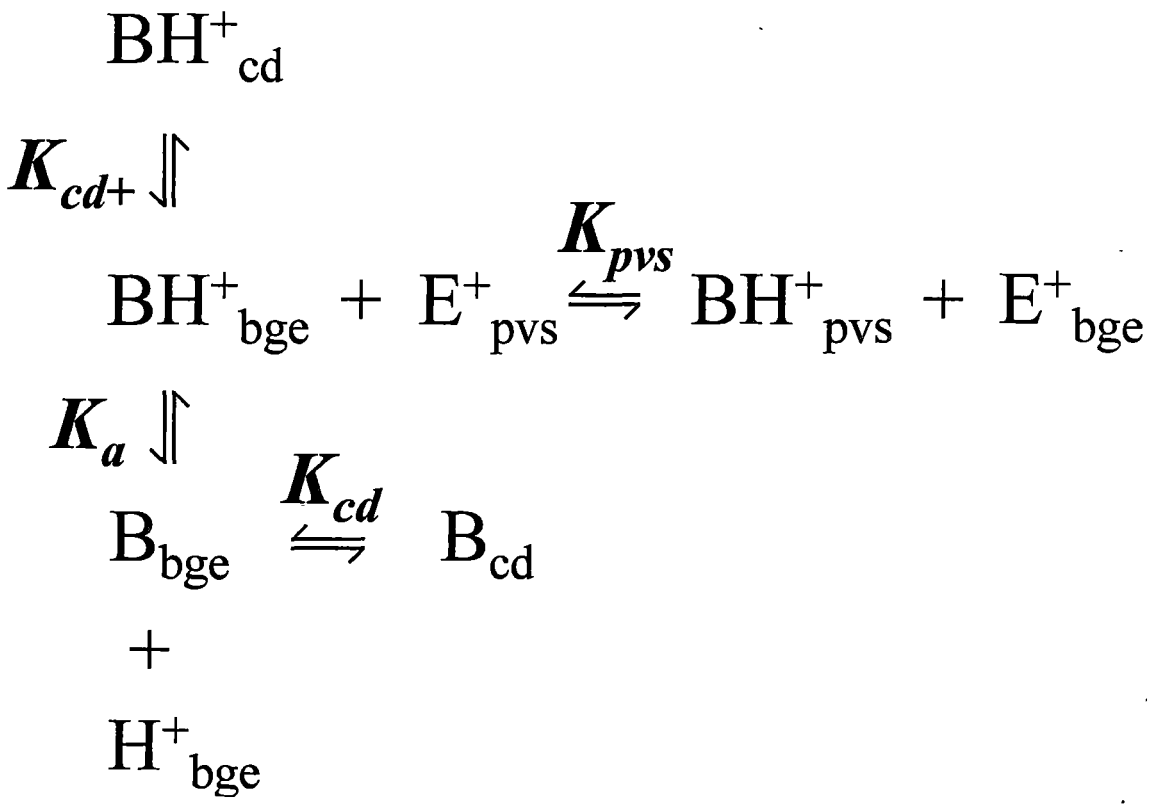

Figure 5.2: Schematic showing the likely equilibrium processes present in the current 3-dimensional system with the variables being [PVS], [β-CD] and pH. K_{pvs} is the ion-exchange selectivity coefficient between the analytes and the PVS. K_{cd} and K_{cd+} are the equilibrium constants between the β-CD and the neutral and protonated base respectively. B and BH^+ represent the neutral and protonated base respectively. E^+ represents the competing ion (Na^+ for the work presented here). The subscripts bge, pvs and cd refer the appropriate species in the electrolyte, PVS or cyclodextrin phases respectively.

In the above equilibria the subscript "bge" refers to species in the electrolyte while "cd" and "pvs" refer to species bound to the cyclodextrin and PVS respectively. K_a is the acid dissociation constant, K_{cd} and K_{cd+} are the equilibrium constants for the interaction between the neutral analyte with the cyclodextrin and charged analyte with the cyclodextrin respectively. K_{pvs} is the equilibrium constant associated with the interaction between the cationic analytes and the anionic PVS.

5.5 System I

5.5.1 Selectivity

Separations of anions performed using PDDAC as a p-SP showed that hydrophobic interactions between the polymer and small organic anions were very weak, see Chapter 3. It therefore can be reasonably assumed that PVS would also show only very weak hydrophobic interactions and should exhibit predominantly IE interactions with small organic cations. This can be seen in Figure 5.3 which shows the effect of adding 2%(w/v) PVS to the electrolyte. It can be seen that the addition of PVS decreased the mobility of all the analytes, with the magnitude of this interaction differing between analytes and therefore leading to changes in selectivity. It is also evident that addition of PVS to the electrolyte affected the anilines and benzylamines more than the pyridines, indicating that pyridines had the weakest interactions with PVS.

If the interaction between PVS and the bases was predominantly IE in nature, increasing the concentration of the competing ion in the electrolyte should decrease these interactions. A similar effect should be observed if the competing ion was replaced by a stronger competing ion, for example by replacing a monovalent

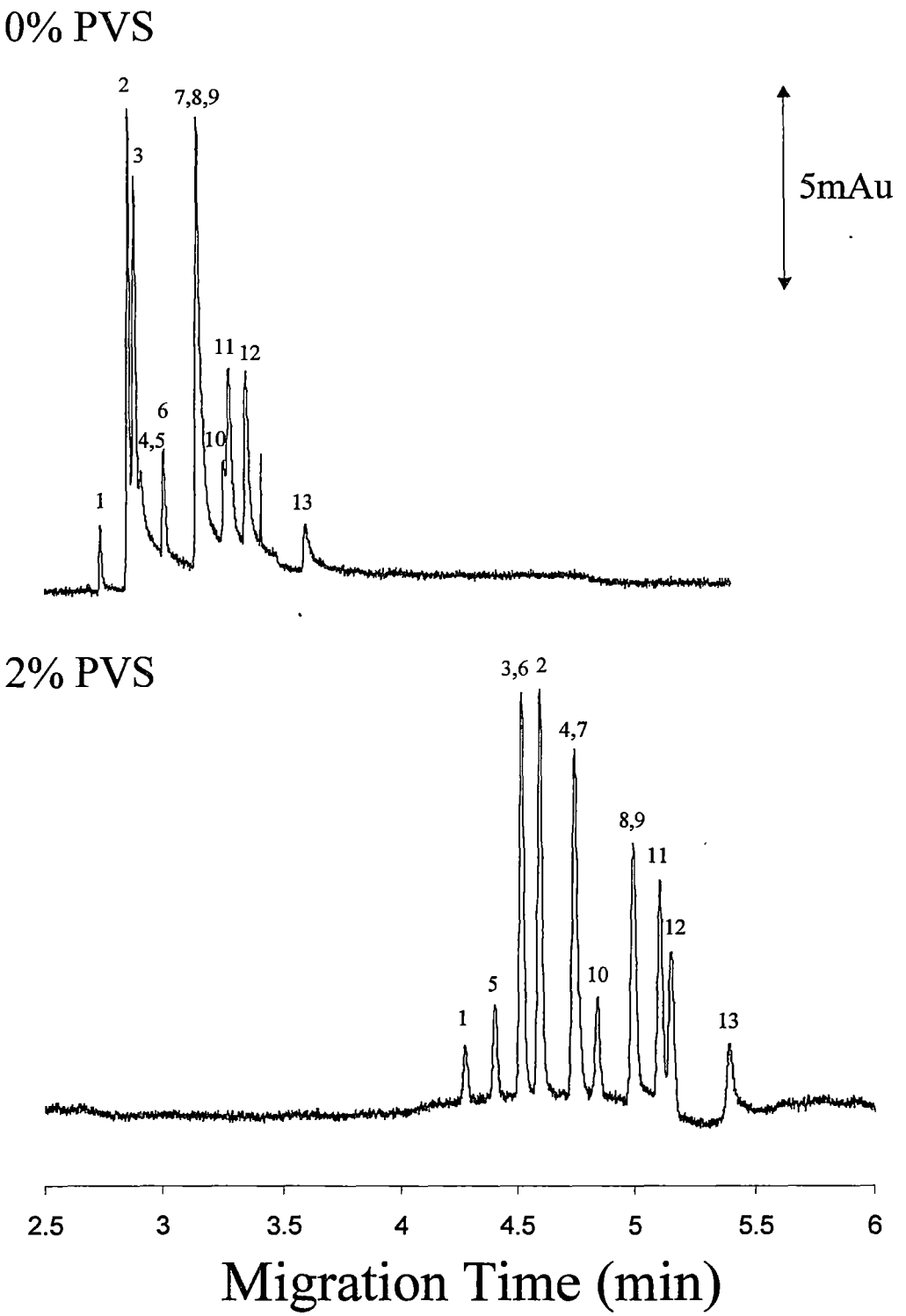

Figure 5.3: Effect of %PVS on the separation of the 13 aromatic bases. Peaks are 1=pyridine, 2=*m*-aminopyridine, 3=*p*-aminopyridine, 4=*o*-aminopyridine, 5=picoline, 6=ethylpyridine, 7=quinoline, 8=aniline, 9=benzylamine, 10=*t*-butylpyridine, 11=methylbenzylamine, 12=ethylaniline and 13=pentylaniline. Conditions: 20mM citrate electrolyte, pH 3.50. Capillary: 50μm x 50cm (41.5cm to detector), detection at 208nm.

competing ion with a divalent ion. Figure 5.4 shows the effect of increasing the concentration of the competing ion and also changing the competing ion from Na^+ to Mg^{2+}. In accordance with the predicted IE mechanism the mobilities of all analytes increased with increasing competing ion concentration and Mg^{2+} produced more pronounced changes in analyte mobility than Na^+ due to the stronger IE interactions of the divalent Mg^{2+}.

For the proposed system to be practically useful, both the IE and hydrophobic interactions should be independent so that varying the extent of one interaction should have little effect on the other. In the previous work with anions, see Chapter 3, an equivalent separation system comprising PDDAC and β-CD did exhibit independent IE and hydrophobic interactions. It can be reasonably assumed that the current system should also exhibit independent interactions.

Under a given set of experimental conditions, the system exhibited good reproducibility with migration times for the analytes varying by less than 2% RSD over 15 consecutive 10 min runs. The capillary coating used was also very stable with the migration time of the EOF varying by less than 2.4% RSD over the same set of runs.

5.5.2 Modelling

The equilibria shown above for system I are characterised by the equibrium contants K_{cd+} and K_{pvs} with the former being a hydrophobic interaction constant between the protonated analyte and the β-CD and the latter being the ion-exchange selectivity coefficient describing the ion-exchange competition for the PVS p-SP between the protonated analyte and the eluent competing cation (E^+). These equilibria are defined as:

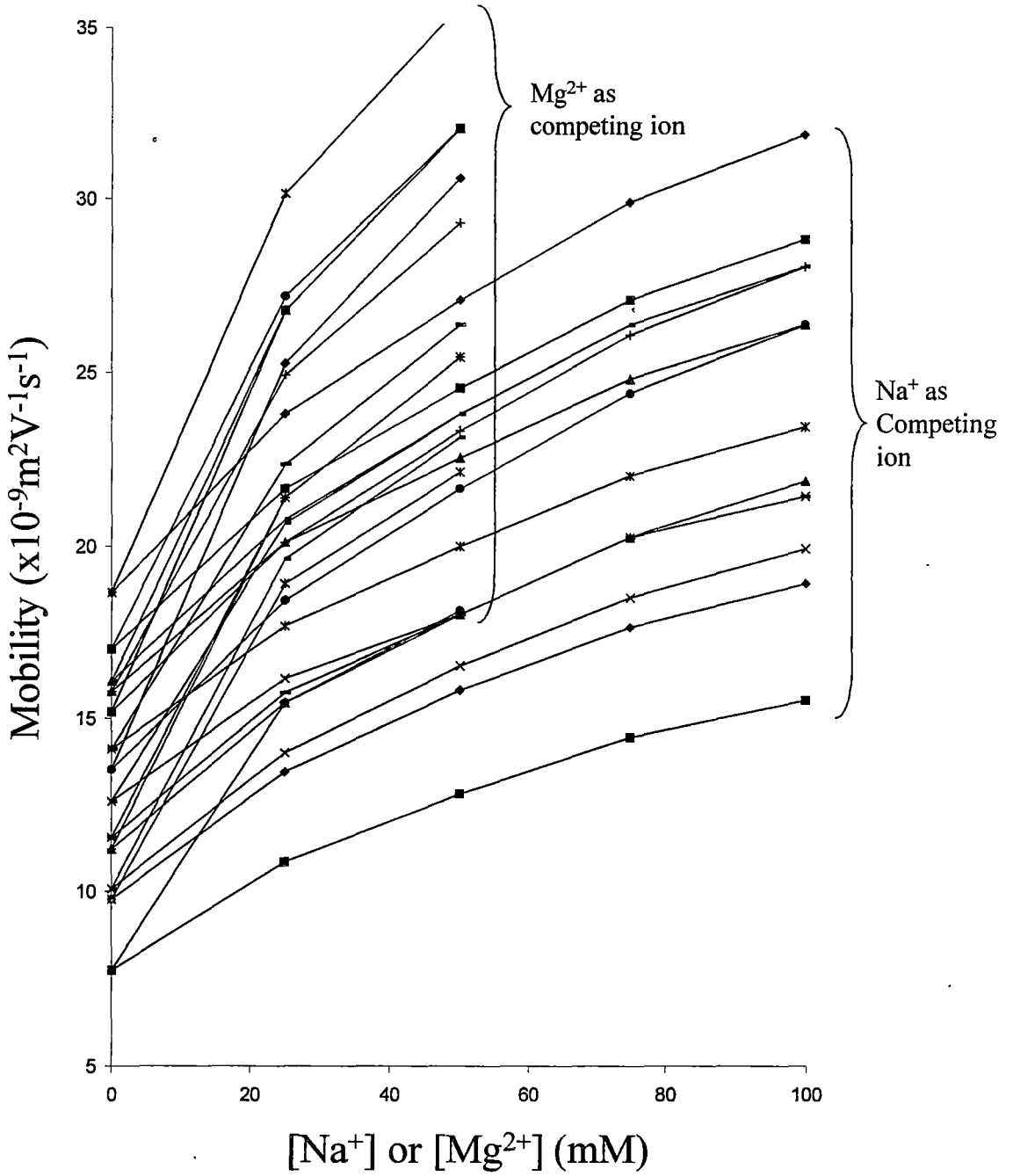

Figure 5.4: Effect of competing-ion type and concentration on the separation of aromatic bases. Conditions: 20mM citrate electrolyte, pH 3.50.

$$K_{cd+} = \frac{[BH^+]_{cd}}{[BH^+]_{bge}} \tag{5-1}$$

$$K_{pvs} = \frac{[BH^+]_{pvs}[E^+]_{bge}}{[BH^+]_{bge}[E^+]_{pvs}} \tag{5-2}$$

where $[BH^+]_{bge}$, $[BH^+]_{pvs}$ and $[BH^+]_{cd}$ refer to the concentrations of the protonated analyte in the electrolyte, PVS and cyclodextrin phases, respectively. $[E^+]_{bge}$ and $[E^+]_{pvs}$ refer to the concentration of the competing ion (Na^+ in this work) in the electrolyte and PVS phases, respectively.

Retention factors for both the cyclodextrin and PVS can be determined. In the case of PVS this can be derived from ion-chromatography theory, see Chapter 3,

$$k'_{poly} = \frac{w_{poly}}{V_{bge}} \left(K_{poly}\right)^{1/y} \left(Q/y\right)^{x/y} [E^+]^{-x/y} \tag{5-3}$$

where w_{poly} is the weight of the PVS pseudo-SP, V_{bge} is the volume of the electrolyte, Q is the ion-exchange capacity of the ion-exchange pseudo-SP, $[E^+]$ is the concentration of the competing ion, while x and y are the charges on the analyte and eluent ion, respectively (both 1 in the current work).

An equivalent expression for k'_{cd} can be derived from first principles, see Chapter 3,

$$k'_{cd} = \frac{V_{cd}}{V_{bge}} K_{cd+} \tag{5-4}$$

where V_{bge} and V_{cd} are the volumes of the electrolyte and cyclodextrin phases, respectively.

For two independent pseudo-SPs the total retention factor, k'_t, of the system can be represented as a linear combination of the individual retention factors,

$$k'_t = k'_{cd} + k'_{pvs} \tag{5-5}$$

substituting for k'_{cd} and k'_{pvs} in eqn (5-5) leads to a final expression for the retention factor of the system,

$$k'_t = \left(\frac{V_{cd}}{V_{bge}}\right) K_{cd+} + w_{\%} K_{pvs} Q [E^+]^{-1} \tag{5-6}$$

where $w_{\%}$ is now the weight percent of polymer in the electrolyte. The observed mobility of an analyte can be expressed in terms of this retention factor, see Chapter 3,

$$\mu_{obs} = \frac{1}{1+k'} \mu_{bge} + \frac{k'}{1+k'} \mu_{sp} \tag{5-7}$$

where μ_{obs} is the observed mobility of the analyte while μ_{bge} and μ_{sp} are the mobilities of the analytes in the electrolyte and p-SP, respectively. Expanding the second term of eqn (5-7) to accommodate the two independent p-SPs gives,

$$\mu_{obs} = \frac{1}{1+k'_t} \mu_{bge} + \frac{k'_{cd}}{1+k'_{cd}} \mu_{cd} + \frac{k'_{pvs}}{1+k'_{pvs}} \mu_{pvs} \tag{5-8}$$

where μ_{cd} and μ_{pvs} are the mobilities of the analytes in the cyclodextrin and PVS phases, respectively. Expanding eqn (5-8) by including previous equations gives a final equation for the separation.

Initial application of this equation to the separation of the 13 bases showed that the $[E^+]^{-1}$ relationship, from eqn (5-6), did not accurately represent the observed trends in μ_{obs}. This is in agreement with results found for the IE separation of cationic opiate compounds using a sulfated cyclodextrin as a p-SP, see Chapter 4. Replacing this with an $[Na^+]^{-x}$ term, eqn (5-9), dramatically improved the results allowing the model

to accurately predict the observed separations of the 13 bases. This outcome is most probably due to the fact that the displacement of Na^+ ions by the bases is not a 1:1 process, as assumed from ion-chromatographic theory. This might be attributable to the fluid nature of the polymer which could cause some of the sulfonate IE sites to be inaccessible to the bases at various times. Since the exact displacement ratio will depend on a range of parameters and will be difficult to predict, its value was determined by non-linear regression, together with other unknown parameters in eqn (5-9).

$$\mu_{obs} = \frac{1}{1+\left(\frac{V_{cd}}{V_{bge}}\right)K_{cd+} + w_{\%}K_{pvs}Q[Na^+]^{-x}}\mu_{bge} + \frac{\left(\frac{V_{cd}}{V_{bge}}\right)K_{cd+}}{1+\left(\frac{V_{cd}}{V_{bge}}\right)K_{cd+}}\mu_{+cd} + \frac{w_{\%}K_{pvs}Q[Na^+]^{-x}}{1+w_{\%}K_{pvs}Q[Na^+]^{-x}}\mu_{pvs} \qquad (5\text{-}9)$$

In eqn (5-9) $w_{\%}$ is defined by the %(w/v) of PVS in the electrolyte. Q is also related to the %PVS and can be estimated by the number of repeat units in the polymer. V_{cd} can be estimated from the individual cavity volume of each β-CD molecule ($0.346nm^3$ [10]). $[Na^+]$ is defined by the concentration of sodium citrate added to the electrolyte while the remaining parameters, K_{cd+}, K_{pvs}, μ_{bge}, μ_{cd} and μ_{pvs} must be determined by non-linear regression.

5.5.3 Application of the migration model

Eqn (5-9) contains 6 unknowns, K_{cd+}, K_{pvs}, μ_{bge}, μ_{cd}, μ_{pvs} and x. Normally at least 7 experimental points would be required to estimate these constants, but it should be recognised that three of these constants, K_{cd+}, K_{pvs} and μ_{bge}, are specific to a particular analyte, while the remainder relate to the separation system and remain the same for all analytes. This permits the use of fewer experimental points when solving the equation and five experimental points comprising the four corner points and centre point of the 2-dimensional experimental space defined by 0-1%(w/v) PVS and 0-10mM β-CD were used as the primary dataset. A further 8 points within the experimental space, the validation set, were used to evaluate the predictive power of the model.

Table 5.3 shows the constants obtained from the non-linear regression of eqn (5-9) using the primary data set. The constants obtained in this way agreed with expected trends, especially the K_{cd+} values. Values within each group increased with increasing alkyl chain length for all classes of compounds (i.e. pyridines, anilines and benzylamines). The largest values of K_{cd+} were obtained for *t*-butylpyridine, ethylaniline and pentylaniline. It can also be seen that anilines exhibited slightly larger K_{cd+} values than the corresponding pyridines, indicating slightly stronger interactions with the β-CD. It should be noted that although the analyte-cyclodextrin interaction has been described as a hydrophobic interaction, it is possible that other interactions, e.g. host-guest complexation, hydrogen bond acceptor etc. occur simultaneously, hence the K_{cd+} terms may cover more than simply hydrophobic interactions. Values obtained for K_{pvs} also agreed with the expected trends. The largest values were observed for the aminopyridines and benzylamines, while the lowest values were for the alkyl substituted pyridines, in agreement with Figure 5.3.

Table 5.3: Parameters derived from non-linear regression of eqn (5-9)

Analyte	K_{pvs}	K_{cd+}	μ_{bge} [1]
Pyridine	4.69	1.32	40.6
Picoline	4.16	1.46	35.9
4-Ethylpyridine	4.05	1.84	33.4
4-*t*-Butylpyridine	4.00	66.91	27.7
Quinoline	3.81	3.42	30.2
o-Aminopyridine	5.47	1.47	35.9
m-Aminopyridine	5.12	1.31	37.4
p-Aminopyridine	4.65	1.39	36.7
Aniline	4.80	3.42	30.2
4-Ethylaniline	4.74	32.94	25.8
4-Pentylaniline	3.95	499.20	21.3
Benzylamine	4.95	3.42	30.2
4-Methylbenzylamine	4.78	9.70	27.3
μ_{pvs} [1]		-22.7	
μ_{cd} [1]		7.3	
x		2.1	

[1] - $x10^{-9} m^2 V^{-1} s^{-1}$

It is also interesting to note that values of K_{pvs} decreased with increasing alkyl chain length, implying that the alkyl substituent exerted some hindering effect on the IE interaction with PVS. These results also showed that it was unlikely that the PVS exhibited any significant hydrophobic interaction with the analytes since this would result in an increase in K_{pvs} values with increasing alkyl chain length on the analyte.

System constants obtained were also within expected ranges. The mobility of the analyte-PVS complex would be expected to be negative since the overall charge on the PVS will remain negative even during interaction with the bases. This was reflected in the observed value of -22.7×10^{-9} $m^2V^{-1}s^{-1}$ for μ_{pvs}. It was also expected that the mobility of the analyte-cyclodextrin complex would be greater than zero, but substantially lower than the mobility of the free analytes. The observed value of $+7.3 \times 10^{-9}$ $m^2V^{-1}s^{-1}$ for μ_{cd} supported this hypothesis. The x value obtained was close to 2 implying a squared relationship between μ_{obs} and $[E^+]$. Interestingly this value was exactly the same as that obtained when modelling the IE separation of cationic opiate compounds using a sulfated cyclodextrin as a p-SP, see Chapter 4.

Figure 5.5 shows the correlation obtained between the observed and predicted mobilities for the entire data set, i.e. 169 points. It can be seen that a high degree of correlation was obtained with an r^2 value of 0.999.

5.5.4 Optimisation

Having an accurate model capable of predicting mobilities allows for the system to be optimised using an appropriate algorithm. This optimisation was performed using both the NRP and MR criteria detailed in Chapter 2.

Using the optimisation process outlined in Chapter 2 optimal conditions were calculated to be 0mM β-CD/1.0% PVS and 2.0mM β-CD/0.95% PVS for the NRP

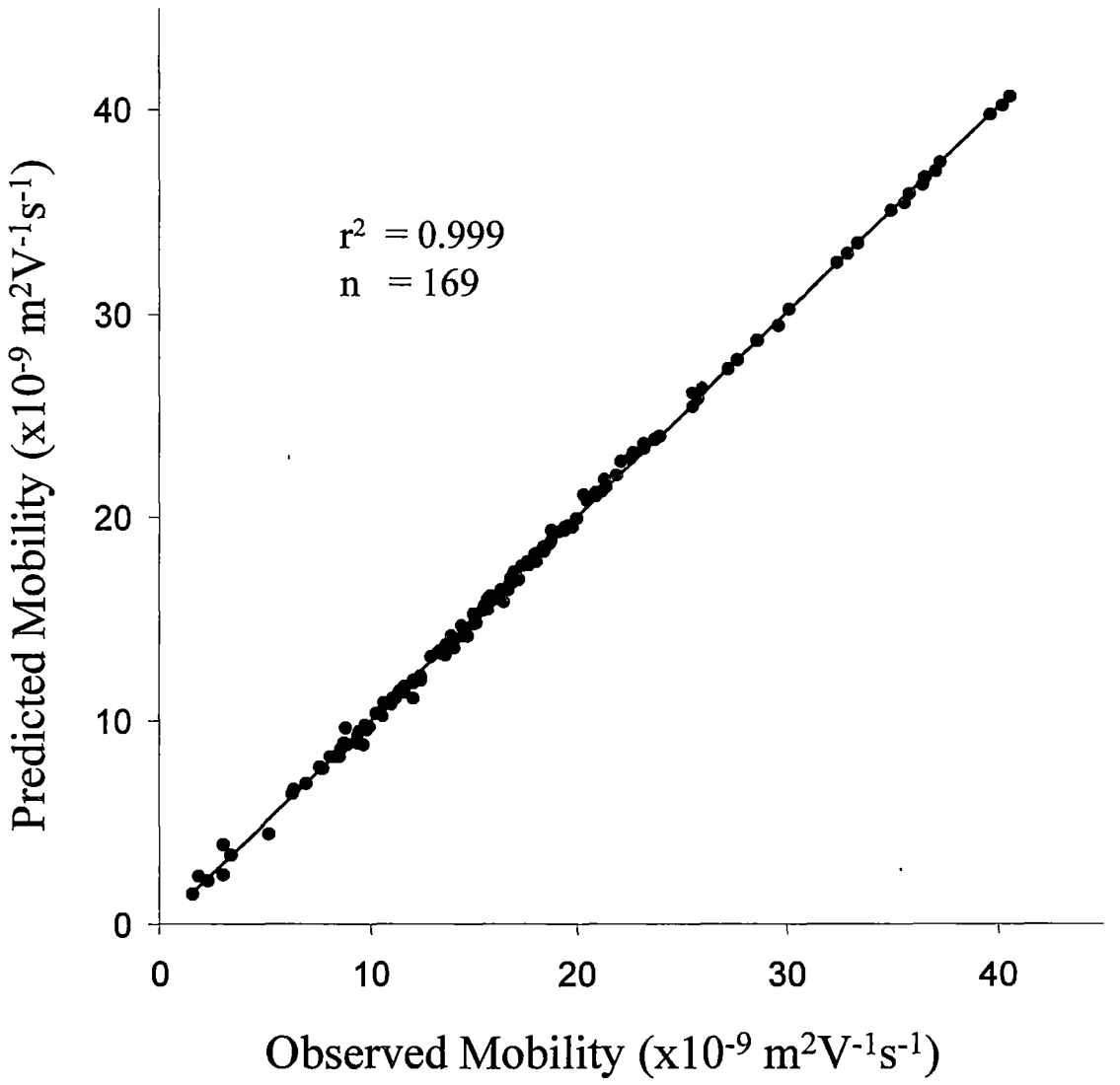

Figure 5.5: Correlation between observed and predicted mobilities using eqn (5-9) and constants shown in Table 5.3. Points used to derive constants also shown.

and MR criteria, respectively. Separations performed under both these sets of conditions are shown in Figure 5.6. It can be seen that both conditions led to at least partial separation of all analytes, with the NRP criterion yielding the better separation (Figure 5.6 a.). The agreement between observed and predicted migration times for both optima was less than 1% for most analytes (23 of the 26 peaks) and less than 2.6% for the other three. It should also be noted that the separation between aniline and benzylamine will always be problematic using only %PVS and [β-CD] as variables since these analytes exhibit identical K_{cd+} and μ_{bge} values and very similar K_{pvs} values. It can be seen that both criteria utilise high levels of PVS trying to exploit this small difference. This problem is potentially avoidable if pH is used as an experimental variable since these two analytes have very different pK_a values (4.60 and 9.35 for aniline and benzylamine, respectively).

5.6 System II

5.6.1 Selectivity

It has been shown that the addition of β-CD to the electrolyte has a greater effect on the more hydrophobic analytes. The use of aromatic bases having a large range of pK_a values (see Table 5.2) allows pH to be employed as an additional parameter to control selectivity. It can be expected that pH should affect the interaction between the aromatic bases and the cyclodextrin due to varying the extent of ionisation of the bases. The effect of pH is thus two-fold, firstly the mobility of the analytes will be varied and secondly the extent of interaction between the analytes and the cyclodextrin will also be affected.

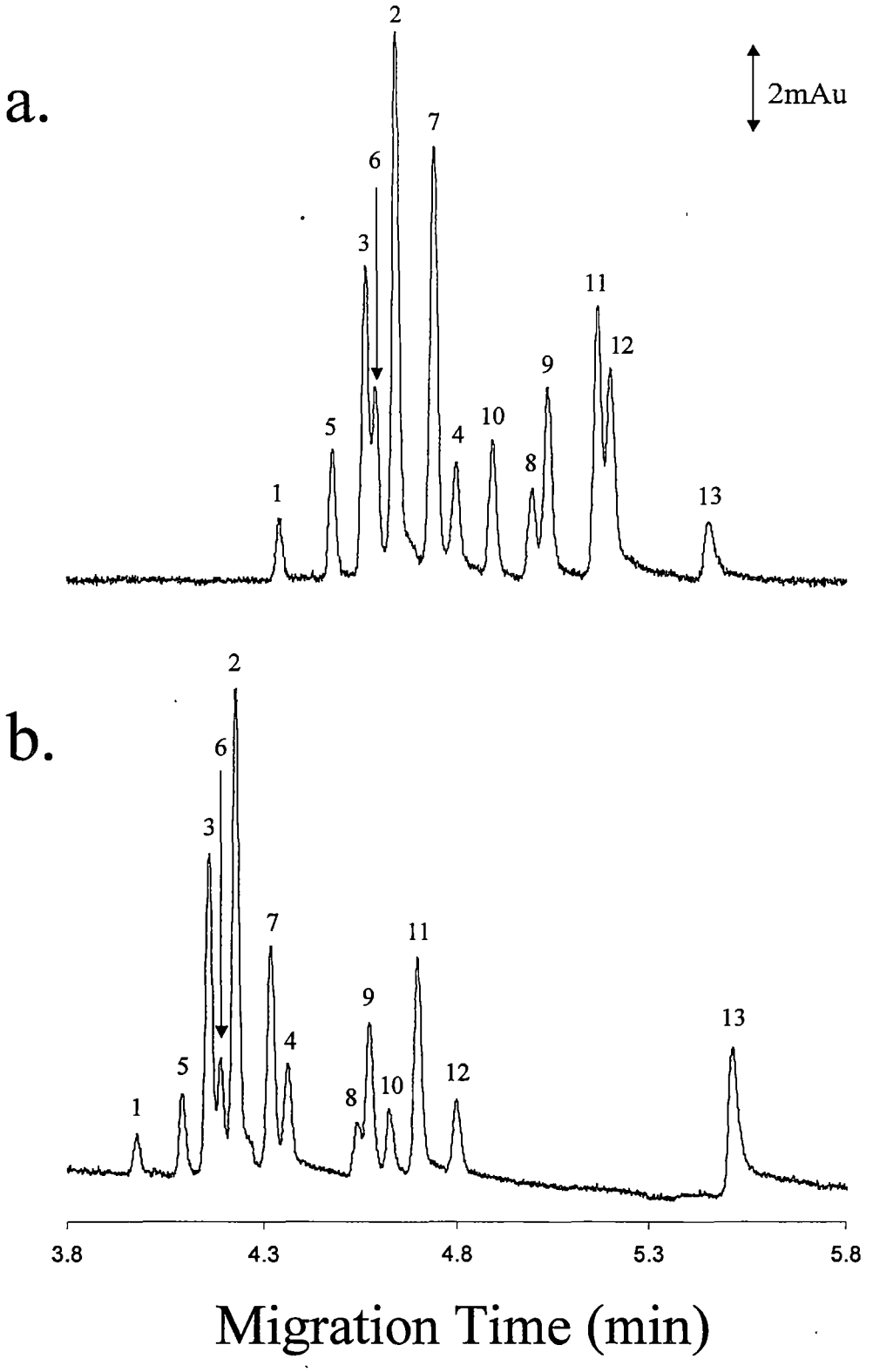

Figure 5.6: Optimal separations calculated with eqn (5-9) and using a) the normalised resolution product criterion and b) the minimum resolution criterion. Conditions: a) 0mM β-CD and 1.0% PVS. b) 2.0mM β-CD and 0.95% PVS. Peaks are 1=pyridine, 2=*m*-aminopyridine, 3=*p*-aminopyridine, 4=*o*-aminopyridine, 5=picoline, 6=ethylpyridine, 7=quinoline, 8=aniline, 9=benzylamine, 10=*t*-butylpyridine, 11=methylbenzylamine, 12=ethylaniline and 13=pentylaniline. General conditions: 20mM Citrate, pH 3.50. Capillary: 50μm x 50cm (41.5cm to detector), detection at 200nm.

5.6.2 Modelling

Since the extent of ionisation of the bases will most likely affect their interaction with the cyclodextrin the assumption that $K_{cd} = K_{cd+}$ cannot be made. The equilibrium constants can thus be defined as follows:

$$K_a = \frac{[B]_{bge}[H^+]_{bge}}{[BH^+]_{bge}} \quad \Rightarrow \quad [BH^+]_{bge} = K_a^{-1}[B]_{bge}[H^+]_{bge} \qquad (5\text{-}10)$$

$$K_{cd} = \frac{[B]_{cd}}{[B]_{bge}} \quad \Rightarrow \quad [B]_{cd} = K_{cd}[B]_{bge} \qquad (5\text{-}11)$$

$$K_{cd+} = \frac{[BH^+]_{cd}}{[BH^+]_{bge}} \quad \Rightarrow \quad [BH^+]_{cd} = K_{cd+}[BH^+]_{bge} \qquad (5\text{-}12)$$

The retention factor, k', can be derived from first principles

$$k' = \frac{n(analyte)_{sp}}{n(analyte)_{mp}}$$

where $n(analyte)_{sp}$ and $n(analyte)_{mp}$ refer to the number of moles of analyte in the stationary and mobile phases, respectively. For the system described here

$$k' = \frac{n(B)_{cd} + n(BH^+)_{cd}}{n(B)_{bge} + n(BH^+)_{bge}} \qquad (5\text{-}13)$$

$$\Rightarrow \quad k' = \frac{[B]_{cd}V_{cd} + [BH^+]_{cd}V_{cd}}{[B]_{bge}V_{bge} + [BH^+]_{bge}V_{bge}} = \left(\frac{V_{cd}}{V_{bge}}\right)\left(\frac{[B]_{cd} + [BH^+]_{cd}}{[B]_{bge} + [BH^+]_{bge}}\right) \qquad (5\text{-}14)$$

where V_{cd} and V_{bge} refer to the volume of the cyclodextrin and electrolyte phases, respectively.

Substituting eqn (5-11), (5-12) and (5-13) into eqn (5-14) gives

$$k' = \left(\frac{V_{cd}}{V_{bge}}\right)\left(\frac{K_{cd} + K_a^{-1}[H^+]_{bge} K_{cd+}}{1 + K_a^{-1}[H^+]_{bge}}\right)$$

Replacing K_a and $[H^+]_{bge}$ with pK_a and pH leads to

$$k' = \left(\frac{V_{cd}}{V_{bge}}\right)\left(\frac{K_{cd} + 10^{(pK_a - pH)} K_{cd+}}{1 + 10^{(pK_a - pH)}}\right) \qquad (5\text{-}15)$$

In eqn (5-15) V_{cd} can be estimated from the individual cavity volume of each cyclodextrin molecule (0.346nm^3 [10]).

The observed mobility of an analyte can be expressed in terms of this retention factor, see Chapter 3,

$$\mu_{ob} = \frac{1}{1+k'}\mu_{bge} + \frac{k'}{1+k'}\mu_{cd} \qquad (5\text{-}16)$$

where μ_{ob} is the observed mobility of the analyte while μ_{bge} and μ_{cd} are the mobilities of the analytes in the electrolyte and cyclodextrin phases, respectivily.

For weak bases the observed mobility is a function of pH due to the extent of ionisation of the analytes and can be described as follows [11]:

$$\mu_{ob} = \alpha \mu_{act} \qquad (5\text{-}17)$$

where $\alpha = \left(\frac{10^{(pK_a - pH)}}{1 + 10^{(pK_a - pH)}}\right)$, μ_{obs} is the observed mobility and μ_{act} is the mobility of the fully protonated species.

On increasing the pH of the system from 3 to 7 there is also an increase in the ionic strength, noted by an increase in current. This increase leads to a decrease in observed mobilities which previous work has taken into account with a $1/\sqrt{I}$ term [12], where I is the ionic strength of the system. In the current model the decreasing

mobilities observed on increasing pH (and therefore ionic strength) was accounted for with a $1/\sqrt{pH}$ term. This simply and accurately described the observed decrease in mobilities on increasing pH.

$$\mu_{ob} = \frac{b}{\sqrt{pH}} \tag{5-18}$$

where b is a constant relating to the mobility at zero pH.

Combining eqn (5-16), (5-17) and (5-18) gives

$$\mu_{ob} = \frac{\alpha}{\sqrt{pH}}\left(\frac{1}{1+k'}b_{bge} + \frac{k'}{1+k'}b_{cd}\right) \tag{5-19}$$

where μ_{ob} is the observed mobility, b_{bge} and b_{cd} are constants relating to the mobility of the analyte in the electrolyte and cyclodextrin phases, respectively, at zero pH where all analytes are fully protonated. Applying eqn (5-19) to the 14 analytes showed good agreement between predicted and observed mobilities, but on increasing pH, b_{cd} was observed to decrease. This is most likely due to the increasing amounts of the non-protonated analyte interacting strongly with the cyclodextrin and leading to decreased mobilities for the analyte-cyclodextrin complex. This was accounted for by including a further α term in the model, which dramatically improved the results. The final model used for the system is as follows

$$\mu_{ob} = \frac{\alpha}{\sqrt{pH}}\left(\frac{1}{1+k'}b_{bge} + \frac{k'}{1+k'}\alpha b_{cd}\right) \tag{5-20}$$

where α and k' are defined as above.

5.6.3 Application of the migration model

Since eqn (5-20) contained 4 unknowns with two variables, namely pH and [β-CD], a minimum of 5 experiments was needed to determine these unknowns. A parameter space covering pH 3.5-7.2 and 0-10 mM β-CD was chosen. The selected pH range covered most of the pK_a values for the analytes, while β-CD has limited solubility above 10mM. The primary dataset needed to determine the four constants in the system comprised the four corner points and centre point of the parameter space. Data were also acquired at 20 additional points throughout the parameter space and comprised the validation set used to evaluate the predictive power of the model.

Table 5.4 lists the constants obtained using non-linear regression and the primary dataset. It can be seen that the values of K_{cd} and K_{cd+} obtained agree with the expected trends in hydrophobicity of the analytes. For example K_{cd} and K_{cd+} for the anilines increased from aniline through to heptylaniline. It can also be seen that the values of K_{cd} were far greater than those for K_{cd+}, which would be expected since it can be reasonably assumed that the hydrophilic charged group on the analyte will cause decreased interaction of the analyte with the hyrophobic core of the β-CD. It can also be seen that the anilines interacted more with the β-CD than the pyridines, reflected by the larger K_{cd} and K_{cd+} values, with only 4-*t*-butylpyridine having a reasonably large K_{cd} value. The model also gives insight into the mobility of the charged analyte-cyclodextrin complex, however these values can only be used for analytes that have an appreciable interaction with the cyclodextrin in their charged form, ie 4-pentylaniline and 4-heptylaniline. For these analytes it can be seen that the mobilities of the complexes for both species were very similar, ~$14 \times 10^{-9} m^2 V^{-1} s^{-1}$. It can also be seen that the mobilty of the complex was much less (approximately a third) than that for the free analyte, as would be expected.

Table 5.4: Parameters derived from non-linear regression of eqn (5-20)

Analyte	K_{cd+}	K_{cd}	b_{bge}	b_{cd}
	$x10^3$		$x10^{-9}m^2V^{-1}s^{-1}$	
Pyridine	0.02	0.00	84.1	0.0
Picoline	0.02	0.00	74.0	0.0
4-Ethylpyridine	0.03	0.07	68.9	0.7
4-*t*-Butylpyridine	0.34	15.05	57.2	1.2
Quinoline	0.04	0.21	64.8	4.9
p-Aminopyridine	0.02	0.00	78.9	0.0
m-Aminopyridine	0.02	0.00	77.1	0.0
o-Aminopyridine	0.02	0.03	73.5	0.0
Aniline	0.06	0.42	66.4	28.3
4-Ethylaniline	0.40	2.09	54.7	17.6
4-Pentylaniline	2.38	76.43	44.9	14.1
4-Heptylaniline	2.64	106.90	38.2	14.7
Benzylamine	0.04	0.00	63.0	0.0
4-Methylbenzylamine	0.10	0.00	57.6	0.0

The K_{cd} values obtained here can be compared with those obtained previously for aromatic anions using a similar modelling procedure, see Chapter 3. K_{cd} values of 2.38 x 10^3 and 2.64 x 10^3 obtained for 4-pentylaniline and 4-heptylaniline, respectively, were of similar magnitude to those obtained previously for 4-propylbenzoate, 4-t-butylbenzoate and 4-heptylbenzoate (2.54 x 10^3, 3.50 x 10^3 and 3.08 x 10^3, respectively). This would be as expected since both the aromatic anions and aromatic cations should interact in a similar manner with the neutral cyclodextrin and hence should yield similar values of K_{cd}. The slight differences are most probably due to the different functional groups, in a similar way that the anilines and pyridines interact to differing degrees.

Figure 5.7 shows the correlation between mobilities predicted for the validation set using eqn (5-20) and parameters derived from the primary data set (shown in Table 5.4) and the observed mobilities. A total of 350 data points was contained in the validation set and a high degree of correlation was obtained, (r^2 = 0.995). It should also be noted that the validation set was obtained using more than one capillary, showing that the system was very reproducible even after replacement of the capillary and re-coating with a fresh layer of PDDAC and dextran sulfate.

The procedure outlined provides a means to determine interaction constants between the neutral and charged forms of weak bases (the method could easily be applied to weak acids) with neutral cyclodextrins.

5.6.4 Optimisation

Optimisation was performed using the NRP and MR criteria, outlined in Chapter 2.

The resolution surface produced over the entire experimental space using the NRP criterion is shown in Figure 5.8. From Figure 5.8 it can be seen that the optimum

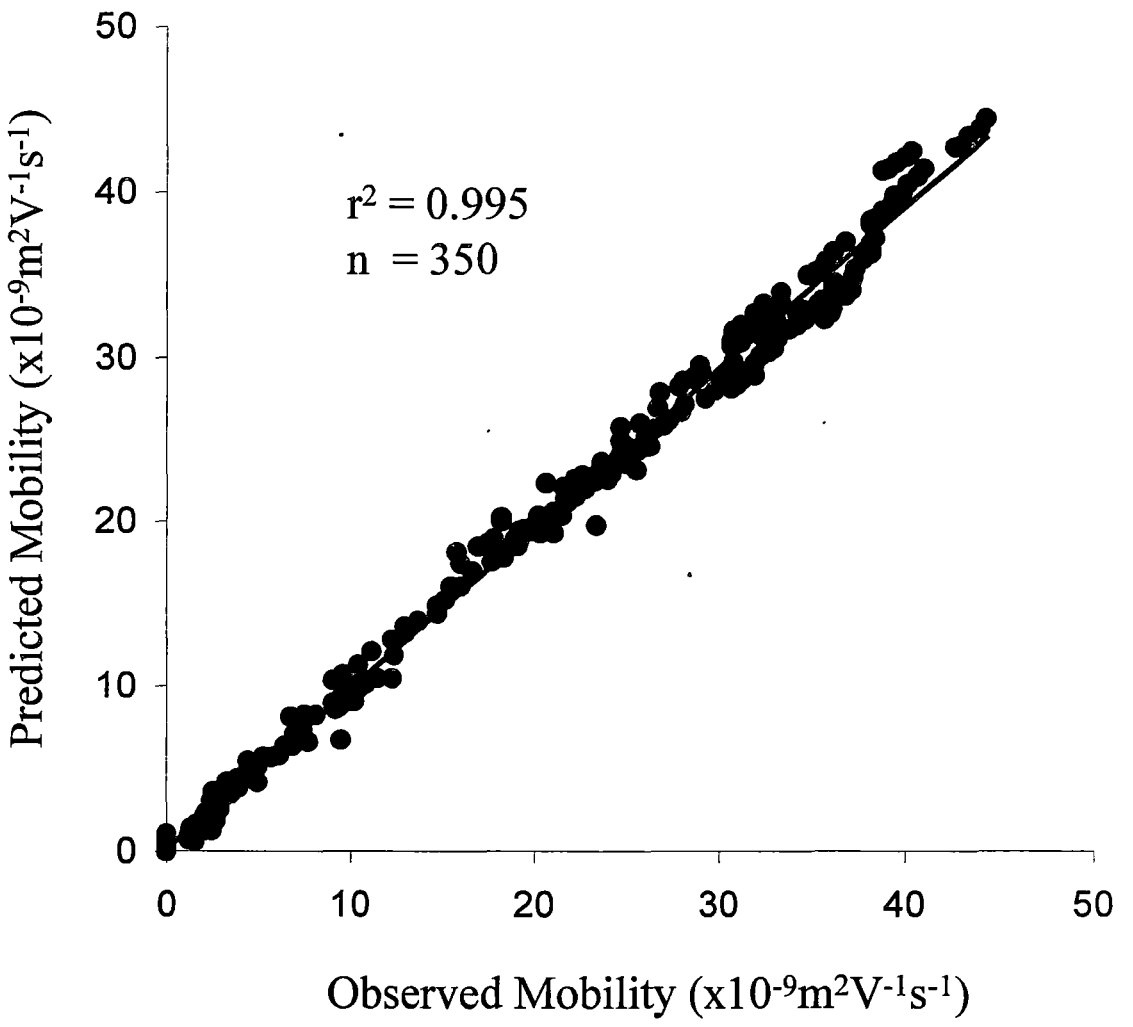

Figure 5.7: Correlation between predicted and observed mobilities at 25 points within the experimental space. The 5 points used to derive the constants are also included.

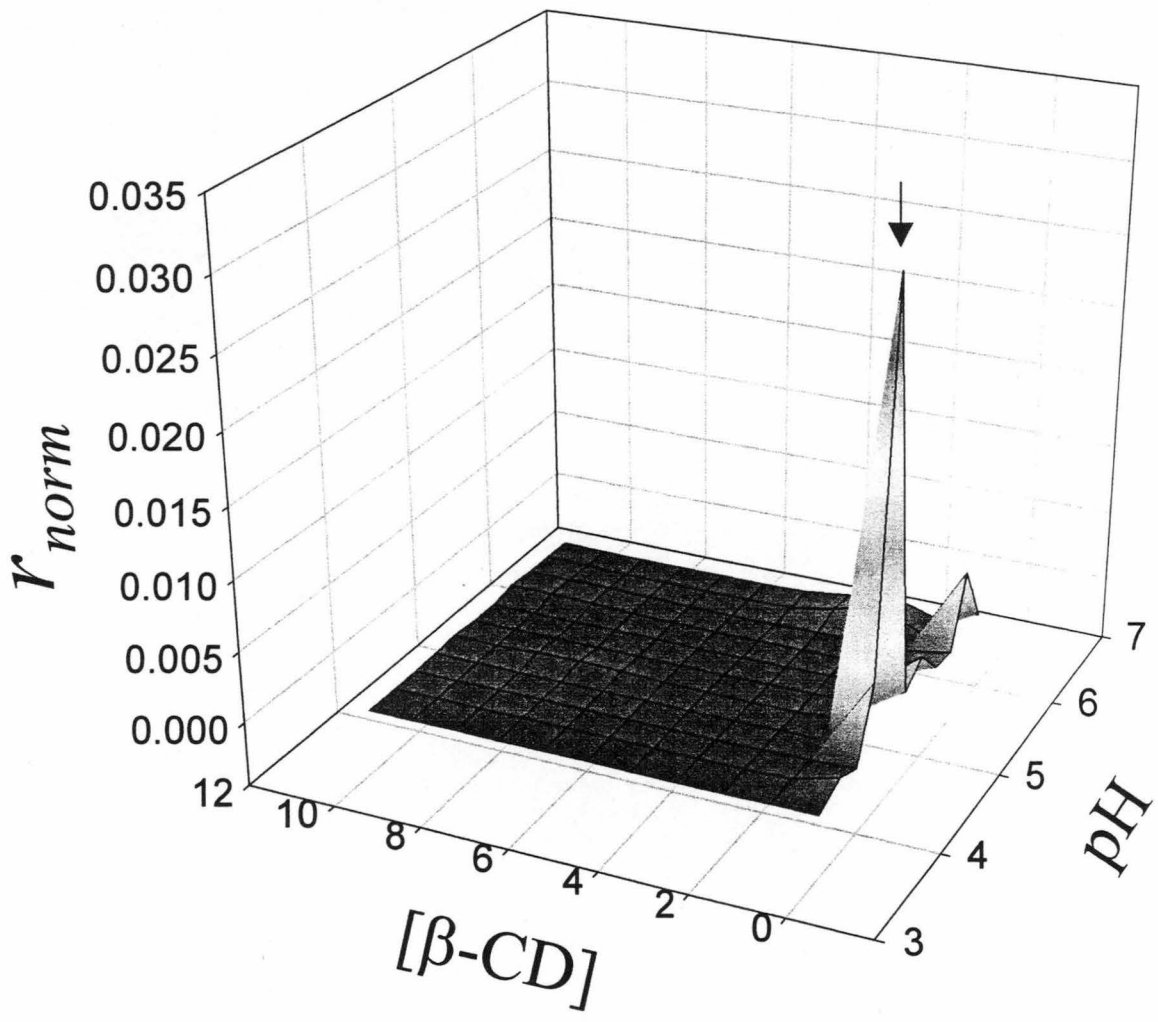

Figure 5.8: Resolution surface obtained using the normalised resolution product and the constants outlined in Table 5.4. Optimum conditions are pH 4.50 and 0 mM β-CD.

separation should occur at pH 4.50 and [β-CD] = 0. It can be seen that this is the only condition that offers reasonable resolution over the entire experimental space using the NRP criterion. This occurs as a result of the need to separate a large number of analytes using mainly pH to influence selectivity. It is interesting to note that the optimal separation predicts 0mM β-CD in the electrolyte, showing that although analyte-cyclodextrin interactions play a major role in the separations, they are not necessary to provide an optimal separation. Figure 5.9 a) shows the separation obtained at these conditions and the predicted separation is shown in Figure 5.9 b). Whilst there was good agreement between the predicted and observed migration mobilities (<2.5%), it is evident that not all of the peaks were resolved, especially picoline, o-aminopyridinepyridine and pyridine, 4-methylbenzylamine and 4-*t*-butylpyridine, aniline and 4-pentylaniline. This resulted from the fact that the main control on the selectivity of the system arose from changes in pH, hence complete resolution of all 14 analytes was difficult to achieve, especially in under 2 min.

The system was also optimised using the MR criterion, see Chapter 2. Figure 5.10 shows the observed and predicted separations using this criterion. It can be seen that the conditions predicted using the MR criterion differed from those predicted by the NRP criterion. Again it can be seen that not all peaks were resolved, especially from the EOF. This was due to the model not taking into account the width of the EOF peak, which was a very large negative dip. Analytes predicted to have low mobilities would theoretically be separated from a narrow EOF peak, but in reality were not separated when a very broad EOF peak was observed. Despite this, the predicted electropherogram agreed well with the observed electropherogram, with differences between predicted and observed mobilities being <5%. It should be noted that in

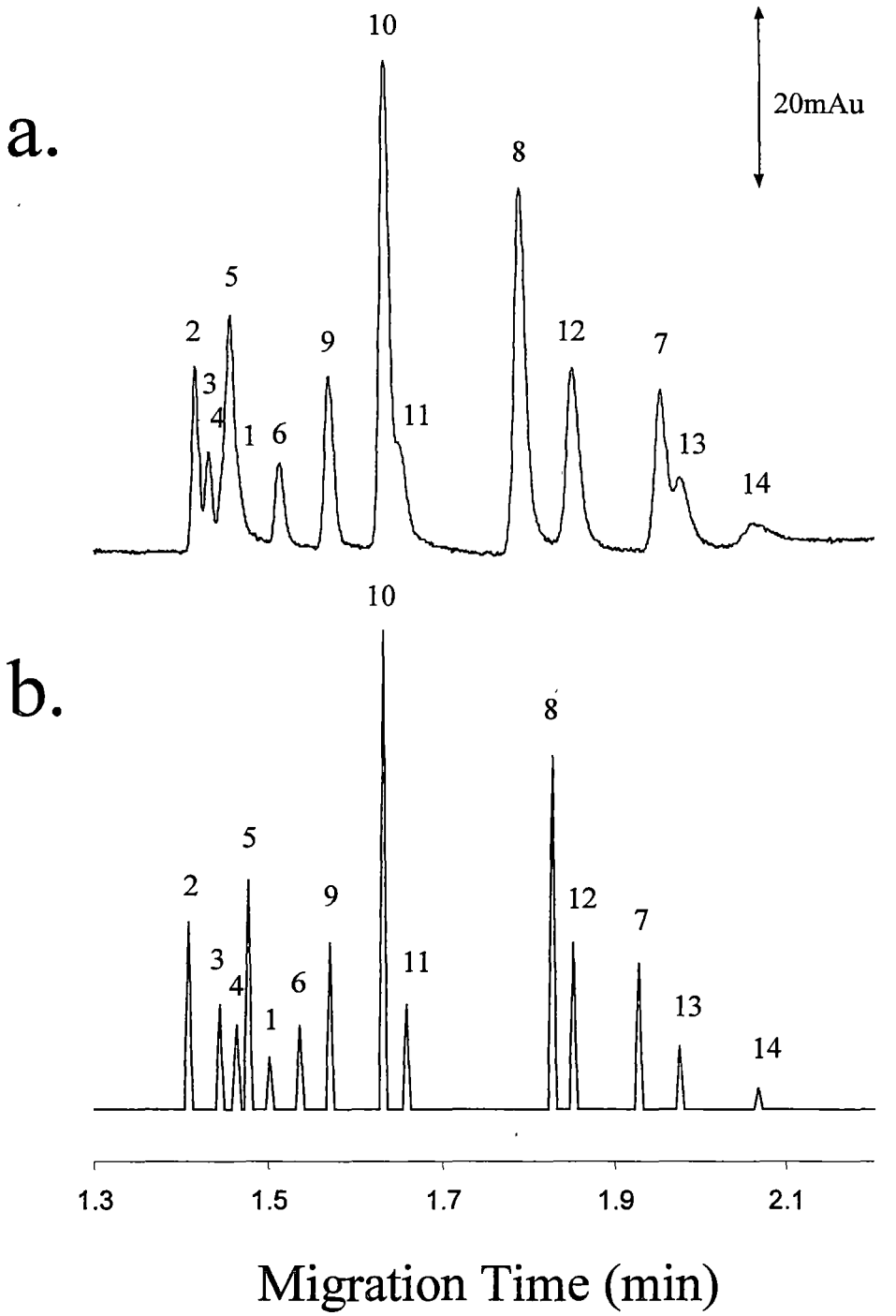

Figure 5.9: Optimum separation of the 14 aromatic bases calculated using the normalised resolution product criterion. a) Observed electropherogram, b) Predicted electropherogram. Peaks are: 1=pyridine, 2=*p*-aminopyridine, 3=*m*-aminopyridine, 4=picoline, 5=*o*-aminopyridine, 6=4-ethylpyridine, 7=aniline, 8=quinoline, 9=benzylamine, 10=4-methylbenzylamine, 11=*t*-butylpyridine, 12=4-ethylaniline, 13=4-pentylaniline and 14=4-heptylaniline. Conditions: electrolyte, 20 mM citrate at pH 4.50 and 0 mM β-CD. Capillary: 50μm x 35cm (26.5cm to detector), detection at 195nm.

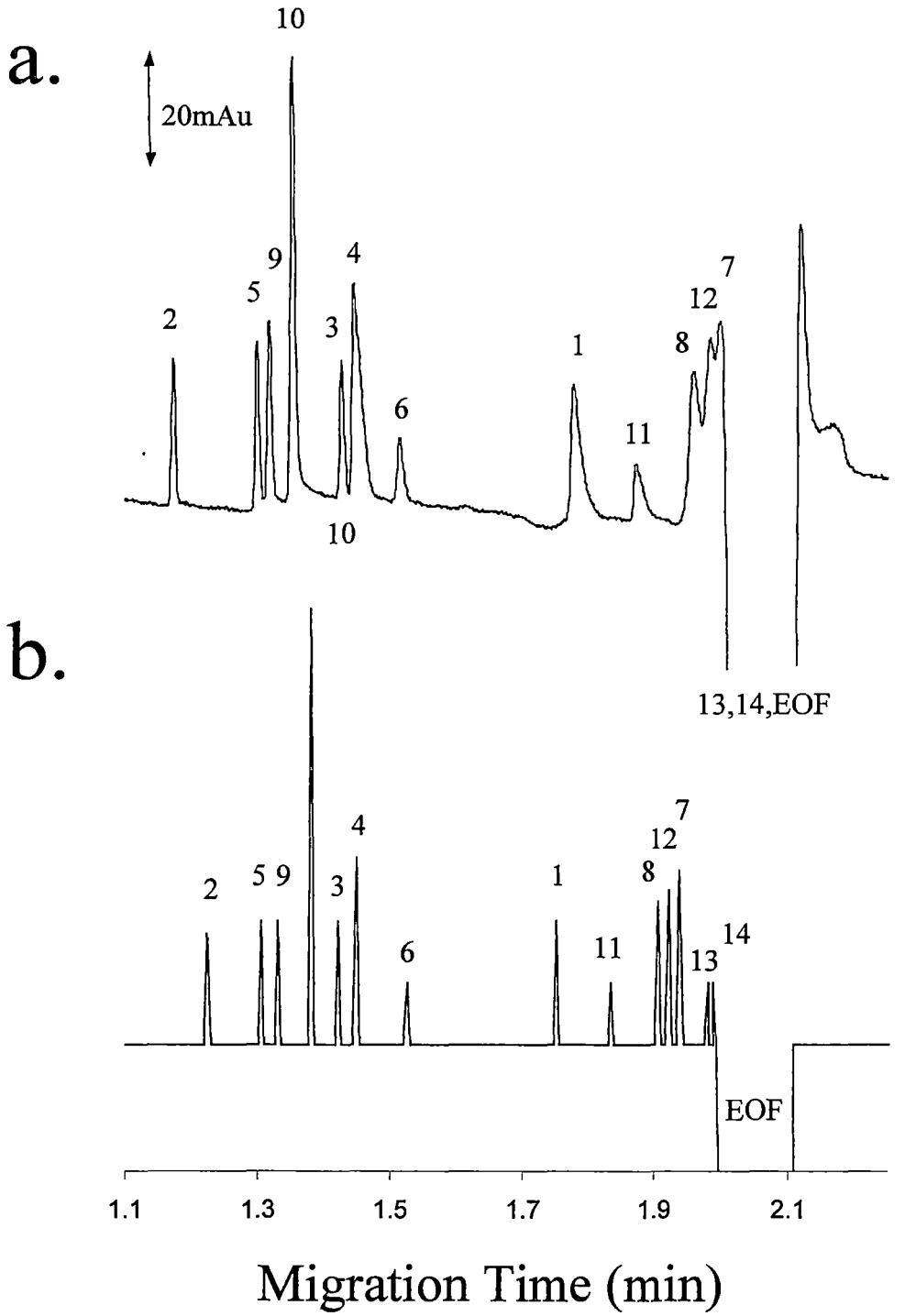

Figure 5.10: Optimum separation of the 14 aromatic bases calculated using the minimum resolution criterion. a) Observed electropherogram, b) Predicted electropherogram. Peaks are: 1=pyridine, 2=*p*-aminopyridine, 3=*m*-aminopyridine, 4=picoline, 5=*o*-aminopyridine, 6=4-ethylpyridine, 7=aniline, 8=quinoline, 9=benzylamine, 10=4-methylbenzylamine, 11=*t*-butylpyridine, 12=4-ethylaniline, 13=4-pentylaniline and 14=4-heptylaniline. Conditions: 20 mM Citrate at pH 5.75 and 2.0mM β-CD. Other conditions as in Figure 5.9.

Figure 5.9 and Figure 5.10 the predicted electropherograms were based on migration times calculated by the model, but peak height and widths were simply chosen to match the observed electropherograms.

5.6.5 Tuning the separation selectivity

The availability of a model that describes the observed migration behaviour leads to the possibility of using this model to predict the conditions needed to achieve the migration of analytes in a desired sequence. This can be of an advantage when determining a trace analyte in the presence of a major matrix component. The method used to predict electrolyte compositions needed for analytes to migrate in a desired order was to use the model to maximise the mobility difference between the target analytes whilst also avoiding co-migration of peaks or overlap with the EOF.

Four analytes were chosen as a test mixture, namely pyridine, 4-*t*-butylpyridine, *m*-aminopyridine and 4-methylbenzylamine. Figure 5.11 shows separations where the migration order of pyridine and 4-*t*-butylpyridine are reversed. When pyridine was to migrate before 4-*t*-butylpyridine (Figure 5.11 a.), the model predicted the maximum [β-CD] and a low pH, while for the reversed order (Figure 5.11 b.) it predicted no β-CD and a pH intermediate between the pK_a values of pyridine and 4-*t*-butylpyridine (5.17 and 5.99, respectively). Figure 5.12 shows an example where co-migration of peaks is a potential problem at the conditions calculated for maximum separation of pyridine and *m*-aminopyridine, if only these two analytes are considered in the optimisation. Figure 5.12 a. shows the conditions calculated for the maximum separation of pyridine and *m*-aminopyridine (with pyridine migrating first) and with the requirement that all analytes in the mixture are separated (pH 3.50 and 1.06 mM

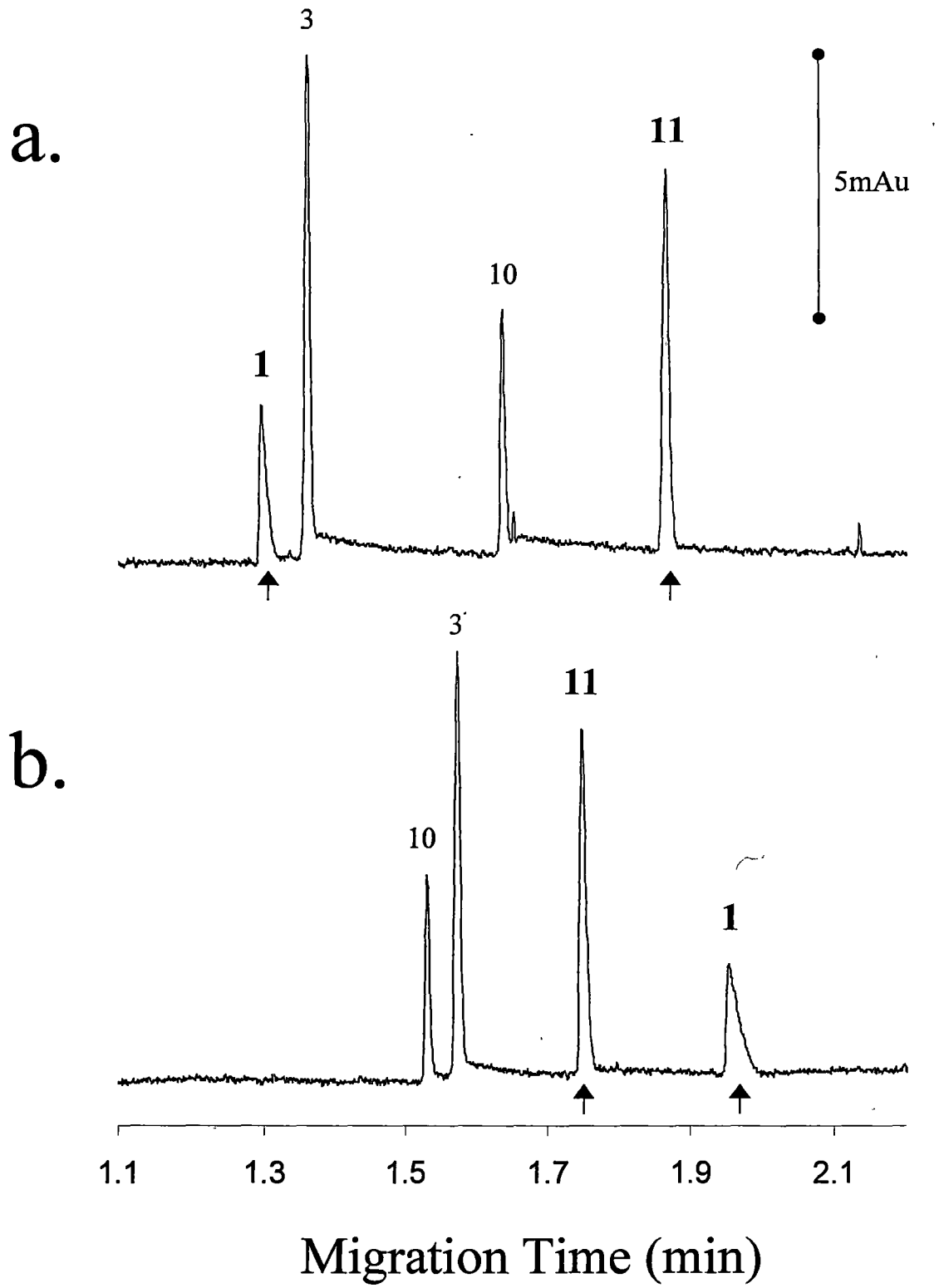

Figure 5.11: Manipulation of separation selectivity for pyridine and *t*-butylpyridine. a) Pyridine before *t*-butylpyridine. Conditions: pH 3.50 and 10 mM β-CD. b) *t*-Butylpyridine before pyridine. Conditions: pH 5.75 and 0 mM β-CD. Other conditions as in Figure 5.9.

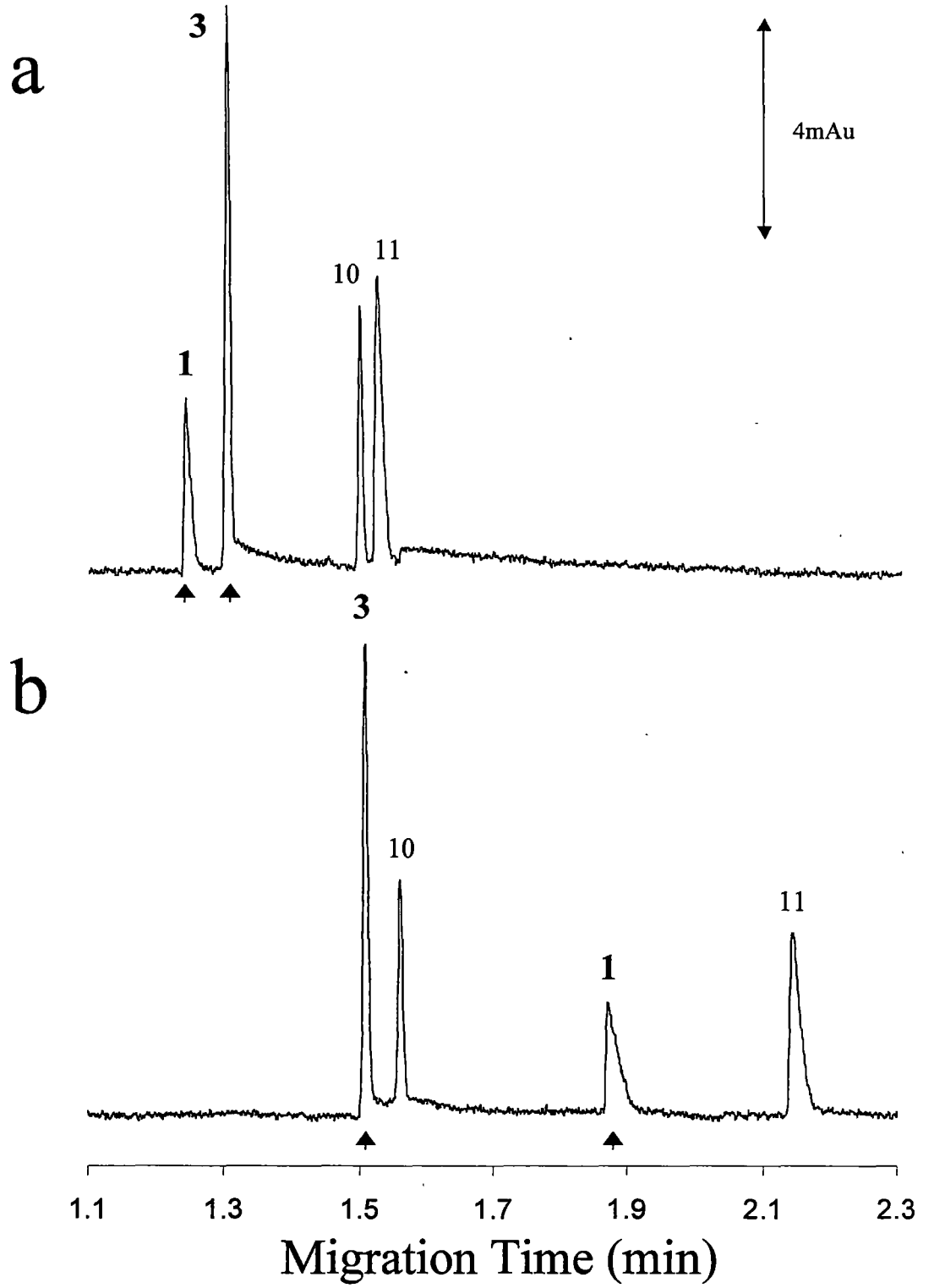

Figure 5.12: Manipulation of separation selectivity for pyridine and *m*-aminopyridine. a) Pyridine before *m*-aminopyridine. Conditions: pH 3.50 and 1.06 mM β-CD. b) *m*-Aminopyridine before pyridine. Conditions: pH 5.50 and 3.42 mM β-CD. Other conditions as in Figure 5.9.

β-CD), whilst Figure 5.12 b. shows the reverse separation order (pH 5.50 and 3.42 mM β-CD).

As well as taking into account resolution between analytes, the separation of analytes from the EOF has been included. Figure 5.13 shows an example where the migration order of *m*-aminopyridine and 4-methylbenzylamine was to be varied. In the case where *m*-aminopyridine was to migrate first, the separation is straightforward (Figure 5.13 a.). However, for the reversed order, conditions for maximum separation of these two analytes was predicted where *m*-aminopyridine had minimum mobility, i.e. at a high pH where it is not protonated and its separation from the EOF peak is problematic. When consideration was given in the optimisation procedure to separation of analytes from the EOF, the electropherogram shown in Figure 5.13 b. resulted. In this separation it can now be seen that all the peaks were resolved from the EOF and from each other.

5.7 Full system

From the above work it can be seen that it is possible to successfully model individual subsystems of the total system shown in Figure 5.2. However, the inclusion of all three variables, pH, [β-CD] and [PVS] has a complicating effect on the analyte-additive interactions. The effect of pH on the analyte-β-CD interactions have been explained above, but in a similar way it can be expected that by altering the extent of ionisation of the bases, the IE interactions with the PVS will also vary since only the protonated base will undergo IE interactions.

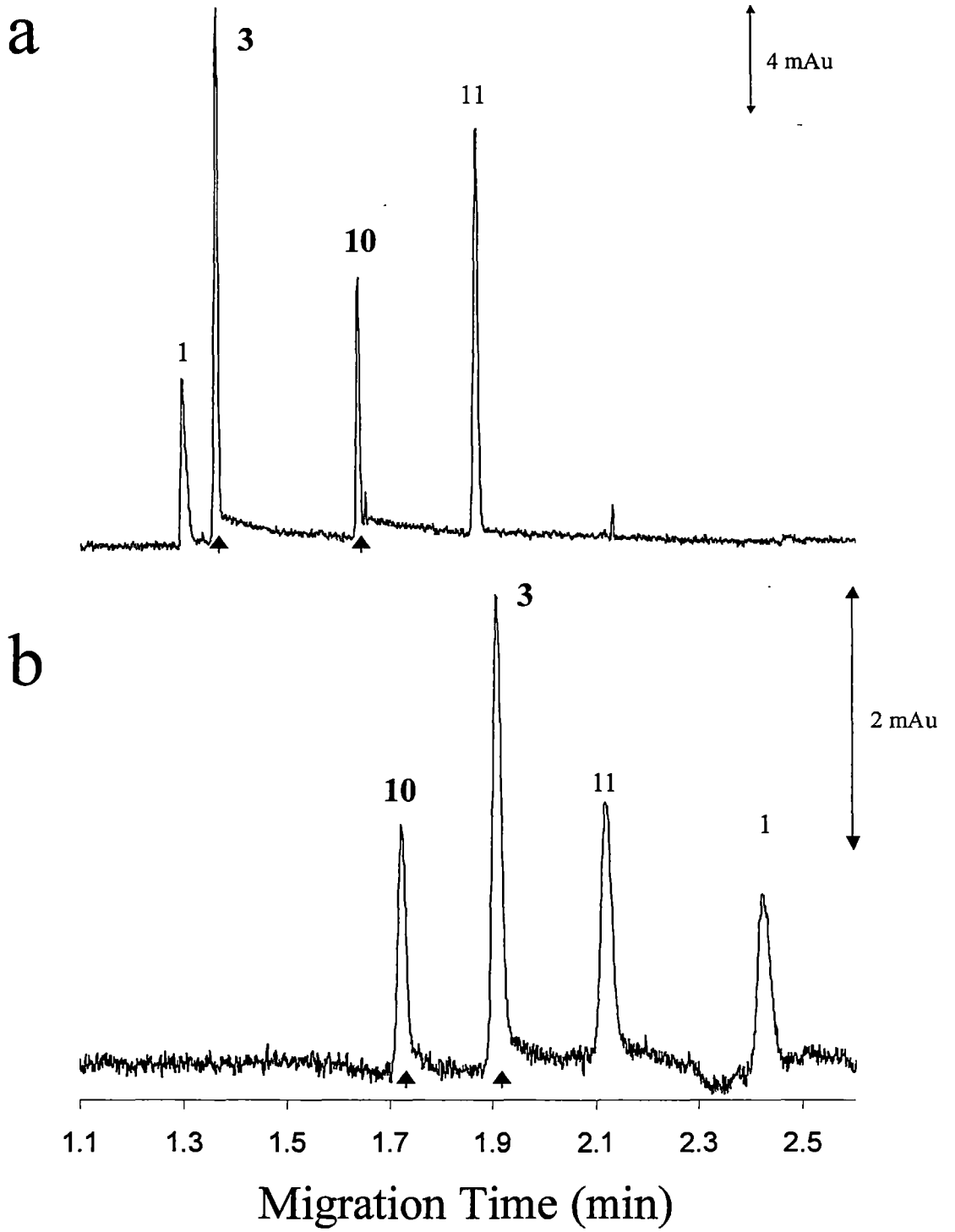

Figure 5.13: Manipulation of separation selectivity for *m*-aminopyridine and 4-methylbenzylamine. a) *m*-Aminopyridine before 4-methylbenzylamine. Conditions: pH 3.50 and 10 mM β-CD. b) 4-Methylbenzylamine before *m*-aminopyridine. Conditions: pH 6.00 and 0 mM β-CD. Other conditions as in Figure 5.9.

5.7.1 Modelling

Inclusion of pH as a variable in the system has a complicating effect on the interactions of the analytes with both β-CD and PVS, as discussed above. However, assuming independent interactions and combining eqn (5-9) and eqn (5-20) leads to a final model for the full system shown in Figure 5.2.

$$\mu_{obs} = \frac{\alpha}{\sqrt{pH}}\left(\frac{1}{1+k'_{cd}+k'_{pvs}}b_{bge} + \frac{k'_{cd}}{1+k'_{cd}}\alpha b_{cd} + \frac{k'_{pvs}}{1+k'_{pvs}}\alpha b_{pvs}\right) \qquad (5\text{-}21)$$

where $k'_{cd} = \left(\frac{V_{cd}}{V_{bge}}\right)\left(\frac{K_{cd}+10^{(pK_a-pH)}K_{cd+}}{1+10^{(pK_a-pH)}}\right)$

and $k'_{pvs} = w_{\%}K_{pvs}Q[E^+]^{-1}\left(\frac{10^{(pK_a-pH)}}{1+10^{(pK_a-pH)}}\right)$

All the parameters in eqn (5-21) have been defined previously.

5.7.2 Application of the Full Migration Model

Eqn (5-21) utilises the experimental parameters %PVS, [β-CD] and pH. As such, a 3-dimensional experimental space defined by the variables 0-1% PVS, 0-10mM β-CD and pH 3.5-7.2 was chosen. Initially, experimental conditions at the 8 corner points and the centroid point were chosen as the primary data set, but this led to relatively poor predictability of observed migration times for a further 12 points contained within the experimental space, giving $r^2 = 0.937$ for the correlation between observed and predicted mobilities. This corresponded to differences in observed and predicted mobilities of up to $\pm 12 \times 10^{-9} m^2V^{-1}s^{-1}$. Correlation was improved ($r^2 = 0.986$) when a more complete set of 21 points was used as the primary data set, see Figure 5.14, but was inadequate to enable sufficiently accurate prediction of migration times for

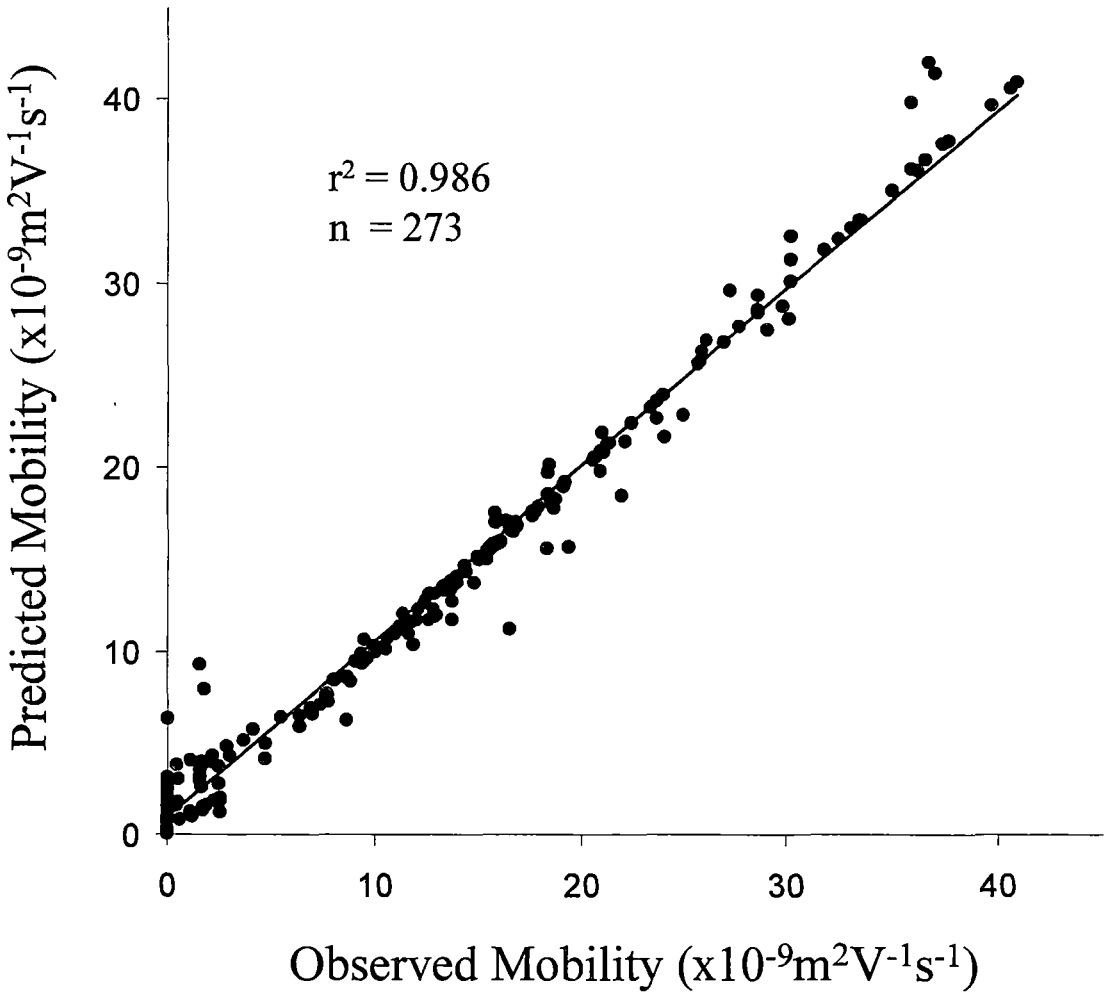

Figure 5.14: Correlation between observed and predicted mobilities using eqn (5-21) and 21 different conditions within the experimental space. All points shown were used to derive the contants for the model.

optimisation purposes (i.e. <5% error). The cause of this is the complexity of the 3-dimensional model and the relatively large number of constants which need to be calculated. This limits the use of non-linear regression.

5.7.3 Artificial neural networks

Since the separation system could not be modelled accurately using the above approaches, artificial neural networks (ANN) were investigated. These have previously been shown to be applicable to complex CE systems [13-15] having a range of input and output parameters. ANNs are a soft modelling approach that do not require any explicit knowledge of the system being modelled. This is an advantage for complicated systems where several parameters can affect the observed separation.

For the current system, the three variables, %PVS, [β-CD] and pH were used as the input layer while the 13 mobilities (one for each analyte) were used as the output layer. The structure of the ANN was optimised by varying the number of hidden layers and nodes and the best architecture was determined to be 3 input parameters, 2 hidden layers comprising 20 nodes each and the 13 output parameters.

The ANN was trained using the full data set of 21 points and then used to predict optimum separations using both the NRP and MR criteria. The same iterative optimisation procedure used earlier was again employed. Predicted optimal conditions were 0.3% PVS, 0mM β-CD at pH 3.75 for the NRP criterion. Agreement between predicted and observed migration times was within 1.4% using the NRP criterion and less than 4.2% for the MR criterion. In the case of optimisation using the MR criterion it was necessary to constrain the calculations to accept only analyte mobilities greater than $2 \times 10^{-9} m^2 V^{-1} s^{-1}$ in order to avoid overlap of analyte peaks with

the large negative baseline disturbance caused by the EOF peak. This ensured that all peaks in the resultant electropherogram were well separated from the EOF. The optimal conditions calculated using this modified criterion were 0.9% PVS, 5mM β-CD at pH 3.50 and observed migration times under these conditions agreed with predicted values to within 1.5%. Separations obtained using the optimal conditions for both optimisation criteria are shown in Figure 5.15. Both approaches yielded good separations, with most of the peaks being resolved fully. It is also interesting to note that both optima utilise low pH conditions (3.75 and 3.50) which are very close to the fixed pH used in the simplified model (3.50). This suggests that the ability to vary pH did not significantly influence the ability to separate this particular set of analytes. That is, introduction of a 3-dimensional experimental space in this example offered little improvement over the 2-dimensional experimental space.

5.7.4 Tuning the separation selectivity

The major advantage in having several independent interactions operating within a system is the increased selectivity control that can be achieved. As an example, the peaks for aniline and benzylamine can be considered. As mentioned above and shown in Table 5.3 and Table 5.4, these two analytes showed very similar mobilities and interactions with both p-SPs and their separation can therefore be expected to be difficult. By using the ANN model of the 3-dimensional system, it is possible to predict the conditions needed to obtain the separation for a desired migration order of these analytes. This is shown in Figure 5.16 where aniline migrated before benzylamine under the conditions shown in Figure 5.16 a., and in the reverse migration order under the conditions shown in Figure 5.16 b. The optimal separation with aniline migrating before benzylamine was achieved with protonated analytes (pH

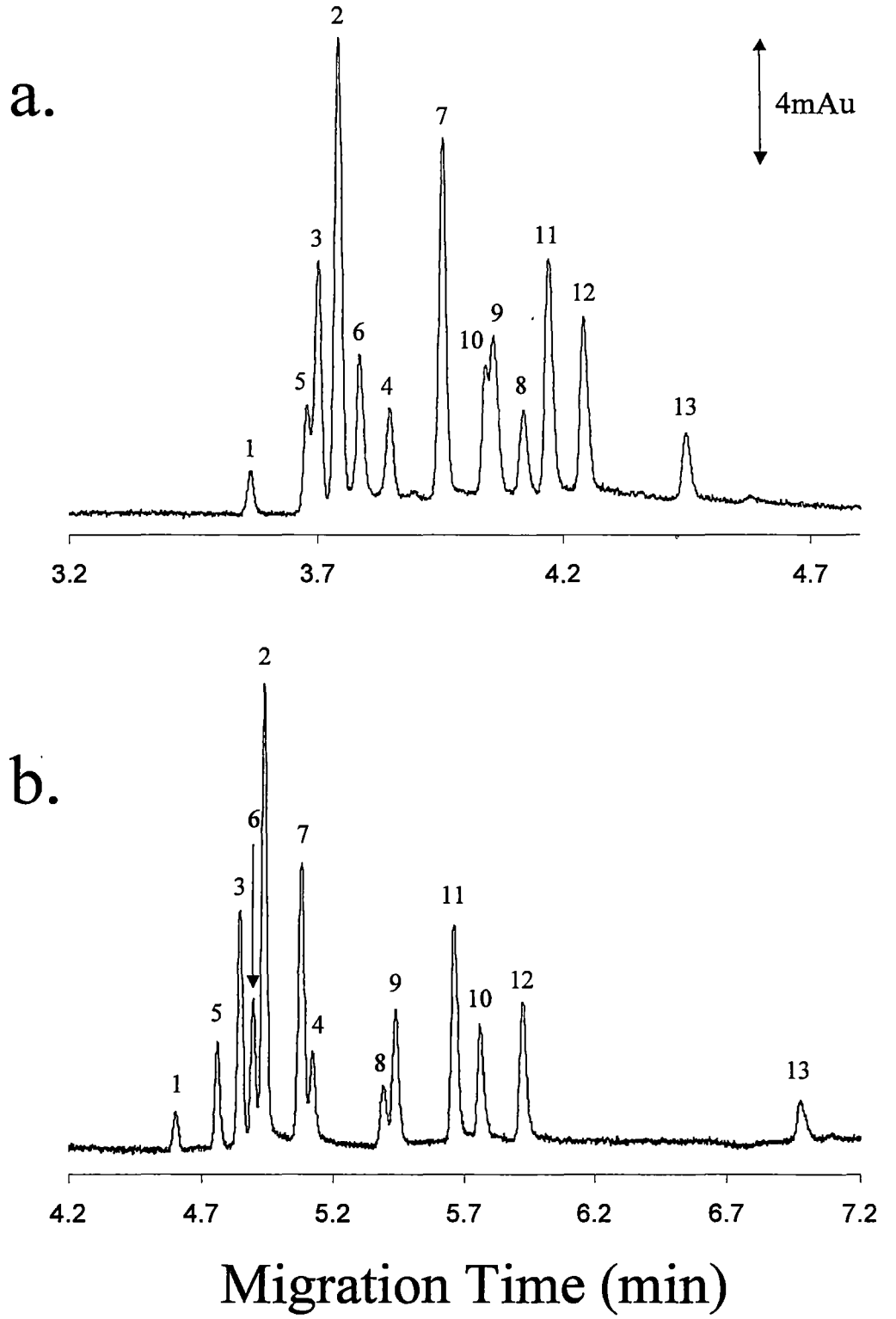

Figure 5.15: Optimum separations calculated with the ANN and using a) the normalised resolution product criterion and b) the minimum resolution criterion with the additional constrain that all mobilities must be greater than 2 x $10^{-9}m^2V^{-1}s^{-1}$. Conditions: a) 0.3% PVS, 0mM β–CD at pH 3.75. b) 0.9% PVS, 5mM β-CD at pH 3.50. Peaks are 1=pyridine, 2=*m*-aminopyridine, 3=*p*-aminopyridine, 4=*o*-aminopyridine, 5=picoline, 6=ethylpyridine, 7=quinoline, 8=aniline, 9=benzylamine, 10=*t*-butylpyridine, 11=methylbenzylamine, 12=ethylaniline and 13=pentylaniline. General conditions: 20mM Citrate. Capillary: 50μm x 50cm (41.5cm to detector), detection at 211nm.

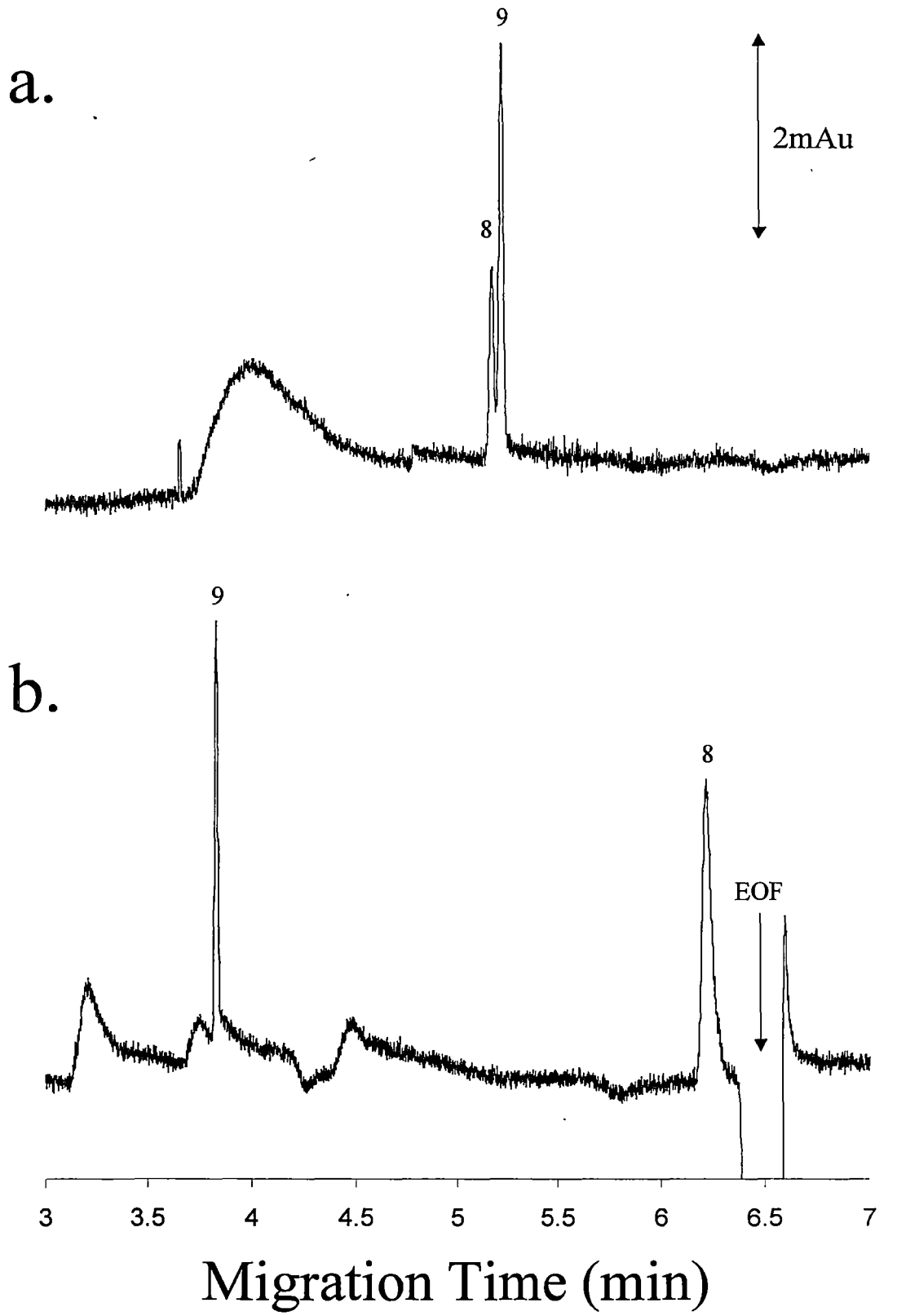

Figure 5.16: Selectivity control offered over aniline and benzylamine. a) Aniline migrating before benzylamine and b) Benzylamine migrating before aniline. Conditions: a) 0.6% PVS, 7mM β-CD at pH 3.50 and b) 0% PVS, 0mM β-CD at pH 5.75. Peaks are 8=aniline and 9=benzylamine. General conditions: 20mM Citrate. Capillary: 50μm x 50cm (41.5cm to detector), detection at 211nm.

3.50) and selecting appropriate values of %PVS and [β-CD]. On the other hand, the reverse migration order could be accomplished using only pH control in the absence of both p-SPs. These very diverse conditions were predicted accurately and rapidly by the ANN. This process could be extended readily to a much wider range of analytes.

5.8 Conclusions

The multi-mode EKC system consisting of polyvinylsulfonate and β-CD as p-SPs combines ion-exchange and hydrophobic interactions as two complementary chromatographic separation mechanisms with an electrophoretic separation. The extent of each interaction can be varied independently by changing the concentration of each p-SP. A mathematical model has been derived which accurately describes the analyte mobilities with differing electrolyte conditions. This model can also be used to successfully optimise the system or the achievement of a desired migration order. The addition of pH as a further experimental parameter limits the application of a physical migration model. However, an artificial neural network was shown to be applicable to this 3-dimensional system and was utilised for the selection of conditions providing the best overall separation or the achievement of a desired migration order. Although a reasonably large number of experimental data points was needed to successfully train the artificial neural network the resultant performance was better than that obtained using the same number of experiments to solve the full mathematical migration model.

The described system is potentially applicable to any analytes that exhibit interactions with PVS and/or β-CD. The system can also be readily modified to suit a particular set of analytes by utilising different pseudo-SPs. One particular area of

application could be in the analysis of pharmaceutically important compounds, since many of these are aromatic bases. The presence of the cyclodextrin could also facilitate the enantiomeric separation while the PVS could aid the electrophoretic separation of different compounds showing very similar electrophoretic mobilities.

5.9 References

1. S.A.C. Wren and R.C. Rowe, *J. Chromatogr.*, 603 (1992) 235.
2. S.A.C. Wren, *J. Chromatogr.*, 636 (1993) 57.
3. S.A.C. Wren and R.C. Rowe, *J. Chromatogr.*, 609 (1992) 363.
4. Y.Y. Rawjee, D.U. Staerk and G. Vigh, *J. Chromatogr.*, 635 (1993) 291.
5. M.E. Biggin, R.L. Williams and G. Vigh, *J. Chromatogr. A*, 692 (1995) 319.
6. Y.Y. Rawjee, R.L. Williams, L.A. Buckingham and G. Vigh, *J. Chromatogr. A*, 688 (1994) 273.
7. B.A. Williams and G. Vigh, *J. Chromatogr. A*, 777 (1997) 295.
8. J.B. Vincent and G. Vigh, *J. Chromatogr. A*, 817 (1998) 101.
9. J.B. Vincent and G. Vigh, *J. Chromatogr. A*, 816 (1998) 233.
10. J. Snopek, I. Jelinek and E. Smolkova-Keulemansova, *J. Chromatogr.*, 452 (1988) 571.
11. R. Kuhn and S. Hoffstetter-Kuhn, *Capillary Electrophoresis: Principles and Practice*, Springer-Verlag, Berlin, 1993.
12. M.C. Breadmore, P.R. Haddad and J.S. Fritz, *Electrophoresis*, 21 (2000) 3181.
13. J. Havel, E.M. Pena, A. Rojas-Hernandez, J.-P. Doucet and A. Panaye, *J. Chromatogr. A*, 793 (1998) 317.
14. L. Pokorna, A. Revilla, J. Havel and J. Patocka, *Electrophoresis*, 20 (1999) 1993.
15. M. Pacheco and J. Havel, *Electrophoresis*, 23 (2002) 268.

Chapter 6

Selectivity Control for Enantiomeric Separations using Dextran Sulfate and Sulfated-Cyclodextrin as Mixed Pseudo-Stationary Phases

6.1 Introduction

The analysis of amino acids is an important area of research in chemistry and biochemistry with EKC being particularly useful for both enantiomeric and non-enantiomeric separation of amino acids. Several additives have been used for the separation of free and derivatized amino acids including micelles, cyclodextrins, crown ethers and proteins [1]. Cyclodextrins are particularly well suited to chiral separations and have the advantage that substituents can be modified to alter their selectivity.

Although the use of additives such as cyclodextrins can facilitate the enantiomeric separation of a wide variety of analytes, the full separation of all peaks in a complex mixture can still be problematic. This can be overcome by varying system parameters such as pH, temperature, applied voltage, use of further additives etc. [2-5]. However, variation of these parameters generally only leads to a small change in the observed selectivity of the system. Furthermore, the selectivity change brought about by variation of these parameters is often unpredictable, with optimisation generally being performed in an empirical manner.

Extensive work has been focused on modelling the enantiomeric separation brought about by the addition of cyclodextrins to the electrolyte. The models range from simple equilibrium-based models [6-8] to more complex models able to handle different types of analytes and cyclodextrins [9-14]. However, these models have generally been used to optimise conditions needed to achieve the best enantiomeric separation between a single pair of enantiomers and not a complex mix of analytes.

Previous chapters have shown that systems comprising cyclodextrins and soluble polymers allow for far greater selectivity control than single additive EKC systems. These systems are also relatively easily modelled, allowing for optimisation and the ability to "tune" the selectivity so as to achieve desired migration orders. The aim of the current chapter is to extend the selectivity control offered in the enantiomeric separation of a test group of three UV absorbing amino acids by accurately modelling a mixed system comprising an anionic cyclodextrin with an anionic polymer, as well as the influence of temperature on the cyclodextrin system alone.

6.2 Experimental

The general details are given in Chapter 2. Detailed conditions are given in each figure caption.

Double-coated capillaries utilising PDDAC and dextran sulfate were used. These were prepared using the same procedure outlined in Chapter 4. The resultant coatings were very robust over the range of [s-β-CD], [dextran sulfate] and temperature used.

6.2.1 Electrolyte preparation

Stock 100mM solutions of phosphoric acid were prepared by dilution of >88% phosphoric acid. 3%(w/v) dextran sulfate solutions were prepared by dissolving the

appropriate amount of solid in 10ml of water. Phosphate electrolytes were prepared by diluting the stock phosphoric acid solution to 20mM and then adding the appropriate amount of s-β-CD or 3% dextran sulfate to give the desired concentration, NaOH was then added to pH 2.0.

6.2.2 *Artificial neural networks*

Calculations using artificial neural networks (ANNs) were performed in the same way as outlined in Chapter 5.

6.3 Effects of Sulfated-β-Cyclodextrin and Temperature

6.3.1 *Selectivity*

Both β- [15] and γ- [16] sulfated cyclodextrins have been used as chiral separating agents. Sulfated-β-CD (s-β-CD) has also been used in the separation of metal ions [17] where the sulfate groups on the cyclodextrin acted as cation-exchangers, analogous to sulfonated cation exchangers. From this it can be expected that the separation mechanism between the s-β-CD and the protonated amino acids will be a combination of host-guest complexation, most likely between the aromatic group on the amino acids and the hydrophobic core of the cyclodextrin, and ion-exchange (IE) interactions between the positive charge on the amino acids and the negative sulfate groups on the cyclodextrin.

Figure 6.1 shows the effect of the addition of s-β-CD on the separation of the three amino acids. It can be seen that even at relatively low cyclodextrin concentrations baseline resolution was obtained for each amino acid. However, full separation of all six enantiomers was not obtained, with co-migration of D-phenylalanine, L-tyrosine

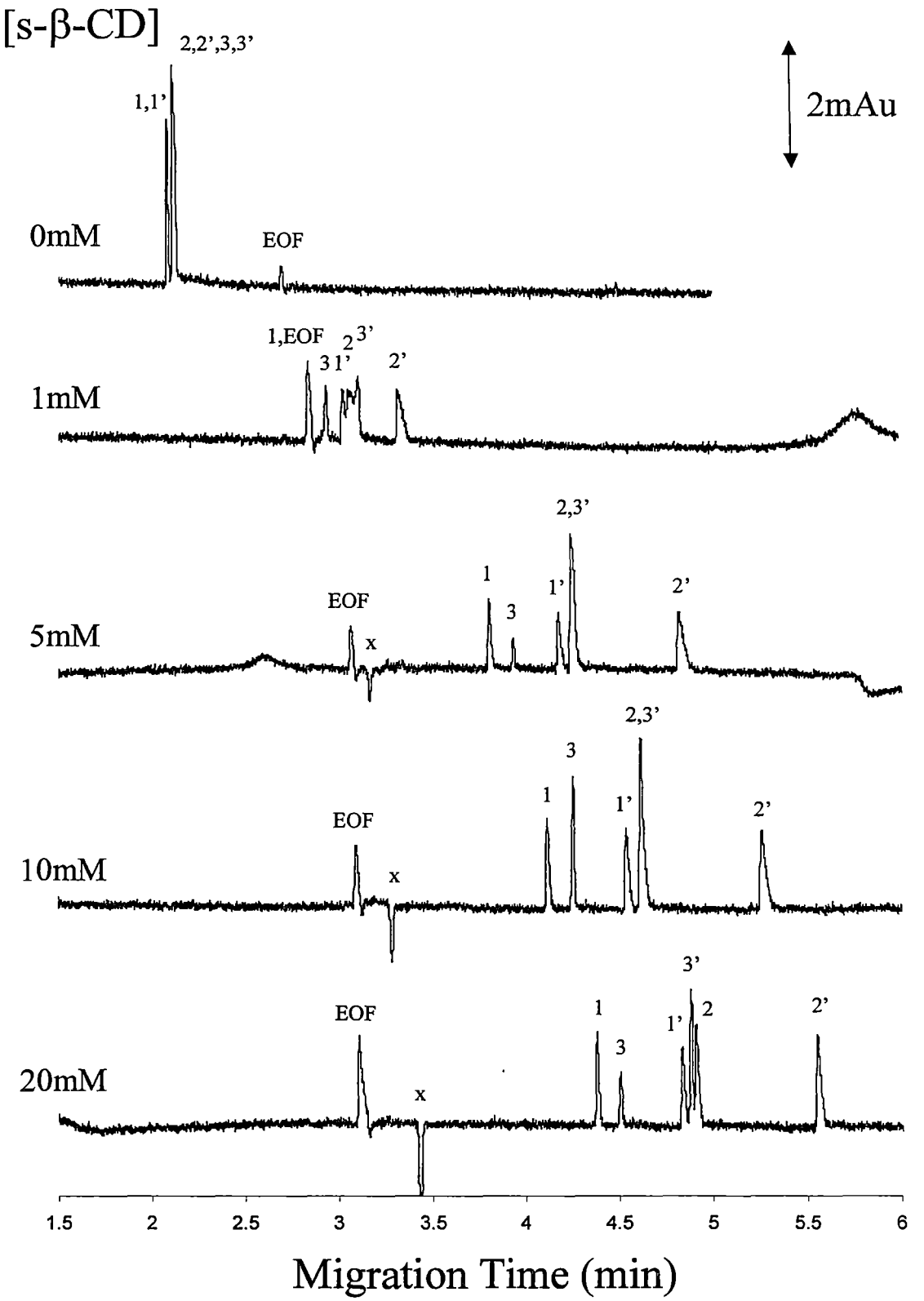

Figure 6.1: Effect of [s-β-CD] on the separation of the 3 amino acids. Peaks are 1=L-Phenylalanine, 1'=D-Phenylalanine, 2=L-Tyrosine, 2'=D-Tyrosine, 3=L-Tryptophan, 3'=D-Tryptophan and x=system peak associated with the addition of s-β-CD. Conditions: 20mM phosphate electrolyte at pH 2.0. Capillary: 25μm x 55cm (46.5cm to detector), separation at 25°C with detection at 210nm.

and D-tryptophan being observed. It can also be seen that the EOF peak co-migrated with L-phenylalanine. On increasing the amount of s-β-CD in the electrolyte, better resolution was obtained with almost baseline resolution being achieved for all six enantiomers at 20mM s-β-CD. It should be noted that the varying peak heights observed for L-tryptophan were due to decomposition in the sample vial. As a result, fresh samples were periodically prepared, leading to the observed difference in peak heights. If quantification was to be performed it would be advisable to regularly replace the sample.

From Chapter 4 and the work by Muzikar *et al.* [17] it can be expected that a major component of the amino acid-cyclodextrin interaction will be IE in nature. The observed separation should therefore be influenced by increasing the concentration of the competing ion in the electrolyte (Na^+ for the work presented here). Figure 6.2 shows the effect of increasing the concentration of sodium chloride in the presence of s-β-CD. It can be seen that as the concentration of competing ion increased, the amount of interaction with the s-β-CD decreased, leading to a separation approaching that of a pure CE system when [NaCl] was sufficiently high.

Temperature is known to have a large effect on enantiomeric separation due to its influence on the analyte-cyclodextrin complexation process. Generally it has been shown that better enantiomeric separations are achieved at lower temperatures [18,19] due to increased migration times and an increase in the stability of the inclusion complex. However, the effect of temperature on the selectivity of enantiomeric systems, has not been comprehensibly evaluated. Figure 6.3 shows the effect of varying temperature on the enantiomeric separation of the three amino acids in the presence of 15mM s-β-CD. Increasing the temperature from 15 to 60°C led to increased mobilities for all of the analytes as expected. However, it can also be seen

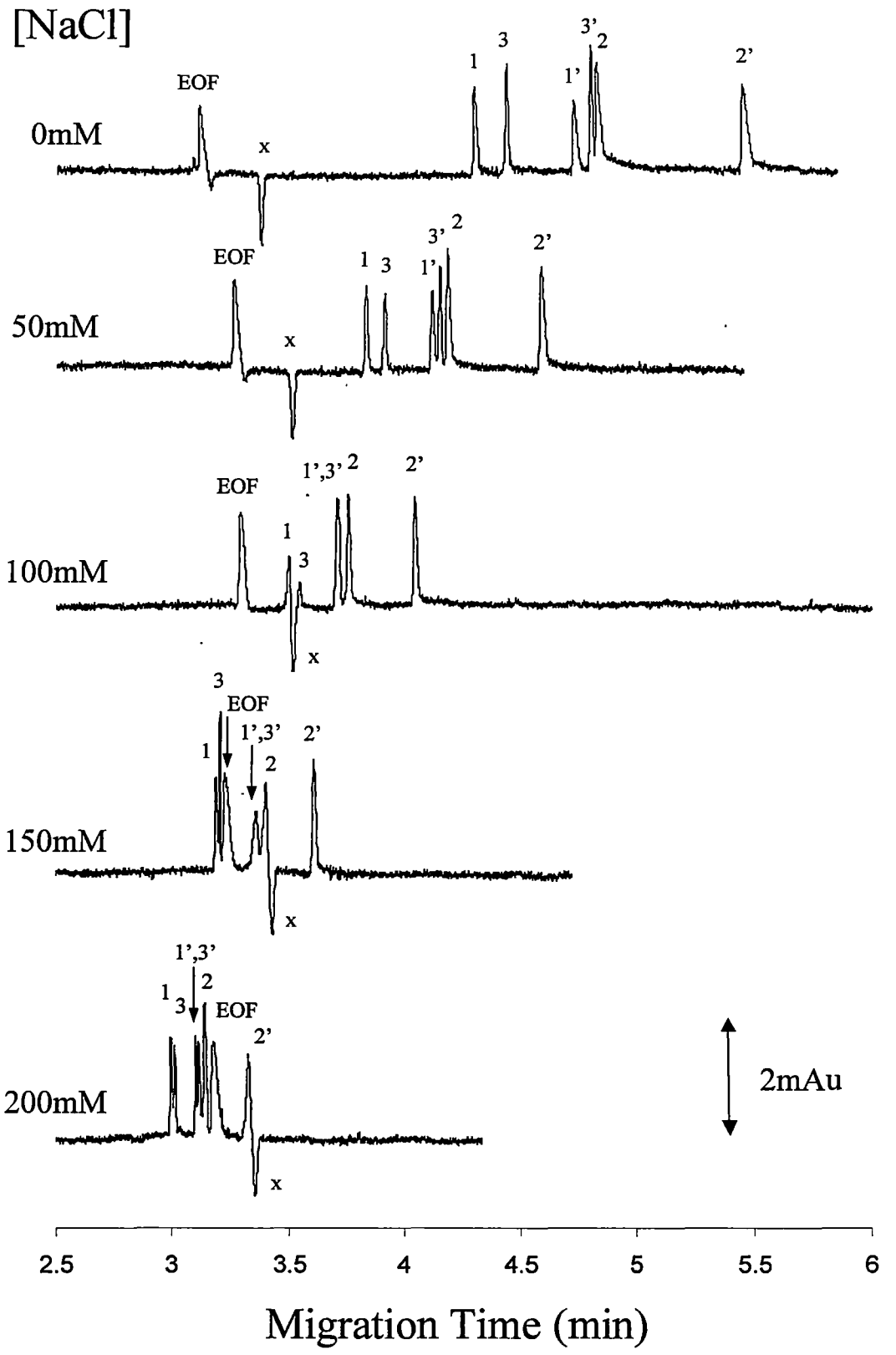

Figure 6.2: Effect of competing ion concentration in a electrolyte containing 15mM s-β-CD. Peaks are 1=L-Phenylalanine, 1'=D-Phenylalanine, 2=L-Tyrosine, 2'=D-Tyrosine, 3=L-Tryptophan, 3'=D-Tryptophan and x=system peak associated with the addition of s-β-CD. Conditions: 20mM phosphate +15mM s-β-CD at pH 2.0. Capillary: 25μm x 55cm (46.5cm to detector), separation at 25°C with detection at 210nm.

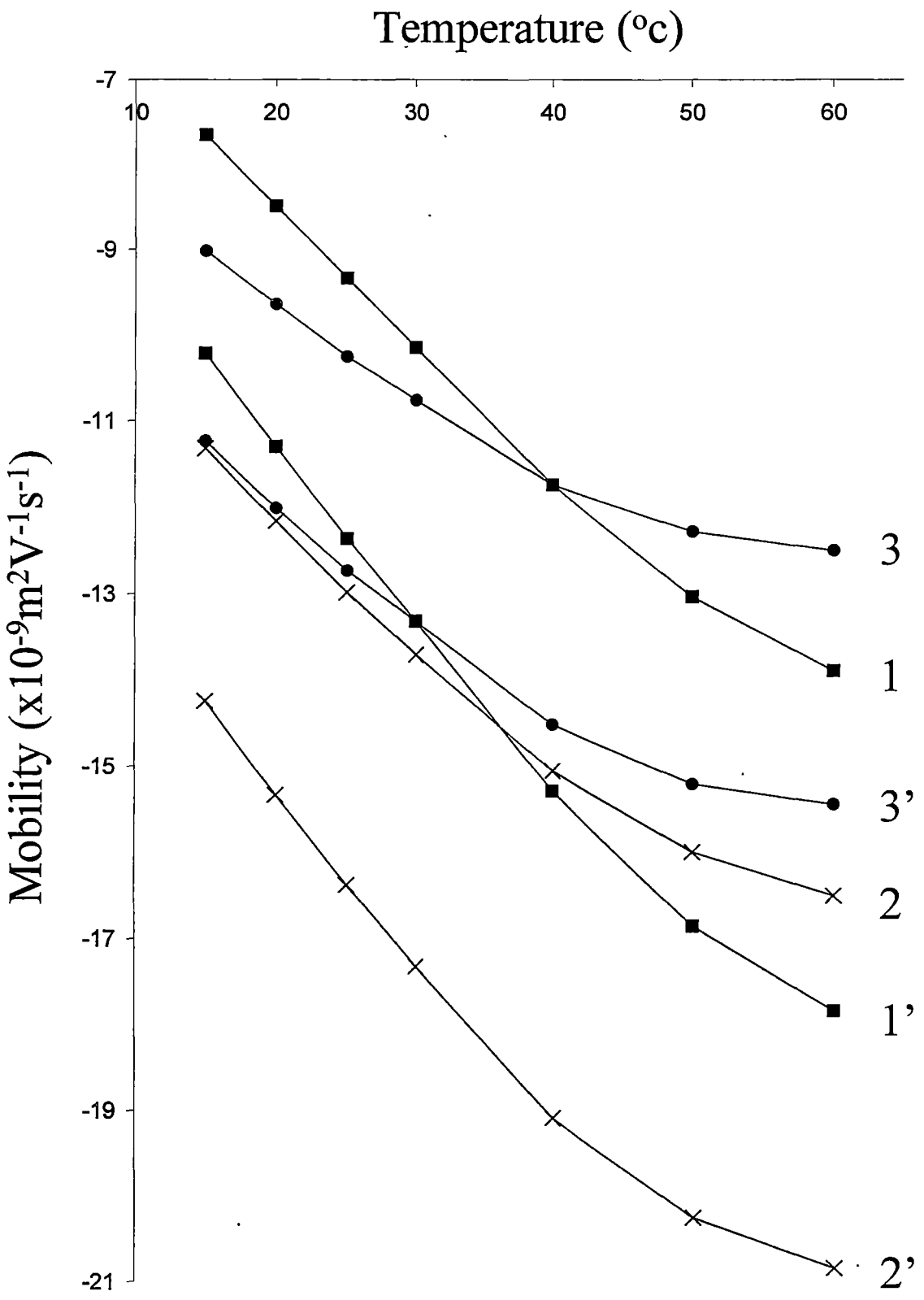

Figure 6.3: Effect of temperature on mobilities of the amino acids in a electrolyte containing 15mM s-β-CD. Peaks are 1=L-Phenylalanine, 1'=D-Phenylalanine, 2=L-Tyrosine, 2'=D-Tyrosine, 3=L-Tryptophan and 3'=D-Tryptophan. Conditions: 20mM phosphate +15mM s-β-CD at pH 2.0

that increasing the temperature also altered the selectivity of the system, with different migration orders observed at 15 and 60°C. It should also be noted that although the resolution decreased on increasing the temperature, even at 60°C baseline resolution of all six enantiomers was achieved.

6.3.2 Modelling

From Figure 6.1 and Figure 6.3 it can be seen that it should be possible to model and optimise the 2-dimensional system using the parameters [s-β-CD] and temperature. However, since the temperature effect is relatively complex and difficult to describe accurately using a physical model, the use of artificial neural networks (ANNs) was investigated.

The 2-dimensional experimental space, 0-20mM s-β-CD and 15-60°C was used comprising a total of 56 points. Different ANN architectures were tested, as was the number of points used to train and validate the model. An ANN having a 2-5-5-6 structure, that is, consisting of 4 layers (2 hidden layers) with 2 nodes in the input layer ([s-β-CD] and temperature), 5 nodes in both the hidden layers and 6 in the output layer (corresponding to the mobilities of the 6 enantiomers), was found to be optimal. Best results were also obtained when 28 points were used to train the ANN with the further 28 points being used to verify the model. Table 6.1 shows the errors associated with differing numbers of training iterations. It can be seen that 20,000 iterations led to the lowest errors in the verification set. Further training iterations, while lowering the error in the training set, increased the error associated with the verifications set. Thus 20,000 iterations were used to train the current model.

Figure 6.4 shows the correlation between observed and predicted mobilities using the ANN. It can be seen that very good correlation was obtained, with an r^2 value of

Table 6.1: Errors vs. training iterations using a 2-5-5-6 ANN.

Number of Training Iterations	*RMS Error in Training Set*	*RMS Error in Verification Set*	*r^2 on Correlation Graph[1]*
1000	1.6940	1.3800	0.9819
3000	0.7023	0.5754	0.9976
7000	0.5144	0.5657	0.9985
10,000	0.3205	0.4805	0.9987
15,000	0.2680	0.3764	0.9992
20,000	0.2030	0.3636	0.9993
30,000	0.1777	0.3911	0.9992
40,000	0.1680	0.4086	0.9992

1 – using all 56 points within the experimental space

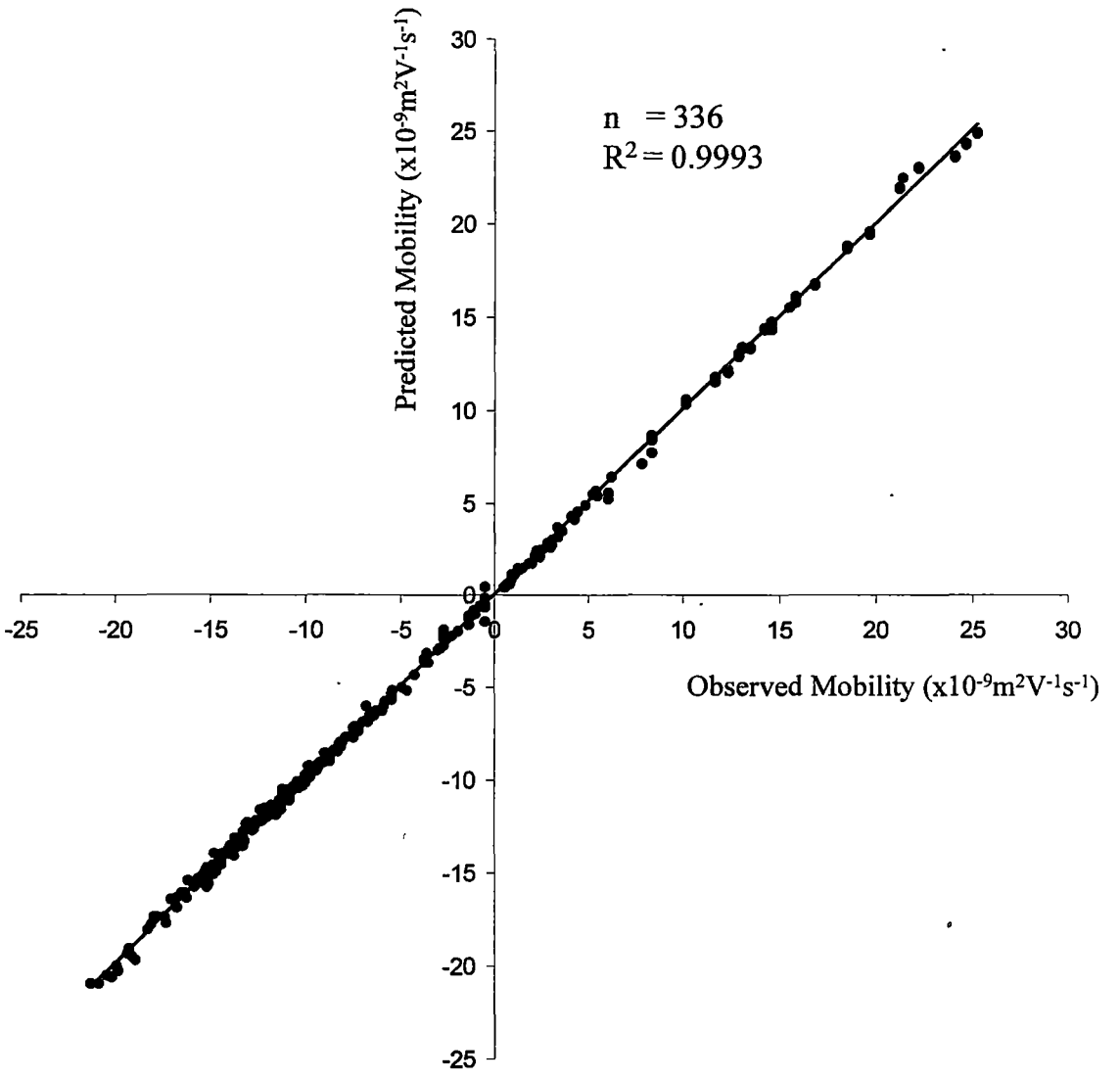

Figure 6.4: Correlation between observed and predicted mobilities using the 2-5-5-6 ANN. All 56 experimental conditions included in the correlation graph, i.e. both those used to train and verify the model.

greater than 0.999. This good correlation allowed the model to accurately predict analyte mobilities anywhere within the 2-dimensional experimental space.

6.3.3 Optimisation

Optimisation was performed using both the NRP and MR criteria as outlined in Chapter 2.

Figure 6.5 shows the observed and predicted separations using conditions calculated with the NRP criterion, whilst Figure 6.6 shows the same information for the MR criterion. It can be seen that both criteria yielded separations with almost baseline resolution of all six enantiomers, but the separation calculated using the NRP criterion gave more evenly spaced peaks than the MR criterion. Both criteria predicted very different electrolyte compositions, with the NRP criterion predicting a low concentration of s-β-CD and low temperature while the MR criterion predicted a high concentration of s-β-CD and a high temperature. Agreement between observed and predicted migration times was also very good for both optima, with differences being less than 1% in both cases. The described system was also very robust, even at higher temperatures, with reproducibility of migration times being less than 1% over 13 successive runs at 60°C.

The model can also be used to individually optimise the separation of each amino acid. Figure 6.7 shows the optimised separations obtained when only individual amino acids were considered. It can be seen that very similar conditions were calculated for each amino acid. It is also interesting to note that a high temperature were predicted for each of the separations, in contrast to previous work which assumed lower temperatures were best for enantiomeric separations [18,19]. The use of higher temperature was also useful since it facilitates fast separations (all under 3.3

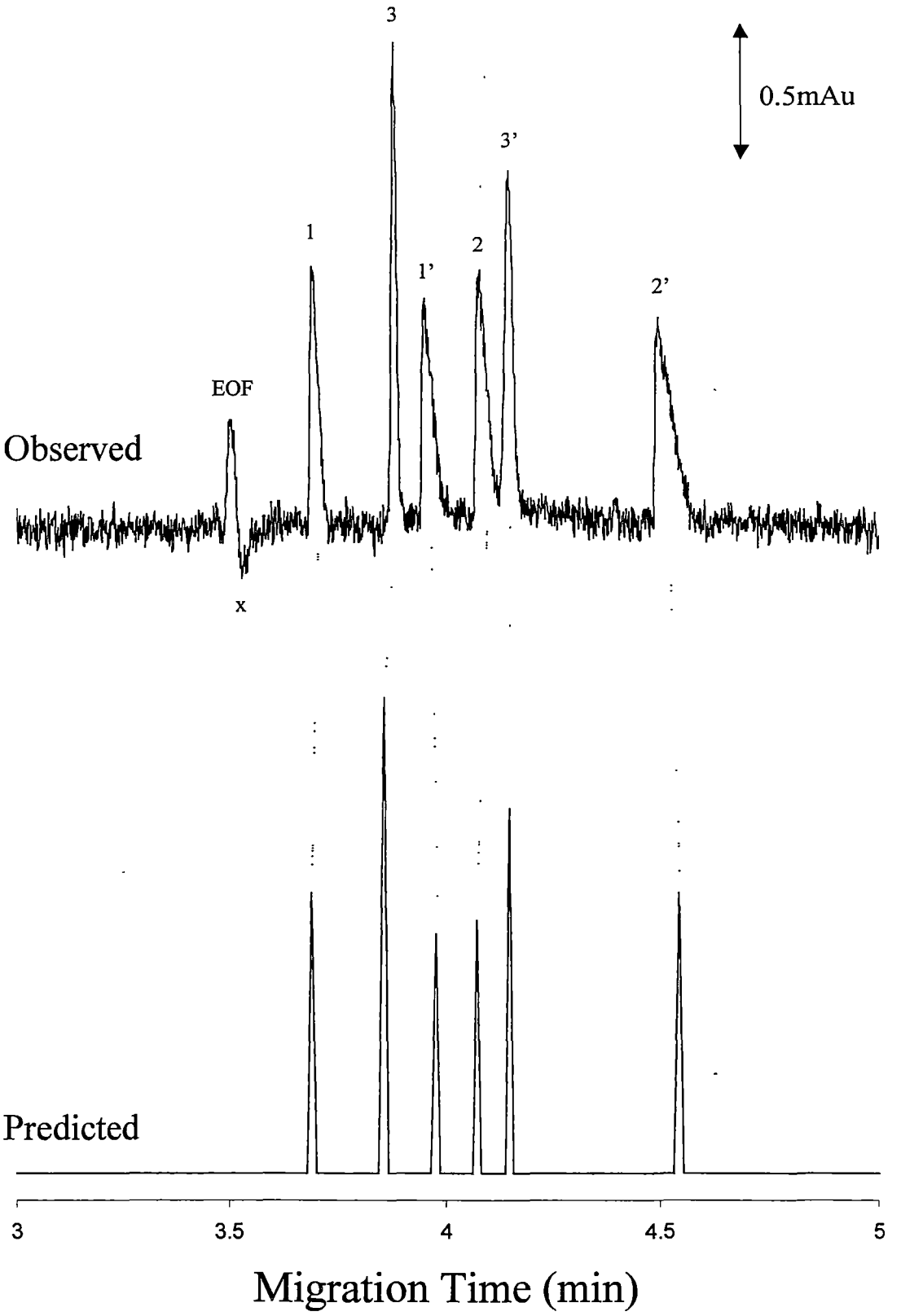

Figure 6.5: Optimised separation at 1.5mM s-β-CD and 15°c. Conditions calculated using the NRP criterion. Peaks are 1=L-Phenylalanine, 1'=D-Phenylalanine, 2=L-Tyrosine, 2'=D-Tyrosine, 3=L-Tryptophan, 3'=D-Tryptophan and x=system peak associated with the addition of s-β-CD. General conditions: 20mM phosphate electrolyte at pH 2.0. Capillary: 25μm x 55cm (46.5cm to detector), with detection at 210nm.

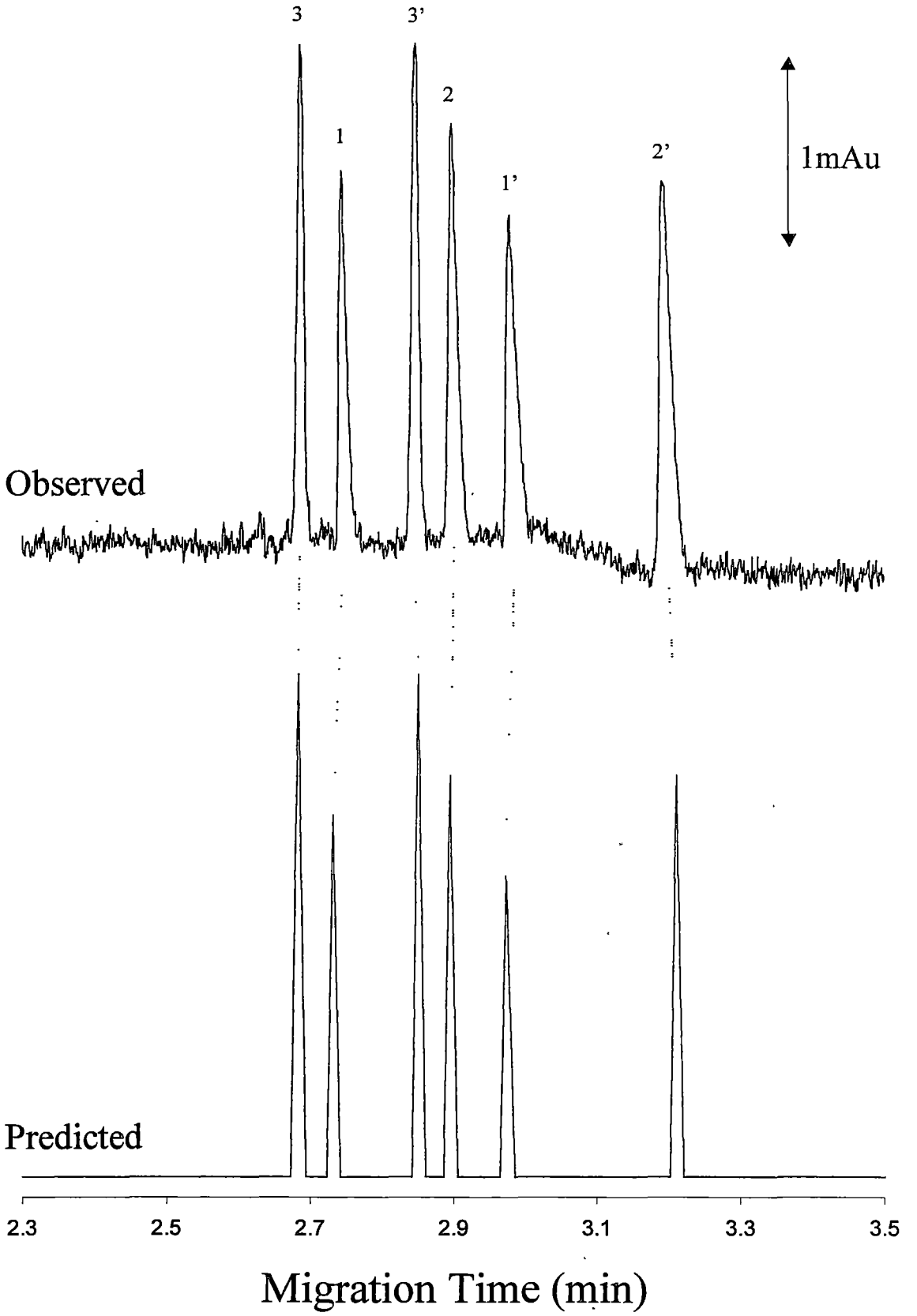

Figure 6.6: Optimised separation at 13mM s-β-CD and 60oc. Conditions calculated using the MR criterion. Peaks are 1=L-Phenylalanine, 1'=D-Phenylalanine, 2=L-Tyrosine, 2'=D-Tyrosine, 3=L-Tryptophan and 3'=D-Tryptophan. General conditions: 20mM phosphate electrolyte at pH 2.0. Capillary: 25μm x 55cm (46.5cm to detector), with detection at 210nm.

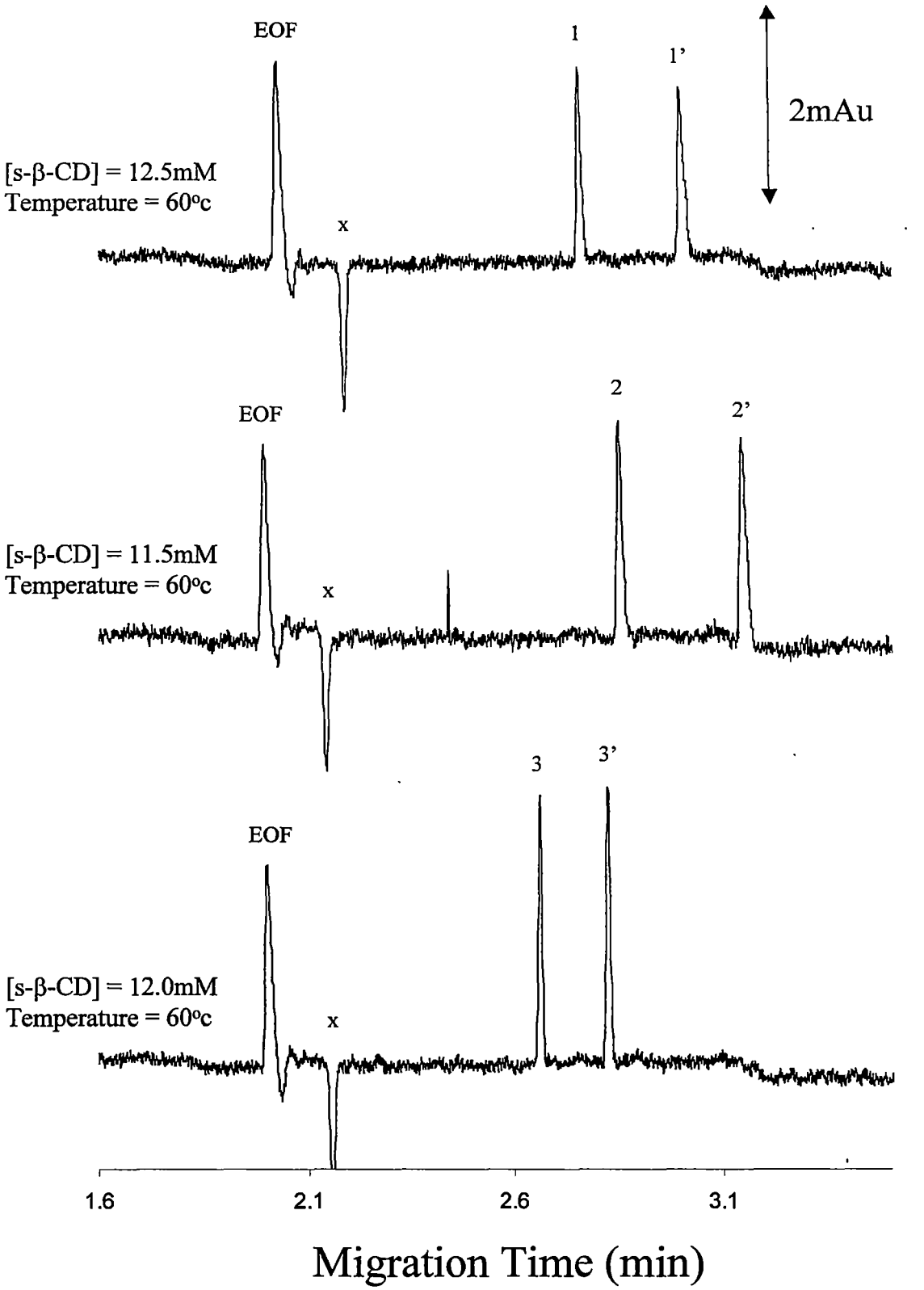

Figure 6.7: Optimised enantiomeric separations for individual amino acids. Peaks are 1=L-Phenylalanine, 1'=D-Phenylalanine, 2=L-Tyrosine, 2'=D-Tyrosine, 3=L-Tryptophan, 3'=D-Tryptophan and x=system peak associated with the addition of s-β-CD. Conditions: 20mM phosphate electrolyte at pH 2.0. Capillary: 25μm x 55cm (46.5cm to detector), with detection at 210nm.

minutes). The best enantiomeric separation is also not achieved at the highest concentration of s-β-CD but at values around 12mM, agreeing with previous work using cyclodextrins where it was found that initially enantiomeric resolution increased on increasing cyclodextrin concentration to some optimum value, after which the resolution tended to decrease [6,7].

6.4 Sulfated-β-Cyclodextrin and Dextran Sulfate System

6.4.1 Selectivity

Previous chapters have shown the advantages for selectivity control from the addition of more than one additive to an EKC system. These systems have involved the combination of a cyclodextrin and a soluble polymer for the separation of both anions and cations. The work presented in this chapter uses the soluble anionic polymer dextran sulfate as a capillary coating, but this polymer also has the potential to interact with the amino acids via an IE mechanism. Figure 6.8 shows the effect of the addition of dextran sulfate on the separation of the amino acids. The straight CE separation led to co-migration of tyrosine and tryptophan. However, addition of dextran sulfate separated out all three amino acids, even at relatively low concentrations of the polymer (around 0.3%(w/v)). Dextran sulfate can be seen to interact most strongly with tryptophan and most weakly with phenylalanine, while showing no enantiomeric selectivity. The splitting that was observed for tyrosine probably resulted from interaction with residual s-β-CD molecules attached to the capillary wall, due to displacement of dextran sulfate molecules. This problem was accentuated because of the small diameter capillaries used (25μm, used so as to decrease high currents encountered on addition of large amounts, >10mM, of

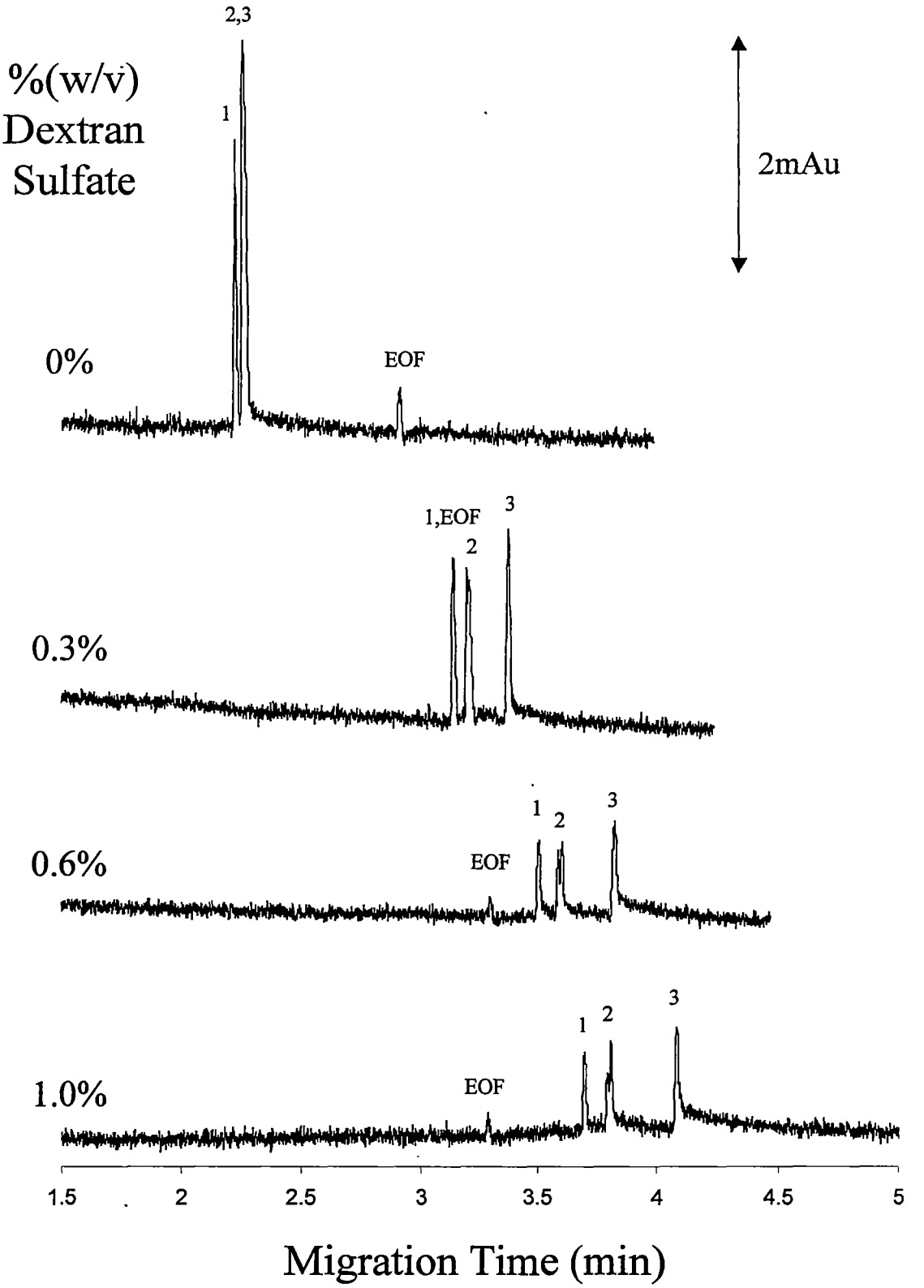

Figure 6.8: Effect of the %(w/v) Dextran Sulfate on the separation of the 3 amino acids. Peaks are 1=DL-Phenylalanine, 2=DL-Tyrosine and 3=DL-Tryptophan. Conditions: 20mM phosphate electrolyte at pH 2.0. Capillary: 25µm x 55cm (46.5cm to detector), separation at 25°C with detection at 210nm.

s-β-CD). This effect was noted only for tyrosine due to the large interaction observed between s-β-CD and D-tyrosine, see Figure 6.1. The interaction between the amino acids and dextran sulfate was most probably IE in nature, supported by the fact that as the competing ion concentration in the electrolyte was increased, observed mobilities tended towards their corresponding CE values (data not shown).

It can be seen from Figure 6.1 and Figure 6.8 that s-β-CD and dextran sulfate offered different selectivities for the three amino acids. Generally s-β-CD interacted strongly with both tyrosine enantiomers, while dextran sulfate interacted most strongly with tryptophan. The combined system comprising both s-β-CD and dextran sulfate added to the electrolyte should combine the enantiomeric separation of the s-β-CD and the selectivity offered by the dextran sulfate.

6.4.2 Modelling

Since both pseudo-SPs are anionic and therefore should have minimal interaction with each other, it can be reasonably assumed that they should interact independently with the amino acids. Figure 6.9 shows the resultant two p-SP system where the association constants for the amino acid-cyclodextrin and amino acid-dextran sulfate complexes are represented by K_{cd} and K_{ds} respectively. These association constants refer to the following equilibria

$$A + CD \overset{K_{cd}}{\rightleftharpoons} A(CD) \qquad (6\text{-}1)$$

$$A + DS \overset{K_{ds}}{\rightleftharpoons} A(DS) \qquad (6\text{-}2)$$

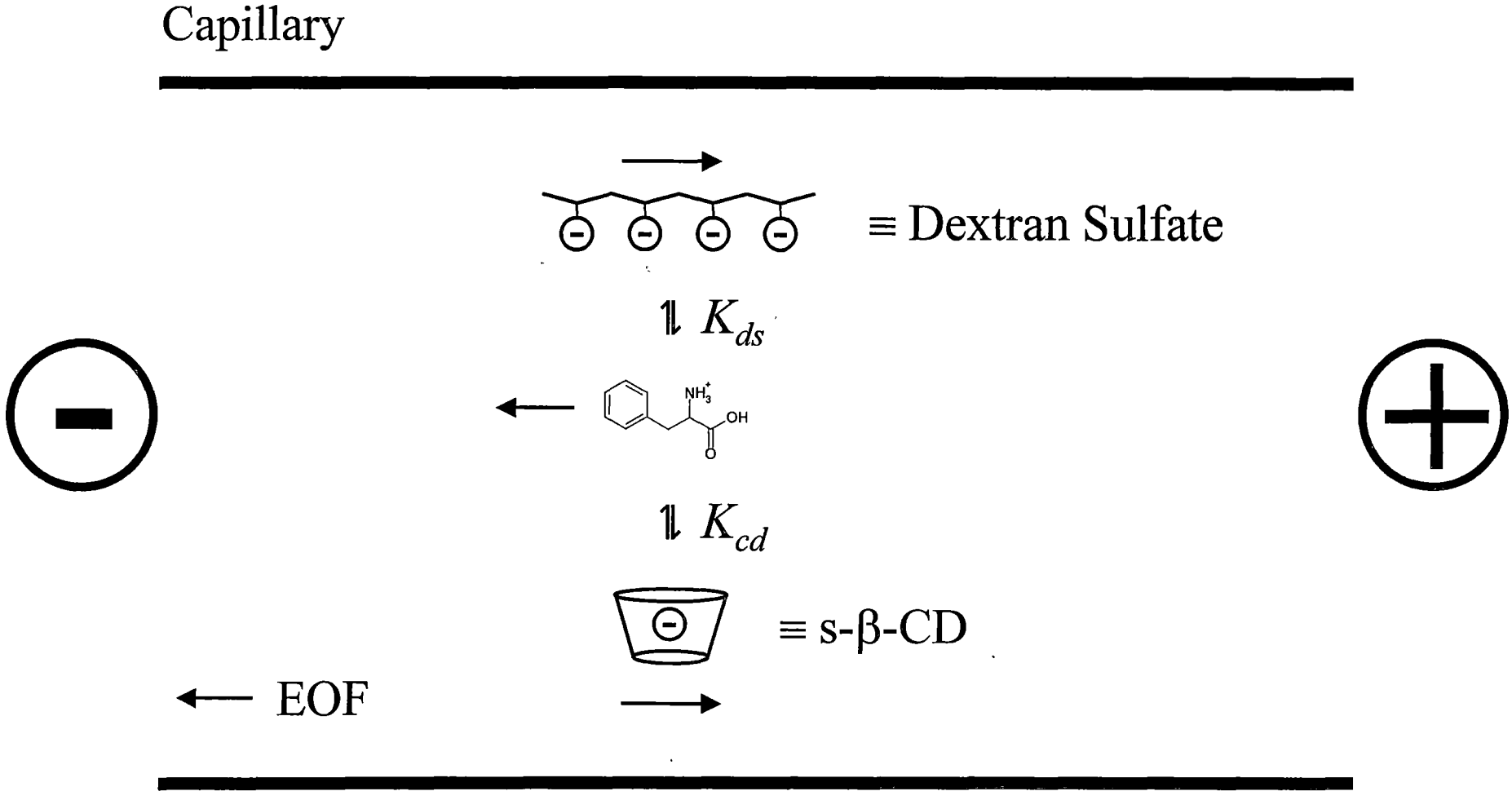

Figure 6.9: Resultant two pseudo-SP system. K_{cd} and K_{ds} represent the association constant for the amino acid and the s-β-CD and dextran sulfate respectively.

where A refers to the amino acid, CD and DS to the cyclodextrin and dextran sulfate respectively and A(CD) and A(DS) to the amino acid-cyclodextrin and amino acid-dextran sulfate complexes respectively.

From eqns (6-1) and (6-2) we can write

$$K_{cd} = \frac{[A(CD)]}{[A][CD]} \tag{6-3}$$

$$K_{ds} = \frac{[A(DS)]}{[A][DS]} \tag{6-4}$$

The observed mobility of an analyte when present in different forms, i.e. when complexed with different additives can be given by

$$\mu_{obs} = f_A\mu_A + f_B\mu_B + f_C\mu_C \tag{6-5}$$

where f is the fraction of analyte and μ is the mobility of the analyte in the various forms. The mobilities of the amino acids in the current system can therefore be represent by the following equation.

$$\mu_{obs} = \frac{[A]}{[A]+[A(CD)]+[A(DS)]}\mu_{bge} + \frac{[A(CD)]}{[A]+[A(CD)]+[A(DS)}\mu_{cd} + \frac{[A(DS)]}{[A]+[A(CD)]+[A(DS)}\mu_{ds} \tag{6-6}$$

Substituting in eqns (6-3) and (6-4) leads to

$$\mu_{obs} = \frac{1}{1+K_{cd}[CD]+K_{ds}[DS]}\mu_{bge} + \frac{K_{cd}[CD]}{1+K_{cd}[CD]+K_{ds}[DS]}\mu_{cd} + \frac{K_{ds}[DS]}{1+K_{cd}[CD]+K_{ds}[DS]}\mu_{ds} \quad (6\text{-}7)$$

This simplifies to

$$\mu_{obs} = \frac{1}{1+k'_{cd}+k'_{ds}}\mu_{bge} + \frac{k'_{cd}}{1+k'_{cd}+k'_{ds}}\mu_{cd} + \frac{k'_{ds}}{1+k'_{cd}+k'_{ds}}\mu_{ds} \quad (6\text{-}8)$$

where $k'_{cd} = K_{cd}[CD]$ and $k'_{ds} = K_{ds}[DS]$.

Eqn (6-8) contains five unknowns, K_{cd}, K_{ds}, μ_{bge}, μ_{cd} and μ_{ds}. The 2-dimensional experimental space consisting of 0-15mM s-β-CD and 0-1%(w/v) dextran sulfate was chosen. For the modelling work [s-β-CD] was replaced with %(w/v) s-β-CD so K_{cd} and K_{ds} values could be compared directly.

6.4.3 Application of the Migration Model

Since eqn (6-8) contains 5 unknowns, a minimum of six experimental points was needed to derive the constants. Although six points gave a satisfactory correlation between predicted and observed mobilities, the best results were obtained when 9 points within the experimental space were used for the non-linear regression. Various layouts of these 9 points were tested, all giving very similar results. For the work here the layout consisting of the 9 points that make a diagonal cross on the experimental space was chosen for the primary set. The further 16 points within the experimental space (the validation set) were used to verify the predictive power of the model

Table 6.2 shows the constants derived using non-linear regression of eqn (6-8). It can be seen that the constants agreed very well with the observed trends. The K_{cd} values were different for each enantiomer, hence leading to enantiomeric separation. It can also be seen that the largest difference in K_{cd} values between enantiomers was for tyrosine. This agreed with the fact that tyrosine showed the best enantiomeric resolution after addition of s-β-CD (~1.135 for tyrosine at 15mM s-β-CD compared to ~1.105 and ~1.085 for phenylalanine and tryptophan, respectively).

K_{ds} values also agreed with expected trends with each amino acid showing very similar values for each enantiomer, agreeing with the fact that dextran sulfate showed no enantiomeric resolution. K_{ds} values were also substantially lower than K_{cd} values implying that the analyte-dextran sulfate interaction was far weaker than the analyte-cyclodextrin interaction. Similar agreement was obtained for the μ_{ds} values, relating to the mobility of the associated amino acid-dextran sulfate complex. These values were all negative since it can be expected that association of a cationic amino acid molecule with the highly charged dextran sulfate should have only a minor effect on the observed mobility of the polymer. Similarly μ_{cd} values were also negative since a 1:1 interaction between an amino acid and the s-β-CD should still leave a highly anionic complex. It was also observed that both enantiomers of each amino acid showed very similar μ_{ds} values but differing μ_{cd} values, agreeing with the chiral and achiral nature of the s-β-CD and dextran sulfate, respectively.

Figure 6.10 shows the correlation between observed and predicted mobilities using eqn (6-8) and the constants shown in Table 6.2. It can be seen that very good correlation was obtained with an r^2 value of 0.998. This showed that the proposed

Table 6.2: Parameters derived from non-linear regression of eqn (6-8).

Analyte	K_{cd}	K_{ds}	μ_{cd}^{1}	μ_{ds}^{1}	μ_{bge}^{1}
L-Phenylalanine	420.1	4.28	-15.1	-10.3	14.8
D-Phenylalanine	520.4	4.27	-18.0	-10.3	14.8
L-Tyrosine	510.1	4.02	-18.6	-11.7	13.8
D-Tyrosine	629.4	3.96	-21.9	-11.7	13.8
L-Tryptophan	410.0	4.87	-16.1	-13.9	13.8
D-Tryptophan	539.8	4.61	-18.3	-14.1	13.8

[1] – $x10^{-9} m^2 V^{-1} s^{-1}$

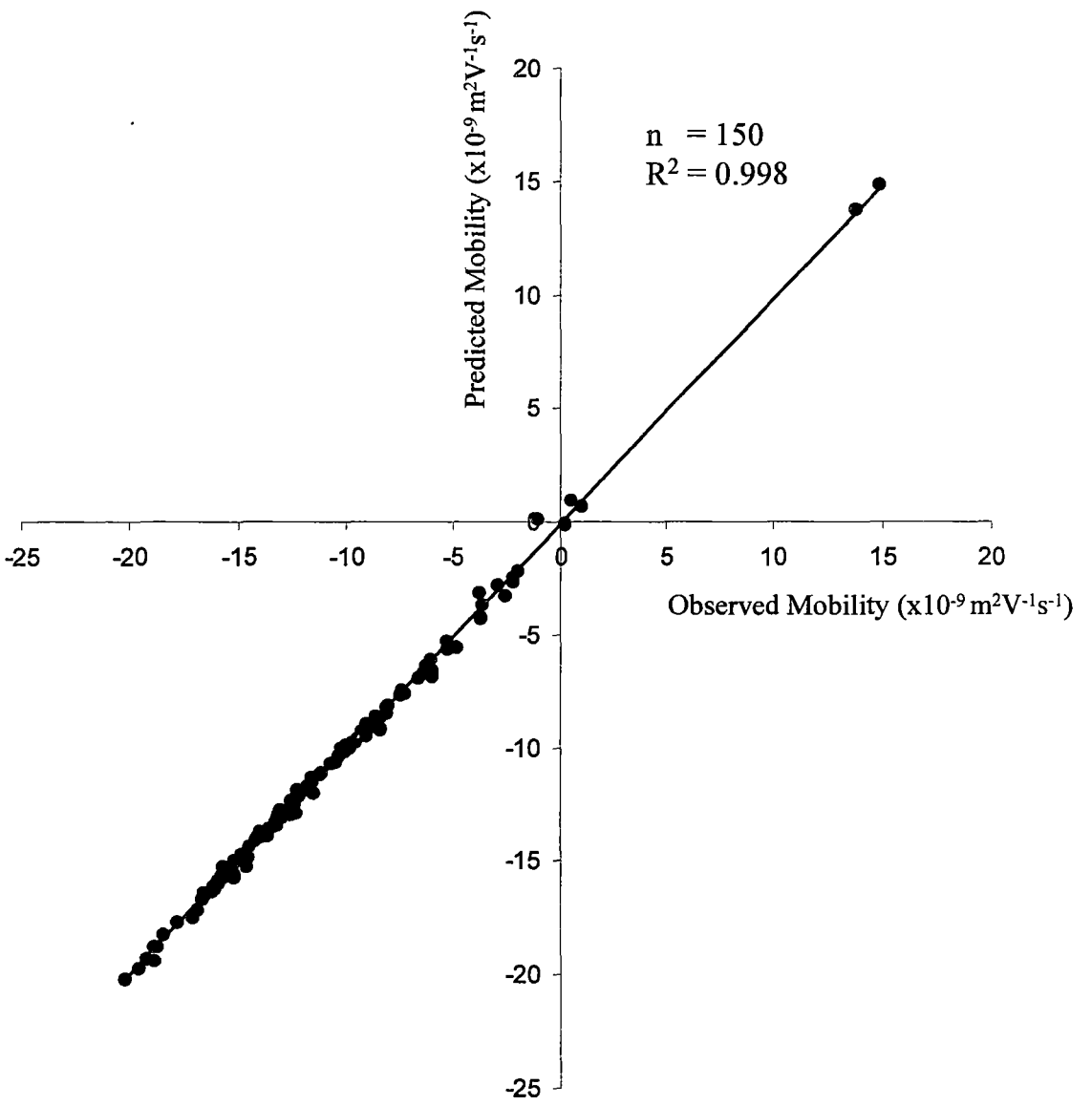

Figure 6.10: Correlation between observed and predicted mobilities using eqn (6-8) and the constants shown in Table 6.2. All 25 experimental conditions included in the correlation graph, i.e. both the primary and verification sets.

model accurately described the two p-SP system. It also supported the earlier assumption that both p-SPs interacted independently with the analytes.

6.4.4 Optimisation

Optimisation of the system was again performed using the NRP and MR criteria, see Chapter 2. The optimum separations are shown in Figure 6.11 and Figure 6.12, along with the predicted separations. Again, agreement between predicted and observed migration times of the optimums was very good with differences of less than 0.5%. The selectivity offered by both criteria again differed with the NRP criterion yielding a more evenly spaced separation. The system was also very robust with variations in migration time being less than 2%RSD over 13 successive runs. Between-column reproducibility was also very good, with the variation in migration times between two different coated capillaries prepared a month apart being less than 2%RSD for the amino acids and less than 2.6%RSD for the EOF.

6.4.5 Tuning the separation selectivity

Previous chapters have shown that having an accurate migration model introduced the ability to predict conditions needed to achieve desired migration orders. However, previous work focussed only on pairs of analytes and not the full system. The ability to control the separation selectivity offers advantages where co-migration is a problem or where peaks are masked by other components present in the sample in much larger concentrations. For the work presented here the full set of enantiomers was included so that the desired migration order of all six enantiomers could be entered into the model and the optimum conditions needed to achieve that order could be calculated.

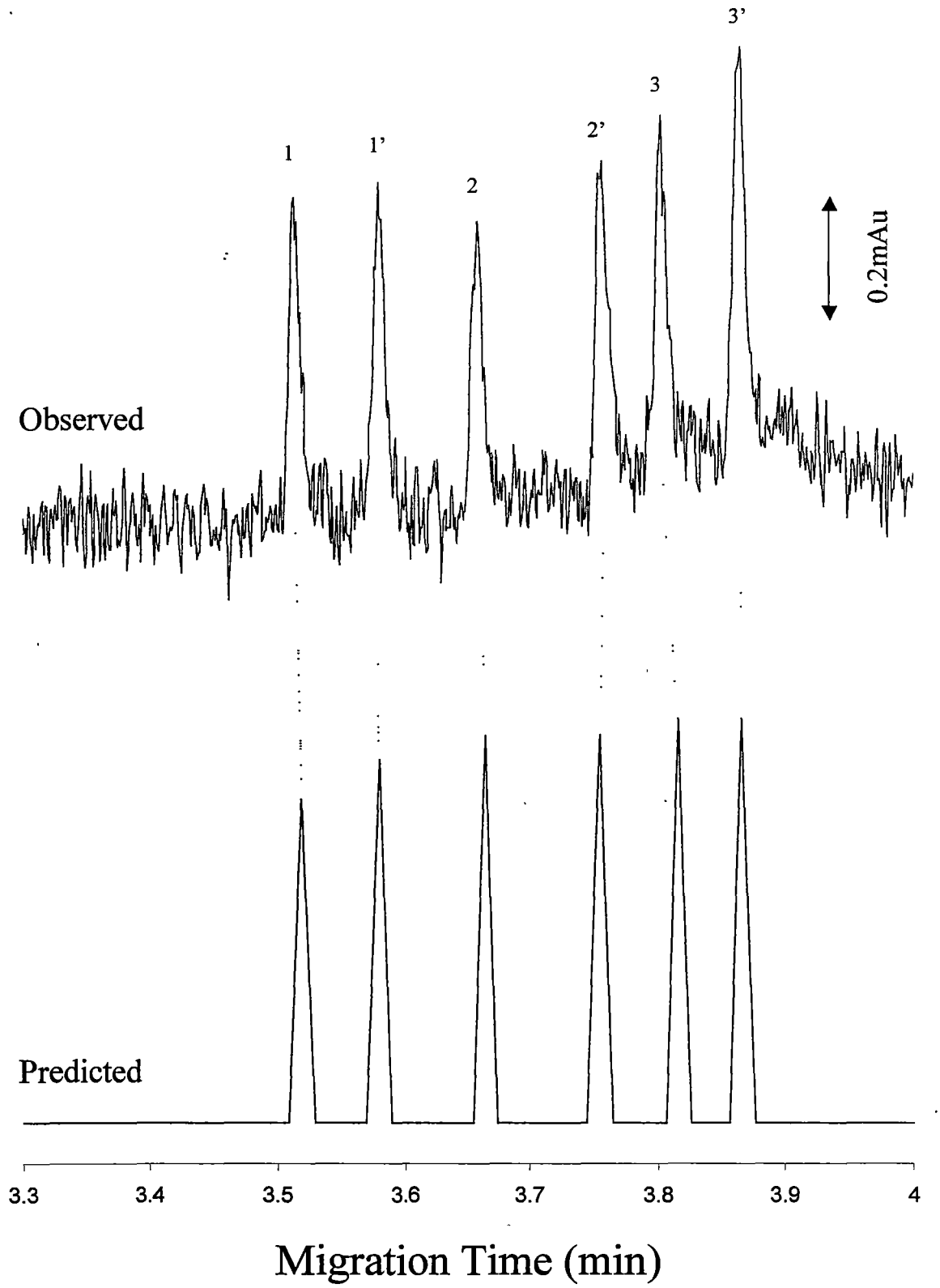

Figure 6.11: Optimised separation at 0.5mM s-β-CD and 0.55% dextran sulfate. Conditions calculated using the NRP criterion and eqn (6-8). Peaks are 1=L-Phenylalanine, 1'=D-Phenylalanine, 2=L-Tyrosine, 2'=D-Tyrosine, 3=L-Tryptophan and 3'=D-Tryptophan. General conditions: 20mM phosphate electrolyte at pH 2.0. Capillary: 25μm x 55cm (46.5cm to detector), separation at 25°C with detection at 210nm.

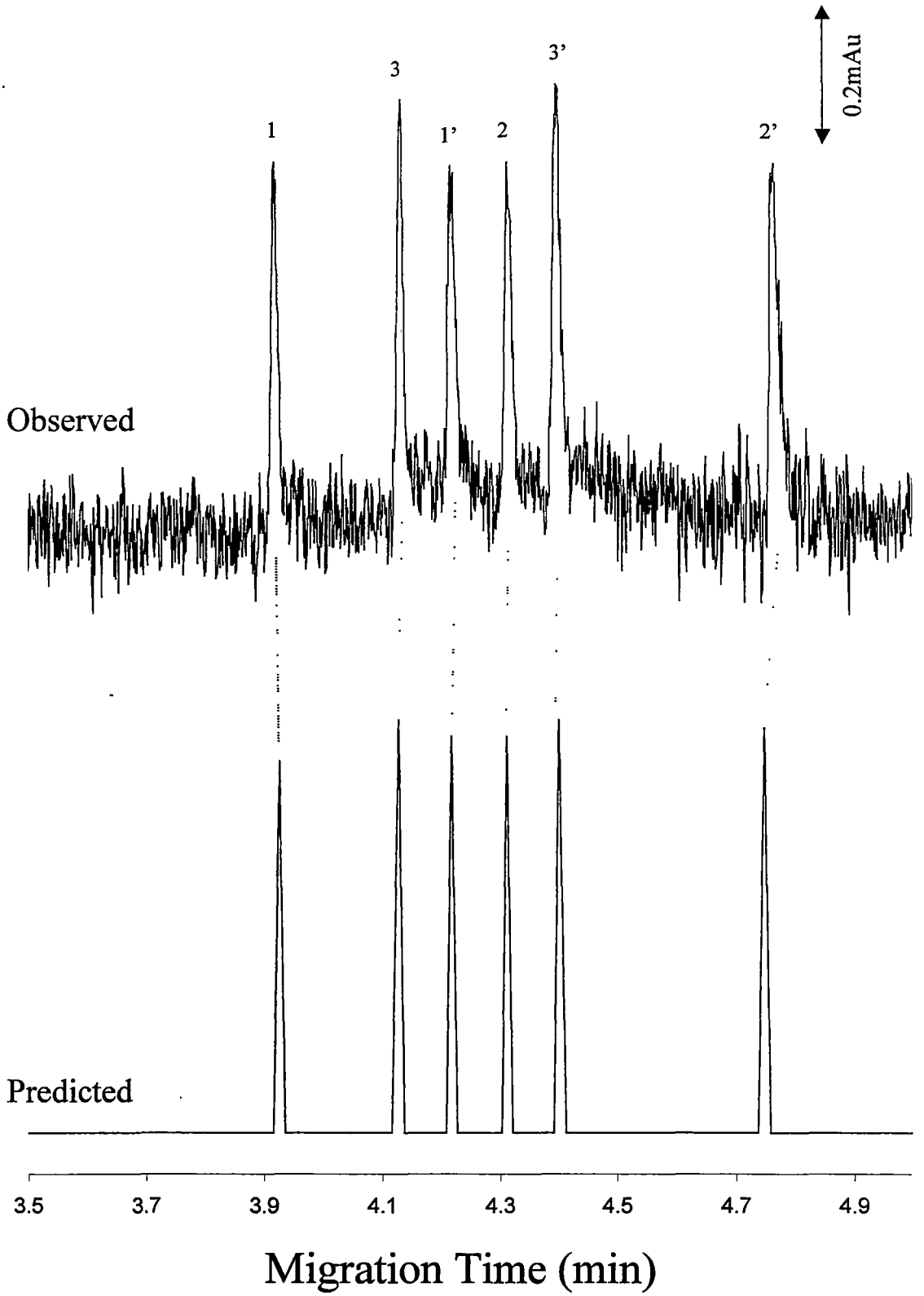

Figure 6.12: Optimised separation at 3.9mM s-β-CD and 0.40% dextran sulfate. Conditions calculated using the MR criterion and eqn (6-8). Peaks are 1=L-Phenylalanine, 1'=D-Phenylalanine, 2=L-Tyrosine, 2'=D-Tyrosine, 3=L-Tryptophan and 3'=D-Tryptophan. General conditions: 20mM phosphate electrolyte at pH 2.0. Capillary: 25μm x 55cm (46.5cm to detector), separation at 25°C with detection at 210nm.

Figure 6.13 shows the optimum separation achieved when the migration order: L-Phenylalanine, D-Phenylalanine, L-Tyrosine, L-Tryptophan, D-Tyrosine and D-Tryptophan was entered into the model using the MR criterion for optimisation. The NRP criterion could also be used but led to a very similar separation due to the small range of conditions that gave rise to this desired migration order. Migration times again agreed very well with those predicted, with differences being less than 0.5% for all analytes. It can be seen for this example that dextran sulfate played an important role since the desired selectivity was not attainable when using s-β-CD alone, see Figure 6.1. The dextran sulfate therefore acted as a "fine tuner", with the ability to move enantiomers around while still maintaining the enantiomeric separation brought about by the s-β-CD. It should be noted that increasing the concentration of dextran sulfate did lead to a decrease in enantiomeric resolution for each amino acid, but baseline resolution of all peaks was maintained.

For situations where a particular migration order was not possible, the model gave the conditions that yielded the separation with as many peaks in the correct position as possible, with those unresolved peaks being forced as close as possible to the desired order, often leading to their co-migration.

It can be seen that although increasing the concentration of dextran sulfate allowed for selectivity control, it also tended to lower peak height, leading to lower sensitivity. For situations where this may be a problem further constraints can be built into the model to minimise the concentration of dextran sulfate needed while still maintaining the desired migration order. Figure 6.14 shows the optimum separations calculated with and without a constraint to limit the amount of dextran sulfate. It can be seen that both conditions led to baseline separation of the six enantiomers, however, when the amount of dextran sulfate was limited (Figure 6.14 b.), larger peaks were

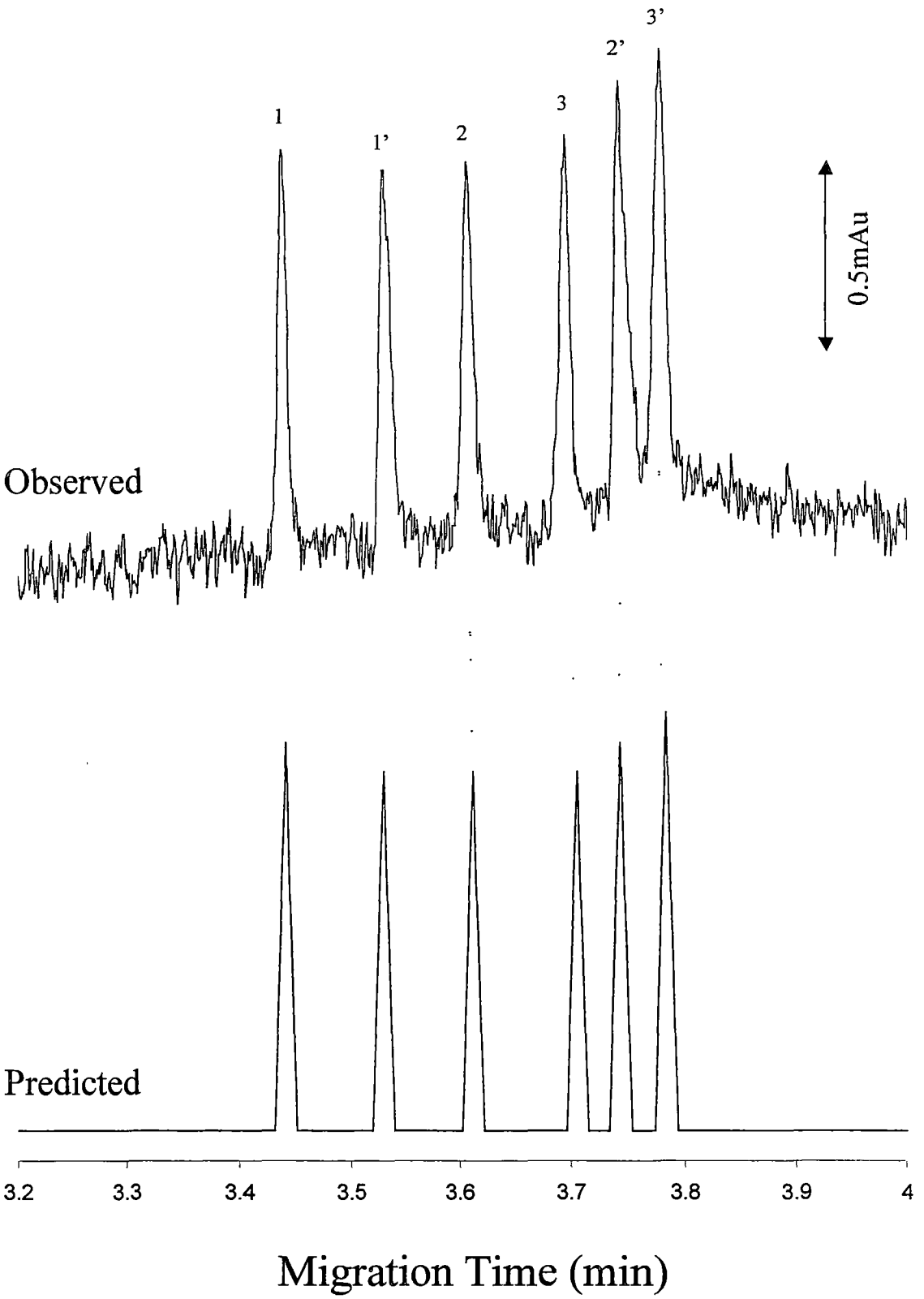

Figure 6.13: Optimised conditions to achieve the migration order: L-Phenylalanine, D-Phenylalanine, L-Tyrosine, L-Tryptophan, D-Tyrosine and D-Tryptophan. Conditions: 0.88mM s-β-CD and 0.58%(w/v) dextran sulfate. Optimum calculated using the MR criterion. Peaks are 1=L-Phenylalanine, 1'=D-Phenylalanine, 2=L-Tyrosine, 2'=D-Tyrosine, 3=L-Tryptophan and 3'=D-Tryptophan. General conditions: 20mM phosphate electrolyte at pH 2.0. Capillary: 25μm x 55cm (46.5cm to detector), separation at 25°C with detection at 210nm.

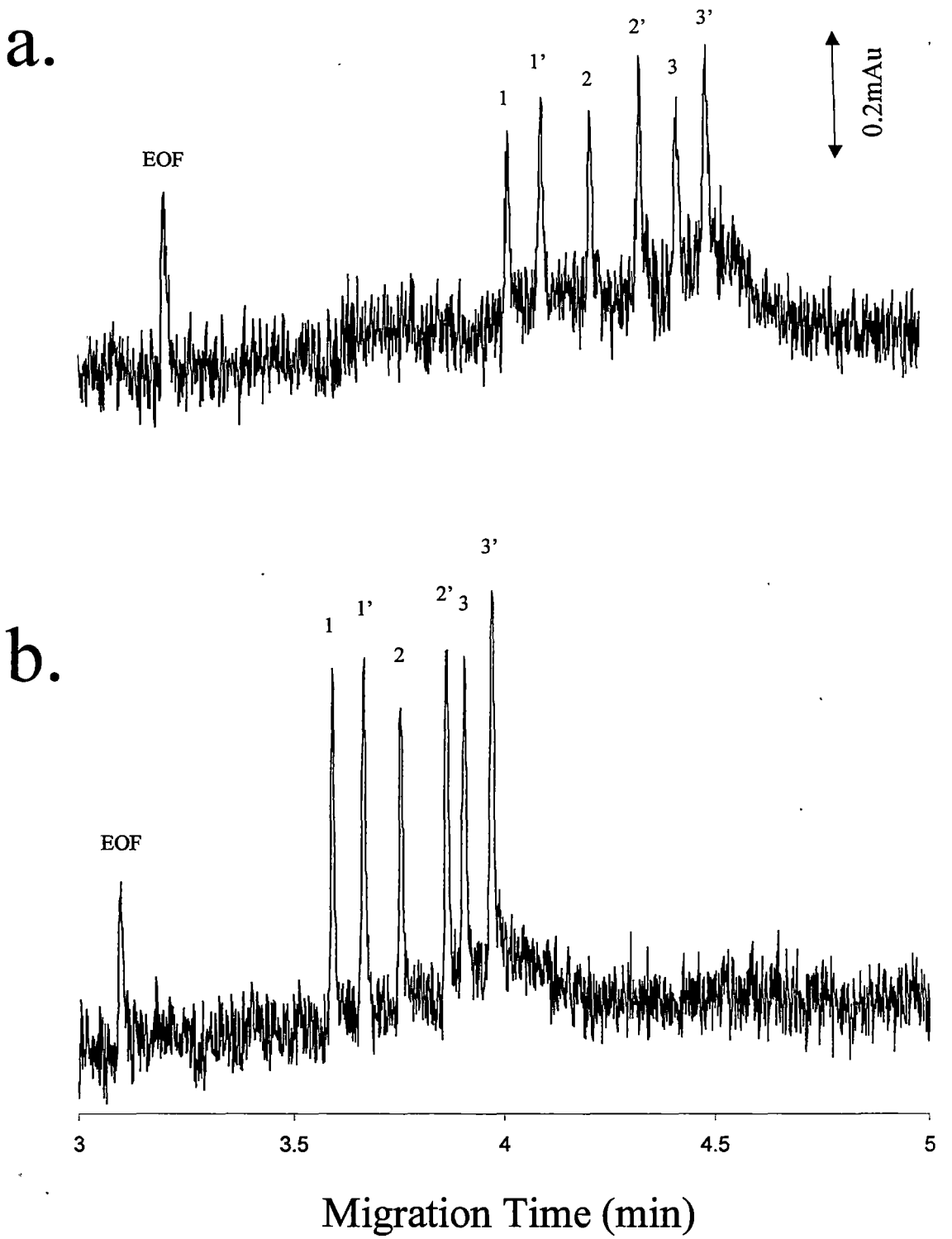

Figure 6.14: Optimised conditions needed to achieve the migration order: L-Phenylalanine, D-Phenylalanine, L-Tyrosine, D-Tyrosine, L-Tryptophan and D-Tryptophan. a. No constraints used for optimisation. Conditions: 1.87mM s-β-CD and 2.4%(w/v) dextran sulfate. b. Additional constraint such that % dextran sulfate kept <1%(w/v). Conditions: 0.87mM s-β-CD and 1.0%(w/v) dextran sulfate. Optimums calculated using the MR criterion. Peaks are 1=L-Phenylalanine, 1'=D-Phenylalanine, 2=L-Tyrosine, 2'=D-Tyrosine, 3=L-Tryptophan and 3'=D-Tryptophan. General conditions: 20mM phosphate electrolyte at pH 2.0. Capillary: 25μm x 55cm (46.5cm to detector), separation at 25°C with detection at 210nm.

observed. This is achieved at the cost of slightly lower resolution, so this would have to be considered if such an approach was to be used.

6.5 Conclusions

The selectivity of enantiomeric separations for three aromatic amino acids (phenylalanine, tyrosine and tryptophan) can be controlled predictably through the use of a sulfated-β-cyclodextrin in combination with either temperature control or the use of the soluble polymer dextran sulfate as a pseudo-stationary phase. In both cases the observed selectivities could be modelled successfully, in the case of temperature using an artificial neural network and in the case of dextran sulfate using a physical model derived from first principles. Both models accurately described the corresponding systems, allowing each to be optimised using various constraints. The use of a physical model also provided useful information about the system, including association constants and analyte-pseudo-stationary phase mobilities. Extension of the physical model allowed for conditions needed to achieve desired migration orders to be calculated, as well as including constraints to improve parameters such as peak height. The increase in selectivity control potentially allows for more complex mixtures of analytes to be separated successfully than would be achievable using a cyclodextrin system alone.

The described systems are potentially applicable to any cationic analytes, such as many pharmaceutically important compounds, that show appreciable interaction with sulfated-β-cyclodextrin. The technique could also be extended to other cyclodextrins as well as different soluble polymers or even different additives, such as crown ethers or ion-pair reagents.

6.6 References

1. J. T. Smith, *Electrophoresis*, 18 (1997) 2377.
2. C. Quang and M. G. Khaledi, *Anal. Chem.*, 65 (1993) 3354.
3. P. Dzygiel, P. Wieczorek and J. A. Jonsson, *J. Chromatogr. A.*, 793 (1998) 414.
4. S. Chinaka, S. Tanaka, N. Takayama, K. Konai, T. Ohshima and K. Ueda, *J. Chromatogr. B.*, 749 (2000) 111.
5. S. Fanali, *J. Chromatogr. A.*, 792 (1997) 227.
6. S. A. C. Wren and R. C. Rowe, *J. Chromatogr.*, 603 (1992) 235.
7. S. A. C. Wren, *J. Chromatogr.*, 636 (1993) 57.
8. S. A. C. Wren and R. C. Rowe, *J. Chromatogr.*, 609 (1992) 363.
9. Y. Y. Rawjee, D. U. Staerk and G. Vigh, *J. Chromatogr.*, 635 (1993) 291.
10. M. E. Biggin, R. L. Williams and G. Vigh, *J. Chromatogr. A.*, 692 (1995) 319.
11. Y. Y. Rawjee, R. L. Williams, L. A. Buckingham and G. Vigh, *J. Chromatogr.*, 688 (1994) 273.
12. B. A. Williams and G. Vigh, *J. Chromatogr. A.*, 777 (1997) 295.
13. J. B. Vincent and G. Vigh, *J. Chromatogr. A.*, 817 (1998) 101.
14. J. B. Vincent and G. Vigh, *J. Chromatogr. A.*, 816 (1998) 233.
15. W. Jianjun, Z. Guojun, Y. Liu and S. Wanru, *Analyst*, 126 (2001) 438.
16. Y. T. Iwata, A. Garcia, T. Kanamori, H. Inoue, T. Kishi and I. S. Lurie, *Electrophoresis*, 23 (2002) 1328.
17. M. Muzikar, J. Havel and M. Macka, *Electrophoresis*, 23 (2002) 1796.
18. A. Guttman and N. Cooke, *J. Chromatogr. A.*, 680 (1994) 157.
19. W. Lindner, B. Bohs and V. Seidel, *J. Chromatogr. A.*, 697 (1995) 549.

Chapter 7

Simultaneous Separation of Anions and Cations using PDDAC and Hexanesulfonate as Mixed Pseudo-Stationary Phases

7.1 Introduction

From the work in Chapter 3 it can be seen that PDDAC is a useful additive for the separation of inorganic and small organic anions. However, these separations result only from IE interactions between the polymer and the analytes. As shown in Chapter 3, the scope of PDDAC-based separations can be increased if further additives are used.

Alkylsulfonates have proven successful as ion-pair (IP) reagents for the separation of cationic analytes, such as drugs, peptides and proteins [1,2]. It has been shown that to bring about changes in selectivity the affinity of the alkylsulfonate for the analytes should differ between analytes. It has also been found that the bulkier the organic group on the sulfonate, the more interaction it appears to have with the analytes [1]. Use of alkylsulfonates as IP reagents, especially ethanesulfonate, has also been shown to dramatically improve peak shapes for basic drugs when added to the electrolyte [3,4]. This is believed to be due to interactions between the cationic drugs and the ethanesulfonate, resulting in a lowering of the effective charge on the drug and hence less interaction with the negative silanol groups on the capillary wall. The addition of alkylsulfonates to a PDDAC system could offer a convenient way to increase

hydrophobicity through the formation of an ion-pair between PDDAC and the alkylsulfonates, possibly leading to different selectivities for hydrophobic analytes. The addition of an alkylsulfonate also potentially allows for selectivity changes to be brought about for the separation of cations. The aim of this chapter was to investigate the possibility of using a combination of PDDAC and alkylsulfonates for the simultaneous EKC separation of anions and cations. The alkylsulfonate should influence the selectivity for both the analyte anions (via IE interactions with the cationic PDDAC) and the analyte cations (via ion-pair interactions with the alkylsulfonate). The possibility of modelling the system was also to be investigated, with an aim to optimise the separation.

7.2 Experimental

The general details are given in Chapter 2. Detailed conditions are given in each figure caption.

7.2.1 Capillary coating procedures

PDDAC-coated capillaries were prepared in a similar manner to those used in Chapter 3.

7.2.2 Electrolyte preparation

A stock 100mM Tris/Cl^- electrolyte was prepared by titration of 100mM Tris to pH 8.0 with HCl, providing a background concentration of 50 mM Cl^- in the stock solution. Individual electrolytes were prepared by dilution of this stock solution to 20 mM Tris/10mM Cl^-. PDDAC was added to the electrolytes as a 2% solution to give concentrations up to 1.0% and hexanesulfonate (as the sodium salt) was added as a 200mM solution to give concentrations up to 110mM.

7.3 Choice of analytes

The main interactions expected between the anions and the p-SPs were IE interactions with the cationic sites on the PDDAC and hydrophobic interactions with the PDDAC/alkylsulfonate complex. A series of analytes was therefore chosen which exhibited different hydrophobicities and IE affinities for PDDAC, see Table 7.1. The inorganic anions, carboxylic acids and sulfonates are known to have differing IE affinities for PDDAC [5], while the varying alkyl chain length should alter the hydrophobicity of the analytes.

A series of opiate compounds was chosen as the cationic analytes, see Table 7.1, as these could be protonated at mid to low pH levels. It was also likely that these analytes would have varying ion-pairing (IP) affinities for long chain alkylsulfonates. The separation of these compounds is also of interest to the pharmaceutical industry and in forensic science, where their determination in a range of samples is performed frequently.

7.4 Effect of pH

In the current system pH was expected to be a major variable since both acids and bases were to be separated simultaneously. Since PDDAC was being used as a p-SP, a reversed EOF was unavoidable. This was advantageous in the case of the anions since it allowed them to be separated in a co-EOF mode, but for the opiates this reversed EOF produced a counter-EOF separation. For maximum interaction between the analytes and the two p-SPs (PDDAC and hexanesulfonate) it was desirable that all analytes be fully deprotonated in the case of the acids or fully protonated in the case of the bases (opiates). Table 7.1 shows the pK_a values for those analytes for which data could be identified and this indicates that the highest pK_a for the acids was

Table 7.1: Choice of analytes and their associated pK_a values.

	Analytes	*pK_a*[1]
Inorganic Anions	Bromide	-
	Iodide	-
	Nitrate	-
Small Organic Anions	Benzenesulfonate	2.55
	4-Toluenesulfonate	-
	4-Ethylbenzenesulfonate	-
	2-Naphthalenesulfonate	-
	Phthalate	2.95, 5.41
	Benzoate	4.20
	4-Toluate	4.36
	4-Propylbenzoate	-
	4-*t*-Butylbenzoate	4.39
	4-Heptylbenzoate	-
Organic Cations	Morphine	7.87(+)
	Thebaine	7.95(+)
	10-OH Thebaine	-
	Codeine	7.95(+)
	Oripavine	-
	Laudanine	-

1 - from Lange's Handbook of Chemistry [8]; (+) – pK_a for protonated species

around 5.4 for the second pK_a of phthalate, while all the opiates had similar pK_a values of around 8. Therefore, for maximum interaction between the analytes and the associated p-SPs a pH of 6.5-7.0 was preferred to allow for fully charged analytes.

Figure 7.1 shows the separations obtained for the opiates from pH 6-8.5 (the separations for the inorganic anions and acids remained constant as expected since they should all be fully protonated over this range). It can be seen that for pH values between 6 and 7.5 (where most of the opiates were protonated) co-elution was a problem due to very similar charge to size ratios for these species. Only at pH values of 8 and 8.5 did separation between the opiates occur, in agreement with Zhang and Thormann [6] who found that a pH value close to the average pK_a of the opiates led to the best separation. It should also be noted that the separations were problematic at pH values of 6.0, 6.5 and 8.5, with unexplained exceedingly long run times or unstable baselines, resulting in the need to prepare new capillaries. Despite this, the stability of the system at pH 8.0 was very good, with reproducible results obtained over a period of weeks with the same capillary. Migration time precision (%RSD values over 12 successive runs) was generally less than 0.4%RSD for most of the anions and less than 1.5% for all the analytes and the EOF. These results were obtained in a PDDAC-coated capillary using a electrolyte consisting of 20mM Tris/HCl electrolyte with 60mM hexanesulfonate. No PDDAC was added to the electrolyte showing that even in the absence of PDDAC, the reversed EOF and analyte migration times were very stable.

7.5 Effect of alkylsulfonates

The effects of alkylsulfonates in the present system were expected to be threefold. Firstly it has been shown that alkylsulfonates can dramatically improve peak shapes

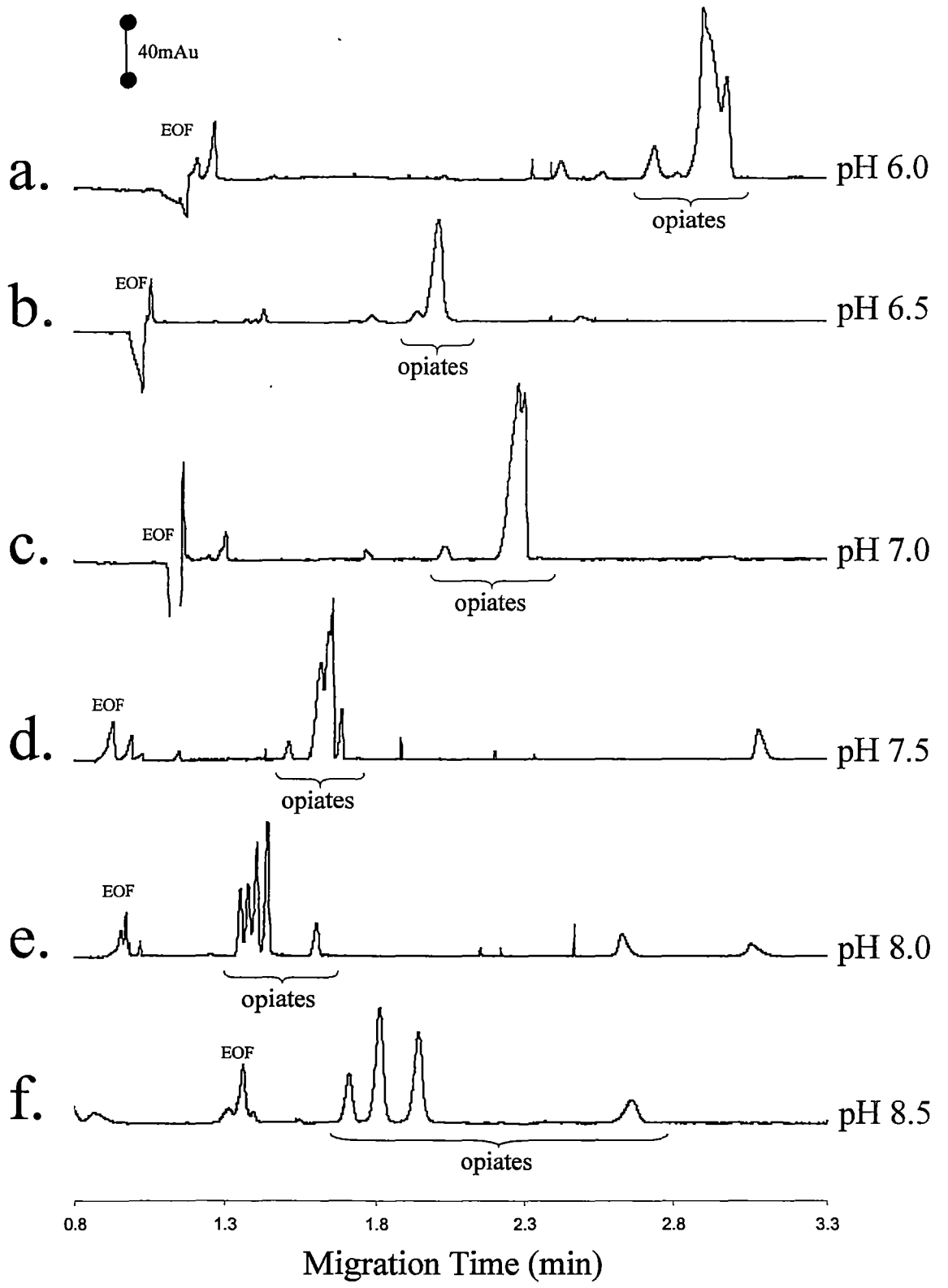

Figure 7.1: Effect of electrolyte pH on the separation of the opiates. a) and b) 20mM BisTris adjusted to pH using HCl. c), d) and e) 20mM Tris adjusted to pH using HCl. Capillary: 50μm x 35cm (26.5cm to detector), with detection at 200nm.

for certain analytes separated in CE [3,4]. Secondly, the alkylsulfonates can act as competing ions, thereby modifying the IE interaction between the anionic analytes and the PDDAC. Thirdly, the alkylsulfonates can increase the hydrophobicity of the PDDAC pseudo-SP by forming ion-pairs with the quaternary ammonium groups. The latter two effects will be discussed in more detail later.

The ability of alkylsulfonates (mainly ethanesulfonate) to improve peak shapes for cationic analytes has been attributed to a reduction in the interaction between the analytes and the capillary wall as a result of electrostatic IP interactions between the sulfonate and the analytes. In the current system the capillary wall has been coated with the cationic PDDAC, hence any electrostatic interactions between cations and the capillary surface should be eliminated and this explains the very good peak shapes obtained for all the opiates studied. However, the anionic analytes also showed very poor peak shapes when alkylsulfonates were not included in the electrolyte, see Figure 7.2 a. The peaks were somewhat improved on addition of PDDAC to the electrolyte, presumably due to competing interaction between PDDAC molecules in the electrolyte and those bound to the capillary wall, but the biggest improvement in peak shapes was brought about from the addition of alkylsulfonates to the electrolyte, see Figure 7.2 b and c. It can be seen that on addition of up to 110mM hexanesulfonate peak shapes were improved dramatically without modification of the separation selectivity of the system. Efficiencies obtained were between 220,000-255,000 theoretical plates (630,000-730,000 theoretical plates/metre) for all analytes in Figure 7.2 b except phthalate. The effect of alkyl chain length was also investigated, and it was found that very similar improvements in peak shape were obtained when ethane-, hexane- or octanesulfonates were used. The improvement in peak shapes was most probably due to the IE effects of the alkylsulfonate at the

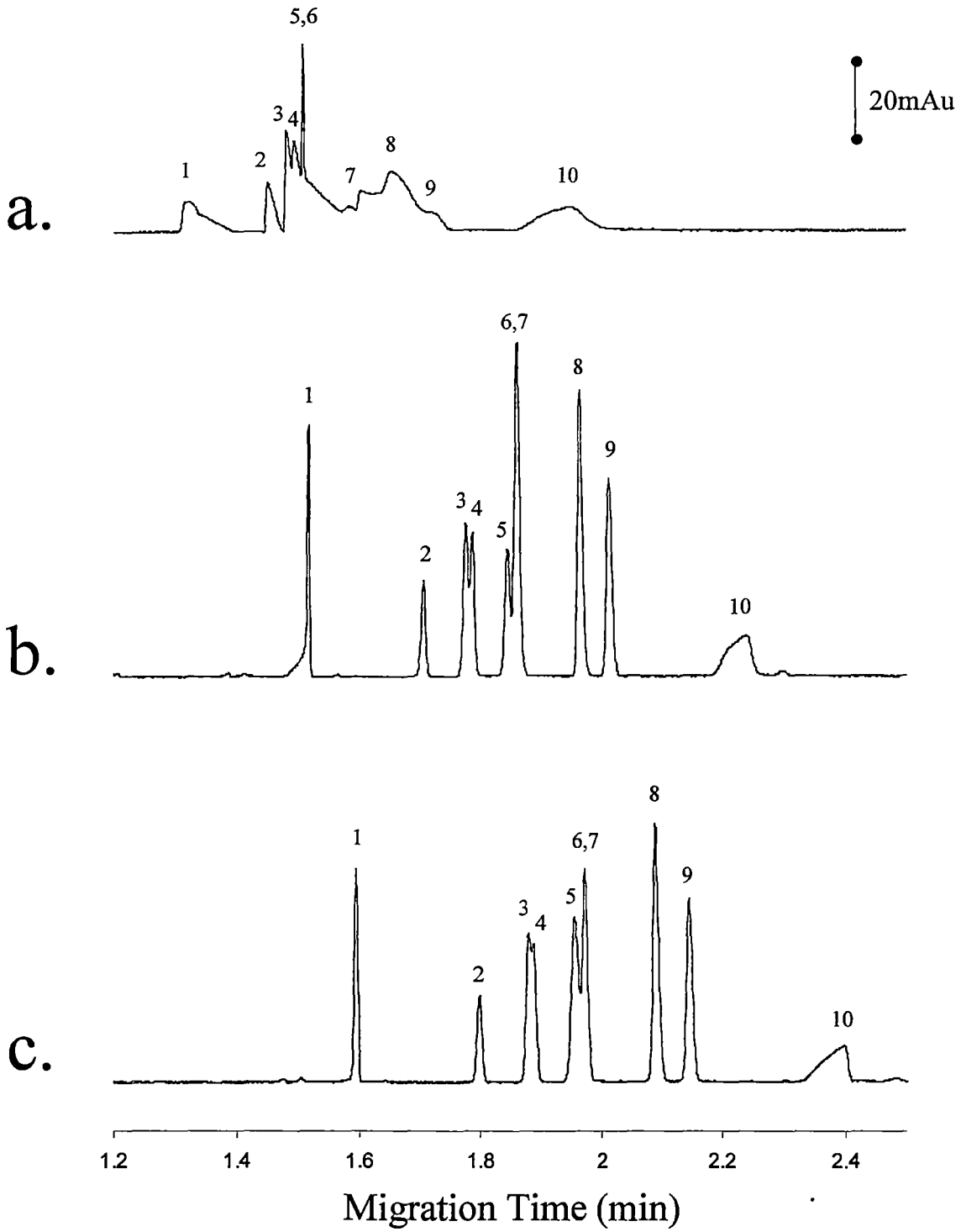

Figure 7.2: Improvement of peak shape on adding hexanesulfonate to the electrolyte. a) no hexanesulfonate, b) 60mM hexanesulfonate and c) 110mM hexanesulfonate. Peaks are 1=phthalate, 2=benzenesulfonate, 3=benzoate, 4=toluenesulfonate, 5=ethylbenzenesulfonate, 6=toluate, 7=naphthalenesulfonate, 8=propylbenzoate, 9=*t*-butylbenzoate and 10=heptylbenzoate. Electrolyte: 20mM Tris, 10mM HCl to pH 8.0. Capillary: 50μm x 35cm (26.5cm to detector), with detection at 200nm.

capillary wall, resulting in less interaction between the analyte anions with the cationic capillary wall. A complicating factor in the improvement offered by the addition of alkylsulfonates is the incompatibility of longer chain sulfonates with PDDAC. It was found that although hexanesulfonate could be added up to 110mM without precipitation of the PDDAC-hexanesulfonate IP, octanesulfonate could only be added up to 25mM before a precipitate formed. Since the aim of the present study was to increase the hydrophobicity of PDDAC, longer chain sulfonates were preferred. As a compromise hexanesulfonate was used for all further studies.

7.6 Selectivity

Reliable manipulation of separation selectivity by introducing new analyte interaction mechanisms can be achieved only if each of the interactions is predictable in its magnitude, thereby allowing the system to be modelled and for selectivity changes to be achieved by simply varying the extent of each interaction. In the current system the selectivity was dependent on the concentrations of PDDAC and hexanesulfonate in the electrolyte. Each of these parameters affects the separation of the anions and cations differently, through IE or IP interactions, respectively. Figure 7.3 shows a schematic of the resultant equilibria operating in this system while Figure 7.4 shows the effect of varying the concentration of hexanesulfonate on the separation of the anions and cations in the presence of 0.5%PDDAC. From Figure 7.3 it can be seen that increasing the concentration of hexanesulfonate in the presence of PDDAC had a two-fold effect on the separation of the anions. Firstly the hexanesulfonate acted as a competing ion, reducing the interaction between the anions and the PDDAC and leading to increased (negative) mobilities. This was observed for all the anions over the range 0-60mM hexanesulfonate, see Figure 7.4 a. Secondly, increasing the

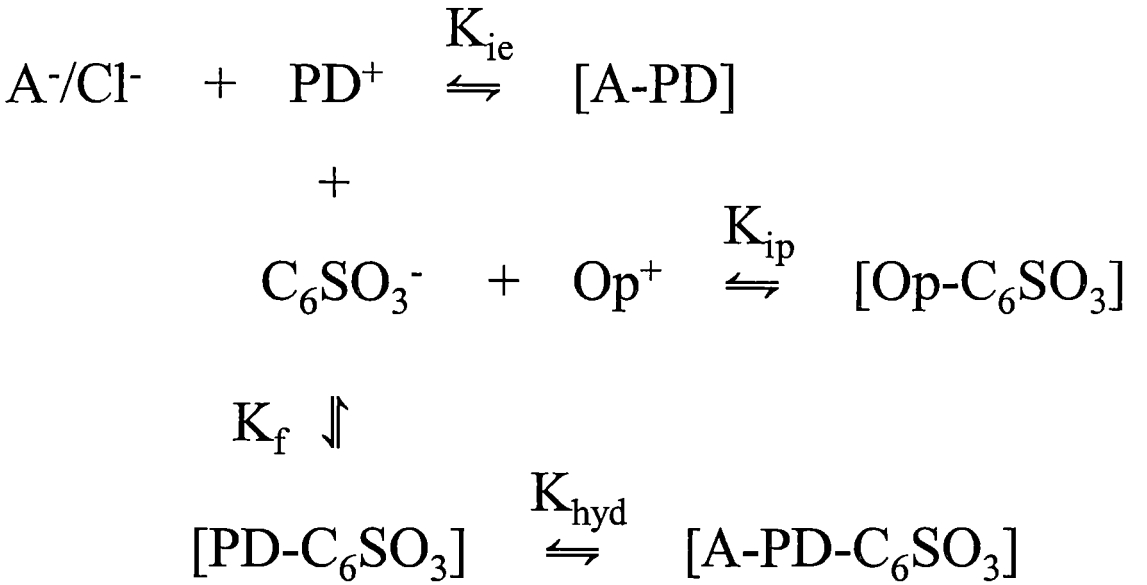

Figure 7.3: Schematic of the simultaneous equilibria operating in the system. A^-, PD^+ and Op^+ refer to the analyte anions, PDDAC pseudo-SP and opiate cations respectively. Species in square brackets refer to associated complexes, eg. [A-PD-C_6SO_3] refers to the anion, PDDAC, hexanesulfonate complex. K_{ie}, K_{ip}, K_f and K_{hyd} are the associated equilibrium constants.

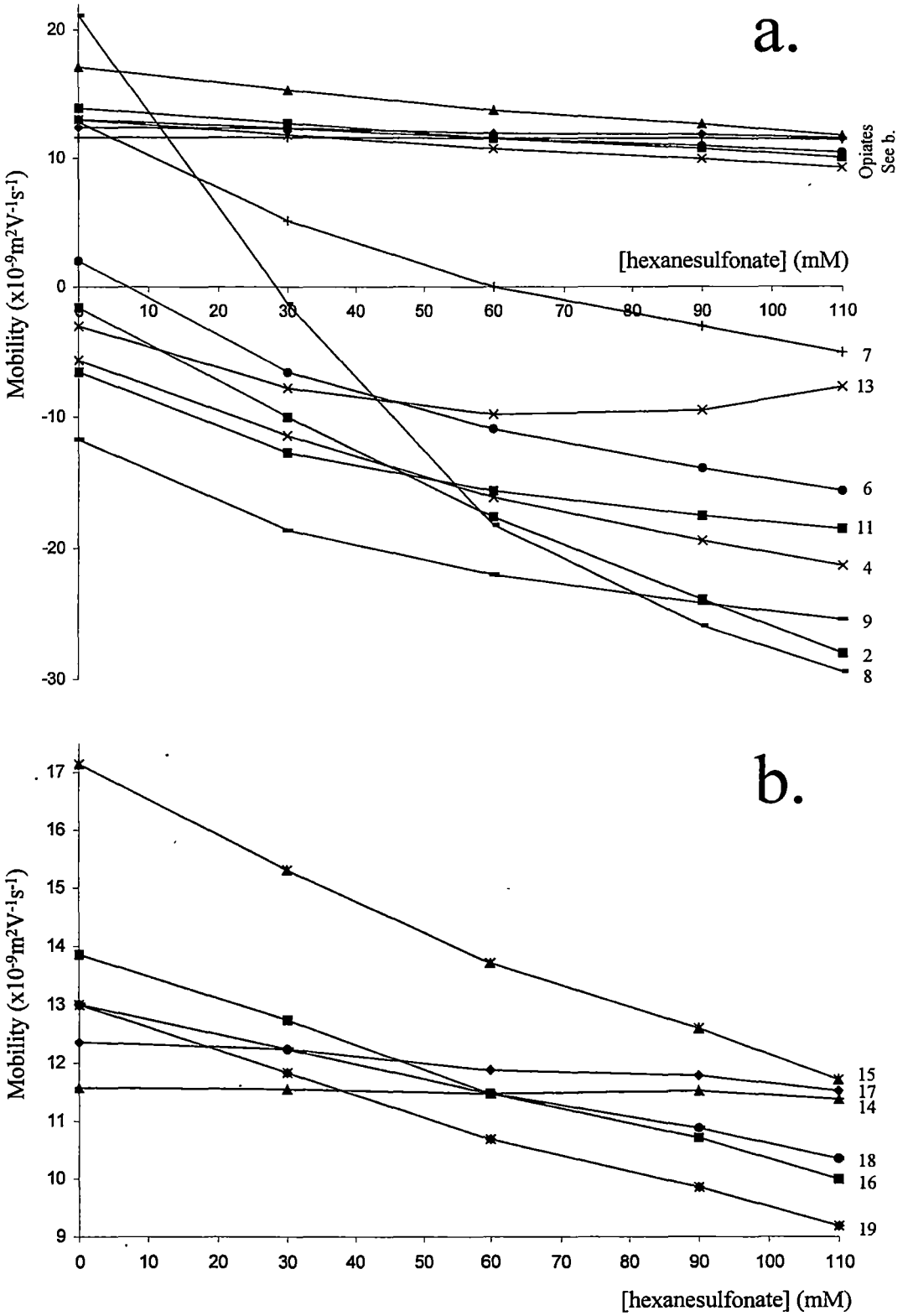

Figure 7.4: Mobility changes resulting from varying [hexanesulfonate] in a electrolyte containing 0.5%PDDAC. a.) shows the mobility changes for a selection of the anions and the opiates while b.) shows the expanded section for the opiates only. Peaks are 2=iodide, 4=benzenesulfonate, 6=ethylbenzenesulfonate, 7=naphthalenesulfonate, 8=phthalate, 9=benzoate, 11=propylbenzoate, 13=heptylbenzoate, 14=morphine, 15=10-OH thebaine, 16=thebaine, 17=codeine, 18=oripavine and 19=laudanine. Electrolyte: 20mM Tris, 10mM HCl to pH 8.0.

hexanesulfonate concentration introduced some hydrophobic interactions with the analytes by increasing the hydrophobic character of the PDDAC due to the formation of IPs between the anionic sulfonate and the cationic polymer. This was observed for heptylbenzoate in Figure 7.4 a. where an increase in hexanesulfonate concentration initially increased the mobility but then later decreased the mobility due to interactions of the hydrophobic part of the analyte with the hydrophobic region of the PDDAC-hexanesulfonate IP. Similar, but less pronounced effects were evident for other hydrophobic analytes. These interactions could be increased by using longer chain alkylsulfonates, but this led to solubility problems for the PDDAC-alkylsulfonate IP.

As well as modifying the mobilities of the anions, increasing the concentration of hexanesulfonate altered the migration of the cations. This can be seen in Figure 7.4 b. where increasing the concentration of hexanesulfonate decreased the mobilities of the cations. Although these results were obtained in a electrolyte containing 0.5% PDDAC, very similar plots were observed for electrolytes containing 0 and 0.25% PDDAC (data not shown). This effect on mobilities was due to IP formation between the analyte cations and the anionic sulfonate, leading to a reduction in charge of the opiates and hence reduced mobility.

7.7 Modelling the system

From Figure 7.3 it can be seen that the observed separation was a result of several competing equilibria. Each of these were well defined, enabling modelling of the system from first principles. However, since the interactions leading to separation differed for the anions and the cations, these were initially modelled separately before being combined into the final model.

7.7.1 Anions

The following equibria apply for the separation of anions in the current system:

$$A^-_{bge} + C_6SO_3^-{}_{ie} \overset{K_{ie}}{\leftrightharpoons} A^-_{ie} + C_6SO_3^-{}_{bge}$$

$$K_h \Updownarrow \qquad\qquad K_f$$

$$A^-_{pds} \qquad PD^+ + C_6SO_3^- \leftrightharpoons PDS^+$$

where A^-_{bge} A^-_{ie} and A^-_{pds} refer to the anionic analytes in the electrolyte, PDDAC and PDDAC-hexanesulfonate phases, respectivily. $C_6SO_3^-{}_{bge}$ and $C_6SO_3^-{}_{ie}$ refer to the hexanesulfonate in the electrolyte and PDDAC phases respectivily while PD^+ refers to the PDDAC molecules in the electrolyte. The three equilibrium constants, K_{ie}, K_h and K_f refer to the IE selectivity and hydrophobic selectivity between the analytes and the PDDAC and PDDAC-hexanesulfonate phases, respectivily, while K_f is the formation constant for the PDDAC-hexanesulfonate IPs. These equibrium constants are defined by the following equations:

$$K_{ie} = \frac{[A^-{}_{ie}][C_6SO_3^-{}_{bge}]}{[A^-{}_{bge}][C_6SO_3^-{}_{ie}]} \tag{7-1}$$

$$K_{hyd} = \frac{[A^-{}_{pds}]}{[A^-{}_{bge}]} \tag{7-2}$$

$$K_f = \frac{[PDS^+]}{[PD^+][C_6SO_3^-]} \tag{7-3}$$

where the species are labelled as in the above equibria. It should be noted that $[PD^+]$ refers to the unit concentration of quaternary ammonium groups in the electrolyte, not the %(w/v) of PDDAC added to the electrolyte. The associated retention factor for the polymer phase, k'_{ie}, can be derived from ion-chromatogaphy theory, see Chapter 3,

$$k'_{ie} = \frac{w_{poly}}{V_{bge}}(K_{ie})^{1/y}(Q/y)^{x/y}[C_6SO_3^-]^{-x/y} \quad (7\text{-}4)$$

where w_{poly} is the weight of PDDAC p-SP, V_{bge} is the volume of electrolyte, Q is the ion-exchange capacity of the PDDAC, $[E]$ is the concentration of the competing ion while x and y are the charges on the analyte and eluent ions, respectively.

An equivalent expression for the retention factor associated with the PDDAC-hexansulfonate phase, k'_{hyd}, can be derived from first principles:

$$k'_{hyd} = \frac{n(A^-)_{sp}}{n(A^-)_{bge}} = \frac{[A^-_{pds}]V_{pds}}{[A^-_{bge}]V_{bge}}$$

where $[A^-_{pds}]$ and $[A^-_{bge}]$ are the concentrations of the analyte in the PDDAC-hexanesulfonate and electrolyte phases, respectivily, while V_{pds} and V_{bge} are the volumes of the PDDAC-hexanesulfonate phase and electrolyte, respectively. Substituting for $[A^-_{pds}]$ from eqn (7-2) leads to:

$$k'_{hyd} = \left(\frac{V_{pds}}{V_{bge}}\right)K_{hyd} \quad (7\text{-}5)$$

The value for V_{pds} is not known, but we can make the assumption that:

$$\left(\frac{V_{pds}}{V_{bge}}\right) \propto [PDS^+] \Rightarrow \left(\frac{V_{pds}}{V_{bge}}\right) = m[PDS^+] \quad (7\text{-}6)$$

where $[PDS^+]$ is the concentration of the PDDAC-hexanesulfonate phase in the electrolyte and m is an arbitary constant. Substituting eqn (7-6) into eqn (7-5) and combining with eqn (7-3) leads to:

$$k'_{hyd} = mK_f K_{hyd}[PD^+][C_6SO_3^-]$$

Combining m, K_f and K_{hyd} into one constant, K_H, leads to a final expression for k'_{hyd}:

$$k'_{hyd} = K_H[PD^+][C_6SO_3^-] \quad (7\text{-}7)$$

The observed mobility of an analyte can be expressed in terms of this retention factor, see Chapter 3,

$$\mu_{ob} = \frac{1}{1+k'}\mu_{bge} + \frac{k'}{1+k'}\mu_{sp} \quad (7\text{-}8)$$

where μ_{ob} is the observed mobility of the analyte while μ_{bge} and μ_{sp} are the mobilities of the analyte in the electrolyte and p-SP, respectively. In the case of two interactions, IE and hydrophobicity, leading to two retention factors, eqn (7-8) can be rewritten as:

$$\mu_{ob} = \frac{1}{1+k'_t}\mu_{bge} + \frac{k'_{ie}}{1+k'_{ie}}\mu_{poly} + \frac{k'_{hyd}}{1+k'_{hyd}}\mu_{pds} \quad (7\text{-}9)$$

where μ_{bge}, μ_{poly} and μ_{pds} are the mobilities of the analyte in the electrolyte, PDDAC and PDDAC-hexanesulfonate phases, respectively. k'_t is the sum of the individual retention factors:

$$k'_t = k'_{ie} + k'_{hyd} \quad (7\text{-}10)$$

Expanding eqn (7-10) by including previous equations gives:

$$\mu_{ob} = \frac{1}{1+K_H[PD^+][C_6SO_3^-]+w_{poly}K_{ie}Q[C_6SO_3^-]^{-1}}\mu_{bge}$$

$$+\frac{w_{poly}K_{ie}Q[C_6SO_3^-]^{-1}}{1+w_{poly}K_{ie}Q[C_6SO_3^-]^{-1}}\mu_{ie} + \frac{K_H[PD^+][C_6SO_3^-]}{1+K_H[PD^+][C_6SO_3^-]}\mu_{pds}$$

A complicating factor is the use of $[C_6SO_3^-]$ in the equation for the IE interaction. This is not strictly accurate as the couter-ion on PDDAC was chloride and the Tris electrolyte was made up to its operating pH using HCl, hence a proportion of the

competing ions in the electrolyte were chloride ions. This can be accounted for by replacing $[C_6SO_3^-]$ in eqn (7-4) with $[C_6SO_3^-+1/dQ+0.01]$ where Q is the ion-exchange capacity of PDDAC which relates to the amount of chloride added to the system by the PDDAC, d is a constant accounting for the difference in eluting strength between chloride and hexanesulfonate, while 0.01M is the concentration of chloride added by the Tris/HCl electrolyte. We can also make the assumption that μ_{ie} and μ_{pds} are equal, since the mobility of the large, polymeric PDDAC molecule should stay reasonably constant even after interaction with the analytes or the hexanesulfonate. Including this term leads to the final model for the separation of the anions in the current system:

$$\mu_{ob} = \frac{1}{1+K_H[PD^+][C_6SO_3^-]+w_{poly}K_{ie}Q[C_6SO_3^- +\frac{1}{d}Q+0.01]^{-1}}\mu_{bge}$$

$$+\frac{w_{poly}K_{ie}Q[C_6SO_3^- +\frac{1}{d}Q+0.01]^{-1}}{1+w_{poly}K_{ie}Q[C_6SO_3^- \frac{1}{d}Q+0.01]^{-1}}\mu_{ie}+\frac{K_H[PD^+][C_6SO_3^-]}{1+K_H[PD^+][C_6SO_3^-]}\mu_{ie} \qquad (7\text{-}11)$$

7.7.2 Cations

The following equilibria apply to the separation of the opiates:

$$Op^{+}_{bge} + C_6SO_3^{-}{}_{bge} \overset{K_{ip}}{\rightleftharpoons} OpC_6SO_{3\,bge}$$

$$+$$

$$Cl^{-}_{1e}$$

$$K_s \Updownarrow$$

$$C_6SO_3^{-}{}_{1e}$$

$$+$$

$$Cl^{-}_{bge}$$

where Op^{+}_{bge}, $C_6SO_3^{-}{}_{bge}$ and $OpC_6SO_{3\,bge}$ refer to the opiates, hexanesulfonate and opiate-hexanesulfonate IP in the electrolyte, respectively, while $C_6SO_3^{-}{}_{1e}$ refers to the hexanesulfonate in the PDDAC phase. Cl^{-}_{1e} and Cl^{-}_{bge} refer to the chloride present in the polymer and electrolyte phases, respectively. K_{ip} and K_s are the IP association constant and IE selectivity coefficient for the associated equilibria. If we initially consider only the IP interaction between the opiates and the hexanesulfonate, the following equilibrium equation applies:

$$K_{ip} = \frac{[OpC_6SO_{3\,bge}]}{[Op^{+}{}_{bge}][C_6SO_3^{-}{}_{bge}]} \qquad (7\text{-}12)$$

where Op^{+}_{bge}, $C_6SO_3^{-}{}_{bge}$ and $OpC_6SO_{3\,bge}$ refer to the free opiate, hexanesulfonate and opiate-hexanesulfonate IP in the electrolyte, respectively. Since the mobility of the IP can be assumed to be zero due to neutralisation of the charge on forming the IP, we can write:

$$\mu_{ob} = \alpha\mu_{bge}$$

where μ_{ob} is the observed mobility, μ_{bge} is the mobility of the free, protonated opiate and α is the fraction of the opiate present in the protonated form, i.e. not ion-paired to the hexanesulfonate. α is defined by:

$$\alpha = \frac{[Op^{+}{}_{bge}]}{[Op^{+}{}_{bge}] + [OpC_6SO_{3\,bge}]} \tag{7-13}$$

rearranging eqn (7-12) and substituting into eqn (7-13) gives:

$$\mu_{ob} = \frac{\mu_{bge}}{K_{ip}[C_6SO_3{}^{-}{}_{bge}] + 1} \tag{7-14}$$

This equation describes the separation of opiates in the presence of hexanesulfonate, but does not take into account the reduction in the amount of available hexanesulfonate in the presence of PDDAC. This can be accounted for by considering the IE interaction between the PDDAC and the hexanesulfonate. This equibrium is described by the following equation:

$$K_s = \frac{[Cl^{-}{}_{bge}][C_6SO_3{}^{-}{}_{ie}]}{[Cl^{-}{}_{ie}][C_6SO_3{}^{-}{}_{bge}]} \tag{7-15}$$

where $[Cl^{-}{}_{bge}]$ and $[Cl^{-}{}_{ie}]$ are the concentrations of chloride in the electrolyte and PDDAC phases, respectively, while $[C_6SO_3{}^{-}{}_{bge}]$ and $[C_6SO_3{}^{-}{}_{ie}]$ are the concentrations of hexanesulfonate in the electrolyte and PDDAC phases, respectively. Using the same considerations as when modelling the anions above we can define the retention factor, k'_{ip}, in terms of various parameters of the system, in a manner similar to eqn (7-4):

$$k'_{ip} = \frac{w_{poly}}{V_{bge}}(K_s)^{1/y}(Q)^{x/y}[E]^{-x/y} \tag{7-16}$$

This can be simplified since now the only competing ion, $[E]$, is the chloride added with the PDDAC (equivalent to Q) or as HCl (10mM) allowing eqn (7-16) to be simplified to:

$$k'_{ip} = K_s w_{poly} \frac{Q}{Q + 0.01} \tag{7-17}$$

The total number of moles of hexanesulfonate can be written as:

$$n(C_6SO_3^-) = n(C_6SO_3^-)_{bge} + n(C_6SO_3^-)_{poly} \tag{7-18}$$

Combining eqn (7-18) with the definition of k'_{ip}:

$$k'_{ip} = \frac{n(C_6SO_3^-)_{poly}}{n(C_6SO_3^-)_{bge}}$$

leads to:

$$n(C_6SO_3^-)_{bge} = \frac{n(C_6SO_3^-)}{1 + k'_{ip}} \tag{7-20}$$

where $n(C_6SO_3^-)$, $n(C_6SO_3^-)_{bge}$ and $n(C_6SO_3^-)_{poly}$ are the total number of moles of hexanesulfonate added and the number of moles in the electrolyte and polymer phases, respectively. This can be converted to concentrations since both are defined in terms of the volume of electrolyte:

$$[C_6SO_3^-{}_{bge}] = \frac{[C_6SO_3^-]}{1 + k'_{ip}} \tag{7-21}$$

Substituting for $[C_6SO_3^-{}_{bge}]$ into eqn (7-14) leads to the final equation:

$$\mu_{ob} = \frac{\mu_{bge}}{K_{ip}\left(\frac{[C_6SO_3^-]}{1 + K_s w_{\%} Q(Q + 0.01)^{-1}}\right) + 1} \tag{7-22}$$

7.7.3 Total System

Combining eqn (7-11) and (7-22) to describe the separation of the mixture of anionic and cationic analytes gives:

$$\mu_{ob} = \frac{\left[\begin{array}{l} \dfrac{1}{1+K_H[PD^+][C_6SO_3^-]+w_{poly}K_{ie}Q[C_6SO_3^- +\frac{1}{d}Q+0.01]^{-1}}\mu_{bge} \\ +\dfrac{w_{poly}K_{ie}Q[C_6SO_3^- +\frac{1}{d}Q+0.01]^{-1}}{1+w_{poly}K_{ie}Q[C_6SO_3^- \frac{1}{d}Q+0.01]^{-1}}\mu_{ie}+\dfrac{K_H[PD^+][C_6SO_3^-]}{1+K_H[PD^+][C_6SO_3^-]}\mu_{ie} \end{array}\right]}{K_{ip}\left(\dfrac{[C_6SO_3^-]}{1+K_s w_{\%}Q(Q+0.01)^{-1}}\right)+1} \qquad (7\text{-}23)$$

In eqn (7-23) Q is related to the %PDDAC and can be estimated by the number of repeat units in the polymer while the remaining parameters, K_{ie}, K_H, K_{ip},K_s,μ_{bge} and μ_{ie} must be determined by non-linear regression.

7.8 Application of the migration model

Since eqn (7-23) contained 6 unknowns with two variables, namely %PDDAC and [hexanesulfonate], a minimum of 7 experiments was needed to determine the unknowns. A two dimensional set of data for retention factors covering the parameter space determined by 0-0.5% PDDAC and 0-110mM hexanesulfonate was chosen and comprised 15 data points. Non-linear regression on the 7 points within the experimental space, the primary data set, was used to determine the 6 constants. The total data set comprising of 15 points was then used to evaluate the predictive power of the model.

Table 7.2 shows the constants obtained by non-linear regression of the primary data set. The three constants, K_{ie}, K_H and K_{ip}, relate directly to the interaction of the analytes with the PDDAC, PDDAC-hexanesulfonate IPs and hexanesulfonate, respectively. The K_{ie} values follow the expected sequence of IE selectivity coefficients of the analytes observed on strong base anion-exchangers. For example

Table 7.2: Parameters derived from non-linear regression of egn (7-23)

Analyte	K_{ie}[1]	K_H[1]	K_{ip}	μ_{bge}[2]	μ_{ie}[2]
Bromide	0.98	0.06	0	-74.2	-27.7
Iodide	2.16	0.06	0	-71.0	-5.6
Nitrate	1.08	0.08	0	-65.7	-28.1
Benzenesulfonate	0.81	0.04	0	-32.0	-6.8
4-Toluenesulfonate	0.88	0.04	0	-29.3	-4.6
4-Ethylbenzenesulfonate	1.06	0.04	0	-27.6	-3.4
2-Naphthalenesulfonate	1.88	0.00	0	-26.8	8.1
Phthalate	7.17	0.00	0	-37.0	26.3
Benzoate	0.86	0.06	0	-30.0	-16.3
4-Toluate	0.72	0.06	0	-27.4	-12.7
4-Propylbenzoate	0.83	0.08	0	-24.4	-9.6
4-*t*-Butylbenzoate	0.84	0.08	0	-23.1	-9.1
4-Heptylbenzoate	0.66	1.51	0	-17.8	-4.4
Morphine	0	0	1.82	11.7	0
Thebaine	0	0	7.02	13.8	0
10-OH Thebaine	0	0	7.69	17.0	0
Codeine	0	0	2.42	12.5	0
Oripavine	0	0	5.41	12.9	0
Laudanine	0	0	7.42	12.9	0
K_s[1]			0.43		
d			24.4		

[1] – x10^3; [2] – x10^{-9} $m^2V^{-1}s^{-1}$

phthalate has the largest K_{ie} value (the only divalent anion in the sample) while naphthalenesulfonate has the second largest value, in agreement with previous studies [5]. It can also be seen that the inorganic anions generally have higher K_{ie} values than the organic sulfonates or acids, while the sulfonates have higher values as a group than the carboxylic acids, again in agreement with Chapter 3. The K_H values generally reflect the hydrophobicities of the analytes with the only analyte showing an appreciable value being heptylbenzoate. This is in agreement with Figure 7.4 a. where only heptylbenzoate showed significant hydrophobic interaction on addition of hexanesulfonate. However, it should be noted that K_H is a combination of three constants (see eqn (7-7)) and hence only gives a guide to the hydrophobic interaction between analytes and the p-SP. Table 7.2 also shows the IP association constants for the opiate-hexanesulfonate IPs. The values obtained agree with the trends observed in Figure 7.4 b. and show that each of the opiates have different affinities for hexanesulfonate, except for 10-OH thebaine and laudanine. The last constant in Table 7.2, K_s, relates to the strength of interaction between hexanesulfonate and PDDAC and can be seen to be approximately half that of the aromatic sulfonates. This is in agreement with the IE selectivity coefficients reported by Breadmore *et al.*[7] for a strong base anion exchange column.

The remaining two parameters listed in Table 7.2, μ_{bge} and μ_{ie} relate to the mobilities of the analytes in the electrolyte and p-SPs, respectively. The values obtained for μ_{bge} correlate well with observed mobilities in electrolytes containing no PDDAC or hexanesulfonate. Values obtained for μ_{ie} were initally assumed to be the same for all analytes, but this assumption does not correlate with observed trends. In practice, the observed limiting mobility obtained on increasing PDDAC concentration (μ_{ie}) was not the same for each analyte. The cause of this could be the relatively small PDDAC

concentration range investigated or the relatively weak interaction of some of the analytes with PDDAC, meaning that some of the analytes will never be as retarded as the more strongly interacting analytes such as phthalate. Results were dramatically improved by assuming different μ_{ie} values for each analyte. From the values for μ_{ie} in Table 7.2 it can indeed be seen that the more striongly interacting analytes, iodide, naphthalenesulfonate and phthalate showed the greatest variation between μ_{bge} and μ_{ie}, as would be expected.

Figure 7.5 shows the correlation between predicted and observed mobilities over the entire experimental space using eqn (7-23) and the constants shown in Table 7.2. It can be seen that correlation was good for all the analytes with the exception of phthalate. Including phthalate in the correlation led to an r^2 value of 0.993 whereas excluding phthalate improved the correlation to 0.996. These values are very good considering the complexity of the system and the required model. The reason for the poor correlation of phthalate is unknown but could be related to its very large interaction with PDDAC compared to the other analytes.

7.9 Optimisation

Optimisation was performed using both the NRP and MR criterions as outlined in Chapter 2. The same optimisation process as that outlined in Chapter 2 was used, however, a predefined limit of $\pm$ $2x10^{-9}$ $m^2V^{-1}s^{-1}$, was used as the cut off for a successful optimum rather than 5% since many of the mobilities were very small, $>5x10^{-9}m^2V^{-1}s^{-1}$, and thus percentage errors were not practical.

Figure 7.6 and Figure 7.7 show the optimum separations obtained using both the NRP and MR criteria. Figure 7.6 shows the optima calculated for the separation of all 19 analytes. It can be seen that the optimum calculated using the NRP criterion

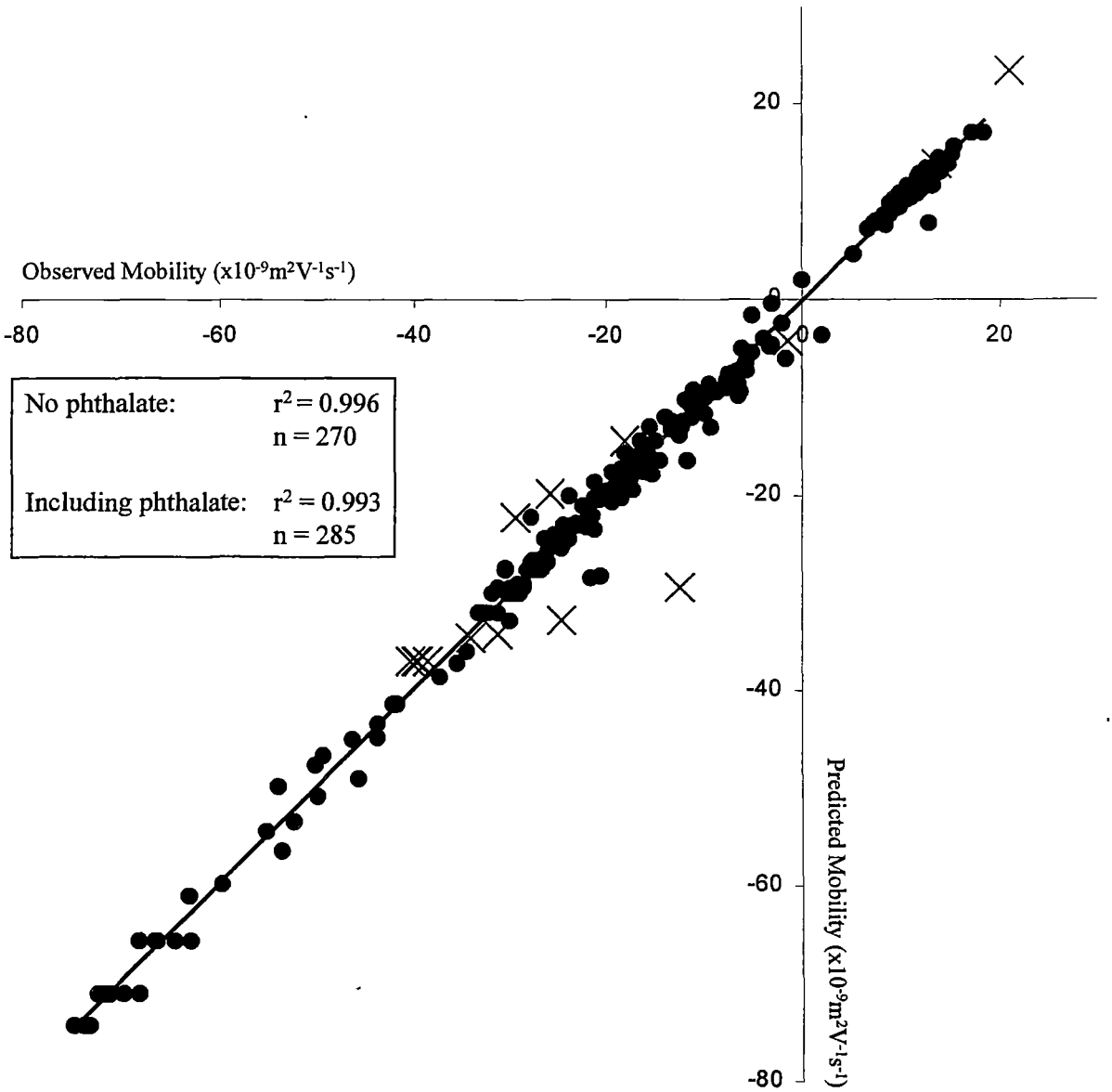

Figure 7.5: Correlation between observed mobilities and those predicted using eqn (7-23) and constants shown in Table 7.2. • = all analytes excluding phthalate, × = phthalate. Points used to derive constants are also included.

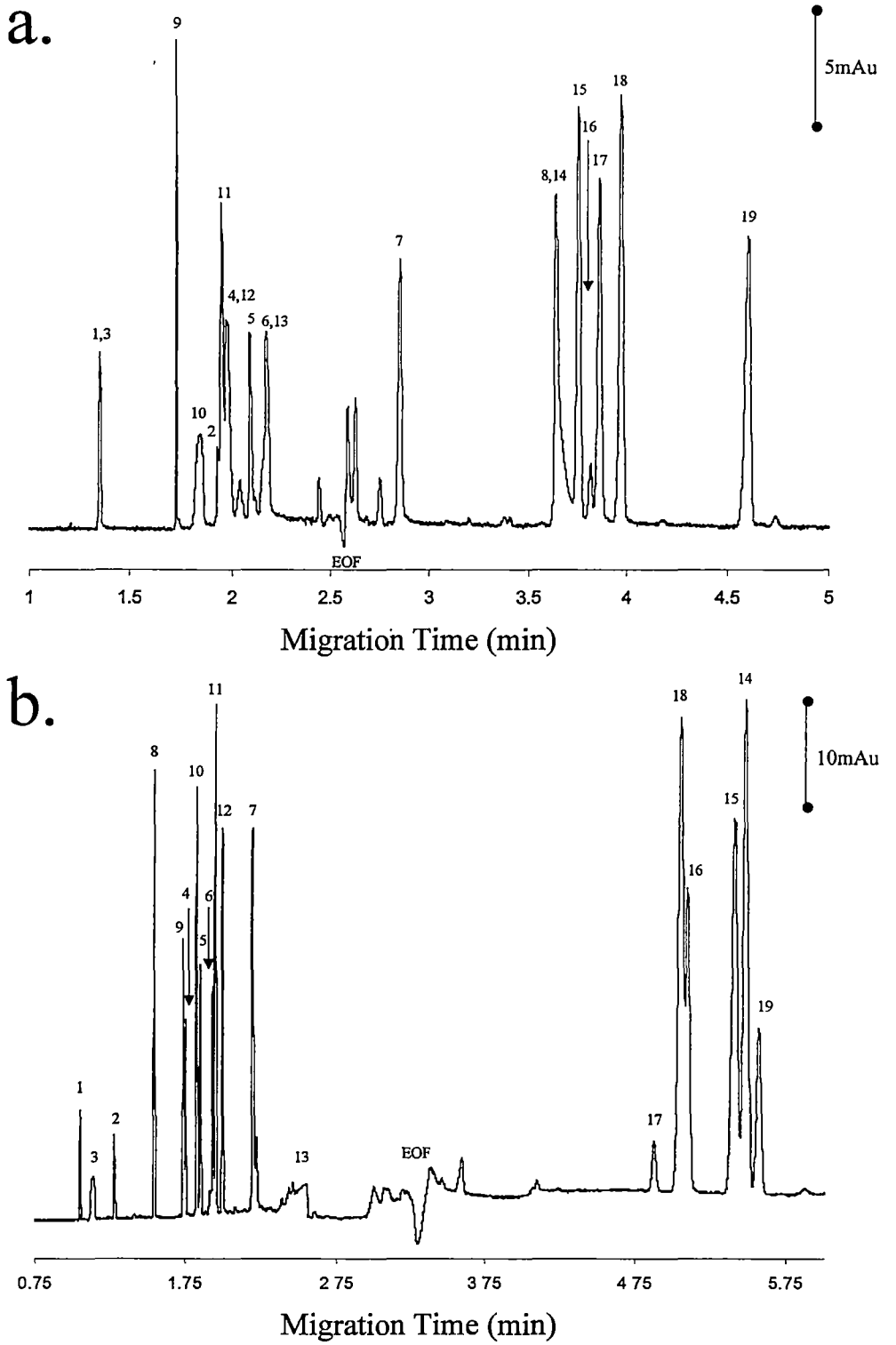

Figure 7.6: Optimised separations for all 19 analytes calculated using the normalised resolution product criterion a.) and the minimum resolution criterion b.). a.) 0.15%PDDAC and 0mM $C_6SO_3^-$, b.) 0.15%PDDAC and 100mM $C_6SO_3^-$. Peaks are 1=bromide, 2=iodide, 3=nitrate, 4=benzene sulfonate, 5=toluenesulfonate, 6=ethylbenzenesulfonate, 7=naphthalenesulfonate, 8=phthalate, 9=benzoate, 10=toluate, 11=propylbenzoate, 12=*t*-butylbenzoate, 13=heptylbenzoate, 14=morphine, 15=codeine, 16=oripavine, 17=laudanine, 18=thebaine and 19=10-OH thebaine. Electrolyte: 20mM Tris, 10mM HCl to pH 8.0. Capillary: 50μm x 35cm (26.5cm to detector) with detection at 205nm

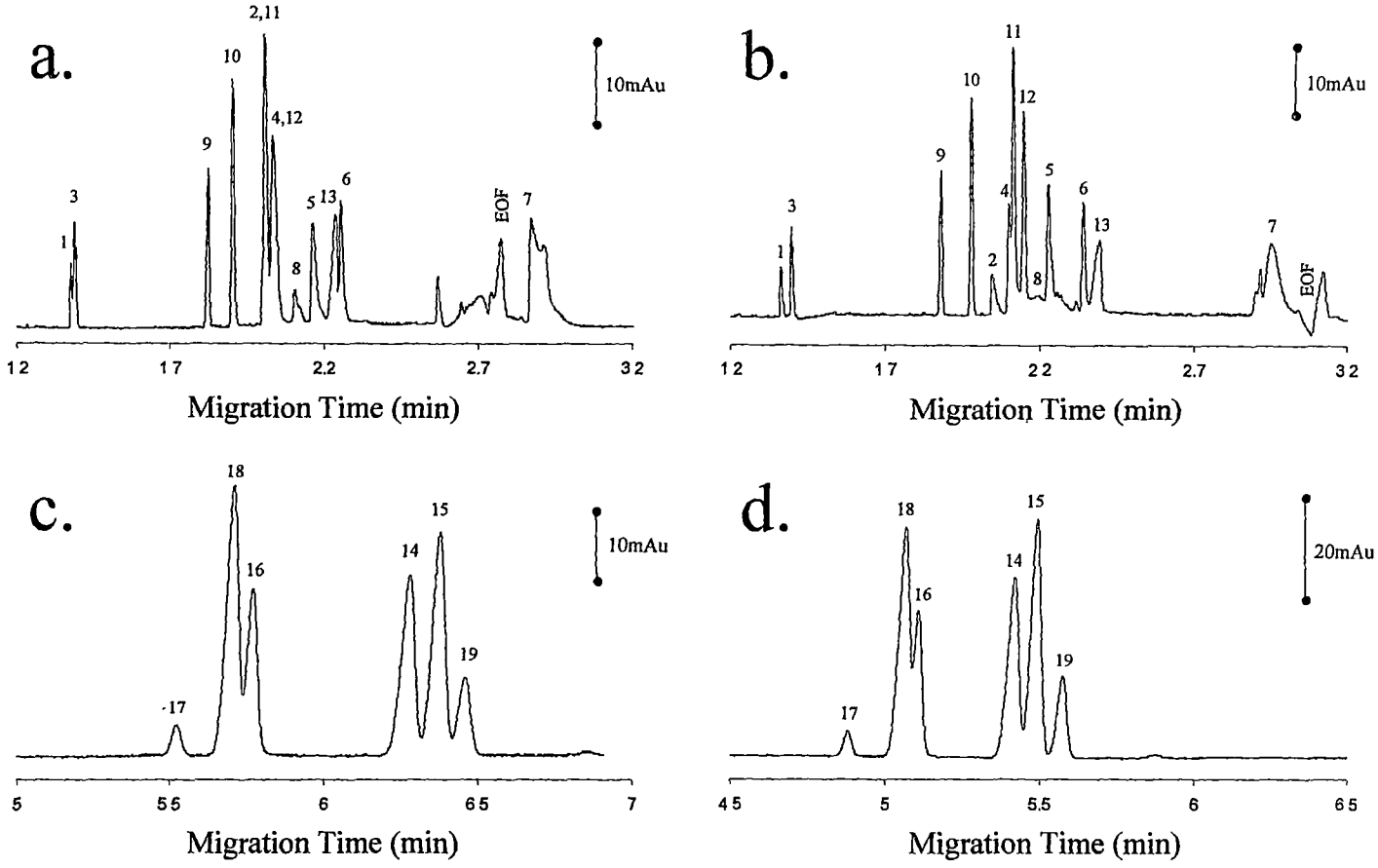

Figure 7.7: Optimised separations for the anions and opiates calculated using the normalised resolution product criterion, a.) and c.) and the minumum resolution criterion, b.) and d.). a.) 0.20%PDDAC and 10mM $C_6SO_3^-$, b.) 0.40%PDDAC and 50mM $C_6SO_3^-$, c.) 0%PDDAC and 110mM $C_6SO_3^-$ and d.) 0.15%PDDAC and 100mM $C_6SO_3^-$. Peaks are 1=bromide, 2=iodide, 3=nitrate, 4=benzenesulfonate, 5=toluenesulfonate, 6=ethylbenzenesulfonate, 7=naphthalenesulfonate, 8=phthalate, 9=benzoate, 10=toluate, 11=propylbenzoate, 12=*t*-butylbenzoate, 13=heptylbenzoate, 14=morphine, 15=codeine, 16=oripavine, 17=laudanine, 18=thebaine and 19=10-OH thebaine. Electrolyte: 20mM Tris, 10mM HCl to pH 8.0. Capillary: 50μm 35 cm (26.5cm to detector) with detection at 205nm.

(Figure 7.6 a.) did not lead to full separation of all the analytes, especially aromatic sulfonates and carboxylates. However, the optimum calculated using the MR criterion provided an acceptable separation for all 19 analytes, Figure 7.6 b. In both cases the predicted and observed mobilities varied by less than 2 x 10^{-9} $m^2V^{-1}s^{-1}$, except for phthalate which varied by up to 15 x 10^{-9} $m^2V^{-1}s^{-1}$, showing that although the model accurately predicted the migration of monovalent anions, it was less reliable for the divalent phthalate. The relatively poor performance of the NRP criterion suggested that trying to achieve an even spread of peaks over the entire separation is impractical. Furthermore, the optimum shown in Figure 7.6 a. was obtained without any hexanesulfonate present in the electrolyte, leading to poor peak shapes and hence reduced resolution. On the other hand, peak shapes in Figure 7.6 b. are generally good with the exception of heptanesulfonate, possibly due to further interactions with the p-SPs which are not considered in the model.

The model also allows the separation of the anions or the opiates to be optimised separately, see Figure 7.7. As with optimisation of all 19 analytes the MR criterion provided better optima for the separation of the anions alone, see Figure 7.7 a. and b. It can be seen that the optimum electrolyte composition determined using the MR criterion, (0.4%PDDAC and 50mM hexanesulfonate) led to almost full separation of all 13 anions, see Figure 7.7 b. whereas the optimum electrolyte composition determined using the NRP criterion (0.2%PDDAC and 10mM hexanesulfonate) gave co-migration of some of the aromatic sulfonates and carboxylates. It should also be noted in Figure 7.7 b. that naphthalenesulfonate migrates close to the EOF, leading to a slightly deformed peak. This is not accounted for within the model and is thus unavoidable unless further constraints are built in.

Figure 7.7 c. and d. shows the optimum separations for the six opiates calculated using both the normalised resolution product and minimum resolution criteria. It can be seen that in both cases very similar separations were obtained, leading to separation of the mixture in under 7 min.

7.10 Conclusions

A system consisting of PDDAC and hexanesulfonate as p-SPs for the simultaneous separation of organic anions and cations has been demonstrated. The IE, hydrophobic and IP interactions between the p-SPs and the analytes can be varied to modify the observed selectivity of the system simply by changing the concentrations of PDDAC or hexanesulfonate. A mathematical model has been derived which describes the observed separation in terms of the various equilibrium processes taking place. This model can be used to not only obtain useful constants related to analyte-SP interactions but also to optimise the system for the separation of anions and cations separately, or for separation of the complete mixture.

The described separation system is potentially applicable to any mixture containing organic anions and cations, particularly in the analysis of pharmaceutically important compounds. The advantage of the described system is the degree of control that can be offered in the separation of complex mixtures due to the competing, complementary equilibria involved in the separations.

7.11 References

1. M. K. Weldon, C. M. Arrington, P. L. Runnels and J. F. Wheeler, *J. Chromatogr. A.*, 758 (1997) 293.
2. C. M. Shelton, J. T. Koch, N. Desai and J. F. Wheeler, *J. Chromatogr. A.*, 792 (1997) 455.
3. W. Ding and J. S. Fritz, *Anal. Chem.*, 70 (1998) 1859.
4. J. Li and J. S. Fritz, *J. Chromatogr. A.*, 840 (1999) 269.
5. M. C. Breadmore, P. R. Haddad and J. S. Fritz, *Electrophoresis*, 21 (2000) 3181.
6. C. Zhang and W. Thormann, *J. Chromatogr. A.*, 764 (1997) 157.
7. M. C. Breadmore, M. Macka, N. Avdalovic and P. R. Haddad, *Anal. Chem.*, 73 (2001) 820.
8. J. A. Dean, *Lange's Handbook of Chemistry*, McGraw-Hill, New York, 1992, 14. Ed.

Chapter 8

General Conclusions

The following general conclusions can be made regarding the selectivity control offered over electrokinetic chromatography (EKC) systems using various soluble additives.

In the separation of anions, ion-exchange (IE) and hydrophobic interactions can be introduced into an EKC system using a combination of a cationic polymer and a neutral cyclodextrin. With the proviso that each of these stationary phases acts independently with the analytes, it is possible to vary the extent of each interaction by simply changing the concentration of each additive. Furthermore, IE interactions can also be modified via the addition of a competing ion to the electrolyte. Using these methods it is possible to separate analytes based not only on their functional group and charge, but also structural differences such as hydrophobicity.

Accurate descriptions of such systems are possible using physical models derived from first principles. For the dual stationary phase system the model was based on electrophoretic separation, IE and hydrophobic interactions, thereby allowing the observed selectivity of the system to be controllable over a 3-dimensional space. The model could be successfully applied to a range of UV absorbing inorganic and small organic anions and gave good agreement between predicted and observed mobilities. Furthermore constants obtained for the model could be readily explained in terms of the IE selectivity coefficients and hydrophobicities of the analytes.

The separation of cations is potentially more useful than the corresponding systems for anions due to the large number of organic cations routinely used in the

pharmaceutical industry. Introduction of IE interactions for the separation of opiate alkaloids (separated as cations) was demonstrated using an anionic cyclodextrin. This allowed selectivity changes to be brought about by varying the composition of the electrolyte. Application of a physical model was also possible to accurately describe the system and predict optimum conditions using various optimisation criteria.

Increasing the complexity of multiple additives in EKC systems potentially increases the number of possible migration sequences achievable for the analytes of interest. However, a complicating factor is that the increased selectivity control may not be predictable due to competing interactions between the analytes and the additives and between the additives themselves.

Application of a dual-additive system to the separation of cations was possible using the same approach as used for anions, but pH could also be included as a further variable due to the large range of pK_a values exhibited by organic bases. The use of a physical model can accurately describe individual analyte-additive interactions, but it is not possible to extend the model to describe the whole system. Artificial neural networks (ANNs) were shown to perform better for such complicated systems where equivalent physical models performed poorly and could be successfully applied to dual-additive EKC systems with a number of input parameters.

Selectivity control for enantiomeric separation was demonstrated using a combination of a cyclodextrin and a soluble polymer. In such a system mobility changes could be introduced by varying the electrolyte composition. In this way desired migration orders and optimised separations could be obtained relatively simply using a physical model that accurately described the observed separations.

As well as electrolyte composition, temperature could be used to modify the observed selectivity. This allowed a simple means to optimise the chiral separations and could also be accurately modelled using a relatively simple ANN.

The potential for controllable selectivity changes for the simultaneous separation of anions and cations was demonstrated using a combination of a cationic polymer and an anionic ion-pair reagent. Predictable selectivity changes were obtained due to differing interactions between the analytes and the individual and combined additives used. The system could be modelled successfully using a physical model.

It can be seen that the introduction of combined pseudo-stationary phases increases the selectivity control offered over various systems for the separation of anions, cations and the simultaneous separation of both anions and cations. Furthermore, useful information can be obtained about analyte-additive interactions using relatively few experiments and derived physical models. Although many suitable additives exist, a potential limitation to this approach is the fact that any additives used need to not only exhibit interactions with the analytes of interest, but to also be compatible with each other and not lead to precipitation or other complicating effects. In practice, such effects exclude combinations of many additives.

Finally it should be noted that further research is needed in the following areas.

(i) The analytes examined in the current research have been used to test the present systems. Application of those systems outlined in the work to real analytical problems, especially in the area of chiral separations, is an obvious area of future research. This, however, will have to be undertaken on a case-by-case basis to see how the present systems tolerate real sample matrices and other problems associated with real samples.

(ii) A large number of potentially suitable polymers and cyclodextrins exhibiting different selectivities is available. Systems exhibiting unique selectivities are therefore possible by investigating mixed systems comprising these additives.

(iii) Several different classes of additives, including dendrimers, crown ethers, resorcarenes, calixarenes, proteins, nanoparticles etc. are available and provide varied interactions with various analytes. These can be potentially used in combination with other additives, allowing for greater selectivity control.

(iv) Although the systems described in this work contained no more than two additives, potentially more additives can be included to increase the selectivity control offered over a system. However, it is desirable in such systems that each pseudo-stationary phase interacts in an independent fashion with the analytes, as well as not interacting to a significant extent with the other additives found in the system. Although sections of the work presented here suggest that this may be a problem, investigation of such systems would still be worthwhile, especially towards specific applications.

(v) Mixed systems utilising a pseudo-stationary phase combined with a solid stationary phase (open tubular, packed or monolithic columns) have not been reported and could offer advantages over mixed pseudo-stationary phases. Solid stationary phases also have the ability to exhibit multiple simultaneous interactions with analytes thus increasing the selectivity that can be offered by such systems.

(vi) Although selectivity changes that have been described thus far are based on analyte-stationary phase interactions, it is possible to introduce "apparent" selectivity changes in the simultaneous separation of anions and cations by

using a dual end injection approach where anions are injected from one end while cations are injected from the other end. In such systems the "apparent" selectivity can be varied by simply changing the position of the detector. Combining such a system with methods presented in this work could allow for far greater selectivity control over observed separations.

(vii) A limitation of the work described is that only UV absorbing analytes were considered. The use of indirect detection could potentially increase the number of analytes applicable to the current separations. This approach, however, could be problematic due to system peaks and other complications, so other detection methods such as contactless conductivity detection could offer the ability to investigate a wide range of analytes.